Solid dispersions: Formulation, characterisation, permeability and genomic evaluation

Muhammad Sheraz Akbar Khan

Doctor of Philosophy

ASTON UNIVERSITY

March 2010

Aston University

Solid dispersions: Formulation, characterisation, permeability and genomic evaluation

Muhammad Sheraz Akbar Khan

Doctor of Philosophy

March 2010

Poor water solubility is characterised by low dissolution rate and consequently reduced bioavailability. Formulation of solid dispersion of the drug has attracted considerable interest as a means of improving dissolution process of a range of poorly water soluble drugs. This current study investigates the formulation of solid dispersion for a range of poorly water soluble drugs with varying physicochemical properties including paracetamol, sulphamethoxazole, phenacetin, indomethacin, chloramphenicol, phenylbutazone and succinylsulphathiazole.

Solid dispersions were prepared using various drugs to polymer ratios. PEG 8000 was selected as a carrier in the solid dispersions. The study revealed that inclusion of drug within the polymeric matrix, ratio of drug to polymer and physicochemical properties of the drug molecules enhance the dissolution rate. Characterisations of the solid dispersions were performed using DSC, FTIR and SEM. These studies revealed that all seven drugs were present in the amorphous form within the solid dispersions and there was a lack of interaction between the PEG 8000 and drug. Stability studies for solid dispersions showed that all seven drugs studied were unstable at accelerated conditions (40°C±2°C/75%RH±5%RH) whereas, they were found to be stable for 12 months at room conditions.

Permeability of indomethacin, phenacetin, phenylbutazone and paracetamol were higher for solid dispersions as compared to drug alone across Caco-2 cell monolayers. From the cell uptake studies it was shown that PEG 8000 enhanced rhodamine123 uptake which suggested that PEG 8000 may increase the permeability of these drugs in solid dispersions. Gene expression profiles analyzing the expression changes in the ABC and solute carrier transporter during permeability studies.ABCA10, ABCB4, ABCC12, SLC12A6, MCT13, SLC22A12 and SLC6A6 gene expression were increased by indomethacin alone whereas solid dispersion of indomethacin resulted in a slight increase in expression. ABCC12 and SAMC gene expression was increased in case of paracetamol alone but slightly increased when exposed to solid dispersion of paracetamol.

Key words: PEG 8000, dissolution, stability studies, Caco-2, microarray.

Acknowledgements

First of all I would like to say thanks to my supervisors, Dr. Afzal R Mohammed, Dr. Hannah K Batchelor and Professor Yvonne Perrie for their guidance, support and help throughout my studies. Thank you Afzal for all your encouragement.

There are so many people to thank along the way;

Professor Baz Jackson for the ITC studies (School of Biosciences, University of Birmingham, United Kingdom).

Dr. Peter J Hanson for the cell culture work.

Dr. Ayesha S Rahman for the microarray work (School of Biosciences, University of Birmingham, United Kingdom).

Mr. Chris Bache, Mr Jiteen H Kansara, Christine Jakeman and Mrs Karen C Farrow.

Finally, thanks to my parents for their unconditional love and support.

Table of contents

List of figures

List of tables

Abbreviations used in this study

2X	2times
18S	18 Svedberg
28S	28 Svedberg
@	At
%	Percentage
Ω	Ohm
µL	Microlitre
µg/mL	Microgram per millitre
λmax	Wavelength maximum
aa-dUTP	5-(3-Aminoallyl)-2'-Deoxyuridine-5'-Triphosphate
ABC-transporter	ATP-binding cassette transporter
ABC-me	ABC-mitochondrial erythroid
ACE-inhibitors	Angiotensin-converting enzyme inhibitors
ATP	Adenosine triphosphate
A2E	*N*-retinylidene-*N*-retinyl-ethanolamine
ß-lactam antibiotics	Beta lactam antibiotics
BBB	Blood-brain barrier
BCS	Biopharmaceutics Classification System
BRB	Blood retinal barrier
BSA	Albumin from Bovine serum
cAMP	Cyclic adenosine monophosphate
cGMP	Cyclic guanosine monophosphate

CDER	Center for Drug Evaluation and Research
cDNA	Complementary deoxyribonucleic acid
cm^{-1}	A reciprocal centimeter
cells/ cm^2	Cells per square centimeter
cm/s	Centimeter per second
CYP P450	Cytochrome P450
cm^2	Square centimeter
Da	daltons
DAPI	4',6-Diamidino-2-phenylindole dihydrochloride
DMEM	Dulbecco's modified Eagle's medium
DNA	Deoxyribonucleic acid
DSC	Differential scanning calorimetry
EDTA	Ethylenediaminetetraacetic acid
e.g.	exempli gratia ('for sake of an example')
etc	et cetera
FBS	Fetal bovine serum
FDA	Food and drug administration
FDR	False discovery rate
FTIR	Fourier transform infrared spectroscopy
GABA	γ-amino butyric acid
GSH	Glutathione
GIT	Gastro-intestinal tract
g/mol	Gram per moles

ΔG	Free energy change
h	Hour
hrs	Hours
HBSS	Hank's balanced salt solution
HEPES	4-(2-hydroxyethyl)-1-piperazineethanesulfonic acid
hNET	Human norepinephrine transporter
HPLC	High performance liquid chromatography
Hyper DSC	Hyper differential scanning calorimetry
ΔH	Binding enthalpy
H_2O	Water
ICH	International Conference on Harmonization
i.e	id est
IND	Indomethacin
IR spectra	Infrared spectra
ITC	Isothermal titration calorimetry
L	Litre
K	Binding constant
KATP	ATP-sensitive potassium
KCC3	K^+ Cl^- cotransporters
kDa	Kilodaltons
m	Meter
mA	milliampere
mAU	milli-absorbance unit

MCT	Monocarboxylate cotansporter
MDR	Multidrug resistance
mRNA	Messenger ribonucleic acid
MRP	Multidrug resistance protein
min	minute
mins	minutes
mL	millilitre
mM	milliMolar
mPa.S	milli pascal second
ms	millisecond
mTP	mitochondrial targeting presequence
N	Stoichiometry
NaOH	Sodium hydroxide
NBF	Nucleotide binding folds
NEAA	Non-essential amino acids
nm	nanometer
n=3	Triplicate
Papp	Permeability coefficients
PARA	Paracetamol
PBS	Phosphate-buffered saline
PCA	Principle component analysis
PCR	Polymerase chain reaction
PEG	Polyethylene glycol

PEGs	Polyethylene glycols
PEG 300	Polyethylene glycol molecular weight 300
PEG 600	Polyethylene glycol molecular weight 6000
PEG 8000	Polyethylene glycol molecular weight 8000
P-gp	Phosphoglycoprotein
pH	Potential of hydrogen
PKC	Paroxysmal kinesigenic choreoathetosis
PM	Physical mixture
PMT	Photo-multiplier tube
PVP	Polyvinylpyrrolidone
RH (r.h)	Relative Humidity
rpm	Revolutions per minute
RNA	Ribonucleic acid
RPE	Retinal pigment epithelial cells
rRNA	Ribosomal Ribonucleic acid
R^2	Coefficient of Determination
s (sec)	Second
SAM	Significant analysis of microarrays
SAMC	S-adenosylmethionine carrier
SD-PARA	Solid dispersion of paracetamol
SD-IND	Solid dispersion of indomethacin
SDS	Sodium dodecyl sulfate
SD	Solid dispersion

S.D	Standard deviation
SEM	Scanning electron microscopy
SLC transporters	Solute carrier transporters
SSC	Saline-sodium citrate
SUR2	Sulsonyl urea receptor
ΔS	Entropy change
TAE	Tris-acetate-EDTA
TAPL	Transporter associated with antigen processing (TAP)-like
TC-Plate	Tissue culture plate
TEER	Transepithelial electrical resistance
TGA	Thermo gravimetric analysis
TM	Transmembrane
UGT/ UDP-glucuronosyltransferase	Uridine 5'-diphospho-glucuronosyltransferase
WHO	World Health Organization
w/w	weight by weight

Chapter 1

Introduction

1.1 Physiology of the gastro-intestinal tract (GIT)

The gastro-intestinal tract consists of esophagus which is 25 cm in length, followed by the stomach. The volume of the stomach changes with the change in the amount of food present in it, whereas its length is approximately 25 cm. The volume of an empty stomach is approximately 50 mL yet its volume can become as much as 4 L when it is dilated by food (Curtis and Barnes, 1994). The stomach is divided into three main parts: the fundus, the body and the pylorus region. The curved uppermost part of stomach is fundus which pushes gastric contents towards pylorus region by its slow continuous contractions. Body is the largest part of the stomach which acts as a reservoir and stores the indigested food and liquids for a certain time period. The lowest part of the stomach is pylorus region; it prevents larger particles of food from entering into the small intestine. There are millions of deep gastric pits in the smooth lining of the stomach, through which the gastric juice produced by the gastric glands enters the stomach. The gastric juice consists of water, hydrochloric acid, pepsin and intrinsic factors. The environment inside the stomach is kept extremely acidic (pH 1-2.5) through hydrochloric acid. It kills the bacteria that are present in food and it is also vital for the activation and optimal activity of pepsin. The breakdown of proteins is carried out through pepsinogen, an inactive enzyme of pepsin. Vitamin B12 is absorbed in the small intestine by intrinsic factor which is a glycoprotein.

The extreme acidity and the presence of pepsin; which is capable of digesting the stomach itself, provides the most rough conditions in the digestive tract to which mucosa of the stomach is exposed. Thick alkaline mucus is secreted by the stomach which

prevents stomach mucosa from digestion. The thick mucus layer is responsible for limiting the absorption inside the stomach despite its large epithelial surface. The underlying tissue layers are kept protected by tight junctions in the epithelial cells of the mucosa from the gastric juice of the stomach. Damaged epithelial cells are shed and replaced quickly, with the whole stomach epithelium being replaced every 3-6 days. The partially digested food then reaches the small intestine, the longest part of the gastro-intestinal tract. It is divided into three main parts. The first 20-30 cm of the small intestine is called duodenum (pH 5.5-6) which have deeply folded mucous membrane in its thick wall, containing duodenal digestive gland and Brunner's glands. An alkaline secretion free from enzymes is produced by the Brunner's glands to neutralise the hydrochloric acid present in the gastric juice. This causes a change in the pH of chyme (the food/gastric fluid matter) that enters the small intestine.

The jejunum (pH 6.0-7.0) and the ileum (pH 7.0-7.5) are the continuation of the duodenum and constitute the remaining part of the small intestine. Although the jejunum has a thicker wall than either the ileum or duodenum, small intestine cannot be differentiated completely as its parts are not demarcated but are distinct in properties. The small intestine is approximately 2 m long. The small intestine is highly specialised for the purpose of absorbing nutrients. Along with the advantage of being greater in length, small intestine also has three main structural features which increase surface area and therefore, enhance the uptake of nutrients.

The plicae circulares are large circular folds that increase the surface area. Villi are finger like projections that also contributes to the increase in surface area. Villi have tiny projections on their surface called microvilli which increase the surface area that further enhances the absorption process.

The gastric emptying differs with the amount of food digested (Davis et al., 1988) and with the type of preparation (Christensen et al., 1985). It has been reported that it takes around 3±1 hrs for a dosage form to reach the large intestine (Davis et al., 1986) though another work has reported that the mean small intestine transit time for a radiotelemetry capsule was 5.7±2 hrs (Evans et al., 1988).

The large intestine is much shorter than the small intestine as its length is approximately 1.5 m but its diameter is quite larger as compared to the small intestine. In the large intestine very little digestion and absorption of food is carried out as most of it has already taken place in the small intestine. Bacterial fauna present in the large intestine produces water, electrolytes and vitamins that are to some degree absorbed over the 12 – 24 hrs time period for which the faecal matter remains in the large intestine.

1.2 Biopharmaceutics Classification System (BCS)

The Biopharmaceutics Classification System (BCS) is a scientific method in which drugs are classified according to the solubility in water related to their dose at three different pHs and intestinal permeability (Amidon et al., 1995). The BCS system divides the drug substances into following four classes;

Class 1 (high solubility–high permeability)

Class 2 (low solubility–high permeability)

Class 3 (high solubility–low permeability)

Class 4 (low solubility–low permeability)

However, the dissolution rate is used as a criterion for the classification of rapid release oral dosage forms. The BCS can be used in association with the dissolution of a product to monitor the three basic properties that are the determining factors in the rate and extent of drug absorption from immediate release solid oral dosage forms: dissolution rate, solubility and permeability. The BCS has been successfully used for extended release solid dosage forms besides for immediate release forms and it is regarded as the basic instrument in the development of drugs over the last few years (Lennernas and Abrahamsson, 2005; Wei et al., 2008; Ku, 2008; Grudzien et al., 2009).

1.3 Dissolution rate

According to modified Noyes-Whitney equation (equation 1.1) the dissolution rate can be improved by increasing the surface area available for dissolution, decreasing particle size and/or increasing wettability, decreasing the boundary surface thickness, ensuring sink conditions for dissolution and increasing the apparent saturation solubility (Noyes and Whitney, 1897; Nernst, 1904).

$dC/dt = (AD[Cs - C])/h \rightarrow$ (equation 1.1)

Where,

dC/dt is the rate of dissolution,

A is the surface area available for dissolution,

D is the diffusion coefficient of the compound,

Cs is the solubility of the compound in the dissolution medium,

C is the concentration of drug in the medium at time t and

h is the thickness of the diffusion boundary layer adjacent to the surface of the dissolving compound.

1.4 Solubilisation

Solubilisation is the use of an inert substance to enhance the solubility of a drug. There are different ways in which the solubility and dissolution of a drug can be increased by using adsorbents (Alsaidan et al., 1998; Bogdanova et al., 2007), surfactant (Krasowska, 1980) or co-solvents (Etman and Nada, 1999).

1.5 Micronisation

It has been shown that the dissolution rate of a variety of drugs can be significantly increased and also the apparent equilibrium solubility can be improved by using micronisation. As predicted by the modified Noyes-Whitney equation (equation 1.1) the dissolution rate is associated with the particle size (Maillols et al., 1982). The therapeutic dose of griseofulvin has been reduced to half by micronisation process (Atkinson et al., 1962; Kabasakalian et al., 1970). It has been proved that the bioavailability can be increased through ultra-micronised dispersions of griseofulvin (Straughn et al., 1980). The problem with very small particles is that they cause poor wettability and their handling is also very problematic (Serajuddin, 1999).

1.6 Complexation

Sparingly soluble drugs have been shown to display improved dissolution by the formation of a complex with water soluble complexation agents. The most widely used complexation agents are cyclodextrins. Cyclodextrin complexes are formed by the binding of the hydrophobic core of the agent with the hydrophobic region of the drug (Florence and Attwood, 1988). The characteristic feature of these complexes is that they are reversible; hence facilitating the absorption by releasing the drug from the complex during dissolution as it is soluble in the fluids of the gastro-intestinal tract. Pitha and Pitha (1985) explained that the solubility of the sparingly soluble drugs can be improved by the application of cyclodexrin complexes. Aqueous solution of cyclodextrins was used to increase the solubility of a variety of steroids.

1.7 Chemical modification (Prodrug)

Chemical modification can render a drug into a more soluble prodrug (Albert, 1958), where the prodrug is defined as "a bio-reversible chemical derivative of an active parent drug" (Taylor, 1996). It includes salt forms and complexes which can be easily disassociated from the drug (Anderson, 1985). Diclofenac, for instance, is generally formulated as a sodium and potassium salt whereas, dissolution is greater from potassium salt because potassium salt has very high dissociation rate. The basic objective is to increase the solubility either by introducing an ionisable group or by reducing the lattice enthalpy of a drug (Amidon, 1981).

Salt formation, by its nature requires a drug to be basic or acidic; therefore it is unsuitable for neutral drugs such as griseofulvin (Berge et al., 1977). The possibility of the salt form of a drug to aggregate in the gastro-intestinal tract demolishes any increase in the dissolution rate that was desired to have been attained by this process (Serajuddin, 1999). Numerous drugs along with griseofulvin have been modified into prodrug to enhance their solubility but this does not improve their bioavailability although they have been shown to have the ability to degrade at the intestinal lumen, therefore, a complete knowledge of the kinetics and mechanisms of prodrug degradation is necessary to make their use effective. The factors responsible for this are incomplete conversion, simultaneous breakdown into inactive derivatives and elimination from the body before complete conversion has occurred. To decrease the crystal lattice enthalpy digoxin prodrugs and complexes with hydroquinone are produced and the proof of their effectiveness is that a digoxin prodrug product is available in the United States (Acylanid®) (Higuchi and Ikeda, 1974; Stella, 1975).

1.8 Introduction to solid dispersions

Enhancement of bioavailability of hydrophobic drugs is one of the major challenges in drug development. Of the plethora of pharmaceutical technologies available to address this issue, solid dispersion is one of the useful methods for the dispersion of the drug into an inert, hydrophilic polymer matrix (Chiou and Reigelman, 1971; Serajuddin, 1999). Solid dispersions in water-soluble carriers have attracted considerable interest as a means of improving the dissolution rate, and hence possibly bioavailability of a range of hydrophobic drugs. Although a large number of studies have been published but the

mechanisms underpinning the observed enhancement of the rate of drug release are not yet understood (Sjokvist-Sears and Craig, 1992; Friedrich et al., 2006).

The use of solid dispersions as an effective source of improving the dissolution rate of poorly soluble drugs has been well studied and demonstrated (Chiou and Reigelman, 1971; Corrigan, 1985; Ford, 1986; Craig, 1990). The poorly water soluble drugs are characterised by insufficient bioavailability (low dissolution rates) and absorption in the gastro-intestinal tract. Different methods have been used to increase the dissolution and bioavailability of poorly water soluble drugs including micronisation (Atkinson et al., 1962), the use of surfactants (Khalafallah et al., 1975), and the formation of solid dispersions (Sekiguchi and Obi, 1961). Solid dispersions display an enhanced solubility of drug because of the conversion of the drug's crystal lattice into an amorphous form, particle size reduction and increased wettability by the hydrophilic polymer. Therefore, the same pharmacological results can be obtained from a reduced amount of drug given to the patient.

1.8.1 First generation solid dispersions

It has been shown by Sekiguchi and Obi in 1961 (Sekiguchi and Obi, 1964) that the formulation of eutectic mixtures improved the rate of drug release which in turn increases the bioavailability of poorly water soluble drugs. Solid dispersions systems were developed by Levy (1963) and Kanig (1964), who made solid solutions by using molecular dispersions instead of using eutectic mixtures, with mannitol as carrier. These improvements were due to faster carrier dissolution, releasing particles of drug. These

dispersions prepared using crystalline carriers were described as first generation of solid dispersions. Urea (Sekiguchi and Obi, 1964; Goldberg, et al., 1966b) and sugars (Kanig, 1964) were the first crystalline carriers to be used in dispersions. The major drawback of first generation solid dispersion is that they form crystalline solid dispersions, which being thermodynamically more stable did not release the drug as quickly as amorphous ones.

1.8.2 Second generation solid dispersions

It was noticed in the late sixties (Simonelli et al., 1969; Chiou and Riegelman, 1969), that solid dispersions with drug in the crystalline state are not as effective as amorphous because they are thermodynamically stable (Simonelli et al., 1969; Vippagunta et al., 2006; Urbanetz, 2006). Therefore, second generations of solid dispersions were introduced having amorphous carriers instead of crystalline. Formerly, the drugs were molecularly dispersed in amorphous carriers which are usually polymers in random pattern (Vilhelmsen et al., 2005).

1.8.3 Third generation solid dispersions

Third generation of solid dispersions appeared as the dissolution profile could be increased by using carriers having surface activity and self-emulsifying characteristics. These contain surfactant carriers or a mixture of amorphous polymers and a surfactant as carrier. The third generation solid dispersions stabilise the solid dispersions, increase the bioavailability of the poorly soluble drugs and reduce recrystallisation of drug. The use of

surfactants such as poloxamer 407 as carriers resulted in high polymorphic purity and improved vivo bioavailability (Majerik et al., 2007).

1.8.4 Manufacturing methods for solid dispersions

Melting and solvent evaporation methods are the two major processes of preparing solid dispersions. Sekiguchi and Obi (1961) were the first to use melting method. The method depends on melting either the carrier or the drug or both. One component is melted and the second is dissolved in it. The solution is then cooled to prepare a solid dispersion. Goldberg and co-workers applied temperatures more than 100 °C to prepare paracetamol-urea and chloramphenicol-urea dispersions (Goldberg et al., 1966a; Goldberg et al., 1966b). The solvent evaporation method consists of solubilisation of the drug and carrier in a volatile solvent that is later evaporated (Lloyd et al., 1999; Hasegawa et al., 2005; Rodier et al., 2005).

1.8.5 Proposed mechanisms for drug release from solid dispersions

Different factors influence the enhancement of dissolution rate of solid dispersions. The use of increased amount of urea enhances the dissolution rate of drug as was shown in a study with 20% chloramphenicol and 80% urea (Goldberg et al., 1965). This was due to the reduction in particle size. However, it was later found that the dissolution rate could be improved without any change in the particle size (Sjokvist-Sears and Nystrom, 1988). Non surface active carrier can enhance the wettability of a drug (Chiou and Reigelman, 1971) by reducing the contact angle and thus causing an increase in the surface area available for dissolution. A drug can be retained in the solution by inhibiting its

precipitation with the addition of a polymer (Simoneli et al., 1976; Hilton and Summers, 1986; Usui et al., 1997). The drug dissolves back into the solution, after precipitating out as metastable polymorph as this form is more soluble than the original polymorph of the drug, as highlighted in a study with indomethacin (Ford and Rubinstein, 1978; Hilton and Summers, 1986).

Carrier-controlled or drug-controlled dissolution mechanisms were first proposed by Craig (2002) in which the drug release depends either on the carrier or the drug itself. This method is based on the models proposed by Higuchi et al. (1965) and Higuchi (1967). The dissolution surface is non-disintegrating and the dissolution of both parts is diffusion controlled. The dissolution is controlled through a drug rich dissolving surface, formed only if the drug makes the larger component (Corrigan, 1985). In high polymer loading there is insufficient drug to support the drug controlling layer formed at the dissolving surface. This causes the drug to disperse within the polymer resulting in a carrier-controlled drug release process. In high drug loading solid dispersions, the dissolution rate of the drug can be measured, by considering the polymer as faster dissolving component.

Hence, the dissolution of the drug is controlled by polymer dissolution if the drug forms the minor component in the solid dispersion. The carrier-controlled dissolution was further supported by another study investigating the incorporation of ten drugs into PEG 6000 solid dispersions where identical dissolution rates were reported (Dubois and Ford, 1985). A linear relationship was shown when the dissolution rate was plotted against the

drug content. Carrier-controlled dissolution works up to a limited concentration depending upon the drug (0-2% w/w for phenylbutazone and 0-15% w/w for paracetamol) as is evident from the differences in the linear relationships for various drugs.

Currently, there is no mechanism that can predict the behavior of a drug in solid dispersion, as various factors are pivotal in deciding drug release. Extensive work is required in order to fully understand the association of the carrier and drug in dispersion.

1.8.6 Characterisation of solid dispersions

There are different techniques that have been used to characterise solid dispersions. Among these the most important methods are thermoanalytical, fourier transform infra-red spectroscopy (FTIR), scanning electron microscopy (SEM), thermogravimetric analysis (TGA) and measurement of release rate of the drug. These methods can be employed efficiently to differentiate between solid solutions (molecularly dispersed drug) and solid dispersions in which drug is only partly molecularly dispersed and physical mixtures of drug and carrier. It is difficult to differentiate accurately between molecularly dispersed and non dispersed systems because of the complex composition of these preparations.

Differential scanning calorimetry (DSC) is the most reliable thermoanalytical technique. Processes in which energy is either required or produced can be quantitatively observed with the help of DSC**.** It is a thermal process to find out the heat flow and temperature

related with substance transitions as a function of time and temperature. With the help of DSC we can find melting temperatures as well as monitor and study the thermal behavior of various substances. Interactions between drugs and polymer are generally said to have cause the changes in the exothermic and endothermic peaks (Ribeiro et al., 2005; Borges et al., 2005).

FTIR spectroscopic imaging is regarded as more beneficial than other methods because it takes into account the specific absorbance of molecular vibrations in the sample for quality assessment of biomedical materials. Hence, dyes or various labelling methods are not necessary for seeing chemical components within the sample. It has opened a new horizon of information about structure, conformation and dynamics of various molecular components (Mantsch and Chapman, 1996). It can be applied to follow changes in bonding between functional groups.

SEM has been a process for ultrastructural analysis in the pharmaceutical industry. The characteristic properties of drug crystals like particle size and morphological surface can be known by the preparation method and chemical composition (Ramadan and Tawashi, 1990). Additionally, the shape and granulometric properties of the powder particles can be explained through the range of parameters automatically obtained by connecting SEM with an image processor. As this method is automatic and gives precise measurements, it is time saving as well as reliable, therefore, it gives valid conclusions with smaller number of observations (Paraira et al., 1994).

Isothermal titration calorimeter (ITC) is a powerful technique with high precision that can quickly and directly explain the complete thermodynamic profiles of interaction in a single experiment (Haq et al., 2000; Leavitt et al., 2001). The heat absorbed or generated during binding can be measured by an ITC experiment. It involves the addition of one binding component (titrant) into the other binding component (titrate) over time using single or multiple injections. The absorbed or generated heat is measured as a change in temperature or as the change in power needed to maintain temperature between the sample and a reference cell. Based on the information of the cell volume and the concentration of the reactants the energy is changed into a binding enthalpy. The enthalpy measured includes the heat of binding between titrant and titrate, also any heat sources related with the reaction due to solvent effects, conformational changes and heats of dilution. It involves a very careful preparation of solutions to obtain thermodynamic parameters that accurately show the concern results.

TGA is a powerful technique for studying the changes in weight of a sample when heated, cooled or held at constant temperature. Its main application is to characterise samples with regard to their composition. Thus, the determinations of the moisture content in a solid dispersion can be determined by using TGA.

1.9 Polyethylene glycol (PEG)

Polyethylene glycols (PEGs) are polymers of ethylene oxide, having molecular weight usually falling in the range 200-30000 daltons (Da). PEGs with molecular weights of 1500-20000 Da can be used efficiently in the formation of solid dispersions. PEG

polymers are widely used and employed in different formulations because of low melting point, low toxicity, compatibility with drugs and hydrophilic nature (Chiou et al., 1971). The viscosity of PEG increases with the increase in molecular weight. PEGs are fluid at molecular weights of up to 600 Da, while in the range of 800-1500 Da they are vaseline-like, and tend to be waxy from 2000 to 6000 Da and those with molecular weights of 20000 Da and above form hard, brittle crystals at room temperature. Their ability to solubilise in many organic solvents makes PEGs highly useful for the formation of solid dispersions. The melting point of different molecular weight of PEGs lies under 65 °C (Price, 1994). The low melting point of the polymer is an ideal feature for the formulation of solid dispersions. Additionally, other favourable characteristics that make PEGs more suitable for solid dispersions include their ability to solubilise some compounds (Betageri and Makarla, 1995) and also to improve compound wettability. Aspirin, which is a soluble drug, showed an increase in the dissolution rate when formulated as a solid dispersion in PEG 6000 (Asker and Whitworth, 1975). PEG 8000 formulation displayed enhanced dissolution rates as compared to drug alone (Perng et al., 1998). PEGs with low molecular weight are more likely to cause slightly greater toxicity as compared to those having higher molecular weight (Price, 1994).

In PEGs with molecular weights falling between the ranges of 4000–6000 Da, hygroscopy is not a problem despite the fact that they possess higher aqueous solubility and have melting points above 50 ºC. Formulation of a pharmaceutically acceptable product is difficult if a PEG having very low molecular weight is used as it may result in a product with a sticky consistency (Shah et al., 1995). PEGs with higher molecular

weight are employed to improve the process: PEG 8000 (Perng et al., 1998) and 10000 (Khan and Zhu, 1998) have been shown to increase dissolution rates of the products than the pure drug.

PEG 6000 solid dispersions were used with 14 different drugs revealing that carrier plays a vital role in the formulation of solid dispersions successfully (Dubois and Ford, 1985). Dubois and Ford showed that the carrier governs the release rate and not the properties of the drug, if the dug is found in a low drug/carrier ratio (<2% in the case of phenylbutazone, up to 15% in the case of paracetamol). Further studies suggested that there is an inverse relationship between release rate and the chain length of PEG (Ford et al., 1986). Similar results were obtained in a study for etoposide (Shah et al., 1995) and griseofulvin (Chiou and Riegelman, 1969). However, the release of glyburide PEG 4000 solid dispersion was shown to be slower than an identical solid dispersion in PEG 6000 exhibiting contradictory behavior (Betageri and Makarla, 1995). The capability of PEG 6000 to dissolve increased amounts of drug than PEG 4000 provides the best possible explanation for improved release, causing more drugs to become molecularly dispersed. Additionally, PEG 6000 promotes the dissolution of the carrier by avoiding precipitation of the drug due to its higher viscosity.

PEG molecular weight effects the release rate as is illustrated by the detailed study of phenylbutazone/PEG solid dispersions (Ford et al., 1986).When a low percentage of the drug was used (0.5-2%), the release followed the rank order 1500> 4000> 6000> 20000 at percentages of 3 and 4% the rank order was PEG 1500> 4000> 20000> 6000 and at a

5% loading the order was 20000> 4000> 1500> 6000. The authors deduced from this data that the release is dependent on the extent of the formation of a molecular dispersion, as the rank order is associated with the crystallinity of the solid dispersion. However, chloramphenicol/PEG solid dispersions displayed contradictory results, for which the rank order of release was PEG 6000> 4000> 12000> 20000 (Kassem et al., 1979). The molecular weight of the PEG did not affect the release rate in some cases. For instance, 10% dispersions of naproxen in PEG 4000, 6000 and 20000 displayed identical release rate, as was shown by Mura et al. (1999).

In addition to this, certain problems may arise in subsequent formulation of the solid dispersions into an acceptable dosage form. It becomes very difficult and impossible to manufacture a tablet dosage form if the resulting dispersion is too soft. The reason for this is that the molecular weight of the PEG used is very low or the drug has a plasticising effect on the PEG (Shah et al., 1995). PEG 8000 was selected as a carrier for this study because it has excellent solubility in aqueous medium and low melting point. PEGs show lack of toxicity and immunogenicity; favorable kinetics as well as tissue distribution in the body (Zaplisky and Harris, 1997).

1.10 Dissolution of Polymer

In order to study the dissolution behavior of polymers, different methods and techniques can be employed including differential refractometry, optical microscopy, florescence and gravimetry (Miller-Chou and Koeing, 2003).

The method of differential refractometry works on the principle that as the concentration of the polymer is increased within the solution, the refractive index changes; this is one of the older methods to study polymer dissolution. This technique is sensitive to change in concentration and hence can also be used for detecting any increase that may occur in the polymer concentration. However, there are certain drawbacks of this method as it is only applicable to high polymer concentration and cannot be used for small polymer concentration due to low sensitivity (Miller-Chou and Koeing, 2003). Additionally, it is only applicable to polymer solution alone as the addition of any other substance (drug) will affect the refractive index.

The optical microscopy method provides direct method for observing the polymer dissolution within a given solution. Therefore, it is the most practical technique to study polymer dissolution. The basic limitation is that no quantitative information can be obtained and thus to know the polymer dissolution profile is not possible.

The use of laser inferometry makes it possible to measure the dissolution rates of a polymer (Rodriguez et al., 1985). In this process monochromatic light is passed through a polymer film placed between two mirror lenses. Through the interference lines from the monochromatic light, information about the dissolution of the polymer can be obtained. The main drawback of this technique is that it can only be applied with the transparent film of polymer. In this method the dissolution profiles of the polymer cannot be obtained.

Gravimetric method can be used to follow the dissolution of a polymer. This method involves the preparation of pellets of polymer followed by performing dissolution tests with these pellets. Pellets are weighed periodically at predetermined intervals by stopping the dissolution run. The major shortcoming of this method is the involvement of compression that is required in preparing the pellets. These forces are most likely to destroy the structure of solid dispersion.

Microviscometry has been successfully applied in the polymer dissolution studies of solid dispersions using PVP (Esnaashari et al., 2005). The advantage of this technique is that samples can be taken during dissolution process (both drug and polymer concentration can be determined concurrently) and only a small sample is required. An instrument called Anton Parr microviscometer has the capability of measuring accurately viscosities as low as 0.3 mPa.S.

1.11 Mathematical models

Different mathematical techniques may be used to treat dissolution data (Shah et al., 1998). To determine and study the release mechanism of solid dispersions, the release data were fitted to the Korsemeyer–Peppas equation which is mostly used to describe drug release from polymeric systems (solid dispersions) for binary systems and when the release mechanism is not known or when more than one release mechanism is involved (Korsmeyer et al., 1983). The best fit mathematical model for binary systems ranked in the following order of Korsemeyer–Peppas > Higuchi @ first-order > Hixson-Crowell cube root law zero-order (Ahuja et al., 2007).

1.12 Stability of Solid dispersions

One of the challenges is assuring product stability during drug development in the pharmaceutical industry. Stability refers to the ability of a product to withstand any degradation in the storage time allowed. It is important that a solid dispersion should be stable throughout the shelf life of the product as is the case for any other pharmaceutical product. On storage neither should its dissolution profile nor should any physicochemical properties change.

Indomethacin PEG 6000 dispersions were used for carrying out the earliest stability studies. The dissolution profile exhibited an alteration in drug dissolution when it was stored at temperatures between 25 °C and 45 °C at 71% RH. Crystallisation of indomethacin was said to have taken place because the colour of the tablets became less yellow with time (amorphous indomethacin is yellow, crystalline indomethacin is off-white) which resulted in a decrease in the dissolution profile (Ford and Rubinstein, 1980). A slightest change such as this colour change would raise concerns for any licensed pharmaceutical product. In another study, PEG dispersions of temazepam and triamterene were assessed for their stability profile and various physicochemical parameters including dissolution profile studies were investigated as stability markers (Dordunoo et al., 1997).

In a recent paper seven drugs were studied to determine the influence of functional group on stability of the formulations. Four of the seven drugs studied consisted of carboxylic acid groups; BAY 12-9566, naproxen, ketoprofen and indomethacin, whereas, one had

hydroxyl groups (testosterone), one an amide (phenacetin) and the last consisted of a no proton donating group (progesterone). It was concluded that upon storage, the presence of interacting groups (such as carboxylic acid, hydroxyl) were stable possibly due to inhibition of reverse crystallisation by the interacting functional groups (Gupta et al., 2002).

1.13 Physicochemical properties of drugs

Table 1.1 illustrates the physicochemical properties of seven drugs used as a model drugs as solid dispersions in the current study.

Table 1.1. Physicochemical properties of the drugs used in the current study (drug bank).

Drug	Molecular Weight	Melting Point	H_2O Solubility	LogP
Paracetamol	151.163g/mol	169-170.5°C	14mg/L	0.917
Sulphamethoxazole	253.279g/mol	167°C	610mg/L	2.447
Phenacetin	179.216g/mol	134-136°C	763mg/L	1.667
Indomethacin	357.787g/mol	158°C	0.937mg/L	3.655
Chloramphenicol	323.129g/mol	150.5°C	2500mg/L	1.476
Phenylbutazone	308.374g/mol	105°C	47.5mg/L	4.214
Succinylsulphathiazole	355.38g/mole	186-188ºC	-	-

1.13.1 Paracetamol

Paracetamol is an acylated aromatic amide (Sweetman, 2002). The structure of paracetamol is shown in Figure 1.1. Paracetamol has analgesic and antipyretic properties and weak anti-inflammatory activity. Von Mering introduced it for the first time as an

antipyretic/analgesic in 1893. It has been used in home medication as an analgesic for over 30 years. Paracetamol is used in the symptomatic treatment of moderate pain and fever (Sweetman, 2004).

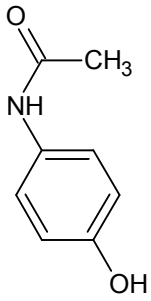

Figure1.1. Structure of Paracetamol

1.13.2 Sulphamethoxazole

Sulphamethoxazole is a sulfonamide drug. The structure of sulphamethoxazole is shown in Figure 1.2. It is a class 2 drug and it has relatively low solubility and high permeability (Sweetman, 2002). It is extensively applied in the treatment of bacterial and protozoal infections.

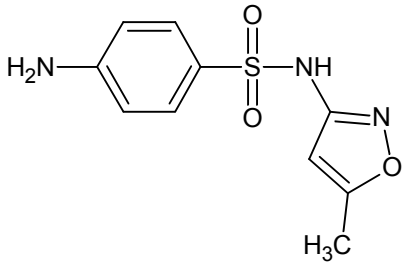

Figure 1.2. Structure of Sulphamethoxazole

1.13.3 Phenacetin

Phenacetin (structure shown in figure 1.3) was introduced for the first time in therapy in 1887. Analgesic mixtures were prepared by using phenacetin with other drug. For a long time it was employed as an analgesic and fever-reducing drug in both human and veterinary medicine.

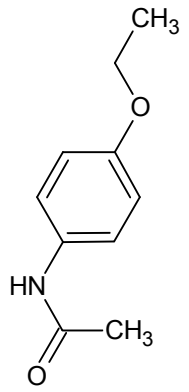

Figure 1.3. Structure of Phenacetin

1.13.4 Indomethacin

Indomethacin is poorly water soluble drug (Hancock and Parks, 2000). It is a member of the non-steroidal anti-inflammatory drugs. It is used for treating pain/swelling involved in osteoarthritis, rheumatoid arthritis and headaches (Sweetman, 2005). It is a class 2 drug (Lobenberg and Amidon, 2000). Due to its hydrophobic nature, it often demonstrates low absorption and low bioavailability; so enhancement in dissolution rate and solubility are important factors for development of drug preparations (Hirasawa et al., 2003). The structure of indomethacin is shown in Figure 1.4.

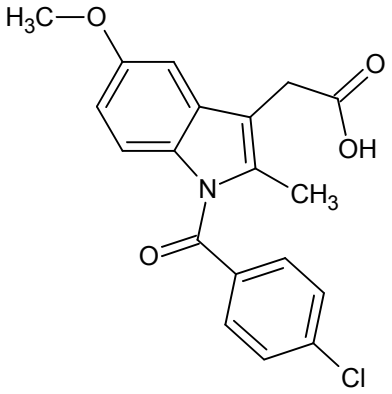

Figure 1.4 Structure of Indomethacin

1.13.5 Chloramphenicol

Chloramphenicol (structure shown in figure 1.5) is a bacteriostatic antibiotic originally derived from the bacterium Streptomyces venezuelae, isolated by David Gottlieb, and introduced into clinical practice in 1949. It was the first antibiotic to be manufactured synthetically on large scale. A vast range of microorganisms can be effectively treated by chloramphenicol; it is active against Gram positive bacteria, Gram negative bacteria and anaerobes (Ambrose, 1984; Kramer, 1984; Sweetman, 2002).

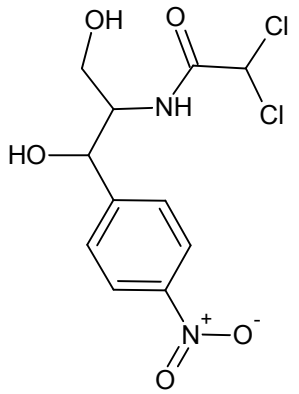

Figure 1.5. Structure of Chloramphenicol

1.13.6 Phenylbutazone

Phenylbutazone (structure shown in figure 1.6) is a non-steriodal anti-inflammatory drug used in the treatment of pain and arthritis. It is mostly used in horses as an analgesic and antipyretic.

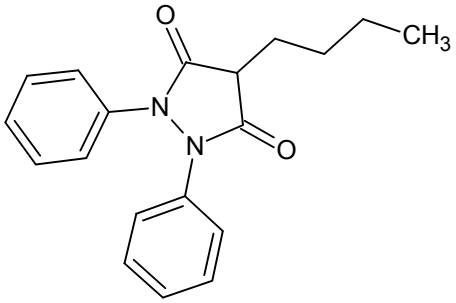

Figure 1.6. Structure of Phenylbutazone

1.13.7 Succinylsulphathiazole

Succinylsulphathiazole is useful as an intestinal antiseptic. The structure of succinylsulphathiazole is shown in figure 1.7. It has a melting point of 186-188 ºC.

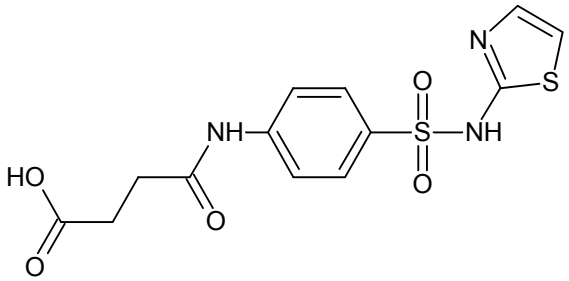

Figure 1.7. Structure of Succinylsulphathiazole

1.14 Permeability and Caco-2 cells

Permeability is the general term that explains the mechanism by which a drug moves and passes across a membrane. The physicochemical properties of a drug, such as its pH, charge, size, lipophilicity and polar surface area influence its permeability (Rowland & Tozer, 1995; Lipinski et al., 2001). The unionized molecules of the drug pass through the intestinal barrier more easily showing that the intestinal pH plays an important role in determining the permeability of the drug (Shore et al., 1957).

Among the various processes involved in the oral drug absorption, the determining factor is the drug permeability to the intestinal membrane in the absorption of the drug. The intestinal permeability of the drug can be determined by applying a variety of *in vivo, in situ* and *in vitro* methods. Along with determining the mechanism of drug absorption, the basic purpose of these studies is to predict oral drug absorption in humans. Cultured epithelial cell lines, most specifically Caco-2 cells, have drawn the focus of the pharmaceutical industry for the last decade. Assays to screen the compounds for evaluating their pharmacokinetic properties, like absorption, metabolism, etc are facing a challenge as it is highly difficult to keep pace with drug development pipeline because of the tremendously large number of compounds that are produced and analysed as potential pharmaceuticals. In vitro model membrane the Caco-2 cell monolayers have been recognised as vital for the rapid screening of the intestinal drug absorption.

Formation of the monolayers from the Caco-2 cells occurs by their spontaneous differentiation into mature cells. Caco-2 cells acquire many characteristic properties of

the absorptive intestinal cells during culture, such as microvilli, enzymes and different carrier mediated transport systems for sugars, amino acids and various drugs (Blais et al., 1987; Hidalgo et al., 1989; Hidalgo and Borchardt, 1990; Hilgers et al., 1990; Dantzig and Bergin, 1990; Chen et al., 1994), despite their origin from colon carcinoma. The transcellular and paracellular movements of drugs through the epithelial layer can be differentiated by the attachment of the adjacent cells via tight junctions formed at the apical sides of the monolayers (Tanaka et al., 1995).

There exists a strong correlation between drug permeability in Caco-2 monolayers and that of intestinal membrane *in vivo*. It has been suggested that oral drug absorption in humans can be detected by the permeability of the drug to Caco-2 monolayers. (Artursson and Karlsson, 1991; Rubas et al., 1993; Stewart et al., 1995; Chong et al., 1996; Lennernas et al., 1996; Yamashita et al., 1997). However, numerous inconsistencies have been reported by these studies that are likely to be present in the experimental conditions including change in pH, shaking rate and solubilising agents in the medium. These conditions can significantly influence the calculated permeability of tested drugs in *in vitro* studies. As the permeability of even monolayers can be affected by the cell culture conditions, it is necessary to develop stable techniques of *in vitro* transport study to have a much reliable prediction of *in vivo* drug absorption.

1.15 Scope of Solid dispersion

Griseofulvin in polyethylene glycol 8000 solid dispersion (Gris-PEG, Novartis) and a nabilone in PVP solid dispersion (Cesamet, Lilly) are the only commercial products that

have been produced commercially and marketed in the last four decades following the initial work of Sekiguchi and Obi (1961), despite the fact that a great deal of work has been done as much as almost 500 papers have been published on this subject and different drug carriers have been tested (Leuner and Dressman, 2000). Chemical or physical instability and scale-up problems are the main factors responsible for the lack in commercial turn around (Serajuddin, 1999; Franco et al., 2001; Craig, 2002).

1.16 Microarray

Microarray is the most widely used method for studying gene expression in many organisms. It has led to large-scale gene discovery and is effectively used for the expression of great number of genes at the same time. Microarray consist of chemically coated glass slides that act as a support onto which DNA segments are arranged and attached on it in a fixed regular pattern. These DNA segments are then covered with a labelled nucleic acid sample. The gene products are labelled either using a fluorescent tag or a radioactive tag, and are washed over the array after being labelled. The DNA segments present on the support hybridise with their complementary sequences of the nucleic acid in the sample. This hybridisation can be measured and analysed with the help of labelling. Laser scanner (for fluorescence) or a phosphorimager (for radioactive materials) are used for detecting hybridisation signals, producing digital images (Chen et al., 1997). Microarray technology is developing rapidly (Blohm and Guiseppi-Elie, 2001; Hughes and Shoemaker, 2001) since microarrays were first reported in the literature in 1995 (Schena et al., 1995). Microarray can also be called as DNA chips, gene chips or DNA arrays. On an array thousands of DNA spots are present and there are numerous

identical DNA molecules found in each spot of lengths varying from 25 to hundreds of nucleotides.

The three main steps that constitute the process of expression analysis include: (1) array fabrication; (2) probe preparation and hybridisation; and (3) data collection, normalisation and analysis.

To study gene expression various techniques have been employed. Microarrays consisting of either oligonucleotides or cDNA fragments are considered to be the most practical method for analysing and studying multiple samples (Schena et al., 1995; Chee et al., 1996).

Biological processes including pathway analysis of specific genes can be effectively characterised using microarrays. Highly accurate maps and sequenced databases for diverse species have made the positional cloning projects extremely easy to carry out. The availability of this extensive data has been proven to be very helpful in further study of genome function.

1.17 Microarray applications

The foremost advantage of DNA microarray technology is its versatility to study the transcript levels of expression of thousands of genes which can be measured in parallel. The high capacity of cDNA microarrays system was first shown by Schena & coworkers to examine the expression of 45 Arabidopsis genes in parallel (Schena et al., 1995). The

cDNA microarray has been observed to exhibit a number of applications in various organisms including plant (Schena, 1996), yeast (Shalon et al., 1996; DeRisi et al., 1997) and human beings. Microarray was also employed to discover novel disease-related genes and investigate complex diseases. For example, inserting human chromosome 6 could reverse the tumorigenic properties of human melanoma cell line UACC-903 as observed by DeRisi et al. (1996). Rheumatoid arthritis and inflammatory bowel disease were examined for their distinctive gene expression by Heller and coworkers (1997). It was established that microarray could be effectively used to identify disease-related genes and study the diseases. The challenge of treating chronic diseases effectively was solved to a greater extend as this method provided an opportunity for drug development and hence improving disease therapies. The function of a particular gene can be ascertained by knowing its expression pattern. A target can be implicated in any pathway or disease without any difficulty by utilising the knowledge of sequence homology to a known gene family along with the selective gene expression.

The alterations in the gene expression caused by a drug can also be detected by the DNA microarray method. It has been shown by Pietu et al. (1996) that the quantitative hybridisation of a high density cDNA array resulted in the expression of novel gene transcript in human muscle cells. The cathepsin K is a novel cysteine protease that is selectively expressed in osteoclasts. This resulted in the development of drugs to inhibit cathepsin K. The gene expression sequence of a particular disease can be detected by the simultaneous measurement of thousands of genes. Microarray technology has also been applied to study ‘‘toxicogenomics’’, investigating the different responses shown by

different individual towards a particular toxic substance due to differences in individual patterns of gene expression (Lettieri, 2006; Ferrer-Dufol and Menao-Guillen, 2009).

DNA microarray was also used to identify the target effects of secondary drugs and also in drug validation studies by Marton (1998). Its effective use in gene discovery, gene expression, and mapping are ample proof of the fact that cDNA microarray technology has developed very rapidly. The correlation of the gene sequences and clinical medicine for both human beings and animals can be obtained by it. The applications of DNA microarray are of great importance in both molecular biology research and clinical diagnostics.

1.18 Aims of the study

In order to enhance the solubility of poorly water soluble drugs, solid dispersions are carried out as it is a highly effective way of increasing the dissolution rate of a drug and thus increasing its solubility. Most drugs used in this study are poorly water soluble and belong to class 2 according to BCS. Phosphate buffer saline (PBS) is used due to its inert nature and exhibits no interaction either with the drug or polymer. PBS having pH value of 7.4 was used as it is similar to the pH condition in the small intestine. Therefore, for all solid dispersions studied the pH during dissolution studies was kept simulate to that in intestinal pH condition.

Chapter 2

Materials and Methods

2.1 Materials

Indomethacin, phenacetin, paracetamol, phenylbutazone, chloramphenicol, sulphamethoxazole, succinylsulphathiazole, phosphate buffered saline tablets, potassium bromide, rhodamine123, bromophenol blue, ethylenediaminetetraacetic acid (EDTA), agarose, ethidium bromide, sucrose, Hepes, hydroxylamine hydrochloride, phenol solution, trpsan blue, 4',6-diamidino-2-phenylindole (DAPI), albumin from bovine serum (BSA V), sodium citrate, sodium chloride, formamide, sodium carbonate and sodium bicarbonate were purchased from Sigma Aldrich, UK.

HPLC grade water, acetonitrile, methanol, glacial acetic acid, absolute ethanol, sodium dodecyl sulphate and hydrochloric acid were obtained from Fisher Scientific, UK.

Dulbecco's modified Eagle's medium (DMEM), fetal bovine serum (FBS), Non-essential amino acids (NEAA) and Hank's balanced salt solution (HBSS) were purchased from Bio Sera, UK.

1% Trypsin–EDTA, 1% pencillin-strepotomycin supplemented with 2 mM glutamine and RNase free water were provided by Gibco Lab. UK.

Poly dA (1 µg/µL) and Human Cot1 DNA were purchased from Invitrogen, UK.

Polyethylene glycol 8000 (PEG 8000) was obtained from Fluka (Biochemika), U.K.

NaOH was provided by Anala R, UK.

1 mL, 2 mL, 5 mL, 10 mL serological pipette, 50 mL centrifuge tubes, 25 cm^2,75 cm^2 cell tissue culture flasks, TC-Plate 6 well sterile with lid, 6 well cell culture plate and 0.2 μm, 0.45 μm syringe filter were provided by Appleton Woods, UK.

Staining trough with drop on lid, Staining jar and lifterslip were provided by VWR, UK.

Caco-2 cell line was purchased from American Type Culture Collection (ATCC), UK.

RNeasy Mini Kit (50) was provided by Qiagen, UK; UV cuvette (50-2000 μL) was obtained from Eppendorf, UK.

Millex-GV syringe filter and MilliPore Pronto Background reduction Kit were provided by Corning, UK.

All other reagents were of analytical grade.

2.2 Spectrophotometric Analysis

Spectrophotometric technique was used to measure and determine the concentration of sample in phosphate buffer saline solution (PBS) of pH 7.4 throughout this study. Measured amounts of the seven drugs were dissolved in PBS and the wavelength for maximum absorption was measured using a Unicam UV-Visible Spectrophotometer between 200 nm- 400 nm. Before any sample analysis was undertaken a baseline scan was obtained using a phosphate buffer saline solution so that any interference could be accounted.

For the calibrations, stock solutions of drugs were prepared at 30 μg/mL in PBS. The linearity of the calibration curve was obtained in a concentration range from 2 μg/mL to 14 μg/mL analysed by UV for indomethacin, phenacetin, paracetamol, phenylbutazone, sulphamethoxazole and succinylsulphathiazole. For chloramphenicol the calibration curve was obtained in a concentration range from 5 μg/mL to 30 μg/mL. Samples were analysed via spectrophotometry at the following wavelengths: paracetamol 240 nm, sulphamethoxazole 252 nm, phenacetin 244 nm, indomethacin 264 nm, chloramphenicol 276 nm, phenylbutazone 236 nm and succinylsulphathiazole 256 nm respectively.

2.3 Preparation of solid dispersion

Solid dispersions containing 5%, 10% and 15% (w/w) drug loading in PEG 8000 were prepared by melted fusion (Dubois and Ford, 1985). The drug and the polymer were heated until the polymer melt. The molten mixture was stirred until the drug was dissolved completely in the melt and a homogeneous solution was obtained. The solution was brought to solidification by pouring it into tablet moulds under ambient conditions.

2.4 Physical mixture

Physical mixtures were prepared by grinding drug (indomethacin, phenacetin, paracetamol, phenylbutazone, chloramphenicol, sulphamethoxazole, succinylsulphathiazole) and PEG 8000 in a mortar for around 15 mins (the percentage drug to PEG 8000 was 5%, 10% and 15% (w/w)).

2.5 Dissolution studies

The drug dissolution from solid dispersion was assessed using *in vitro* dissolution tests. The concentration of drug present in the dissolution media was measured by ultraviolet spectrophotometer at various time points (5, 10, 15, 20, 25, 30 and 60 mins). A Hanson Research apparatus (SRII 6 Flask dissolution test station) fitted with a validata control unit was used for dissolution studies. It was also equipped with 1 L round bottom flasks and baskets that conform to the Apparatus 1 standards laid out in the United States Pharmacopeia. The dissolution testing was carried out at temperature of 37 °C in 1000 mL of dissolution media (PBS), rotated at 100 rpm (Dubois and Ford, 1985). A 5 mL sample was taken at time points 5, 10, 15, 20, 25, 30 and 60 mins and was replaced with fresh 5 mL dissolution media (all experiments were performed in triplicate). All the readings were blanked with the same media as was used in the dissolution study. The absorbance at the measured value for the wavelength of the specific drug was measured by ultraviolet spectrophotometer and the percentage of drug released was calculated using calibration curves. Mathematical modeling for transport mechanism was carried out on GraphPad Prism, version 4 by plotting the fraction of drug released versus time which was fitted to a power function to determine the values of diffusional coefficient n and release constant k.

A sample absorbance reading from the dissolution study in phosphate buffer solution pH 7.4 was found to be 0.783 (figure 3.18) for 10 mins data point of the dispersion containing the paracetamol and PEG 8000. This is converted into a concentration in µg/L using a conversion factor taken from the line of best fit produced using the "LINEST" function in Microsoft Office Excel 2003 from a calibration curve. The

calibration curve including the value produced by the LINEST equation is shown in figure 3.10 and it was found to be 0.0071x-0.015. It therefore follows that:

0.783+0.015 = 0.798 µg/L

0.798/0.071 = 11.239 µg/L

When found that the concentration of paracetamol was11.239 µg/L. As this value was taken after 10 mins of dissolution study, 10 mL of dissolution media had been removed. It therefore follows that:

11.239 * (1000-10)/1

11.127 mg/L

So, 11.127 mg of paracetamol had dissolved after 10 mins of dissolution study from paracetamol solid dispersion. The original weight of paracetamol that was loaded into the dispersion prior to the dissolution study was 25.75 mg.

11.127 * 100/25.75

43.21% of the paracetamol released from solid dispersion after 10 mins of dissolution.

2.6 Microviscometry analysis

Microviscometry was used to measure the dissolution of PEG 8000 from drug-PEG 8000 solid dispersions. The samples were measured on an Anton-Parr AMVn (Austria) version 1.612047 microviscometer, equipped with the visionlab software.

The Anton-Paar AMVn microviscometer in this method uses Stokes law to determine viscosity by measuring time taken for a rolling ball over a fixed distance through the liquid. The following conditions were used for each run sample:

- Temperature 25 °C
- AMVn measuring programme Standard 50 x 4
- AMVn measuring system 15084989

PEG 8000 was dissolved in PBS over the concentration range 2 mg/mL to 10 mg/mL to prepare a calibration. The dissolution of PEG 8000 from the drug polymer mixed systems was measured using microviscometry (Esnaashari et al., 2005) for all samples at all time intervals. All the measurements were done in triplicate.

A sample viscosity reading from the dissolution study in phosphate buffer solution pH 7.4 was found to be 0.9640 for 5 mins data point of one of the dispersion containing indomethacin and PEG 8000. The calibration curve showing the value produced from straight line is shown in figure 3.17 and it was found to be 0.0225x+0.9553. It therefore follows that: 0.9640-0.9553/0.0225, 0.387 * 1000, 387 mg/L. After finding that the concentration of PEG 8000 was 387 mg/L from indomethacin solid dispersion, the original weight of PEG 8000 loaded into the dispersion prior to the dissolution study was 489.25 mg.

387 * 100/489.25

79.10% of PEG 8000 released.

Fraction released of both drug and polymer was calculated from percentage released.

2.7 Differential scanning calorimetry (DSC)

DSC data were obtained using a Perkin-Elmer Diamond DSC with a thermal analyser, equipped with Pyris software. Each sample (2-5 mg) was weighed into a non-hermetically sealed DSC sample pan (Perkin-Elmer) which was then crimped and placed on to the sample furnace. An empty pan was also crimped and this was placed on to the reference furnace.

The following method and conditions were used for each run (Normal DSC):

- Purge gas Nitrogen
- Heating rate 10 °C/min
- Temperature range 0 °C to 300 °C

On completion of a temperature scan, analysis was performed using the Pyris software. The melting points of each peak were derived by measuring the onset temperature.

2.8 Hyper DSC

Hyper DSC is the use of heating rates in excess of 100 °C/min and as much as 500 °C/min, where normal DSC has a range of about 1 °C/min to 20 °C/min. This provides a number of advantages, the most important of which is that hyper DSC can be used to prevent recrystallisation during a fast heating (Pijpers et al., 2002).

Hyper DSC data were obtained using a Perkin-Elmer Diamond DSC with a thermal analyser, equipped with Pyris software. The sample mass was accurately weighed into

a non-hermetically sealed DSC sample pan. This was crimped and placed on the sample furnace. An empty pan was crimped and placed on the reference furnace.

The following method and conditions were used for each run (Hyper DSC):

- Purge gas Helium
- Heating rate 500 °C/min
- Temperature range 0 °C to 300 °C

On completion of a temperature scan, analysis was performed using the Pyris software. The melting points of each peak were derived by measuring the onset temperature. All the measurements were performed in triplicate.

2.9 Infrared spectroscopy (FTIR)

Fourier transform infrared spectroscopy (FTIR) spectra were obtained using FTIR spectrometer Pye Unicam Ltd Cambridge England. The samples were ground and mixed thoroughly with potassium bromide, at 1:100 (sample: potassium bromide) weight ratio. The potassium bromide discs were prepared by compressing the powders at a pressure of 5 tons for 5 mins in a hydraulic press. Scans were obtained at a resolution of 4 cm^{-1}, from 4000 to 400 cm^{-1} at scan rate of 16. All studies were performed in triplicate.

2.10 Scanning electron microscopy (SEM)

Scanning electron microscopy (SEM) is a technique that determines the surface visualisation of substances to size as small as 1 μm. It is used to examine surface

characteristics such as roughness. SEM data were obtained by using a scanning electron microscope, Stereoscan 90 Cambridge, UK. Sample powders were fixed on an aluminum stub using double-sided adhesive carbon tape and coated in vacuum (4 Psi) with a double gold layer in order to make them conductive using Emscope Sputter (SC 500) for 360 s at 10 mA. The samples were then loaded into the SEM to obtain scanning electron micrographs of the sample.

2.11 Thermogravimetric analysis (TGA)

Thermogravimetric analysis (TGA) is a technique used to measure changes in the mass of a sample as a function of temperature or time. It is performed by loading a known weight sample on to a mass pan. The sample then undergoes a heating step at a constant rate and the resultant mass change is plotted against temperature or time.

Thermogravimetric analysis was performed using a Perkin Elmer, (Pyris TGA) instrument with ThermoGravimetric Analyser. A pan base was loaded onto the mass stirrup of the TGA and tared. The pan base was then loaded with known weight of sample evenly spread. This was then transferred onto the TGA and the TGA furnace was raised. A typical heating run consisted of heating the sample from 30 °C to 150 °C at a rate 20 °C/min (Weuts et al., 2004). The average mass loss was calculated for each sample. All the studies were done in triplicate.

2.12 Isothermal titration calorimetry (ITC)

Isothermal titration calorimetry (ITC) was used to detect small heat changes during reaction. ITC measurements were performed on a VP-ITC ultra sensitive titration calorimeter, MicroCal, LLC, Northampton, MA. ITC experiments were carried out at

25 °C. All solutions were thoroughly degassed before use by stirring under vacuum (Thermovac Microcal) for 15 min at 23 °C. All titrations were performed with a 250 μL injection syringe and a stir rate of 307 rpm. Experiments were performed at 25 °C±1°C. A 25 mM phosphate buffer, pH 7.4, was used to prepare all solutions and used for calorimetric experiments. Each binding system was studied in duplicate. The sample cell (volume 1.4413 mL) was loaded with 0.250 mM drug solution and sample syringe was loaded with 2.5 mM PEG 8000. Injections were started after baseline stability had been achieved. The titration of PEG 8000 with drug solution involved 25 consecutive injections, the first being 2 μL, and the remaining ones of 10 μL. In all cases, each injection was done in 20 s at 240 s intervals.

Control experiments were done in which identical aliquots were injected into the buffer solution. The data were collected automatically and subsequently fitted to a one-site binding model by the Origin 7.0 software package supplied by the manufacturer (MicroCal). The enthalpy change for each injection was calculated by integrating the area under the peaks of the recorded time and then corrected with the control titrations. The first injection was not taken into consideration for data analysis. After subtracting the heat of dilution, a non-linear least-squares algorithm along with the concentrations of the titrant and the sample were used to fit the heat flow per injection to an equilibrium binding equation, providing best fit for the values of stoichiometry (N), the change in enthalpy (ΔH), and the binding constant (K). The change in free energy (ΔG) and the change in entropy (ΔS) for the binding reaction were calculated by the fundamental equations of thermodynamics.

2.13 Solubility

For solubility studies excess amount of solid dispersion, physical mixture and drug alone were added in glass tube containing phosphate buffer saline, and stirred for 24 hrs at room temperature. The solutions were filtered through 0.45 μm filter paper (Whatman), diluted, and analysed by UV Spectrophotometer at the corresponding wavelengths for each drug. The experiments were carried out in triplicate.

2.14 Drug content determination

60 mg of solid dispersion was accurately weighed and dissolved in 100 mL of PBS and filtered. Sample (1 mL) was diluted with PBS up to 20 mL and absorbance was measured with a UV spectrophotometer at respective drugs wavelength. The drugs content was calculated using the calibration curve ($R^2 = 0.9999$).

2.15 Stability Studies

Stability testing was carried out to determine the quality of formulation under the influence of temperature and humidity over time. The representative samples of solid dispersions were placed in a controlled temperature and humidity cabinet **(**Firlabo, 6100). An accelerated term stability study was conducted according to the International Conference on Harmonization (ICH), stability protocol, 40°C±2°C/75%RH±5% RH. In order to study the stability of the solid dispersions, the representative samples of solid dispersions were sealed in aluminum foil and stored at room temperature conditions (silica gel to control moisture content) and in a controlled temperature cabinet at 40 °C (75% RH) (silica gel to control moisture content). The physicochemical properties of these dispersions were evaluated after 0,

3 and 6 months for accelerated and 0, 3 and 12 months for samples stored under ambient conditions.

2.16 Culture media composition

- Dulbecco's modified eagle medium (DMEM) 500 mL
- 10% heat inactivated fetal bovine serum 50 mL
- 1% pencillin-strepotomycin supplemented with 2 mM glutamine 5 mL
- 1% non essential amino acid 5 mL

2.17 Procedure for Caco-2 cell culture

Caco-2 cells with passage 70 were obtained from American Type Culture Collection (ATCC) and used at passages 90-100. Cells were grown to 90% confluences in 75 cm^2 T-flasks with DMEM supplemented with 10% FBS, 1% pencillin-strepotomycin supplemented with 2 mM glutamine and 1% NEAA. Culture medium was changed every second day and cells were grown at a temperature of 37 °C and 5% CO_2. For the transport assay, cells were seeded on top of 6 well transwell culture plate inserts (24 mm, 4.7 cm^2) at a density of 2 x 10^5 cells/cm^2. Transwell inserts were used by first adding medium to the 6 well plate, then adding the transwell insert, followed by the addition of the medium and cells to the inside compartment of the transwell insert. Recommended 6 transwell permeable medium volume is 2.6 mL for plate well and 1.5 mL for inside of transwell. An initial equilibrium period was used to improve cell attachment by adding medium to the 6 well plate well and then to the transwell insert. The plate was then incubated for at least 1 h. The cells were then added to fresh medium in the transwell insert and returned to the incubator. The level was checked periodically and fresh medium added as required. The culture medium was replaced

every 24-48 hrs. Transepithelial electrical resistance (TEER) was measured at the start and end of every study.

2.18 Cell quantification

From the cell suspension, 200 µL was removed and mixed with 200 µL of tryptan blue. Using the haemocytomer, cell viability and the cell counts were determined. To each side of the cover slip placed on the haemocytomer, 10 µL of tryptan blue cell suspension was added and viewed microscopically. The viable cells (bright cells) were counted and from this cell concentration was calculated.

$$\text{Average cell per square} = \frac{1+2+3+4+5+6+7+8+9+10}{10}$$

Cells per mL = Average cells per square x dilution factor (2) x $10^{4.}$

2.19 Drug transport studies

Caco-2 monolayers were used 21–25 days after seeding. Apical to basolateral permeability of drug and the solid dispersion was assessed. After 1 h of pre-incubation with drug-free transport medium (Hanks balanced salt solution), the medium containing the drug and the solid dispersion was introduced to the apical side (1.80 mL). To determine the initial concentration (Co), a sample of 300 µL was taken from the apical side (1.5 mL remaining at the apical side). Sample aliquots (300 µL) were taken from the basolateral side at given time intervals (0, 5, 10, 15, 20, 25, 30 and 60 mins). After each sampling, an equal volume of fresh transport buffer (37 °C) was added to the receiver compartment (basal side) and kept the cells at a temperature of 37 °C and 5% CO_2 during experiment. Samples were subsequently analysed by

HPLC. All experiments were performed at 37 °C (n = 3). Apparent permeability Papp (cm/s) was calculated according to the equation 2.1:

$$Papp = dQ/dt \times 1/ACo \quad \rightarrow (2.1)$$

where dQ/dt is the rate of appearance of the drugs on the basolateral side (μg/sec), Co is the initial concentration on the apical side (μg/cm^3) and A is the surface area of the monolayer (cm^2).

After finding that the concentration of indomethacin from solid dispersion was 4.84 μg after 5 mins during permeability study using Caco-2 cells. Apparent permeability coefficient was calculated using equation 2.1.

Whereas

dQ/dt =4.84/5*60 (μg/sec) is the flux across the basolateral side.

A = 4.7 (cm^2) is the area of diffusion.

Co = 750 (μg/cm^3) is the initial concentration of drug in donor compartment.

Papp= dQ/dt x 1/ACo

Papp= (4.84/5*60)/4.7*750

Papp= 4.58 x 10^{-6}.

The permeability coefficients (Papp) were calculated for each time points (5, 10, 15, 20, 25, 30 and 60 mins) and determined the mean value of Papp for each drug and solid dispersion as shown in table 6.3.

2.20 Caco-2 cell uptake studies

Rhodamine123 was used for Caco-2 cell uptake studies.

2.20.1 Preparation of 4% paraformaldehyde in PBS

Two PBS tablets were dissolved in 200 mL distilled water (2X stronger PBS solution). 4 g of paraformaldehyde was added to 50 mL double distilled water and heated to 60 °C. 1 M NaOH (14 drops) was added slowly until the solution was clear and allowed to cool. This was followed by the addition of 50 mL of paraformaldehyde to 50 mL of 2X PBS and stored in a plastic bottle.

2.20.2 Uptake of rhodamine 123 across the Caco-2

Caco-2 cells were maintained in DMEM supplemented with 1% non-essential amino acids, 10% fetal bovine serum, and 1% penicillin streptomycin glutamine in 5% CO_2 atmosphere at 37 °C. The Caco-2 cells were sub-cultured twice during the experimental time period. The cell viability was periodically examined using Trypan blue exclusion assay. After incubation for 60 mins at 37 °C, Hanks balanced salt solution (HBSS) in transwell inserts was removed and plates were washed with PBS.

2.20.3 Fixation and Staining of Caco-2 cells

The cells were fixed with 4% paraformaldehyde at room temperature for 10 mins. They were then washed in PBS, incubated for 5 mins at room temperature with 2 μg/mL DAPI to stain nuclei and washed again in PBS.

2.20.4 Caco-2 uptake of rhodamine123 studied by fluorescence spectroscopy

Individual transwell membrane was mounted on clean glass slides with Vectasheild. The slides were viewed with a Zeiss AXIOCAM (AXIOSKOP WEST GERMANY) for the uptake and distribution. Fluorescence images were obtained at 40X magnifications.

2.21 Drug recovery

The recovery is defined as the amount recovered in the apical and basolateral compartment at the end of the experiment and is expressed as a percentage of the amount added to the donor side at time zero (equation 2.2):

Recovery = (CR, 60 mins × VR + CD, 60 mins × VD)/CD, 0 min × VD × 100 → (2.2)

with CR, 60 mins and CD, 60 mins the concentration measured after 60 mins in the receiver and donor compartment, respectively, CD,0 min the concentration of the test compound in the donor compartment at time zero and VR and VD the volumes buffer added in receiver and donor compartment, respectively.

2.22 HPLC analysis (transport studies) and statistical analysis of data

The HPLC studies were performed using a Dionex 1100 HPLC system with autosampler (AS50), gradient pump (GP50), detector (UVD170U) and a C18 analytical column with a particle size of 5 µm (Phenomenex ODS 3 Column, 4.6 µm × 150 mm). The mobile phase consisted of acetonitrile (50%): double distilled water (50%): 1 mL (per liter of mobile phase) of acetic acid for indomethacin, phenacetin

and phenylbutazone. Indomethacin, phenacetin and phenylbutazone were detected at a wavelength of 264 nm, 244 nm, and 236 nm at a flow rate of 1 mL/min. The mobile phase consisted of acetonitrile (10%): double distilled water (90%) for paracetamol and was detected at a wavelength of 240 nm, at a flow rate of 1 mL/min. The injection volume was maintained at 20 µL. Student's unpaired *t*-test with $P<0.05$ was considered as significant. Statistical significance was calculated by GraphPad prism software.

2.23 Microarrays

The samples (PEG 8000, drugs alone and solid dispersions treated Caco-2 cells and untreated Caco-2 cells) were collected at various time points for transcriptomics directly into a mixture of phenol (5%) and ethanol (95%) in the ratio of 1:5 of phenol-ethanol and sample. The samples were incubated on ice and then pelleted by centrifugation at 5000 rpm at 4 °C for 10 mins and the pellets were stored at -80 °C until RNA extraction. Total RNA was extracted from the bacterial pellets by using an RNeasy kit (QIAGEN) and reverse transcribed and fluorescently labelled with Cy3 and Cy5 dye by using a CyScribe indirect postlabelling kit (GE-healthcare). All the controls and test samples were labelled with Cy3 and Cy5 dyes and single channel hybridisation was carried out.

Prior to hybridisation slides were treated with sodium borohydride from Pronto background reduction kit (Corning) followed by prehybridisation of slides for a minimum of 2 hrs in (20x SSC, 0.1% SDS, BSA 0.1%). For each experiment 80 pmol of Cy3 and Cy5-labelled cDNA was added to a final volume of 80 µL of hybridisation solution containing 30% formamide, 20× SSC, 0.1% SDS, Human Cot1 DNA and

Poly dA (1 ug/uL). The cDNA probes were denatured at 95 °C for 5 mins, centrifuged for 2 mins at full speed and hybridised for 16 hrs at 42 °C. Slides were then washed at 42 °C with 2× SSC-0.1% SDS for 15 mins and at room temperature with 0.2× SSC and twice with 0.05× SSC for 15 mins using Advawash slide washing machine. Slides were dried by low speed centrifugation at 1500 rpm at 25 °C for 10 mins and scanned by using Perkin Elmer Scanarray scanner. The signal intensity of each spot in the microarray was quantified by using scanarray software.

Quantile normalisation, hierarchical clustering, PCA and significant analysis of microaarays (SAM) were performed using TMEV (Saeed et al., 2003) TM4: a free, open-source system for microarray data management and analysis.

2.24 Agarose Gel Electrophoresis

2.24.1 Gel preparation and gel running conditions

Tribase (242 g) and EDTA (18.6 g) were dissolved in 600 mL distilled water. Glacial acetic acid (57.1 mL) was then added and made volume to 1000 mL with distilled water (50x TAE gel buffer). Agarose (1g) was dissolved in 100 mL (1x) TAE gel buffer by heating for 2 mins and allowed it to cool. Then ethidium bromide (4 µL) was added and allowed to set for 60 mins in the gel tray.

The loading dye was prepared by dissolving bromophenol blue (25 mg) and sucrose (4 g) in HPLC grade water (10 mL). Then RNA sample was prepared for gel electrophoresis by mixing of RNA (1 µL), loading dye (2 µL) and RNase free water (7 µL). The sample was run at 80 V for 30 mins in 1x TAE gel running buffer.

Chapter 3

Dissolution Studies

3.1 Introduction

"Dissolution is defined as the process by which a known amount of drug substance goes into solution per unit of time under standardised conditions". The dissolution of drug from a solid dispersion is dependent on the underlying solubility of the polymers (Craig, 2002). This is partially due to the mechanism whereby polymers dissolve due to the diffusion of solvent into the polymer matrix which results in the polymer altering from glassy to the rubbery state. This helps chain disentanglement which results in dissolution (Miller-Chou and Koenig, 2003). The general objectives of the dissolution studies are:

1. Optimisation of therapeutic effectiveness during product development.
2. Assessment of production quality.
3. Prediction of *in vivo* availability.

In order to investigate the dissolution behavior of polymers various methods can be employed; these include differential refractometry, optical microscopy, microviscometry, fluorescence and gravimetry (Miller-Chou and Koeing, 2003). However, microviscometry has been successfully used for the dissolution studies of PVP from a solid dispersion (Esnaashari et al., 2005). When polymer dissolves into solution, the viscosity of solution increases and microviscometry is capable of differentiating the viscosity between low polymer concentration solutions. The benefits of using this method are such that samples can be taken during dissolution run (both drug and polymer concentration can be determined concurrently) and only a small sample (1 mL) is required.

Although a lot of work has been done on the release mechanism, the enhancement of drug release rate is not yet fully explained (Craig, 2002). The release process is complex and different factors such as the properties of drug (solubility) (Sjokvist-Sears and Craig, 1992), physical state (Horter and Dressman, 2001), particle size (Sjokvist-Sears and Nystrom, 1988), dissolution of the polymer (Corrigan, 1985), molecular weight (Craig and Newton, 1992) and the possible drug polymer interaction (Bogdanova et al., 2005) can affect the release process. Craig (2002) presented a drug release model distinguishing between carrier-controlled and drug-controlled dissolution, depending on the solubility of drug in the concentrated polymer layer (Craig, 2002). The model helps to describe the correct way to control the drug release rate from solid dispersions. In dispersions having low drug content, there are two methods for controlling the drug release: carrier-controlled dissolution and drug-controlled dissolution. In the former the dissolution of carrier controls the dissolution of drug while in the later, the physical properties of the drug itself seems to affect the rate of dissolution (Craig, 2002). The first step for both mechanisms involves the formation of a carrier rich dissolving surface. The drug has to pass through this surface so that it can be released into the bulk phase. The next phase involves the dissolution of the drug into the carrier diffusion layer, and then the drug is released into the bulk medium. The second phase is vital in stating which mechanism will follow. Craig (2002) proposed that in case of carrier-controlled dissolution the drug dissolves in the carrier very quickly, causing the drug to disperse molecularly within the diffusion layer. The viscosity of the dissolving surface is sufficient to cause the diffusion of drug through this layer to be very gradual. Therefore, the dissolution of the polymer is the controlling factor in the release of drug. While in drug-controlled dissolution, particles dissolves slowly into diffusion layer,

so are released as solid particles into the bulk medium. Therefore, the properties of the drug such as the particle size and physical form are vital in the drug-controlled dissolution mechanism. There are other descriptions that provide possible explanations for which mechanism can be used for dispersions with high carrier content. As previously discussed that carrier can improve the wetting of drug, it is therefore, obvious that the carrier by improving wetting enables the drug to dissolve quickly into the diffusion layer, in turn causing carrier-controlled diffusion to occur (Chiou and Reigelman, 1971).

In the current study, the *in vitro* drug release data were fitted to Korsemeyer–Peppas model

$Mt/M\sim = Kt^n$ → (equation 3.1)

Where Mt/M~ is the fraction of drug released at time t, κ is the apparent release rate constant that incorporates the structural and geometric characteristics of the drug delivery system and n is the diffusional exponent which characterises the transport mechanism of the drug.

3.2 Aims of the study

The aim of this study was to investigate the effect of PEG 8000 on the drug dissolution profiles. Drug with different polymer concentration in the solid dispersion was studied for their effect on dissolution result. Drug release mechanism was studied based on dissolution of polymer and drug.

3.3 Results and Discussion

3.3.1 UV Analysis of drugs

The optimum absorbance wavelength was measured using Unicam UV-Visible Spectrophotometer. A scan over the range 200-500 nm was performed for each drug and the peak absorbance taken as the λmax for each drug. In some cases the run was only over the range 200-300 nm if the λmax value was within this range.

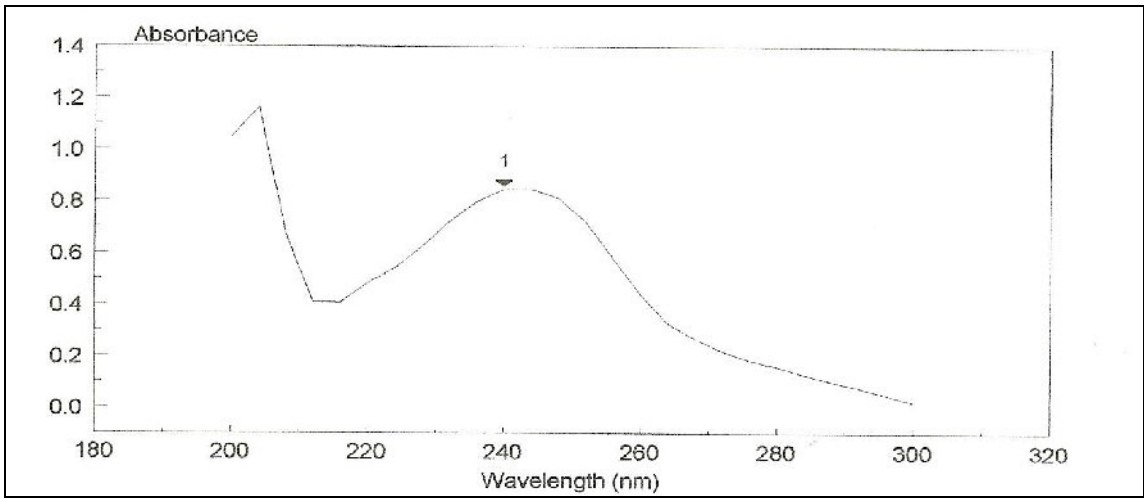

Figure 3.1. UV scan of paracetamol in phosphate buffer saline by Unicam UV, λmax = 240 nm.

The λmax values were; paracetamol 240 nm; sulphamethoxazole 252 nm; phenacetin 244 nm; indomethacin 264 nm; chloramphenicol 276 nm; phenylbutazone 236 nm and succinylsulphathiazole 256 nm in phosphate buffer saline.

Controls of phosphate buffer saline and PEG 8000 in phosphate buffer saline were under identical conditions to the drugs and no UV absorbance was noted for either solution. Figures 3.1-3.9 shows the scanning of paracetamol, sulphamethoxazole, phenylbutazone,

phenacetin, indomethacin, chloramphenicol, succinylsulphathiazole, phosphate buffer saline and PEG 8000.

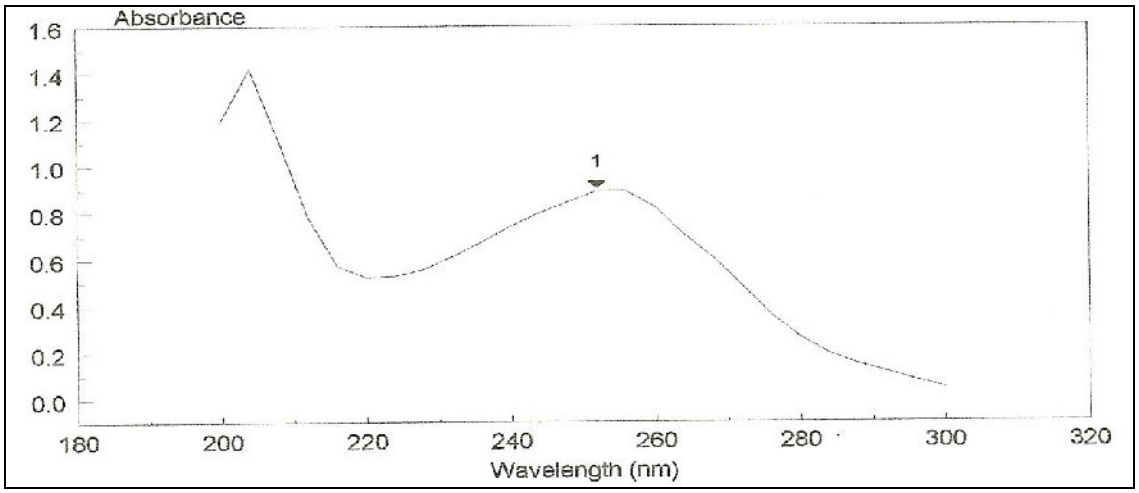

Figure 3.2. UV scan of sulphamethoxazole in phosphate buffer saline by Unicam UV, λmax = 252 nm.

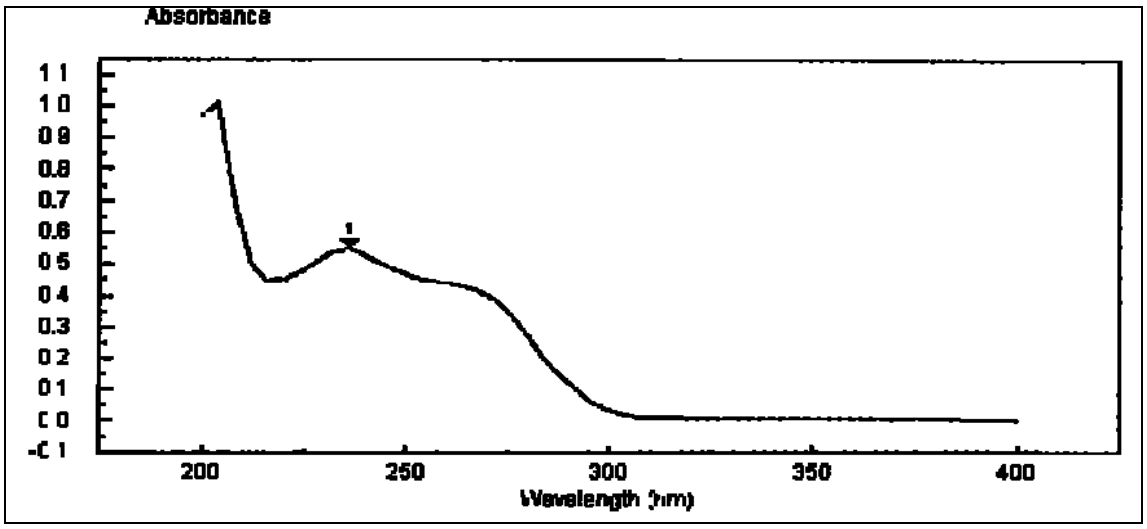

Figure 3.3. UV scan of phenylbutazone in phosphate buffer saline by Unicam UV, λmax = 236 nm.

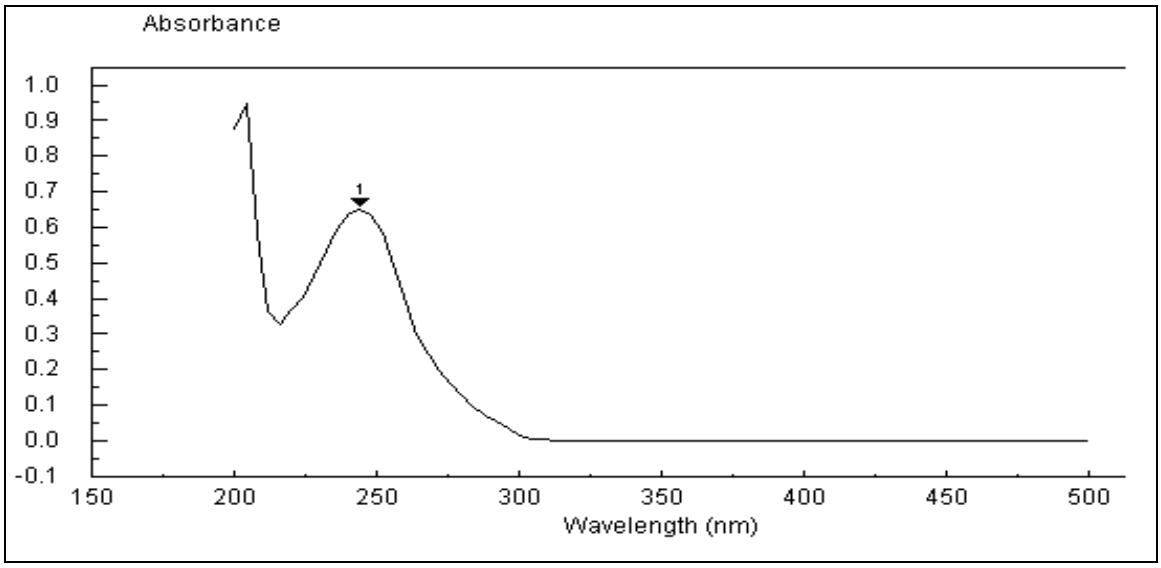

Figure 3.4. UV scan of phenacetin in phosphate buffer saline by Unicam UV λmax = 244 nm.

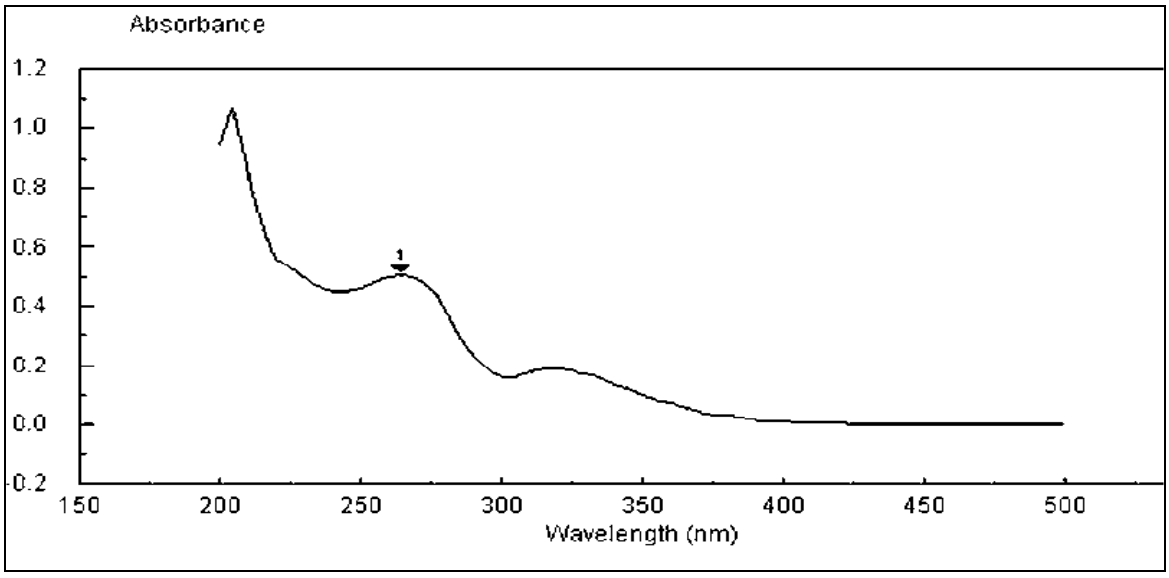

Figure 3.5. Scan of indomethacin in phosphate buffer saline by Unicam UV, λmax = 264 nm.

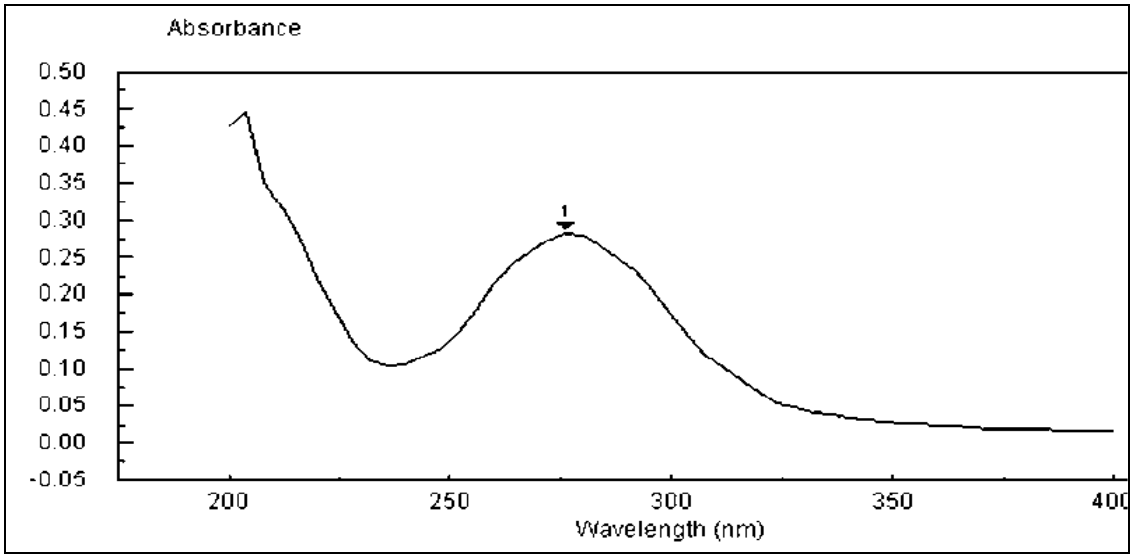

Figure 3.6. UV scan of chlroamphenicol in phosphate buffer saline by Unicam UV, λmax = 276 nm.

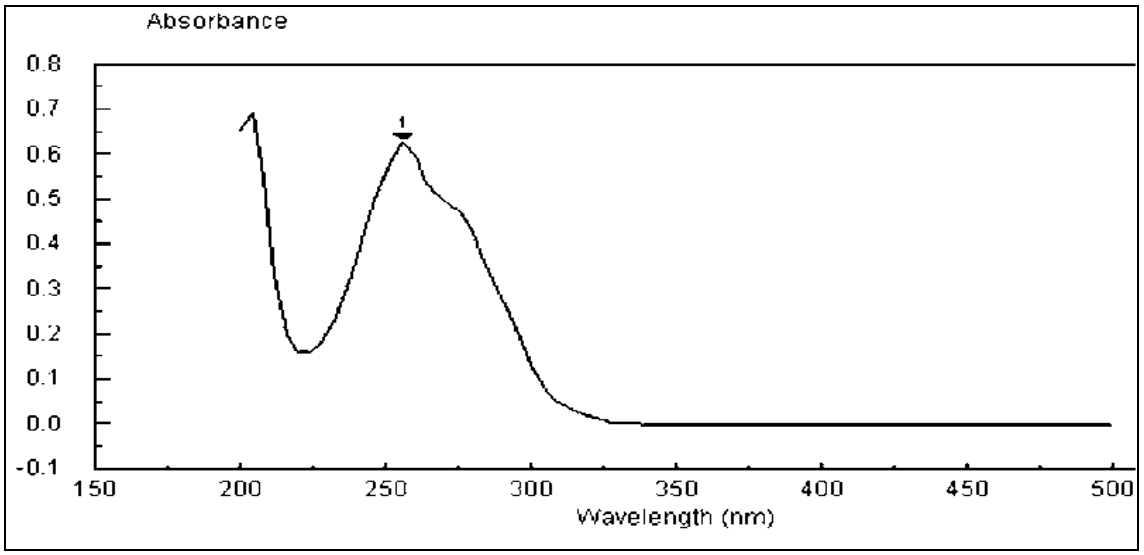

Figure 3.7. UV scan of succinylsulphathiazole in phosphate buffer saline by Unicam UV, λmax = 256 nm.

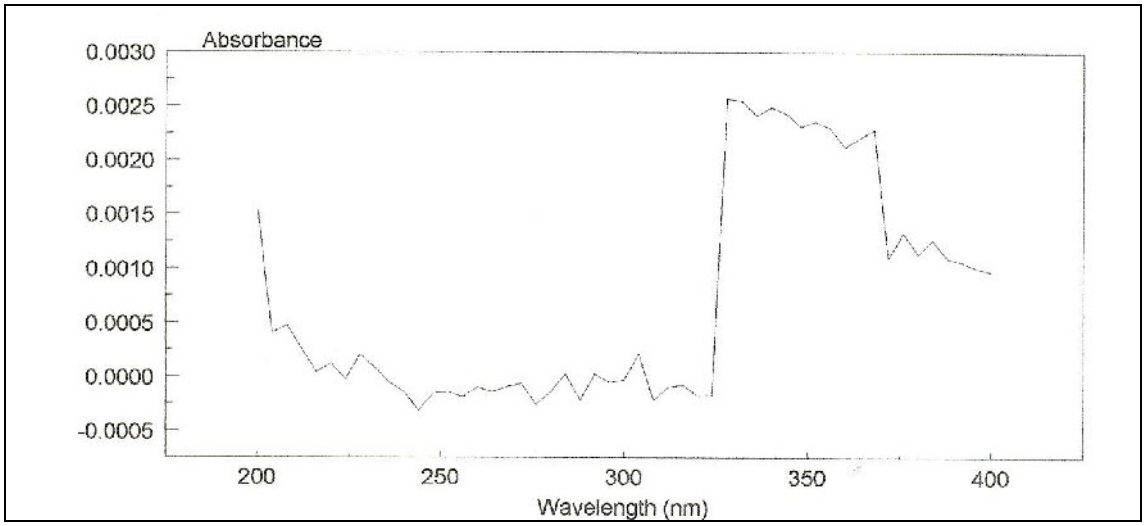

Figure 3.8. UV scan of Phosphate buffer saline blank by Unicam UV.

Figure 3.8 shows that there is no UV absorption in the range relevant to the drug absorption (240-276 nm), therefore there is no interference caused by the presence of phosphate buffer saline. Figure 3.9 highlights that there is no UV absorbance by PEG 8000 in the region of interest for the drugs (240-276 nm).

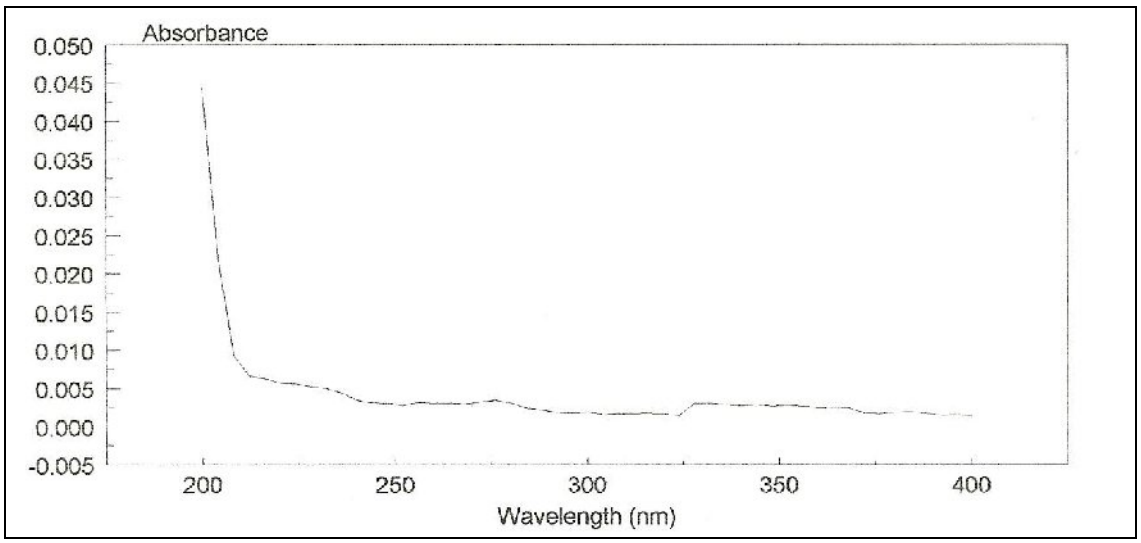

Figure 3.9. UV scan of polyethylene glycol 8000 (50 µg/mL) in phosphate buffer saline by Unicam UV.

3.3.2 Calibrations of drugs via UV and polymer via microviscometry

3.3.2.1 Calibration curve of paracetamol

For the calibration, stock solution of paracetamol was prepared at 30 µg/mL in phosphate buffer saline (pH 7.4). The linearity of the calibration curve (Coefficient of Determination R^2 = 0.99) was obtained in a concentration range from 2 µg/mL to 14 µg/mL by Unicam UV-Visible Spectrophotometer at 240 nm as shown in figure 3.10.

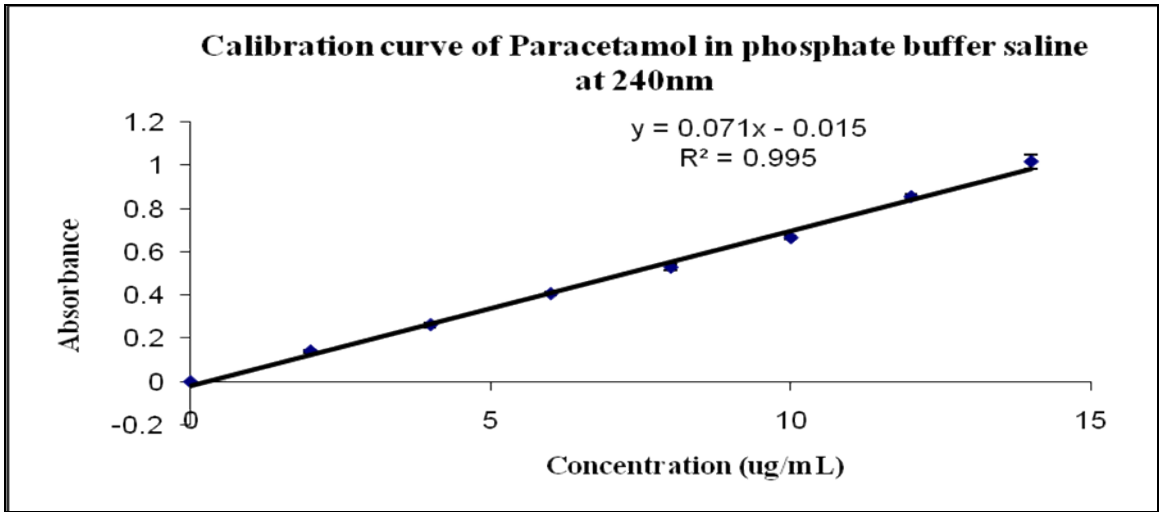

Figure 3.10. Calibration curve of paracetamol in phosphate buffer saline at 240 nm by UV. Data are expressed as mean±S.D (*n* = 3).

3.3.2.2 Calibration curve of sulphamethoxazole

For the calibration, stock solution of sulphamethoxazole was prepared at 30 µg/mL in phosphate buffer saline (pH 7.4). The linearity of the calibration curve (Coefficient of Determination R^2=0.99) was obtained in a concentration range from 2 µg/mL to 14 µg/mL by Unicam UV-Visible Spectrophotometer at 252 nm as shown in figure 3.11.

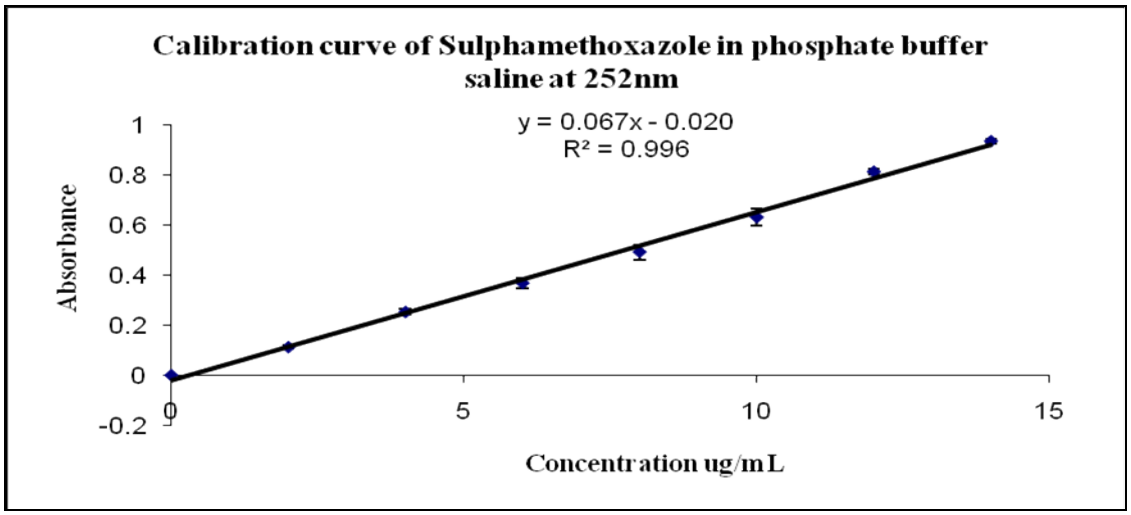

Figure 3.11. Calibration curve of sulphamethoxazole in phosphate buffer saline at 252 nm by UV. Data are expressed as mean±S.D(*n* = 3).

3.3.2.3 Calibration curve of phenacetin

For the calibration, stock solution of phenacetin was prepared at 30 µg/mL in phosphate buffer saline (pH 7.4). The linearity of the calibration curve (Coefficient of Determination R^2=0.99) was obtained in a concentration range from 2 µg/mL to 14 µg/mL by Unicam UV-Visible Spectrophotometer at 244 nm as shown in figure 3.12.

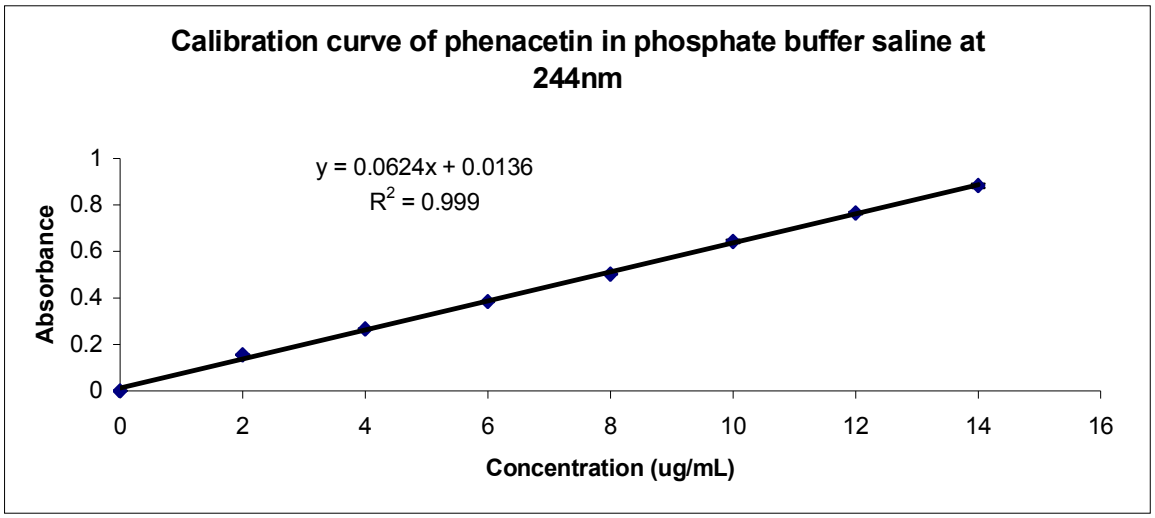

Figure 3.12. Calibration curve of phenacetin in phosphate buffer saline at 244 nm by UV. Data are expressed as mean ± S.D(*n* = 3).

3.3.2.4 Calibration curve of indomethacin

Figure 3.13 shows the calibration curve of indomethacin by UV in phosphate buffer saline (pH 7.4) at 264 nm. Stock solution of indomethacin was prepared at 30 µg/mL in phosphate buffer saline (pH 7.4). A calibration range of 2–14 µg/mL was established with good linearity over the entire working range (Coefficient of Determination R^2=0.99).

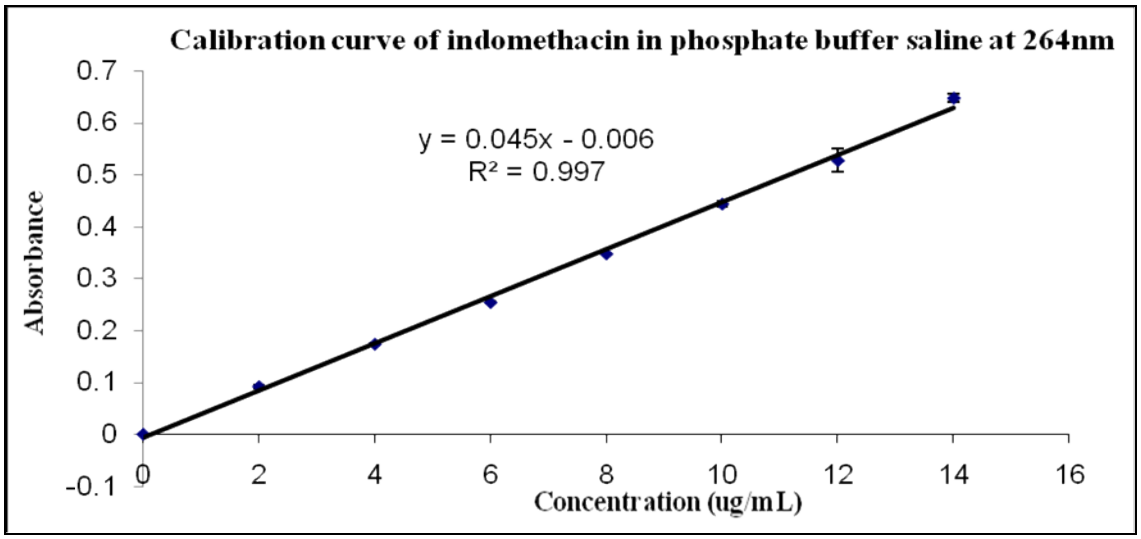

Figure 3.13. Calibration curve of indomethacin in phosphate buffer saline at 264 nm by UV. Data are expressed as mean±S.D(*n* = 3).

3.3.2.5 Calibration curve of chloramphenicol

Figure 3.14 shows the calibration curve of chloramphenicol by UV in phosphate buffer saline (PBS) (pH 7.4) at 276 nm. A calibration range of 5–30 µg/mL was established with good linearity over the entire working range (Coefficient of Determination R^2=0.99).

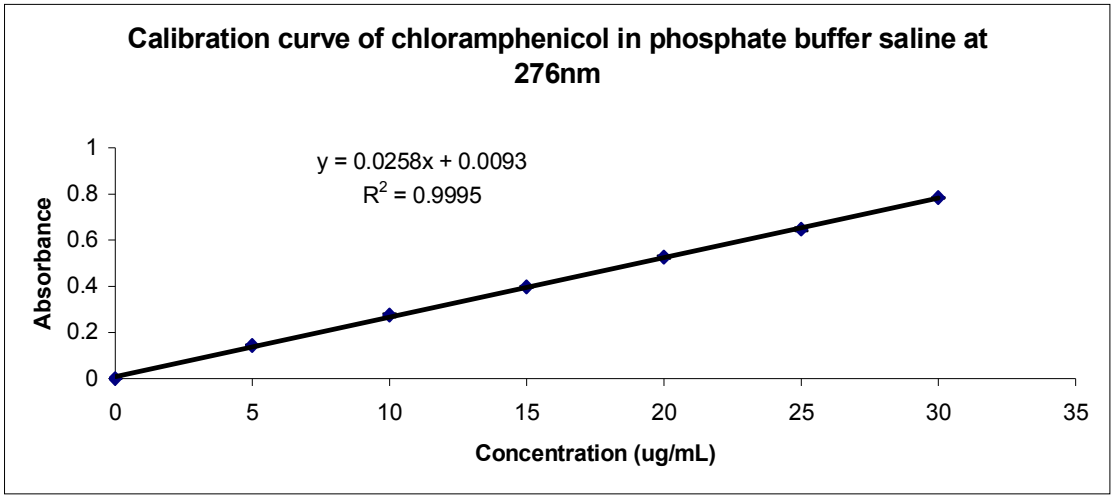

Figure 3.14. Calibration curve of chloramphenicol in phosphate buffer saline at 276 nm by UV. Data are expressed as mean±S.D (*n* = 3).

3.3.2.6 Calibration curve of phenylbutazone

For the calibration, stock solution of phenylbutazone was prepared at 30 µg/mL in phosphate buffer saline (pH 7.4). The linearity of the calibration curve (Coefficient of Determination R^2=0.99) was obtained in a concentration range from 2 µg/mL to 14 µg/mL by Unicam UV-Visible Spectrophotometer at 236 nm as shown in figure 3.15.

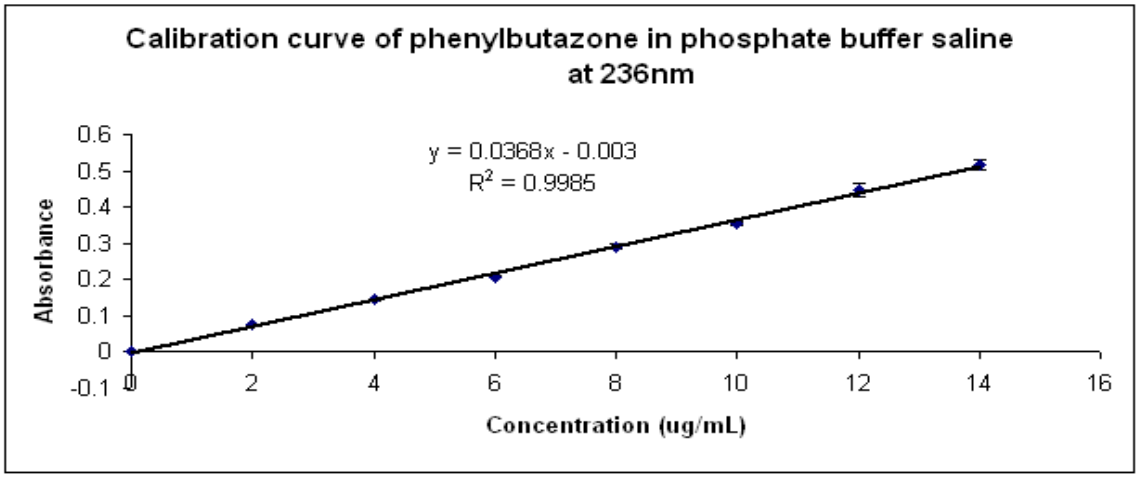

Figure 3.15. Calibration curve of phenylbutazone in phosphate buffer saline at 236 nm by UV Data are expressed as mean±S.D(*n* = 3).

3.3.2.7 Calibration curve of succinylsulphathiazole

For the calibration, stock solution of succinylsulphathiazole was prepared at 30 µg/mL in phosphate buffer saline (pH 7.4). The linearity of the calibration curve (Coefficient of Determination R^2=0.99) was obtained in a concentration range from 2 µg/mL to 14 µg/mL by Unicam UV-Visible Spectrophotometer at 256 nm as shown in figure 3.16.

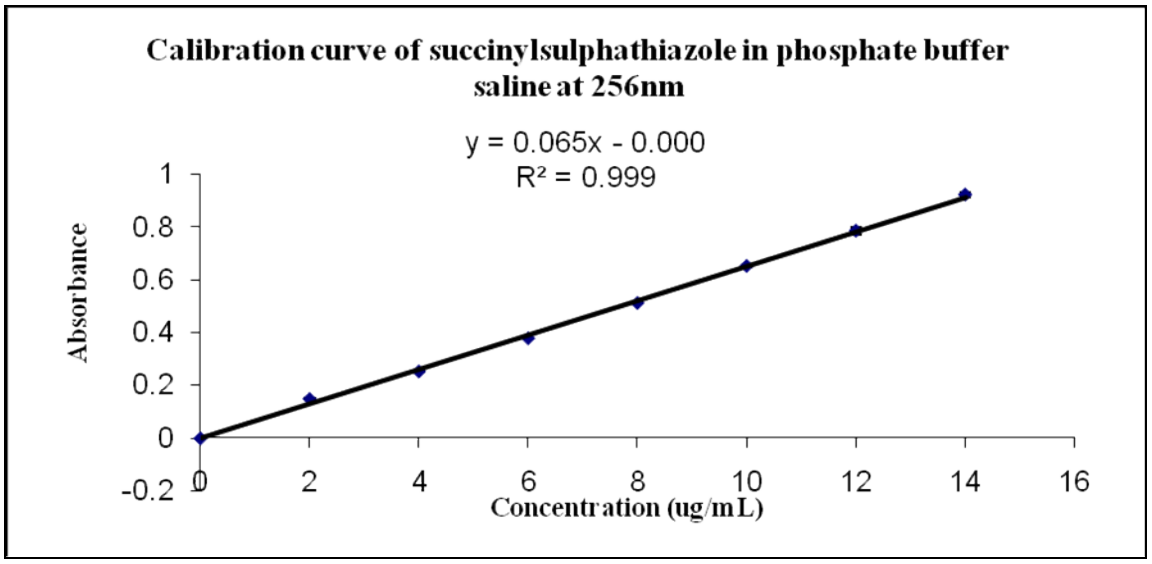

Figure 3.16. Calibration curve of succinylsulphathiazole in phosphate buffer saline at 256 nm by UV. Data are expressed as mean±S.D(*n* = 3).

3.3.2.8 Calibration curve of PEG 8000

For the calibration of PEG 8000, stock solution of polymer was prepared at 30 mg/mL in phosphate buffer saline (pH 7.4). The linearity of the calibration curve (Coefficient of Determination R^2=0.99) was obtained in a concentration range from 2 mg/mL to 10 mg/mL by microviscometry (Esnaashari et al., 2005) as shown in figure 3.17.

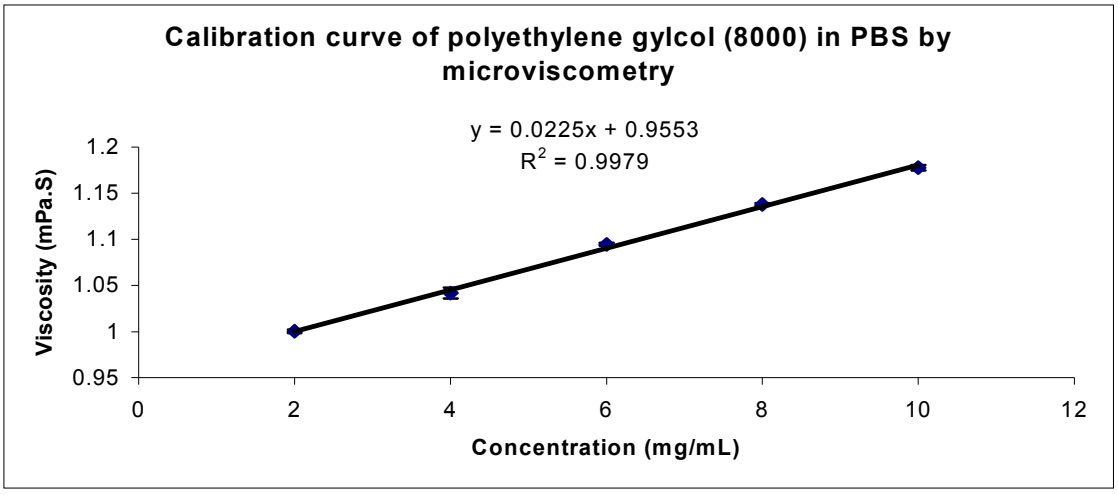

Figure 3.17. Calibration curve of polyethylene gylcol (8000) in phosphate buffer saline by microviscometer. Data are expressed as mean±S.D(*n* = 4).

3.3.3 Drug release studies

3.3.3.1 Dissolution studies of paracetamol

The dissolution profiles of paracetamol from the solid dispersions with 5%, 10% and 15% (w/w) are shown in figure 3.18. The release patterns showed fast dissolution during the first 30 mins. In formulations with weight ratio of PEG 8000, the drug release rate was not affected by the content of PEG 8000, as such in case of 5% (w/w) and 10% (w/w) since they produced a very similar release profile. However, in case of 15% (w/w) showed

decrease of the dissolution rate as compared to lower PEG 8000 concentration. The paracetamol release from the solid dispersion (SD) as compared to the pure drug and physical mixture (PM) are shown in figure 3.19. It was seen that the pure drug crystals showed a slower dissolution as compared to solid dispersion and physical mixture. The paracetamol release was 91% from solid dispersion; 43% from physical mixure and 34% from drug alone after 60 mins.

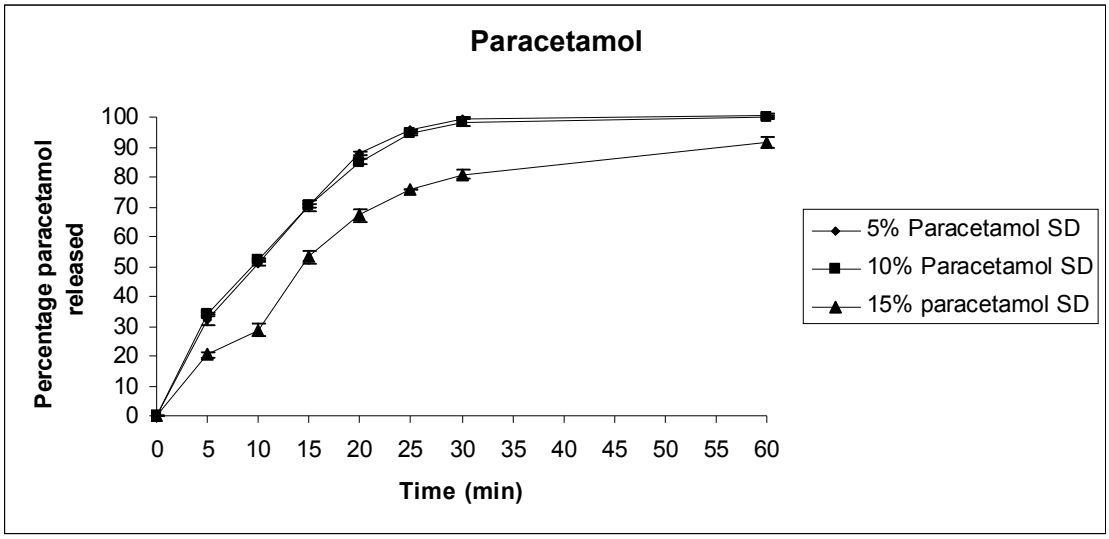

Figure 3.18. Percentage released of paracetamol from solid dispersions; 5%, 10% and 15% (w/w) corresponds to the amount of paracetamol in solid dispersions. Data are expressed as mean±S.D(*n* = 3).

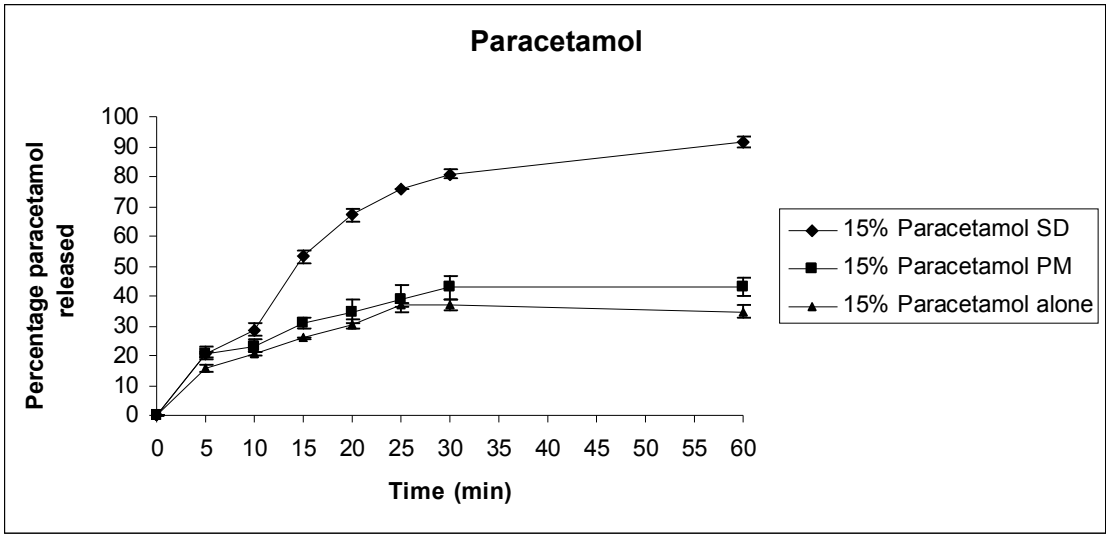

Figure 3.19. Percentage released of paracetamol from solid dispersions, physical mix and drug alone (15% w/w) corresponds to the amount of paracetamol in solid dispersions, physical mix and alone. Data are expressed as mean±S.D(*n* = 3).

3.3.3.2 Dissolution studies of sulphamethoxazole

The release profiles of sulphamethoxazole for 5%, 10% and 15% (w/w) solid dispersions are shown in figure 3.20. The rate and extent of sulphamethoxazole released was faster in 5% (w/w) solid dispersion as compared to 10% and 15% (w/w). The drug released from 5% (w/w) solid dispersion was 100% in 60 mins as compared to 10% and 15% (w/w) solid dispersion (in case of 10% (w/w) drug release was 84% and for 15% (w/w) drug release was 83% after 60 mins. Solid dispersions in PEG 8000 exhibited faster dissolution rates than drug alone and their corresponding physical mixture as shown in figure 3.21. Sulphamethoxazole alone gave the slowest initial dissolution rate with only about 30% of the drug dissolved in 60 mins as compared to solid dispersion and physical mixture. (Drug released was 83% from solid dispersion and 40% from physical mix).

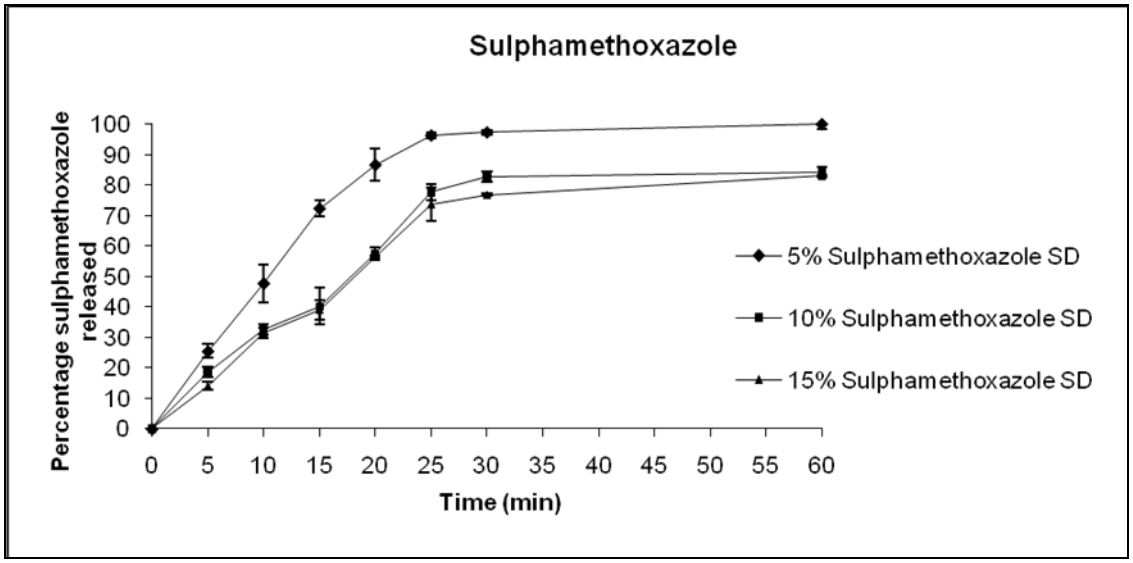

Figure 3.20. Percentage released of sulphamethoxazole from solid dispersions; 5%, 10% and 15% (w/w) corresponds to the amount of sulphamethoxazole in solid dispersions. Data are expressed as mean±S.D(*n* = 3).

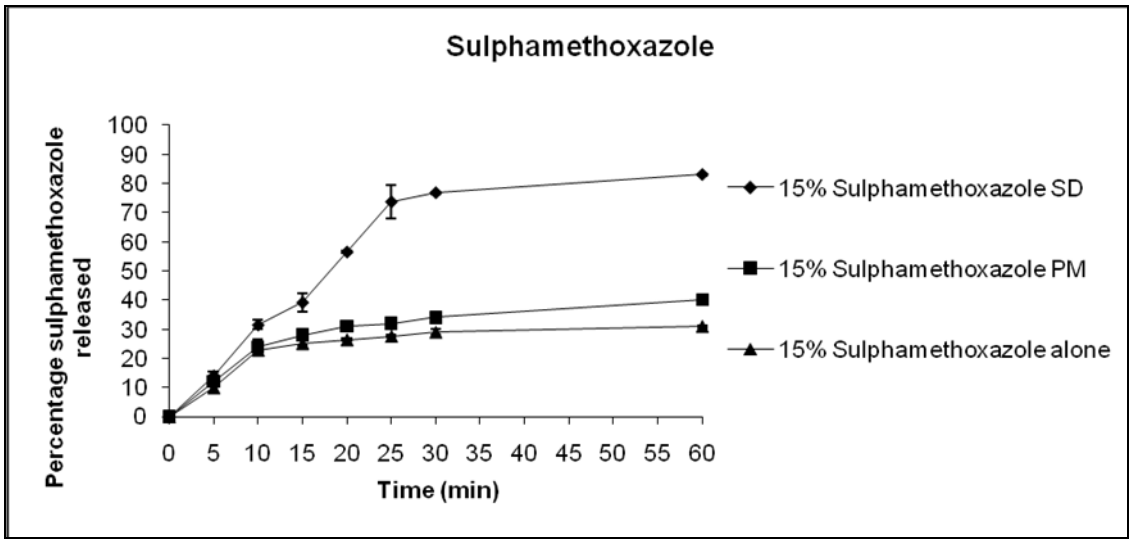

Figure 3.21. Percentage released of sulphamethoxazole from solid dispersions, physical mix and drug alone (15% w/w) corresponds to the amount of sulphamethoxazole in solid dispersions, physical mix and drug alone. Data are expressed as mean±S.D(*n* = 3).

3.3.3.3 Dissolution studies of phenacetin

The 5% (w/w) solid dispersion displayed the best performance, as compared to 10% (w/w) and 15% (w/w) solid dispersions as shown in figure 3.22. Almost 100% drug released

within 30 mins from 5% (w/w) solid dispersion as compared to 10% (w/w) formulation with drug release was 46% after 60 mins. Drug released from 15% (w/w) solid dispersion was 29% over the entire length of time period during dissolution studies. Increasing the concentration of drug in the dispersions leads to a decrease in dissolution rate and release profile. Figure 3.23 indicates that phenacetin released faster in solid dispersion followed by physical mixture and then drug alone over the entire length of time period. But interesting results for first two time points were noticed; drug release was same from solid dispersion, physical mix and drug alone of about 3-4%.

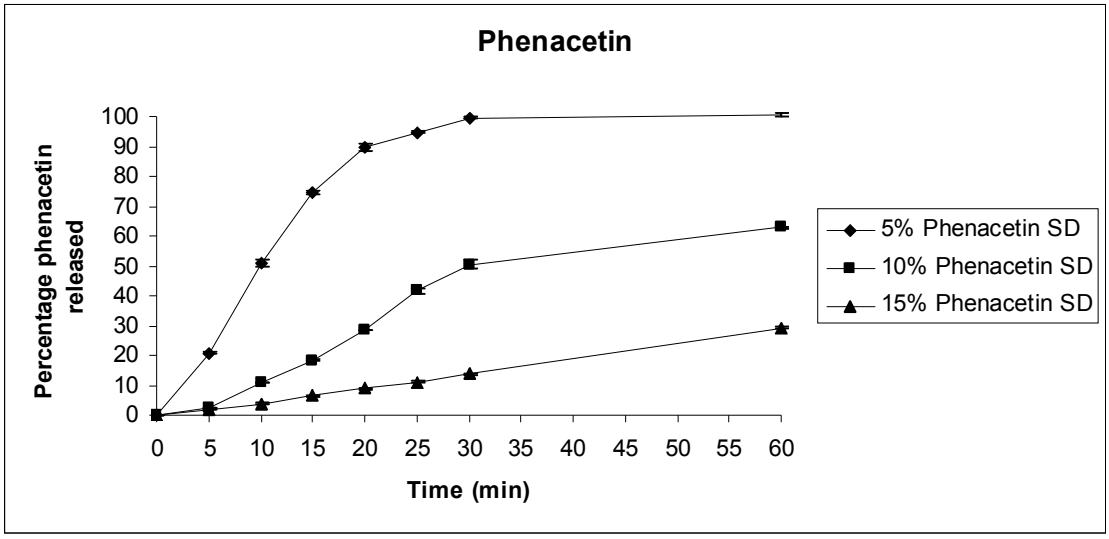

Figure 3.22. Percentage released of phenacetin from solid dispersions; 5%, 10% and 15% (w/w) corresponds to the amount of phenacetin in solid dispersions. Data are expressed as mean±S.D(*n* = 3).

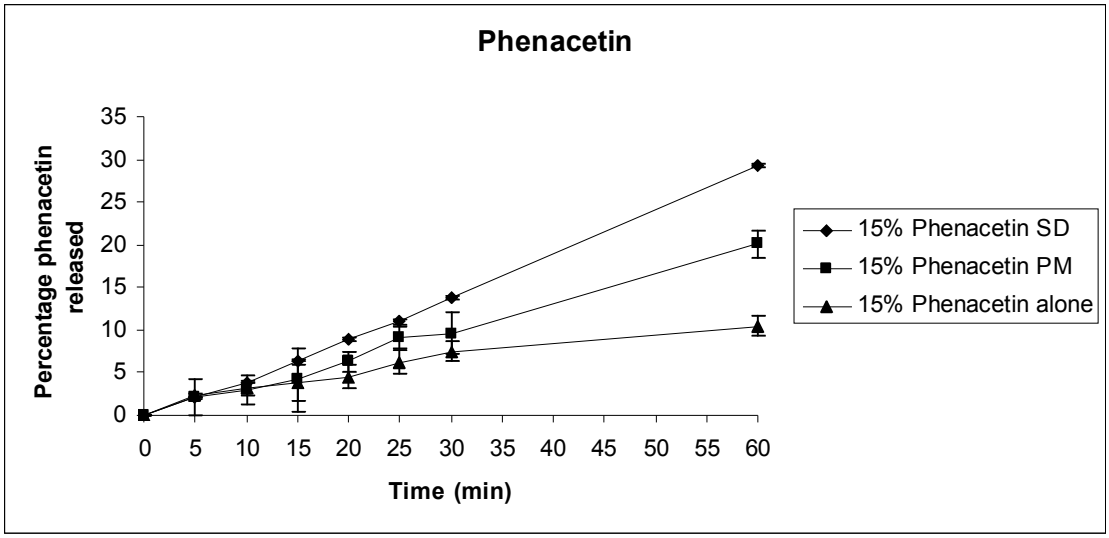

Figure 3.23. Percentage released of phenacetin from solid dispersions, physical mix and drug alone (15% w/w) corresponds to the amount of phenacetin in solid dispersions, physical mix and drug alone. Data are expressed as mean±S.D(*n* = 3).

3.3.3.4 Dissolution studies of indomethacin

Figure 3.24 shows the percentage released of 5%, 10% and 15% (w/w) solid dispersions of indomethacin with PEG 8000 during dissolution studies. The drug release was slower from the dispersions containing high drug content as compared to low drug content formulations. The release profile was not linear over the entire length of time period during dissolution studies. The drug released was almost 100% with 5% (w/w) indomethacin within 30 mins as compared to 10% (w/w) which was 65%. In case of 15% (w/w) solid dispersions the amount of drug released was 45% within 30 mins. Increasing the concentration of PEG 8000 showed faster release of indomethacin from solid dispersions as shown in figure 3.24. As the amount of PEG 8000 increased, a significant increase in the rate and extent of drug released was observed. The release profile of indomethacin from solid dispersion, physical mixture and drug alone of same concentrations are indicated in figure 3.25. The rate and extent of drug release was more from solid dispersion than physical mix and least with drug

alone. In case of solid dispersion the release profile was linear for the first 15 mins and maximum release was observed during 30 mins (45% released). The drug released was 25% for physical mix and 16% for drug alone over the entire length of time period.

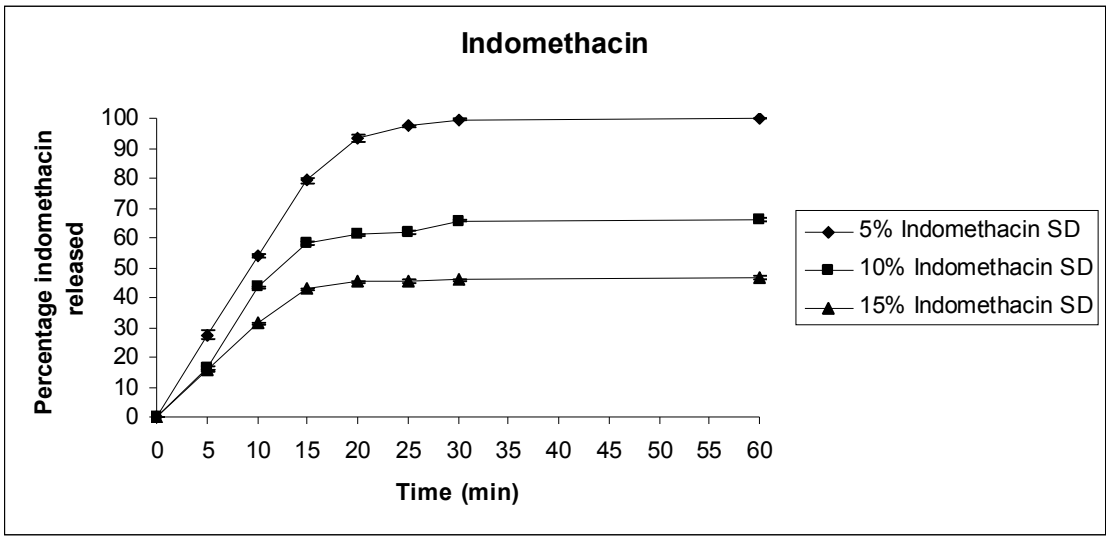

Figure 3.24. Percentage released of indomethacin from solid dispersions; 5%, 10% and 15% (w/w) corresponds to the amount of indomethacin in solid dispersions. Data are expressed as mean±S.D(*n* = 3).

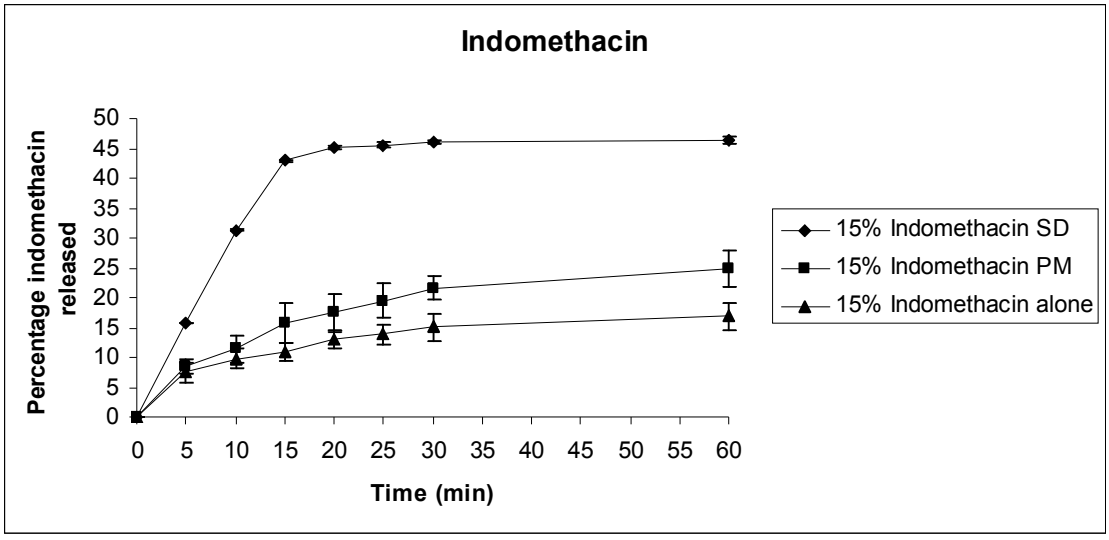

Figure 3.25. Percentage released of indomethacin from solid dispersions, physical mix and drug alone (15% w/w) corresponds to the amount of indomethacin in solid dispersions, physical mix and drug alone. Data are expressed as mean±S.D(*n* = 3).

3.3.3.5 Dissolution studies of chloramphenicol

The dissolution profiles of chloramphenicol from the solid dispersions with 5%, 10% and 15% (w/w) are shown in figure 3.26. The rate and extent of chloramphenicol released was faster in 5% (w/w) solid dispersion as compared to 10% (w/w) and 15% (w/w). The drug released from 5% (w/w) solid dispersion was 100% as compared to 10% and 15% (w/w) solid dispersion over the entire length of time period (in case of 10% (w/w) drug release was 62% and for 15% (w/w) formulation drug release was 45%. Solid dispersions in PEG 8000 exhibited faster dissolution rates than drug alone and their corresponding physical mixture as shown in figure 3.27. It was seen that the pure drug crystals showed a slower dissolution as compared to solid dispersion and physical mixture. Chloramphenicol release was 45% from solid dispersion; 15% from physical mix and 13% from drug alone over the entire length of time period. The release profiles for physical mixture and drug alone looked similar with 15% and 13% drug release during dissolution studies.

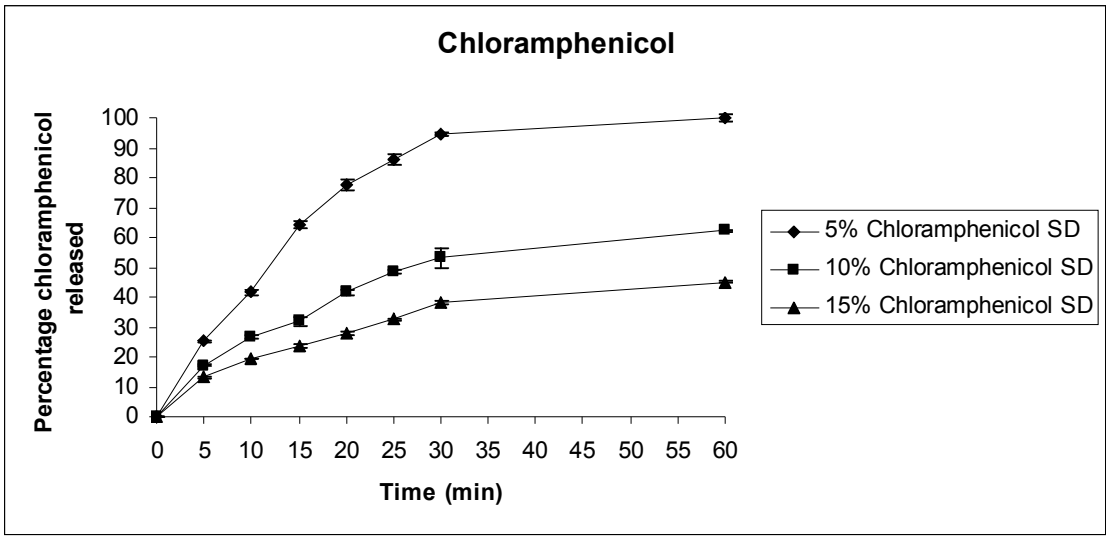

Figure 3.26. Percentage released of chloramphenicol from solid dispersions; 5%, 10% and 15% (w/w) corresponds to the amount of chloramphenicol in solid dispersions. Data are expressed as mean±S.D(*n* = 3).

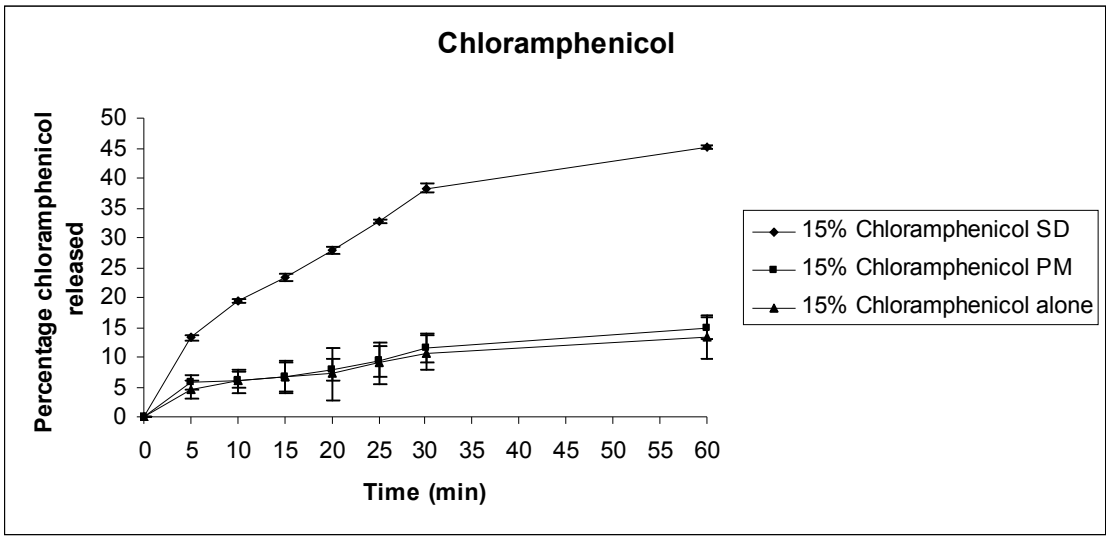

Figure 3.27. Percentage released of chloramphenicol from solid dispersions, physical mix and drug alone (15% w/w) corresponds to the amount of chloramphenicol in solid dispersions, physical mix and drug alone. Data are expressed as mean±S.D(*n* = 3).

3.3.3.6 Dissolution studies of phenylbutazone

The release profiles of phenylbutazone for 5%, 10% and 15% (w/w) solid dispersions are shown in figure 3.28. The rate and extent of phenylbutazone released was faster in 5% (w/w) solid dispersion as compared to 10% and 15% (w/w). The drug released from 5% (w/w) solid dispersion was 100% as compared to 10% and 15% (w/w) solid dispersion over the entire length of time period (in case of 10% (w/w) drug release was 84% and for 15% (w/w) drug release was 73%). Solid dispersions in PEG 8000 showed faster dissolution rates than drug alone and their corresponding physical mixture as shown in figure 3.29. Phenylbutazone alone gave the slowest release with only about 10% of the drug dissolved as compared to solid dispersion and physical mix (drug released was 73% from solid dispersion and 36% from physical mix) over the entire length of time period during dissolution studies. However, similar result as phenacetin for first two time points was

observed; drug release was same from solid dispersion, physical mix and drug alone as shown in figure 3.29 (drug release was 4%).

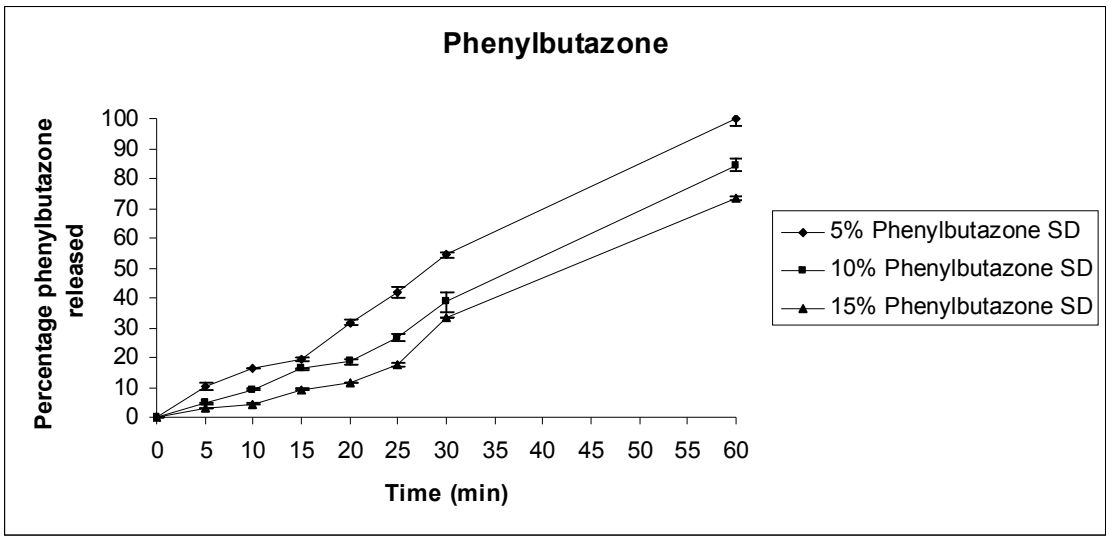

Figure 3.28. Percentage released of phenylbutazone from solid dispersions; 5%, 10% and 15% (w/w) corresponds to the amount of phenylbutazone in solid dispersions. Data are expressed as mean±S.D(*n* = 3).

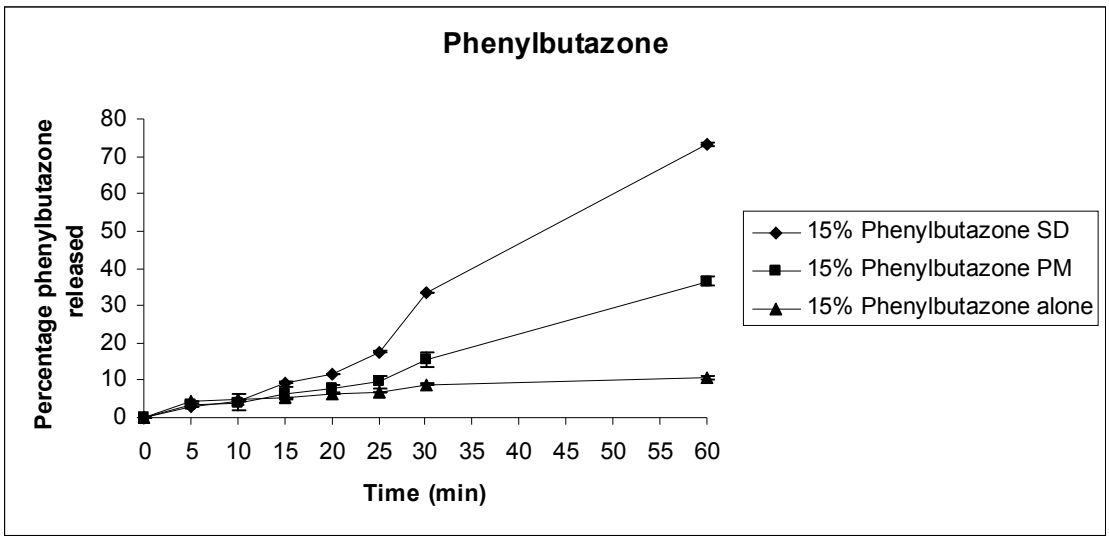

Figure 3.29. Percentage released of phenylbutazone from solid dispersions, physical mix and drug alone (15% w/w) corresponds to the amount of phenylbutazone in solid dispersions, physical mix and drug alone. Data are expressed as mean±S.D(*n* = 3).

3.3.3.7 Dissolution studies of succinylsulphathiazole

Figure 3.30 shows that the percentage of succinylsulphathiazole released over time was fastest for 5% (w/w) loadings compared to 10% and 15% (w/w) loaded solid dispersions. The drug released was almost 100% with 5% (w/w) solid dispersion after 25 mins as compared to 10% (w/w) and 15% (w/w) dispersions. The drug released from 10% (w/w) solid dispersion was 69% and 15% (w/w) solid dispersion was 48% over the entire length of time period. The release profiles of succinylsulphathiazole from solid dispersion, physical mixture and drug alone of same concentrations are shown in figure 3.31. The rate and extent of drug release was more from solid dispersion than physical mixture and least with drug alone. The drug released was 48% for solid dispersion, 26% for physical mixture and 15% for drug alone over the entire length of time period during dissolution studies.

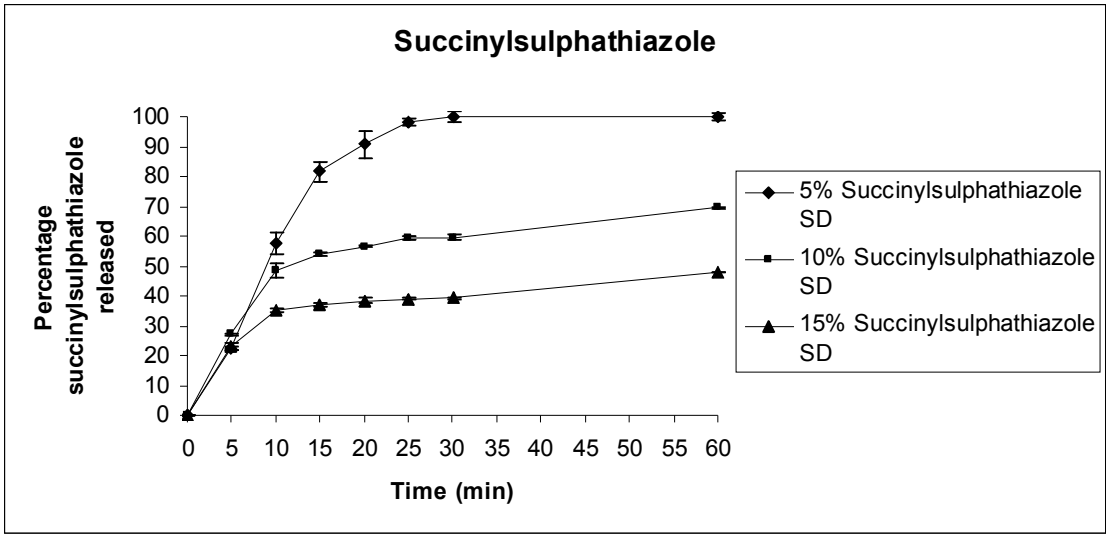

Figure 3.30. Percentage released of succinylsulphathiazole from solid dispersions; 5%, 10% and 15% (w/w) corresponds to the amount of succinylsulphathiazole in solid dispersions. Data are expressed as mean±S.D(*n* = 3).

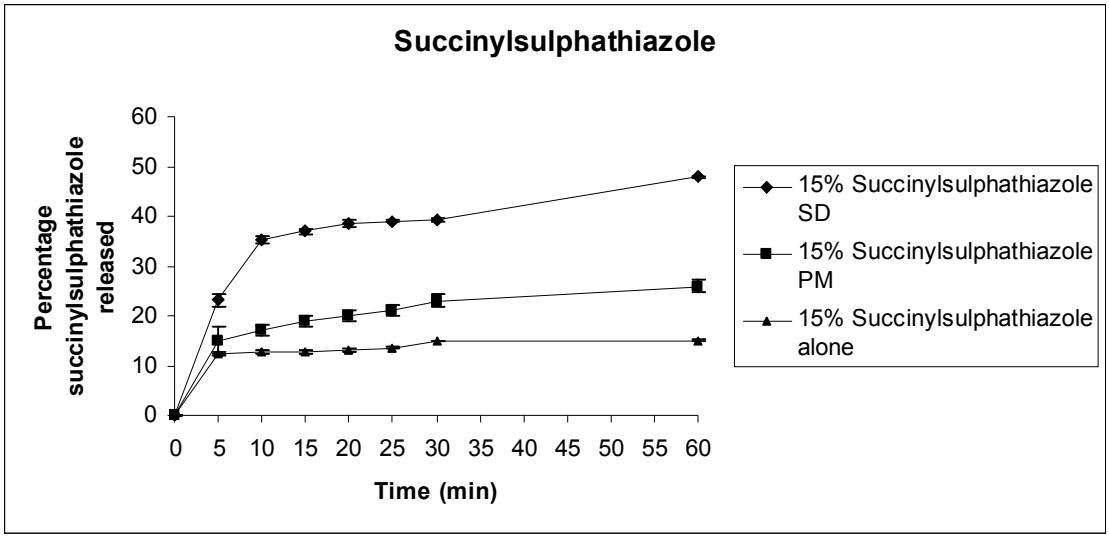

Figure 3.31. Percentage released of succinylsulphathiazole from solid dispersions, physical mix and drug alone (15% w/w) corresponds to the amount of succinylsulphathiazole in solid dispersions, physical mix and drug alone. Data are expressed as mean±S.D(*n* = 3).

3.3.4 Polymer dissolution studies

Figures 3.32-3.34 show drugs released faster or at a similar rate to PEG 8000 e.g paracetamol, sulphamethoxazole and phenacetin.

Figures 3.35-3.38 show PEG 8000 released faster than drugs e.g indomethacin, chloramphenicol, phenylbutazone and succinylsulphathiazole.

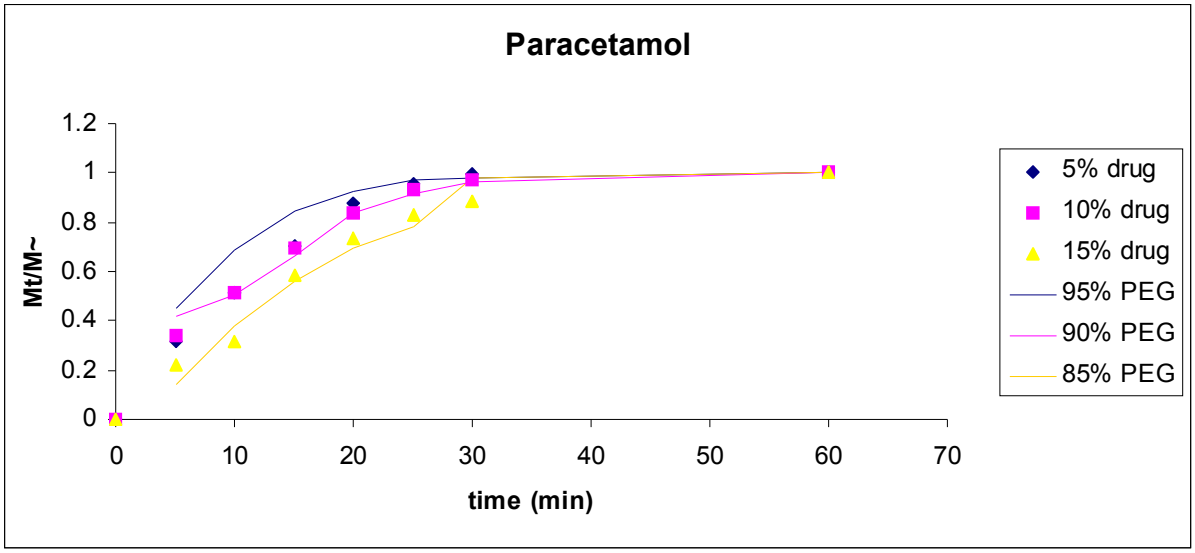

Figure 3.32. Fraction released of both Paracetamol and PEG 8000 from solid dispersions; 5%, 10% and 15% (w/w) correspond to the amount of paracetamol; 95%, 90% and 85% (w/w) correspond to the amount of PEG 8000 in the binary systems (solid dispersion).

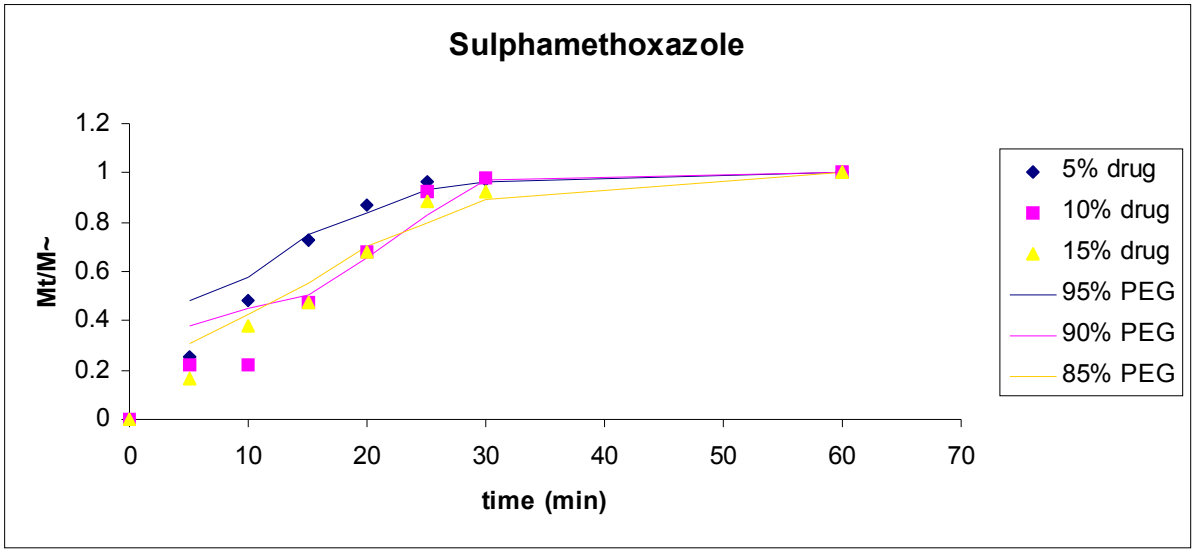

Figure 3.33. Fraction released of both sulphamethoxazole and PEG 8000 from solid dispersions; 5%, 10% and 15% (w/w) correspond to the amount of sulphamethoxazole ; 95%, 90% and 85% (w/w) correspond to the amount of PEG 8000 in the binary systems (solid dispersion).

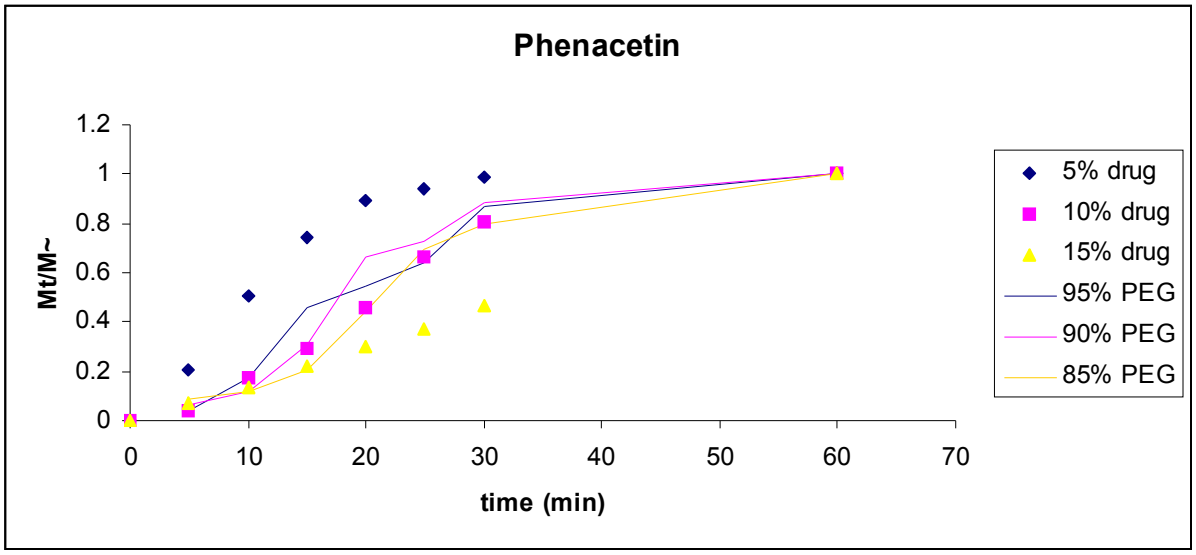

Figure 3.34. Fraction released of both phenacetin and PEG 8000 from solid dispersions; 5%, 10% and 15% (w/w) correspond to the amount of phenacetin ; 95%, 90% and 85% (w/w) correspond to the amount of PEG 8000 in the binary systems (solid dispersion).

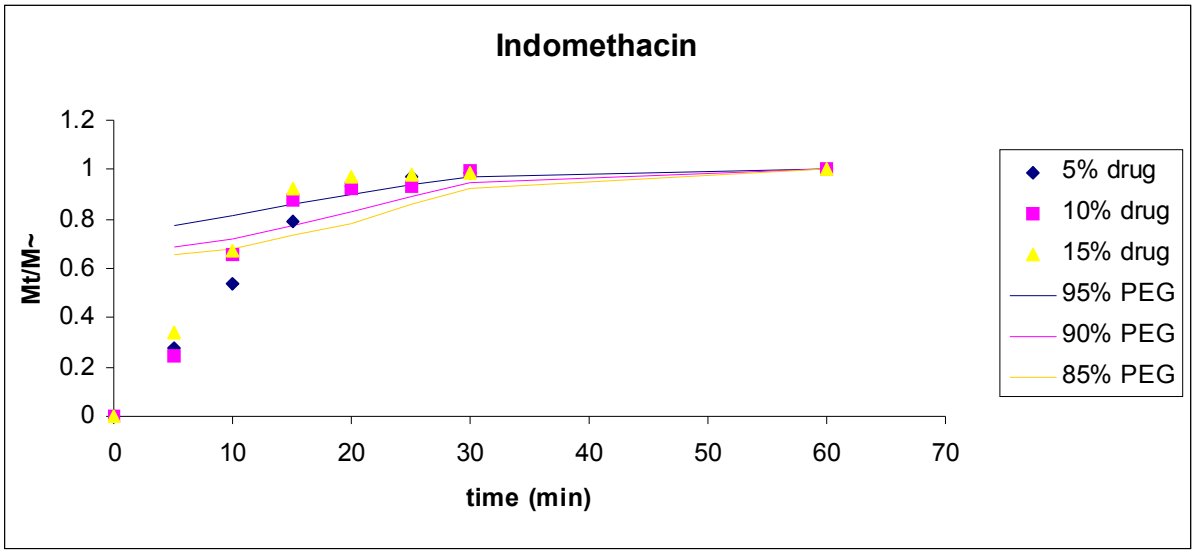

Figure 3.35. Fraction released of both indomethacin and PEG 8000 from solid dispersions; 5%, 10% and 15% (w/w) correspond to the amount of indomethacin ; 95%, 90% and 85% (w/w) correspond to the amount of PEG 8000 in the binary systems (solid dispersion).

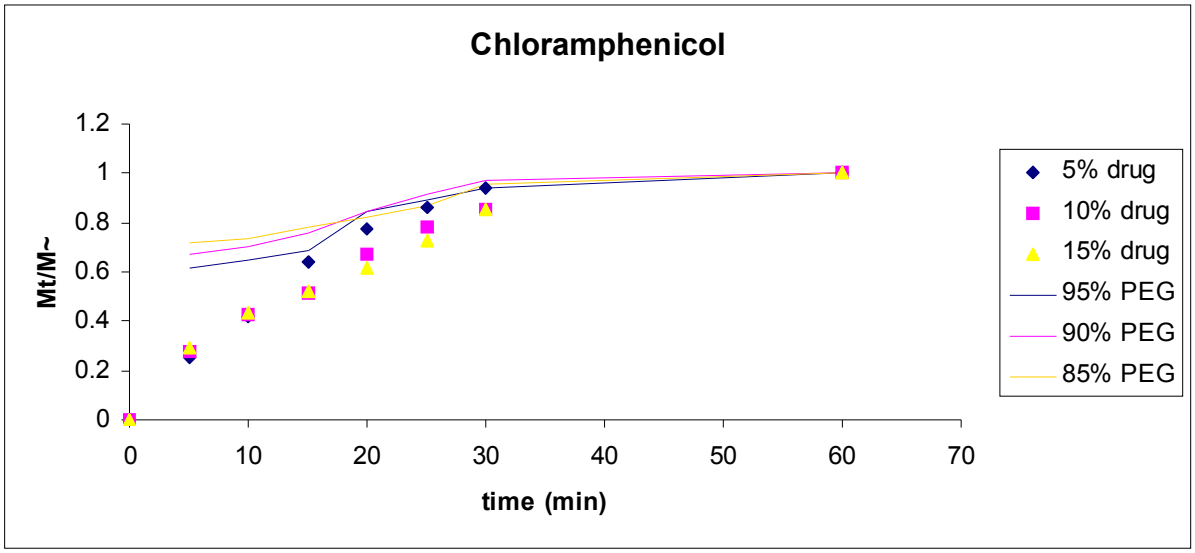

Figure 3.36. Fraction released of both chloramphenicol and PEG 8000 from solid dispersions; 5%, 10% and 15% (w/w) correspond to the amount of chloramphenicol ; 95%, 90% and 85% (w/w) correspond to the amount of PEG 8000 in the binary systems (solid dispersion).

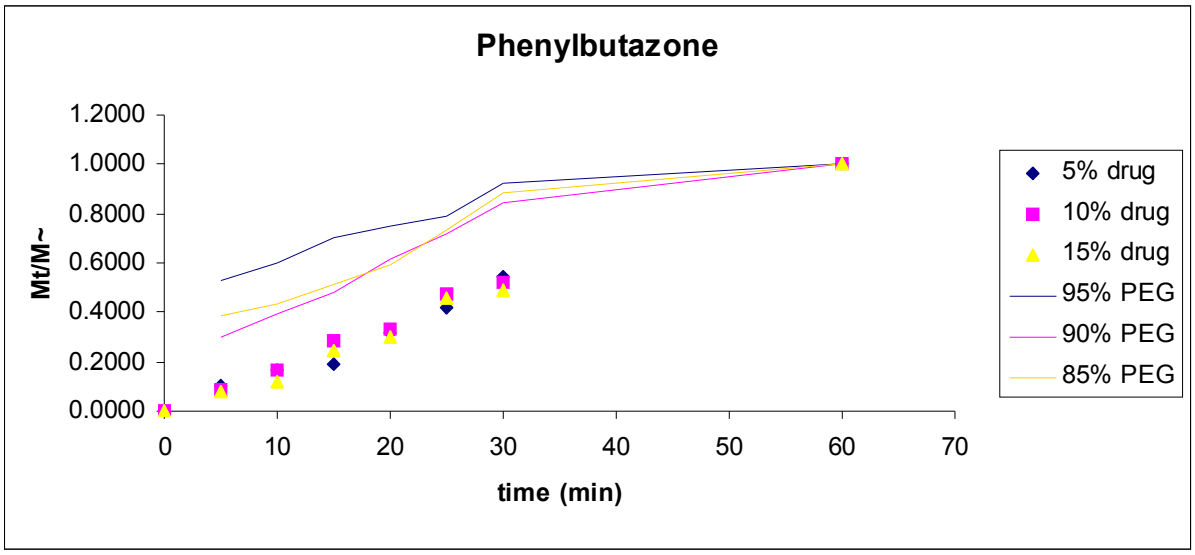

Figure 3.37. Fraction released of both phenylbutazone and PEG 8000 from solid dispersions; 5%, 10% and 15% (w/w) correspond to the amount of phenylbutazone ; 95%, 90% and 85% (w/w) correspond to the amount of PEG 8000 in the binary systems (solid dispersion).

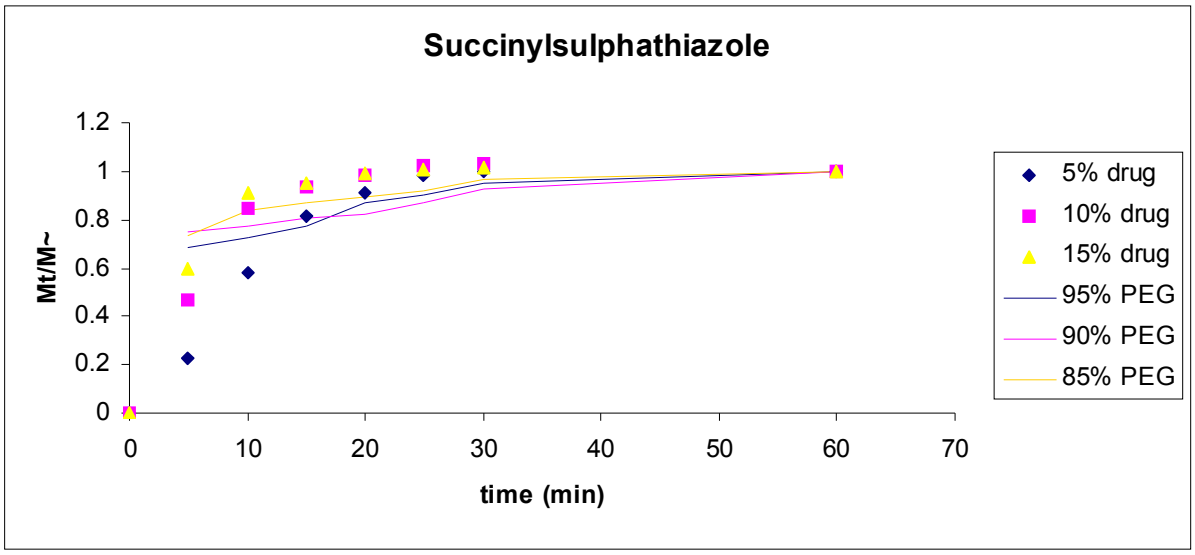

Figure 3.38. Fraction released of both succinylsulphathiazole and PEG 8000 from solid dispersions; 5%, 10% and 15% (w/w) correspond to the amount of succinylsulphathiazole; 95%, 90% and 85% (w/w) correspond to the amount of PEG 8000 in the binary systems (solid dispersion).

Mathematical modeling was performed on GraphPad Prism, version 4 by plotting the fraction of drug released versus time which was fitted to a power function to determine the values of n and K. These models are commonly used for drugs and less frequently used to analyse polymer dissolution, however, in this study it was interesting to use the same model for both drug and polymer release to see how similar the profiles were. The regression (R^2) values for the polymer were lower than the drugs and this may be an artifact from the origins of the equation used.

Table 3.1. Diffusional coefficient, n, release constant K and the correlation coefficient R^2 (Peppas equation) for drug release from 5%, 10% and 15% (w/w) solid dispersions (drug-PEG 8000).

Drugs	Loading % (w/w)	Drug release kinetics			Transport mechanism	Polymer release kinetics			Transport Mechanism
		K	n	R^2		K	n	R^2	
Paracetamol	5	0.113	0.6647	0.9872	Non-Fickian	0.3201	0.3282	0.8283	Fickian
	10	0.1294	0.6142	0.9917	Non-Fickian	0.23359	0.4014	0.902	Fickian
	15	0.0547	0.8387	0.9643	Non-Fickian	0.053199	0.8113	0.8805	Non-Fickian
Sulphamethoxazole	5	0.0779	0.7818	0.9709	Non-Fickian	0.28987	0.3317	0.906	Fickian
	10	0.0368	0.953	0.892	Case II	0.16063	0.4583	0.8987	Non-Fickian
	15	0.0383	0.9603	0.9875	Case II	0.14474	0.5159	0.9543	Non-Fickian
Phenacetin	5	0.0576	0.8808	0.9423	Non-Fickian	0.002934	1.6833	0.9639	Super Case-II transport
	10	0.0031	1.66	0.9906	Super Case-II transport	0.003959	1.6003	0.9615	Super Case-II transport
	15	0.0085	1.0629	0.9965	Super Case-II transport	0.007165	1.3518	0.9195	Super Case-II transport
Indomethacin	5	0.0768	0.8175	0.9738	Non-Fickian	0.65306	0.1149	0.9619	Fickian
	10	0.0747	0.8421	0.8846	Non-Fickian	0.52961	0.1699	0.9371	Fickian
	15	0.1245	0.6804	0.9221	Non-Fickian	0.48623	0.1887	0.923	Fickian
Chloramphenicol	5	0.0652	0.7631	0.988	Non-Fickian	0.41351	0.2269	0.888	Fickian
	10	0.0761	0.6431	0.9937	Non-Fickian	0.46886	0.1902	0.9083	Fickian
	15	0.0977	0.5773	0.9922	Non-Fickian	0.54453	0.1489	0.8985	Fickian
Phenylbutazone	5	0.0116	0.9075	0.977	Case II	0.3074	0.2739	0.9667	Fickian
	10	0.071	0.9766	0.9946	Case II	0.10947	0.5316	0.9681	Non-Fickian
	15	0.0046	1.0554	0.988	Super Case-II transport	0.13969	0.4335	0.9296	Fickian
Succinylsulp-hathiazole	5	0.0483	1.0334	0.9611	Super Case-II transport	0.52254	0.1718	0.9297	Non-Fickian
	10	0.2119	0.5445	0.9075	Non-Fickian	0.60017	0.1207	0.9162	Fickian
	15	0.3513	0.3675	0.8893	Fickian	0.5994	0.1247	0.959	Fickian

Preparation of solid dispersions improved the dissolution rate of all drugs. The solid dispersions of the seven drugs showed that drugs released faster in solid dispersions as compared to pure drug. Solid dispersions of many poorly water-soluble drugs with hydrophilic carrier matrix have been formulated for improving drug dissolution rate (Serajuddin, 1999; Passerini et al., 2002; Seo et al., 2003). Drugs released faster in 5% (w/w) as compared to 10% and 15% (w/w) solid dispersions except for paracetamol solid dispersion where similar release profile was seen for 5% and 10% (w/w) as shown in figures 3.18, 3.20, 3.22, 3.24, 3.26, 3.28 and 3.30. The importance of the carrier to enhance the performance of solid dispersion was illustrated in a study of 14 different drugs formulated as solid dispersions in PEG 6000 (Dubois and Ford, 1985). Dubois and Ford (1985) showed that, when the drug is present in a low drug/carrier ratio, the release rate is dependent only on the carrier and not on the drug properties. Moreover, solid dispersions may improve the bioavailability of poorly soluble drugs by increasing the drug dissolution rate and their saturation solubility in the gastro-intestinal fluids. The use of solid dispersions as a potential means of improving the dissolution behavior of poorly soluble drugs has been well presented and studied (Chiou and Riegelman, 1971; Corrigan, 1985; Ford, 1986; Craig, 1990). Solid dispersions often show an enhanced solubility because of the transformation of the drug's crystal lattice, a reduction of particle size and a better wettability exerted by the hydrophilic carrier. Even the dissolution rate of a relatively soluble drug like aspirin can be improved by formulating it as a solid dispersion in PEG (Asker et al., 1975). Possible mechanisms of increase in dissolution rates for solid dispersions have been proposed by Ford (1986), and include: reduction of particle size, a

solubilisation property of the carrier, improved wettability and dispersibility of a drug in the solid dispersion, conversion of drug into amorphous form.

The results showed that PEG 8000 improved drug dissolution for all the drugs studied. Similar result was shown when poorly soluble diclofenac was coupled with PEG 6000 (Adamo et al., 2005). Chiou and Riegelman (1969) were able to achieve a noticeable increase in the release rate of griseofulvin from solid dispersions in PEG. An increase in the release rate by formulation as a solid dispersion in PEG 4000 has been observed for many drugs, including oxazepam (Gines et al., 1996), piroxicam (Fernandez et al., 1993), zolpidem (Trapani et al., 1999) and glyburide (Betageri et al., 1995). Similarly, a two-fold increase in the release rate of carbamazepine was achieved by formulation as a solid dispersion in PEG 4000 and 6000 and was translated into an increase in the bioavailability relative to a suspension of the drug (El-Zein et al., 1998). Norfoxacin/PEG 6000 solid dispersions also produced a moderate increase in bioavailability (Fawaz et al., 1996). It is well established that materials such as PEG may increase the solubility of a range of drugs, particularly at high concentrations. Further drugs which exhibited elevated release rates when formulated as PEG solid dispersions include Sr33557, a new calcium antagonist (Lheritier et al., 1995), ketoprofen (Margarit et al., 1994), oxazepam (Jachowicz et al., 1993), nifedipine (Suzuki et al., 1997), phenytoin (Jachowicz et al., 1987), ursodeoxycholic acid (Okonogi et al., 1997), fenobrate (Sheu et al., 1994) and prednisolone (Jachowicz, 1987). Perng et al. (1998) achieved a ten-fold increase in the release rate of an experimental 5-lipoxygenase inhibitor with PEG 8000.

Increasing the concentration of drug in the dispersions leads to a decrease in dissolution rate. The drug/carrier ratio in a solid dispersion is one of the main influences on the performance of a solid dispersion. This could possibly be attributed to the wettability offered by the polymer and the conversion of crystalline drug into amorphous form. If the percentage of the drug is too high, it might result in the formation of small drug crystals within the dispersion rather than remaining completely molecularly dispersed thereby ultimately lowering the dissolution rate . On the other hand, if the percentage of the carrier is high, it can promote better wettability with an improved capacity to molecularly disperse the drug resulting in enormous increases in the solubility and release rate of the drug. Similar findings were reported with solid dispersions of lorazepam–PEG where a linear relationship was found between the polymer weight fraction and the dissolution rate constant (Al-Angary et al., 1996). Lin and Cham (1996) showed that solid dispersions of naproxen in PEG 6000 released drug faster when a 5% or 10% naproxen loading was used when compared to 20%, 30% or 50% loading. Dubois and Ford (1985) showed that, when the drug is present in a low drug/carrier ratio the release rate is dependent only on the carrier and not on the drug properties. Similar results were obtained with etoposide (Shah et al., 1995) and griseofulvin (Chiou et al., 1969).

The increased dissolution rate observed in this case can thus be contributed by several factors such as a solubilisation effect of the carrier and improved wettability of the drug. The rate and extent of drug release was more from solid dispersion followed by physical mixture and then drug alone for all formulations as shown in figures 3.19, 3.21, 3.23, 3.25, 3.27, 3.29 and 3.31. The drug released was more from physical mixtures as compared to

drug alone for all drugs. This might be due to lowering of the surface tension effect of PEG 8000 to the medium resulting in wetting of hydrophobic drug crystalline surface. Similar result was obtained by Sekikawa et al. (1979) and Tantishaiyakul et al. (1999). Drug release was same for 15% (w/w) solid dispersion, physical mix and drug alone for first 10 mins in case of phenacetin and phenylbutazone. This might be due to the drug floating on the surface of dissolution medium.

Paracetamol, sulphamethoxazole and phenacetin showed faster release than PEG 8000 as shown in figures 3.32-3.34 while PEG 8000 released faster than indomethacin, chloramphenicol, phenylbutazone and succinylsulphathiazole in solid dispersions (drug-PEG) as shown in figures 3.35-3.38. Theories proposed for the mechanisms governing drug release from solid dispersions are dependent on an understanding of the dissolution behavior of both drug and polymer. Some systems show carrier-controlled release with the rate of release being determined by the dissolution of the polymer and independent of the drug loaded (Corrigan, 1985; Dubois and Ford, 1985) such as indomethacin, chloramphenicol, phenylbutazone and succinylsulphathiazole in the current study while others drugs such as paracetamol, sulphamethoxazole and phenacetin showed that release is dependent on the properties of the drug (Sjokvist-Sears and Nystrom, 1988).

The goodness of fit for various models was investigated for binary systems ranked in the order of Korsemeyer–Peppas > Higuchi @ first-order > Hixson-Crowell cube root law zero-order (Ahuja et al., 2007).

All release data was converted into the fraction of drug released, from the solid dispersions and PEG 8000 and plotted against time. This plot was then fitted to the model described in equation 1, as shown in Figure 3.32-3.38. In this study, all data are fitted theoretical data from the experimental data using Peppas Equation. The kinetics of drugs and polymer release from the three different solid dispersions formulation was analysed using the Peppas and Korsmeyer model given by the following equation (Peppas, 1985).

$Mt/M\sim = Kt^n \quad \rightarrow$ (equation 3.1)

Where Mt/M~ is the fraction of drug released at time t, κ is the apparent release rate constant that incorporates the structural and geometric characteristics of the drug delivery system and n is the diffusional exponent which characterises the transport mechanism of the drug. The release data was fitted into the above model to determine the n values. The transport mechanisms were classified based on the value that n assumes. For a cylinder, the drug transport mechanism is by Fickian diffusion when n=0.45, if $0.45<n<0.89$, it indicated anomalous (non-Fickian) transport and for values of n=0.89, Case II or zero-order release kinetics was indicated (Peppas, 1985). When $n>1$ it indicated Super Case II transport. Case II relates to polymer relaxation, while non-Fickian release is described by two mechanisms, the coupling of drug diffusion and polymer relaxation (Ritger and Peppas, 1987).

Table 3.1 gives the n values for all the solid dispersions that were tested for 5%, 10% and 15% (w/w). Table 3.1 shows that release of paracetamol, indomethacin and chloramphenicol for 5%, 10% and 15% (w/w) from the solid dispersions that were

formulated was by non-Fickian mechanisms. Similar non-Fickian behavior has also been reported previously with the Gelucire dispersions of paracetamol and caffeine (Khan and Craig, 2003). In 5% (w/w) sulphamethoxazole and phenacetin showed non-Fickian behavior; 10% and 15% (w/w) sulphamethoxazole indicated Case II transport while in phenacetin showed super Case II mechanism. Results of 5% and 10% (w/w) for phenylbutazone were Case II transport and for 15% (w/w) solid dispersion was super Case II. The mode of drug release for eleven drugs studied in chitosonium malate matrix was generally non-Fickian and Super Case II type **(**Akbua, 1993). In 5% (w/w) solid dispersion of succinylsulphatiazole was super Case II; 10% (w/w) was non-Fickian and 15% (w/w) was Fickian behavior. The release data showed combined effect of diffusion and relaxational mechanisms for drug release (Sriamornsak et al., 2007). Table 3.1 also shows the release kinetics of PEG 8000. Fickian mechanisms in PEG 8000 as in the case of indomethacin, chloramphenicol, phenylbutazone and succinylsulphathiazole. In the case of paracetamol and sulphamethoxazole it was Fickian to non-Fickian and phenacetin it was super Case II transport.

3.4 Conclusions

The results show the suitability of PEG 8000 as the carrier for solid dispersions of all seven drugs studied. The dissolution rates of physical mixtures were higher in all seven drugs than pure drugs; this being probably caused by wettability of drug due to PEG 8000. Solid dispersions demonstrated higher dissolution rates than those of physical mixtures and drug alone, resulting from the increase in drug wettability caused by carrier. Maximum dissolution rate was obtained with 5% (w/w) drug loading solid dispersions suggesting that high carrier concentration enhanced the dissolution. Microviscometry has shown to be effective method for measuring the dissolution of the PEG 8000 from the solid dispersions. Formulations such as indomethacin, chloramphenicol, phenylbutazone and succinylsulphathiazole showed carrier-controlled release with the release rate being controlled by the dissolution of the polymer while drugs such as paracetamol, sulphamethoxazole and phenacetin demonstrated that release rate is dependent on the properties of the drug.

Chapter 4

Characterisation Studies

4.1 Introduction

The characterisation of solid dispersions was performed using differential scanning calorimetry (DSC), fourier transform infrared spectroscopy (FTIR), scanning electron microscopy (SEM), solubility studies and isothermal titration calorimetry (ITC).

4.1.1 Differential scanning calorimetry (DSC)

DSC was used to detect melting point and quantify transitions and reactions displayed as endothermic and crystallisation (exothermic) events which results in a baseline shift as the specific heat capacity of the sample changes.

4.1.2 Hyper differential scanning calorimetry (Hyper DSC)

Hyper differential scanning calorimetry (Hyper DSC) employs heating rates typically in excess of 100-500 °C/min, whereas normal DSC has a range of about 1-20 °C/min. This provides a number of advantages, the most pertinent of which is that hyper DSC can be used to prevent recrystallisation during a heating step (Pijpers et al., 2002). Hyper DSC cycles were also used to enhance the thermal signal when compared to the standard DSC thermograms. This also had the additional benefit of minimizing changes in morphology and preventing any interactions during the heating process.

4.1.3 Fourier transform infrared spectroscopy (FTIR)

Fourier transform infrared spectroscopy (FTIR) studies were performed to help and assist in the evaluation of any possible chemical (functional group) interactions between drug and PEG 8000. The interactions between drug and the polymer in the solid dispersion or

physical mixture would result in band shifts compared to the spectra for the drug and polymer (Silverstein et al., 1991).

4.1.4 Scanning electron microscopy (SEM)

Scanning electron microscopy (SEM) produces very high magnification images of a sample morphology revealing details about 1 to 5 nm in size. The surface morphology of indomethacin, phenacetin, paracetamol, phenylbutazone, chloramphenicol, sulphamethoxazole, succinylsulphathiazole and its binary systems (solid dispersion) were examined by SEM.

4.1.5 Solubility studies

Solubility studies are important in the drug development. It serves for the identification of screening and bioavailability issues. In biopharmaceutical evaluation of formulation, knowledge of solubility is important for the confirmation of bioavailability results.

4.1.6 Isothermal titration calorimetry (ITC)

Calorimetric techniques are very powerful for studying and understanding biological processes at molecular level. Isothermal titration calorimetry (ITC) can detect the small changes of heat during reaction. It allows for the determination of the thermodynamic parameters such as enthalpy, entropy, Gibbs free energy, heat capacity, binding constant and effective number of binding sites in biological reactions. ITC is the only technique that can establish all of these binding parameters from a single experiment. Other advantages include the measurement of a heat signal (Wiseman et al., 1989).

4.2 Aims of the study

The characterisation was performed to see whether any interactions between drug-excipient have taken place. DSC was used to detect melting point and any transitions which will be displayed as endothermic events and crystallisations for all seven solid dispersions. FTIR was used for determination of any interactions between drug and polymer. SEM at different magnifications was used to investigate the morphological differences of solid dispersions.

Isothermal titration calorimetry (ITC) was used to determine the small changes of heat during titration of drug with PEG 8000 and for the detection of PEG 8000/drug interactions.

4.3 Results and Discussion

4.3.1 Differential scanning calorimetry (DSC)

DSC thermograms of drug alone, solid dispersions and physical mixtures (drug-PEG 8000) for indomethacin, phenacetin, paracetamol, phenylbutazone, chloramphenicol, sulphamethoxazole and succinylsulphathiazole are discussed below:

4.3.1.1 DSC of polymer alone, indomethacin alone, solid dispersion 15% (w/w) (indomethacin-PEG 8000) and physical mixture 15% (w/w) of indomethacin-PEG 8000

Figures 4.1-3 show the DSC thermograms of indomethacin, PEG 8000, solid dispersion 15% (w/w) (indomethacin-PEG 8000) and physical mixture 15% (w/w) of indomethacin-PEG 8000. The thermograms of indomethacin alone and polymer alone exhibited single endothermic peaks at around 159.79 °C and 59.13 °C for indomethacin and PEG 8000, respectively. Investigation of the heating scans of solid dispersion for the drug showed melting peak for the polymer at around 59 °C with no endothermic peak corresponding to the indomethacin (figure 4.1). The absence of a peak at temperatures corresponding to the melting of the drug could potentially be attributed to the solubilisation and distribution of the drug within the hydrophilic polymer matrix resulting in the conversion of crystalline drug into amorphous form. Analogous phenomena have also previously been reported by various researchers (Craig et al., 1991; Guyot et al., 1995; Damian et al., 2000).

However, physical mixtures of indomethacin with the polymer (figure 4.2) resulted in the absence of melting endotherm corresponding to the drug as seen in the thermograms for the solid dispersion. To further investigate the binary physical mixture of indomethacin and polymer, standard DSC at scan rate of 10 °C/min was employed to have an insight into any transitions occurring during slow heating in contrast to faster heating rate used in Hyper DSC. Analysis of samples (physical mixture) containing 20%, 30% and 40% w/w drug content for the indomethacin showed only a single peak corresponding to the melting of the polymer (figure 4.3). These results are in agreement with previous work reported on the thermal analysis of physical mixtures of poorly soluble drugs and polymers. Research published by Ahuja et al. (2007), Abdul-Fattah and Bhargava (2002), have shown that the physical mixtures of the drug candidates resulted in a single peak corresponding to the polymer melt with the peak for the drug absent in the scans for the physical mixture. The lack of the endotherm of the drug has been attributed to the melting and solubilisation of the drug within the molten carrier during the heating of the samples. PEG 8000 is characterised by an onset melt temperature of around 59 °C and the corresponding endotherms for indomethacin occur at 159.79 °C respectively. It may be possible that during the heating process for the analysis of thermograms for the physical mixtures, the molten carrier (which has nearly half the melting temperature when compared to the drug) begins to solubilise the drug thereby dispersing it within its matrix with the consequence that the endotherm for the drug disappears completely. To further explain the DSC results of physical mixtures during heating, the drug may be dissolved in the carrier and no crystalline drug remained as the melting temperature of the drug reached showing only single carrier endotherm.

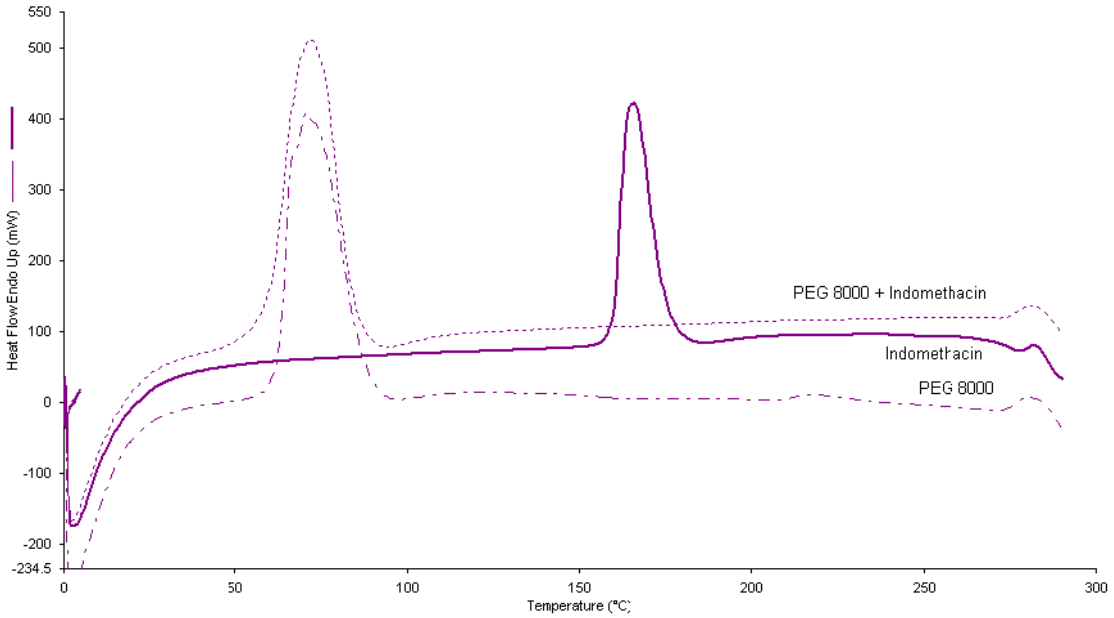

Figure 4.1. Hyper-DSC thermograms of solid dispersion consisting of 15% (w/w) indomethacin, indomethacin alone and PEG 8000 alone.

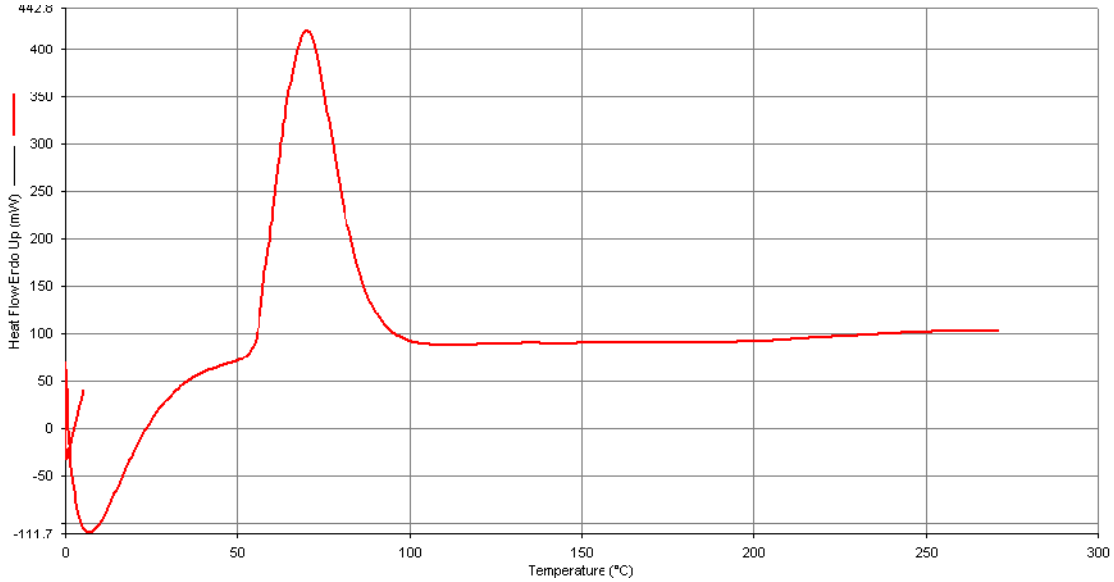

Figure 4.2. Hyper-DSC thermograms of physical mixture consisting of 15% (w/w) indomethacin and PEG 8000.

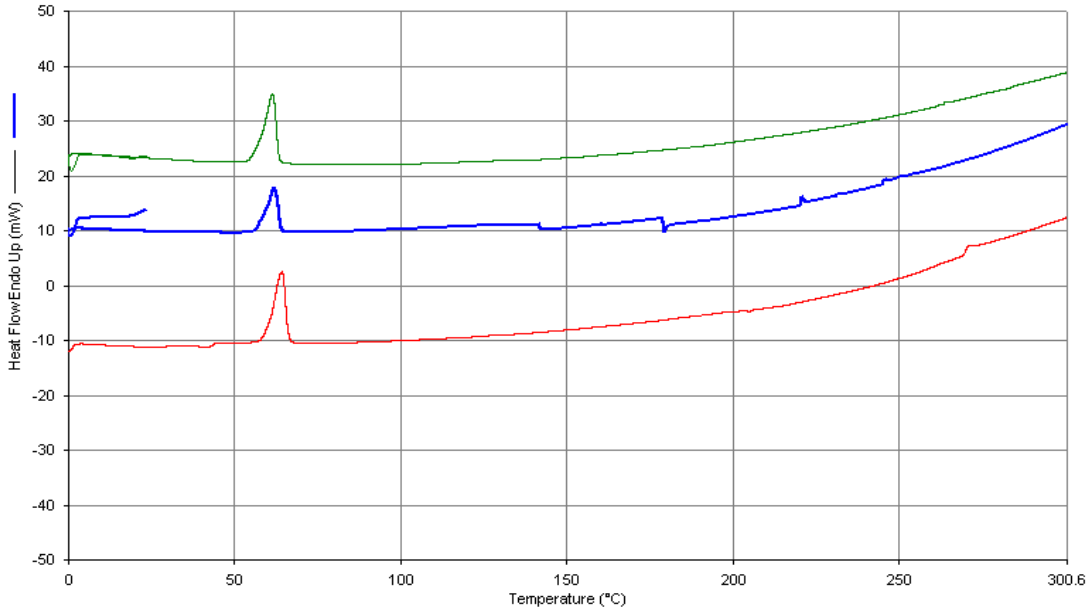

Figure 4.3. DSC thermograms of physical mixture consisting of 20%, 30% and 40% (w/w) (bottom to top) indomethacin and PEG 8000.

4.3.1.2 DSC of polymer alone, phenacetin alone, solid dispersion 15% (w/w) (phenacetin-PEG 8000) and physical mixture 15% (w/w) of phenacetin-PEG 8000

Figures 4.4-5 show the DSC thermograms of phenacetin, PEG 8000, solid dispersion 15% (w/w) and physical mixture 15% (w/w) of phenacetin-PEG 8000. The thermograms of phenacetin alone and polymer alone exhibited single endothermic peaks at around 133.38 °C and 59.13 °C for phenacetin and PEG 8000, respectively. Investigation of the heating scans of solid dispersion for the drug investigated showed melting peak for the polymer at around 59 °C with no endothermic peak corresponding to phenacetin (figure 4.4). The absence of a peak at temperatures corresponding to the melting of the drug could potentially be attributed to the solubilisation of drug within the hydrophilic

polymer matrix resulting in the conversion of crystalline phenacetin into amorphous form.

DSC scan for the physical mixture revealed an interesting profile. Physical mixture of phenacetin with the polymer (figure 4.5) showed two transitions: the first corresponding to the melt of the polymer (PEG 8000) and the second due to the melting of the phenacetin.

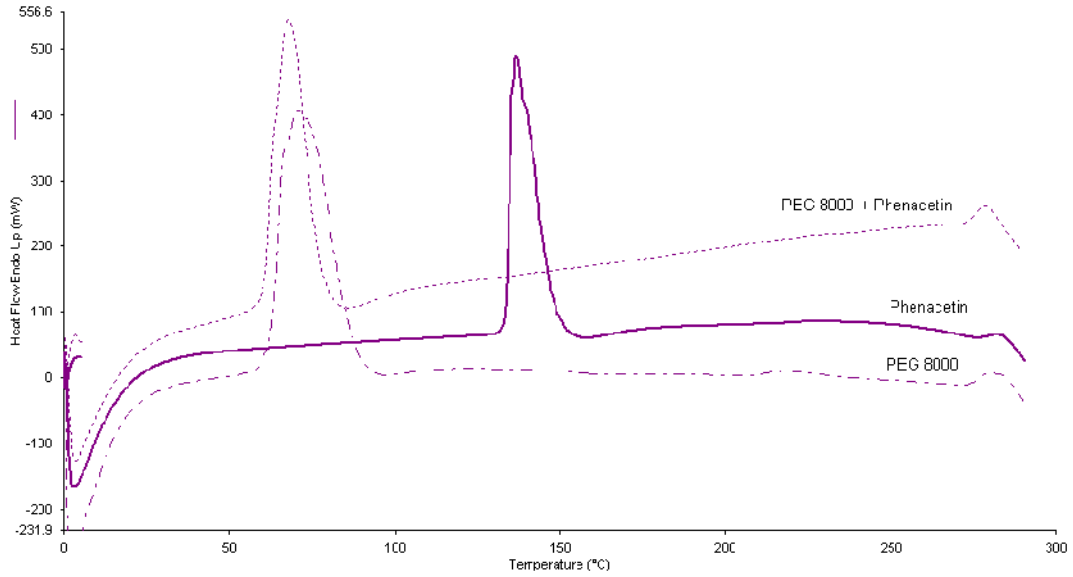

Figure 4.4. Hyper-DSC thermograms of solid dispersion consisting of 15% (w/w) phenacetin, phenacetin alone and PEG 8000 alone.

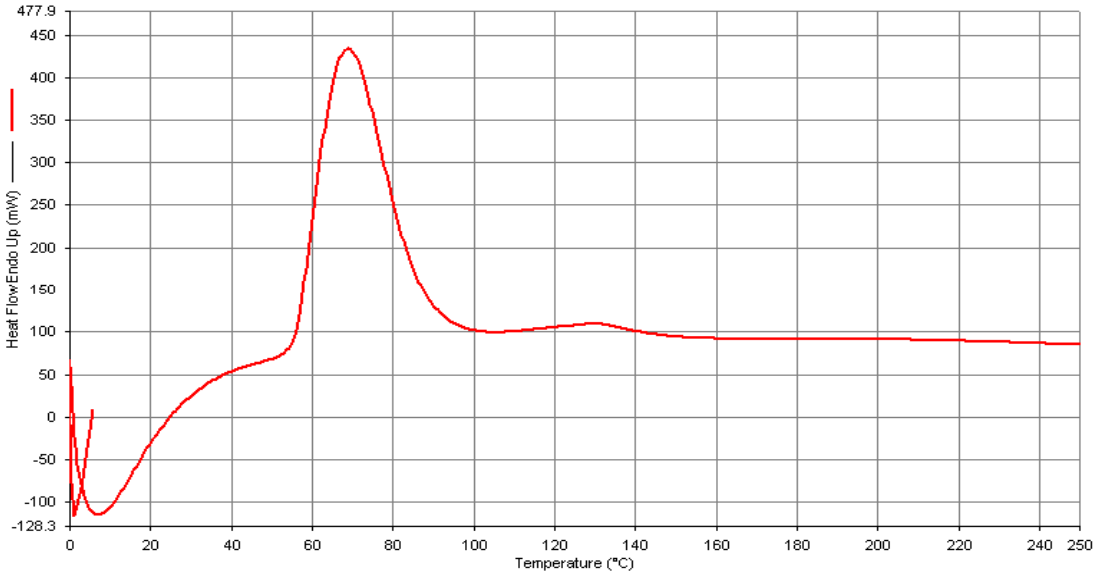

Figure 4.5. Hyper-DSC thermograms of physical mixture consisting of 15% (w/w) phenacetin and PEG 8000.

4.3.1.3 DSC of polymer alone, paracetamol alone, solid dispersion 15% (w/w) (paracetamol-PEG 8000) and physical mixture 15% (w/w) of paracetamol-PEG 8000

Figures 4.6-7 show the DSC thermograms of paracetamol, PEG 8000, solid dispersion 15% (w/w) (paracetamol-PEG 8000) and physical mixture 15% (w/w) of paracetamol-PEG 8000. The thermograms of paracetamol alone and polymer alone exhibited single endothermic peaks at around 166.71 °C and 59.13 °C for paracetamol and PEG 8000, respectively. Investigation of the heating scans of solid dispersion for the drug investigated showed melting peak for the polymer at around 59°C with no endothermic peak corresponding to the paracetamol (figure 4.6). The absence of a peak at temperatures corresponding to the melting of the drug could potentially be attributed to

the solubilisation of drug within the hydrophilic polymer matrix resulting in the conversion of crystalline paracetamol into amorphous form.

Physical mixture of paracetamol with the polymer (figure 4.7) showed two transitions: the first corresponding to the melt of the polymer (PEG 8000) and the second due to the melting of the paracetamol.

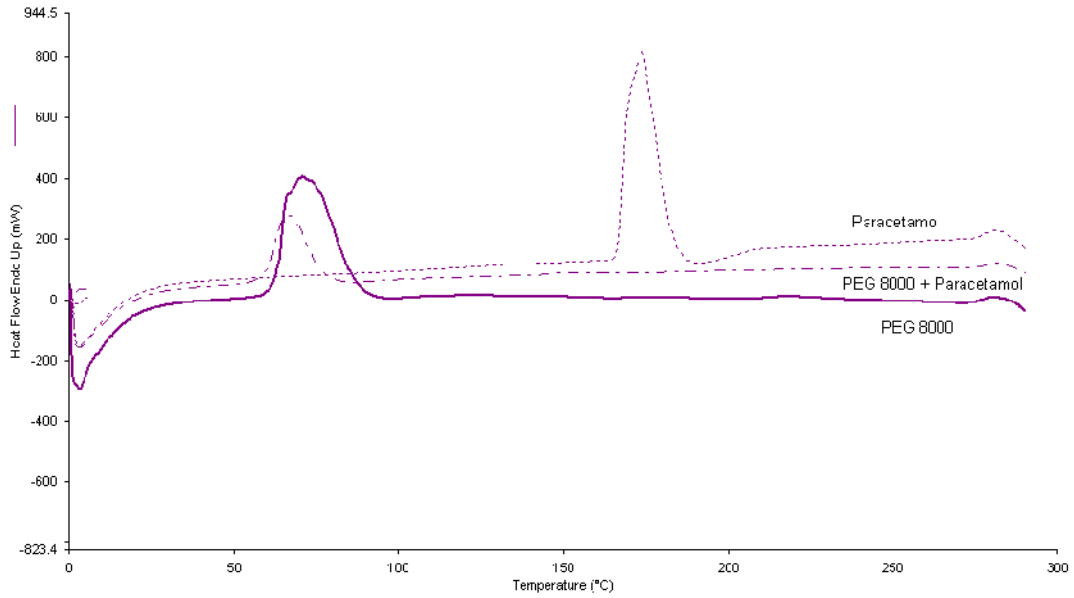

Figure 4.6. Hyper-DSC thermograms of solid dispersion consisting of 15% (w/w) paracetamol, paracetamol alone and PEG 8000 alone.

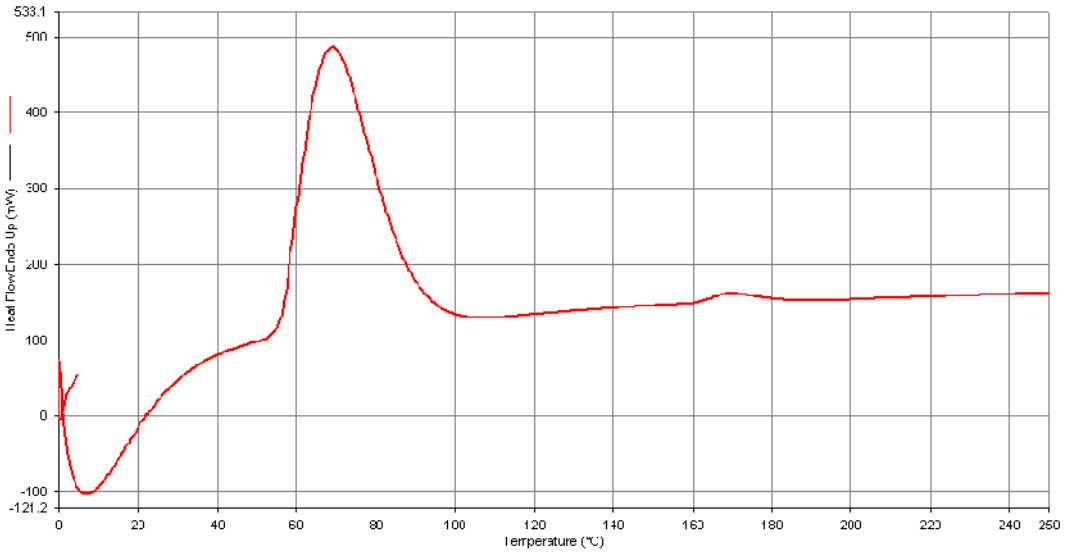

Figure 4.7. Hyper-DSC thermograms of physical mixture consisting of 15% (w/w) paracetamol and PEG 8000.

4.3.1.4 DSC of polymer alone, phenylbutazone alone, solid dispersion 15% (w/w) (phenylbutazone-PEG 8000) and physical mixture 15% (w/w) of phenylbutazone-PEG 8000

Figures 4.8-9 show the DSC thermograms of phenylbutazone, PEG 8000, solid dispersion 15% (w/w) and physical mixture 15% (w/w) of phenylbutazone-PEG 8000. The thermograms of phenylbutazone alone and polymer alone exhibited single endothermic peaks at around 107.70 °C and 59.13 °C for phenylbutazone and PEG 8000, respectively. Investigation of the heating scans of solid dispersion for the drug investigated showed melting peak for the polymer at around 59 °C with no endothermic peak corresponding to the phenylbutazone (figure 4.8). The absence of a peak at temperatures corresponding to the melting of the drug could potentially be attributed to the solubilisation of drug within the hydrophilic polymer matrix resulting in the conversion of phenylbutazone into amorphous form.

Physical mixtures of phenylbutazone with the polymer (figure 4.9) resulted in the absence of melting endotherm corresponding to the drug as seen in the thermograms for the solid dispersion. To further investigate the binary physical mixture of phenylbutazone and PEG 8000, standard DSC at scan rate of 10 °C/min was employed to determine any transitions occurring during slow heating (Normal DSC) in contrast to faster heating rate used in Hyper DSC. Analysis of samples (physical mixture) containing 20%, 30% and 40% (w/w) drug content for the phenylbutazone showed only a single peak corresponding to the melting of the polymer (figure 4.10).

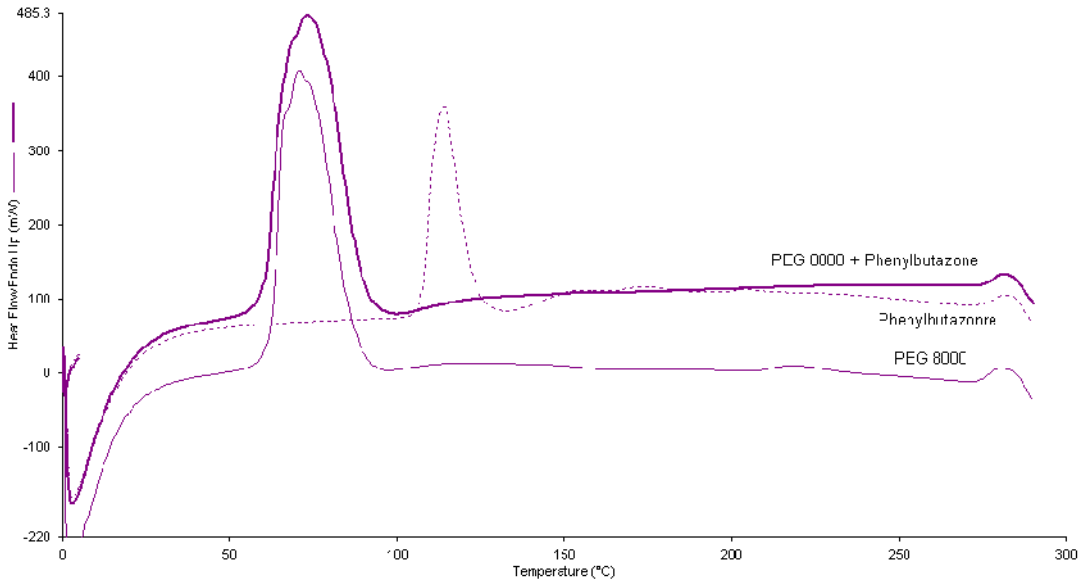

Figure 4.8. Hyper-DSC thermograms of solid dispersion consisting of 15% (w/w) phenylbutazone, phenylbutazone alone and PEG 8000 alone.

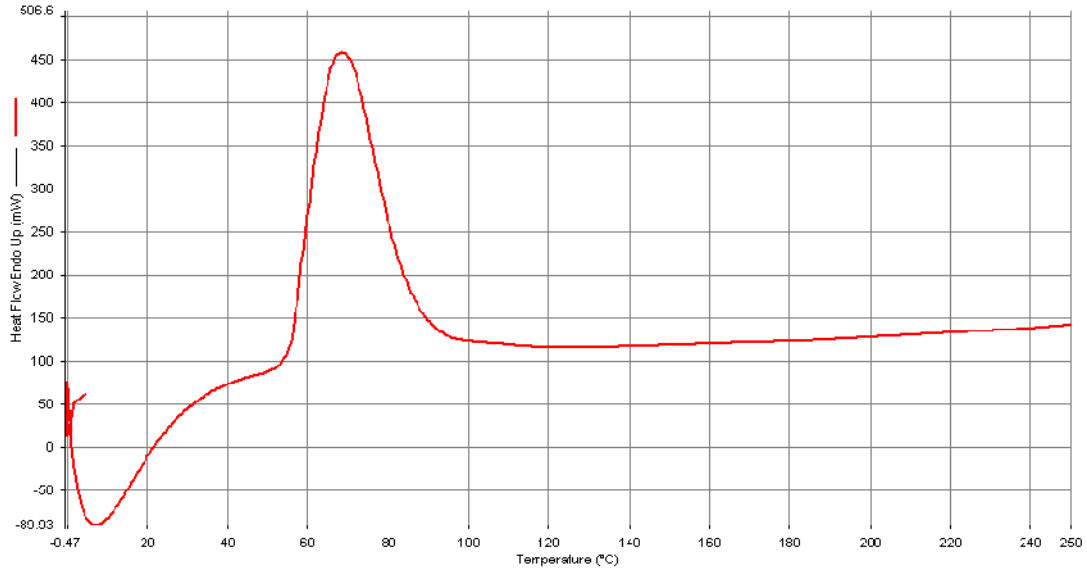

Figure 4.9. Hyper-DSC thermograms of physical mixture consisting of 15% (w/w) phenylbutazone and PEG 8000.

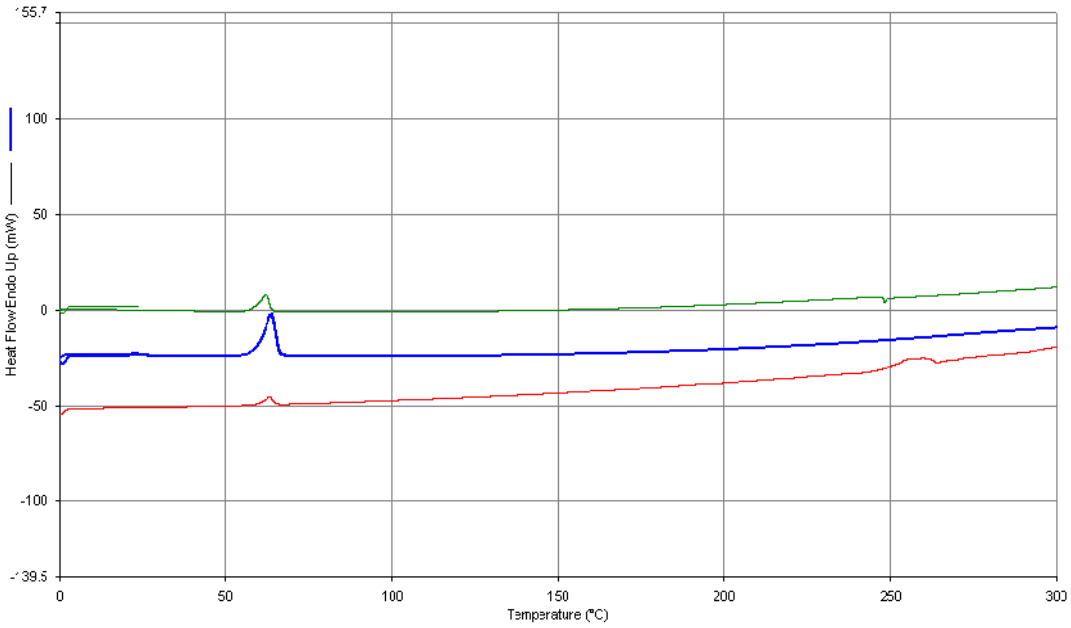

Figure 4.10. DSC thermograms of physical mixture consisting of 20%, 30% and 40% (w/w) (bottom to top) phenylbutazone and PEG 8000.

4.3.1.5 DSC of polymer alone, chloramphenicol alone, solid dispersion 15% (w/w) (chloramphenicol-PEG 8000) and physical mixture 15% (w/w) of chloramphenicol-PEG 8000

Figures 4.11-12 show the DSC thermograms of chloramphenicol, PEG 8000, solid dispersion 15% (w/w) (chloramphenicol- PEG 8000) and physical mixture 15% (w/w) of chloramphenicol-PEG 8000. The thermograms of chloramphenicol alone and polymer alone exhibited single endothermic peaks at around 150.48 °C and 59.13 °C for chloramphenicol and PEG 8000, respectively. Investigation of the heating scans of solid dispersion for chloramphenicol investigated showed melting peak for the polymer at around 59 °C with no endothermic peak corresponding to the drug (figure 4.11). The absence of a peak at temperatures corresponding to the melting of the drug could potentially be ascribed to the dispersion of the drug within the carrier matrix resulting in the loss of crystalline form and conversion into amorphous form. This phenomenon has also been previously presented by Craig et al. (1991), Guyot et al. (1995) and Damian et al. (2000).

Physical mixtures of chloramphenicol with the polymer (figure 4.12) resulted in the absence of melting endotherm corresponding to the drug as seen in the thermograms for the solid dispersion. To further investigate the binary physical mixture of chloramphenicol and standard DSC at scan rate of 10 °C/min was employed to gain insight into any transitions occurring during slow heating (Normal DSC) in contrast to faster heating rate used in Hyper DSC. Analysis of samples (physical mixture) containing

20%, 30% and 40% (w/w) drug content for the chloramphenicol showed only a single peak corresponding to the melting of the polymer (figure 4.13).

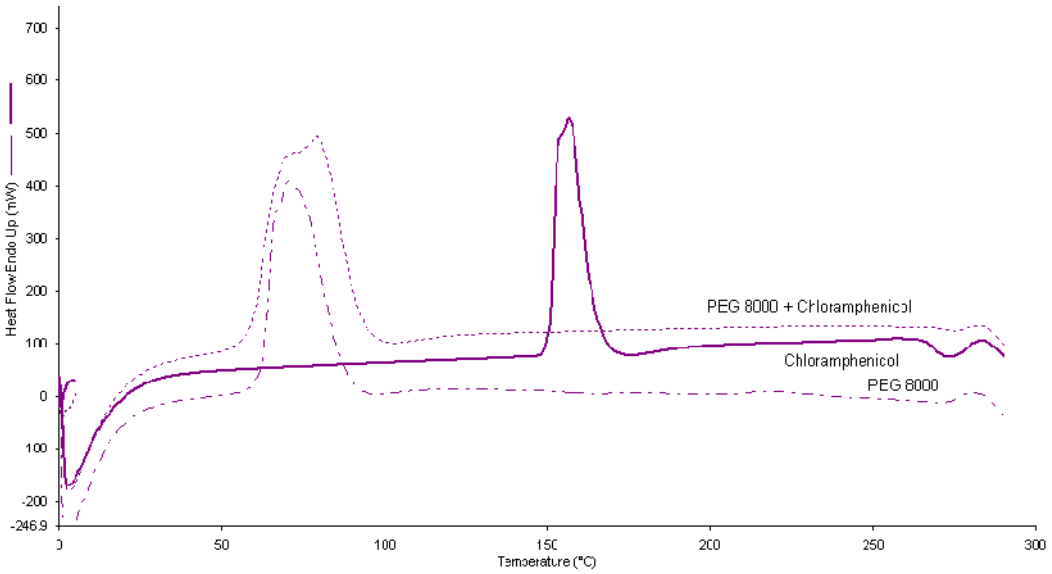

Figure 4.11. Hyper-DSC thermograms of solid dispersion consisting of 15% (w/w) chloramphenicol, chloramphenicol alone and PEG 8000 alone.

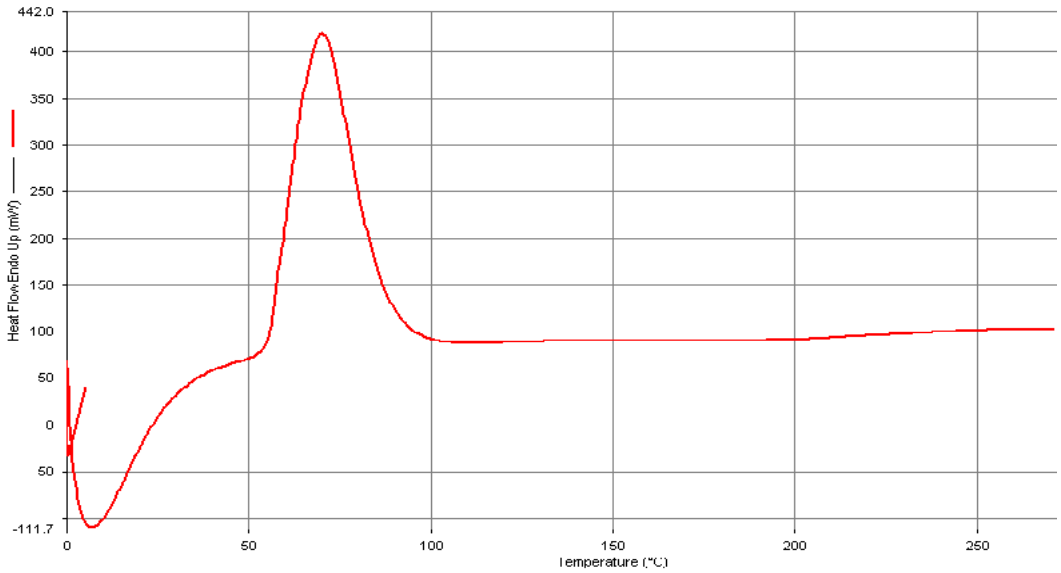

Figure 4.12. Hyper-DSC thermograms of physical mixture consisting of 15% (w/w) chloramphenicol and PEG 8000.

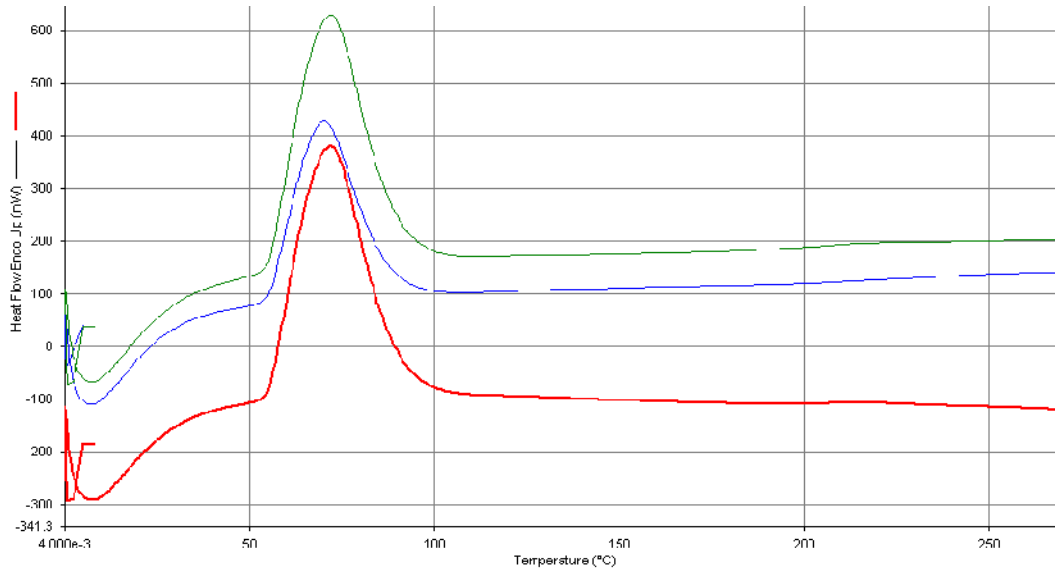

Figure 4.13. DSC thermograms of physical mixture consisting of 20%, 30% and 40% (w/w) (bottom to top) chloramphenicol and PEG 8000.

4.3.1.6 DSC of polymer alone, sulphamethoxazole alone, solid dispersion 15% (w/w) (sulphamethoxazole-PEG 8000) and physical mixture 15% (w/w) of sulphamethoxazole-PEG 8000

Figures 4.14-15 show the DSC thermograms of sulphamethoxazole, PEG 8000, solid dispersion 15% (w/w) and physical mixture 15% (w/w) of sulphamethoxazole-PEG 8000. The thermograms of sulphamethoxazole alone and polymer alone exhibited single endothermic peaks at around 167.22 °C and 59.13 °C for sulphamethoxazole and PEG 8000, respectively. The heating scans of solid dispersion for the drug investigated showed melting peak for the polymer at around 59 °C with no endothermic peak corresponding to sulphamethoxazole (figure 4.14). The absence of a peak at temperatures corresponding to the melting of the drug could potentially be attributed to the solubilisation of drug within

the hydrophilic polymer matrix resulting in the conversion of sulphamethoxazole into amorphous form.

Physical mixtures of sulphamethoxazole with the polymer (figure 4.15) resulted in the absence of melting endotherm corresponding to the drug as seen in the thermograms for the solid dispersion. Analysis of the samples using DSC at scan rate of 10 °C/min was employed to gain insight into any transitions occurring during slow heating in contrast to faster heating rate used in Hyper DSC. Analysis of samples (physical mixture) containing 20%, 30% and 40% (w/w) drug content for the sulphamethoxazole showed only a single peak corresponding to the melting of the polymer (figure 4.16).

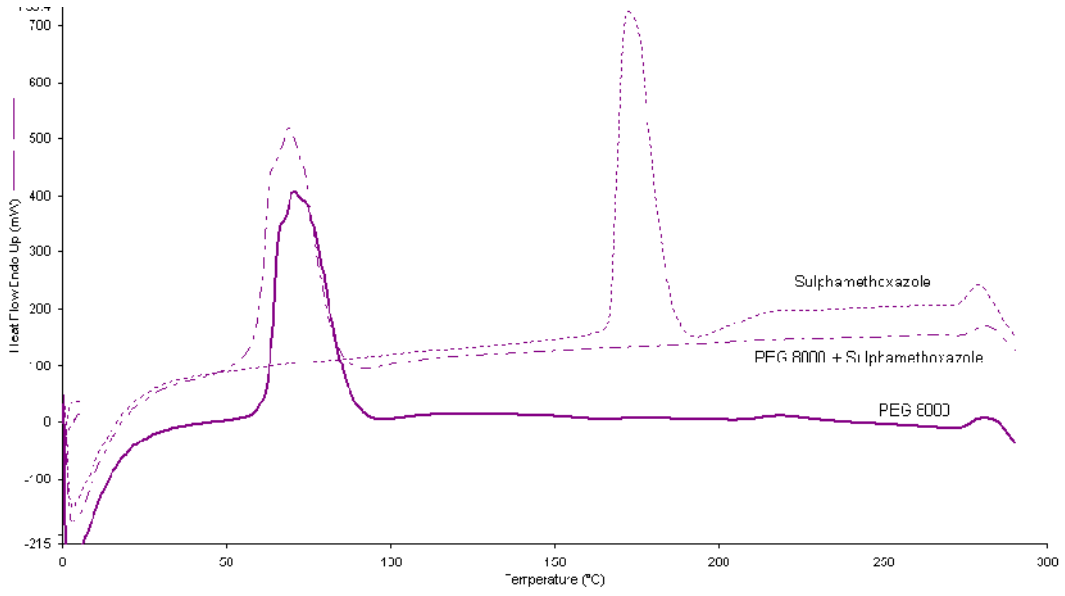

Figure 4.14. Hyper-DSC thermograms of solid dispersion consisting of 15% (w/w) sulphamethoxazole, sulphamethoxazole alone and PEG 8000 alone.

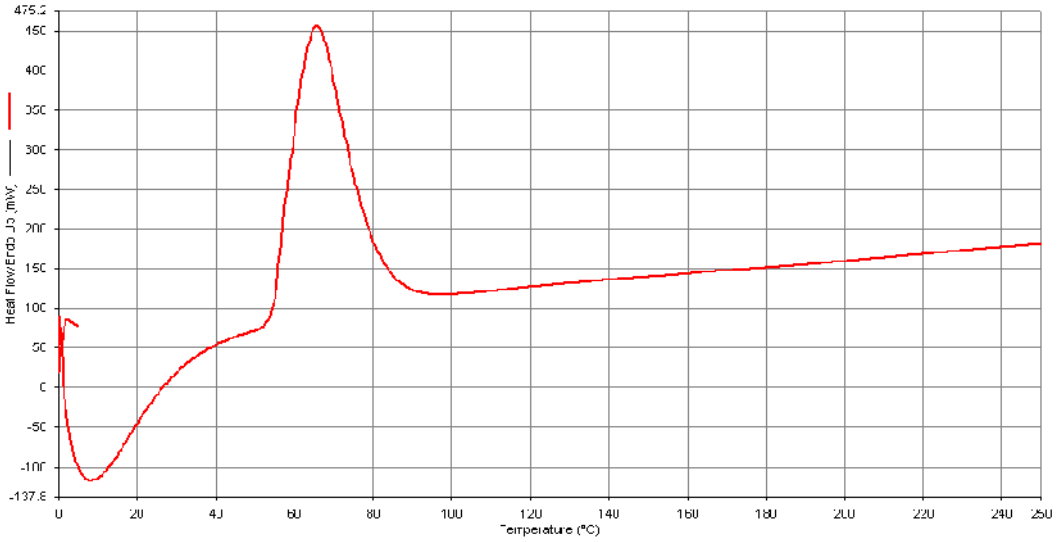

Figure 4.15. Hyper-DSC thermograms of physical mixture consisting of 15% (w/w) sulphamethoxazole and PEG 8000.

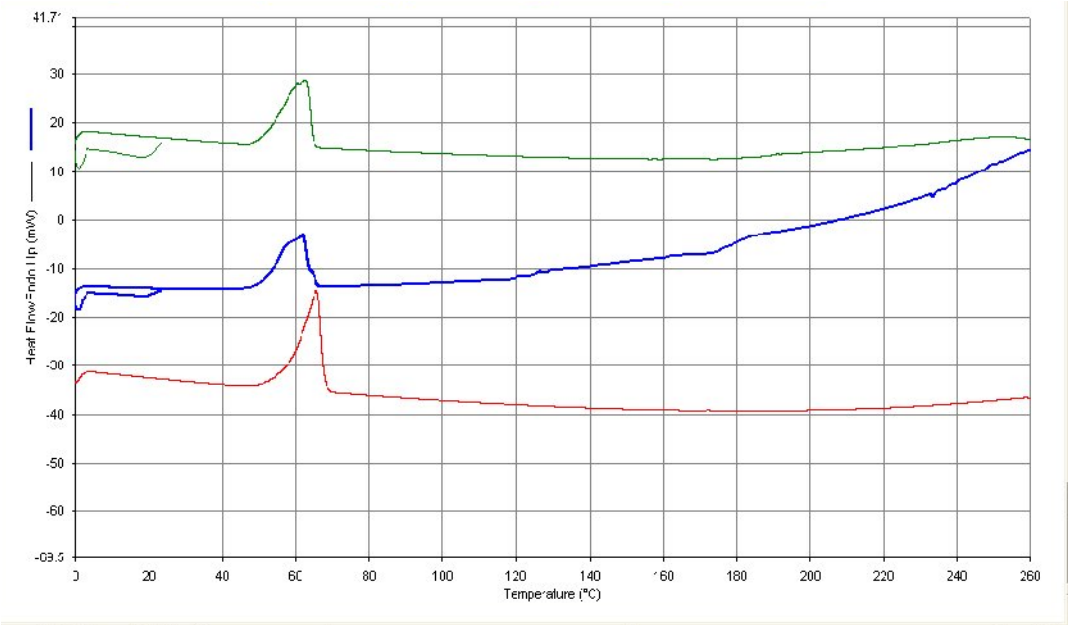

Figure 4.16. DSC thermograms of physical mixture consisting of 20%, 30% and 40% (w/w) (bottom to top) sulphamethoxazole and PEG 8000.

4.3.1.7 DSC of polymer alone, succinylsulphathiazole alone, solid dispersion 15% (w/w) (succinylsulphathiazole-PEG 8000) and physical mixture 15% (w/w) of succinylsulphathiazole-PEG 8000

Figure 4.17-18 show the DSC thermograms of succinylsulphathiazole, PEG 8000, solid dispersion 15% (w/w) and physical mixture 15% (w/w) of succinylsulphathiazole-PEG 8000. In case of succinylsulphathiazole alone, there were two melting endotherms which indicate the presence of more than one polymorphic forms of succinylsulphathiazole. Investigating the heating scans of solid dispersion for succinylsulphathiazole showed melting peak for the polymer at around 59 °C with no endothermic peak corresponding to the drug (figure 4.17). The absence of a peak at temperatures corresponding to the melting of the drug could potentially be ascribed to the dispersion of the drug within the carrier matrix resulting in the loss of crystalline form.

Physical mixtures of succinylsulphathiazole with the polymer (figure 4.18) resulted in the absence of melting endotherms corresponding to the drug as seen in the thermograms for the solid dispersion. The analysis was followed up by DSC at scan rate of 10 °C/min containing 20%, 30% and 40% (w/w) drug and resulted in a single peak corresponding to the melting of the polymer (figure 4.19).

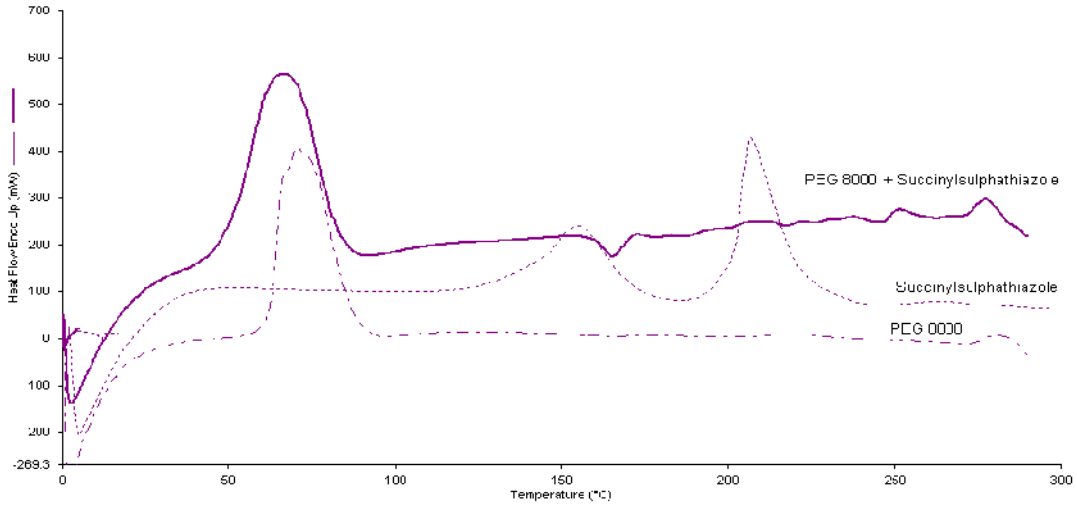

Figure 4.17. Hyper-DSC thermograms of solid dispersion consisting of 15% (w/w) succinylsulphathiazole, succinylsulphathiazole alone and PEG 8000.

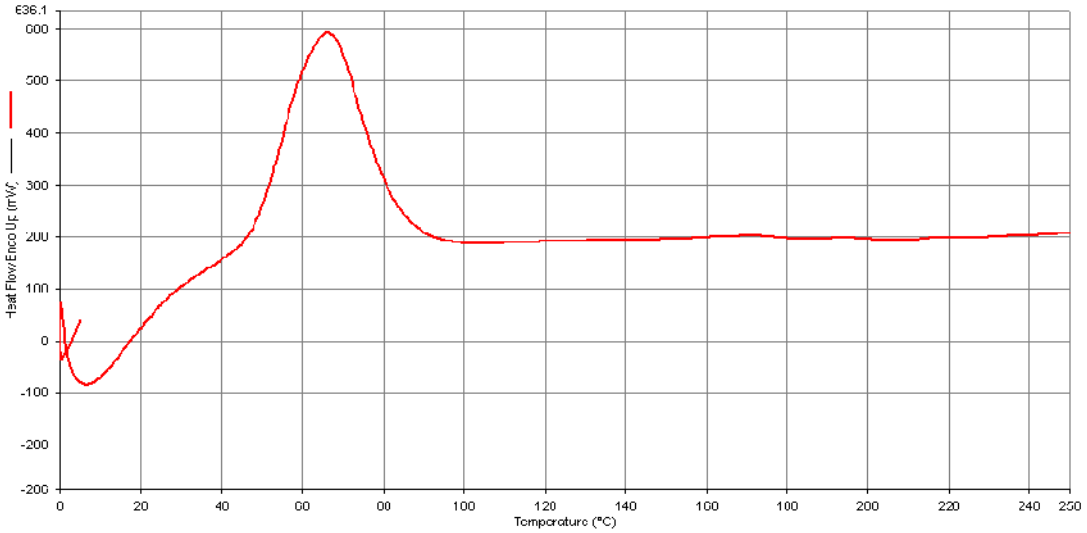

Figure 4.18. Hyper-DSC thermograms of physical mixture consisting of 15% (w/w) succinylsulphathiazole and PEG 8000.

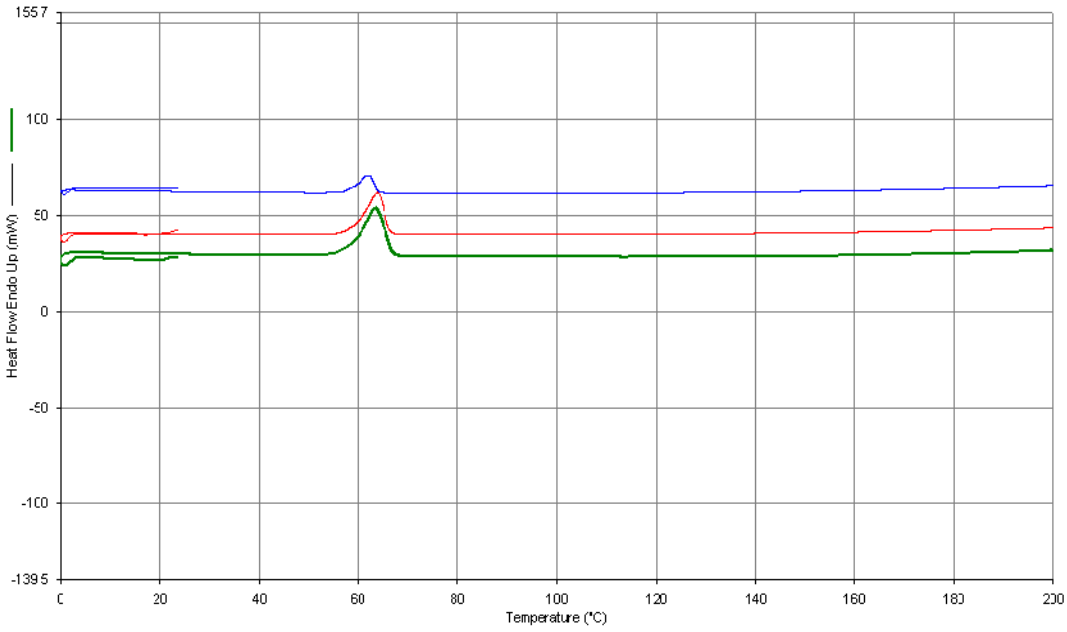

Figure 4.19. DSC thermograms of physical mixture consisting of 20%, 30% and 40% (w/w) (bottom to top) succinylsulphathiazole and PEG 8000.

Table 4.1 shows the summary of melting onset for Drug alone, drug-PEG 8000 15% (w/w) solid dispersion, PEG 8000 alone and physical mixture 15% (w/w) drug-PEG 8000 during DSC studies.

Table 4.1. DSC study of indomethacin, phenacetin, paracetamol, phenylbutazone chloramphenicol, sulphamethoxazole, succinylsulphathiazole, PEG 8000, solid dispersions 15% (w/w) drug-PEG 8000 and physical mixture 15% (w/w) of drug-PEG 8000.

Drug alone, drug-PEG 8000 15% (w/w) solid dispersion, PEG 8000 alone and physical mixture 15% (w/w) drug-PEG 8000	Melting onset
Indomethacin	159.79 °C
Indomethacin - PEG 8000 (15%:85%) solid dispersion	59.70 °C
PEG 8000	59.13 °C
Indomethacin - PEG 8000 (15%:85%) physical mixture	55.25°C
Phenacetin	133.38 °C
Phenacetin- PEG 8000 (15%:85%) solid dispersion	60.35 °C
PEG 8000	59.13 °C
Phenacetin- PEG 8000 (15%:85%) physical mixture	59 °C; 130.47°C
Paracetamol	166.71 °C
Paracetamol-PEG 8000 (15%:85%) solid dispersion	59.97 °C
PEG 8000	59.13 °C
Paracetamol-PEG 8000 (15%:85%) physical mixture	59 °C; 161.17°C
Phenylbutazone	107.70 °C
Phenylbutazone- PEG 8000 (15%:85%) solid dispersion	60.52 °C
PEG 8000	59.13 °C
Phenylbutazone- PEG 8000 (15%:85%) physical mixture	55.53°C
Chloramphenicol	150.48 °C
Chloramphenicol- PEG 8000 (15%:85%) solid dispersion	59.22 °C
PEG 8000	59.13 °C
Chloramphenicol- PEG 8000 (15%:85%) physical mixture	150.47°C
Sulphamethoxazole	167.22 °C
Sulphamethoxazole- PEG 8000 (15%:85%) solid dispersion	59.01 °C
PEG 8000	59.13 °C
Sulphamethoxazole- PEG 8000 (15%:85%) physical mixture	56.55°C
Succinylsulphathiazole	200.68 °C
Succinylsulphathiazole- PEG 8000 (15%:85%) solid dispersion	58.32 °C
PEG 8000	59.13 °C
Succinylsulphathiazole- PEG 8000 (15%:85%) physical mixture	53.18°C

Investigation of the heating scans of solid dispersion for all the drugs investigated showed melting peak for the polymer at around 59 °C with no endothermic peak corresponding to the drug. The absence of a peak at temperatures corresponding to the melting of the drug could potentially be assigned to the solubilisation and distribution of the drug within the hydrophilic polymer matrix resulting in the conversion of crystalline drug form into amorphous form. Similar phenomena have also previously been reported and shown by various researchers (Craig et al. 1991; Guyot et al. 1995; Damian et al. 2000).

DSC scans for the physical mixture revealed an interesting profile. Physical mixtures of phenacetin and paracetamol with the polymer (figures 4.5 and 4.7) showed two transitions: the first corresponding to the melt of the polymer and the second due to the melting of the drug. However, physical mixtures of indomethacin, phenylbutazone, chloramphenicol, sulphamethoxazole and succinylsulphathiazole with the polymer (figures 4.2, 4.9, 4.12, 4.15 and 4.18) resulted in the absence of melting endotherm corresponding to the drug as seen in the thermograms for the solid dispersion.

In order to further investigate the differences in thermal behavior of the physical mixtures (presence and absence of drug endotherms), the samples were subjected to infra red analysis to determine the possibility of any molecular interactions between the two excepients. These results are similar to those presented by Frances et al. (1991) which involved analysis of ciprofloxacin-PEG 6000 physical mixtures and are also similar to the

effects found by Dordunoo et al. (1991) for triamterene and temazepam-PEG physical mixtures.

4.3.2 Fourier transform infrared spectroscopy (FTIR)

In order to further characterise possible interactions between the drug and the polymeric carrier infrared spectra were recorded. Four different spectra comprising of drug only, polymer only, physical mixture of the drug 15% (w/w) with polymer and solid dispersion 15% (w/w) of the drug with the polymer were recorded for each of the drugs investigated.

4.3.2.1 FTIR spectra of polymer alone, indomethacin alone, solid dispersion 15% (w/w) (indomethacin-PEG 8000) and physical mixture 15% (w/w) of indomethacin-PEG 8000

The infra red spectra for the polymer (figure 4.20a) was characterised by sharp peaks at 3450, 2891 and 1148 cm^{-1} corresponding to the stretching associated with O-H, C-H and C-O bonds respectively. The IR spectra for indomethacin (figure 4.20b) was characterised by sharp transition occurring at 2965, 1716, 1612 and 1479 cm^{-1} corresponding to the bond stretching associated with O-H, C=O, NH and C-C bonds respectively. Analysis of the spectra for both the physical mixture (figure 4.20c) as well as the solid dispersion of indomethacin (figure 4.20d) did not reveal any changes for the specific absorption bands for both the polymer as well as the drug suggesting a lack of interaction between the two moieties. Reproducibility of the spectra characteristic of PEG 8000 and indomethacin when analysed as a physical mixture as well as solid dispersion suggested the absence of any interactions between indomethacin and PEG 8000.

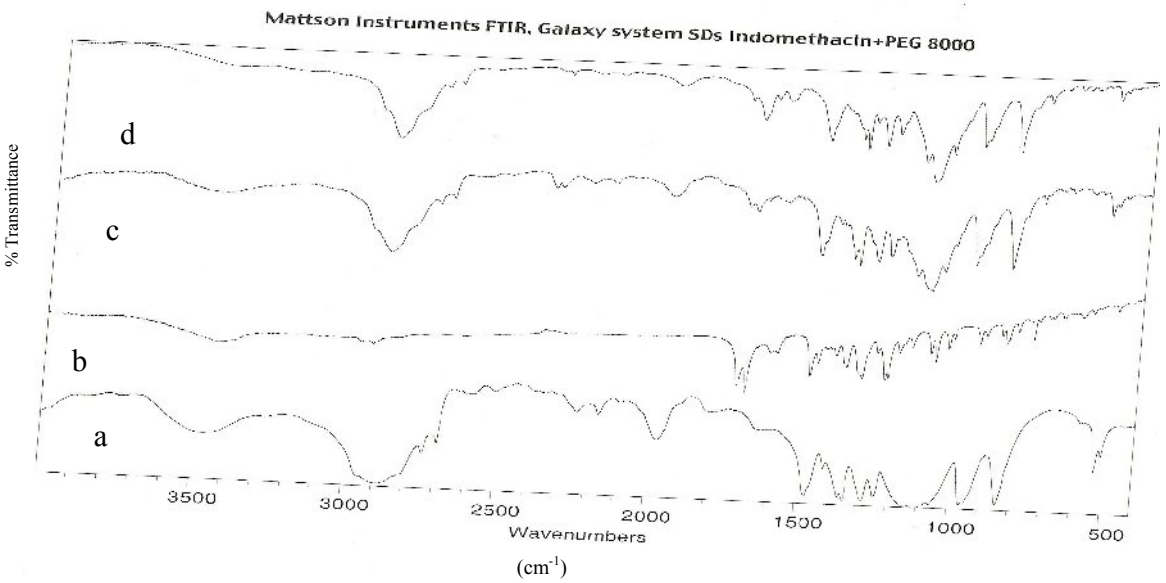

Figure 4.20. Fourier transform infrared spectra of (bottom to top): (a) PEG 8000, (b) indomethacin, (c) physical mixture of PEG 8000 and indomethacin and (d) Solid dispersion of PEG 8000 and indomethacin.

4.3.2.2 FTIR spectra of polymer alone, phenacetin alone, solid dispersion 15% (w/w) (phenacetin-PEG 8000) and physical mixture 15% (w/w) of phenacetin-PEG 8000

The infra red spectra for the polymer (figure 4.21a) was characterised by sharp peaks at 3450, 2891 and 1148 cm^{-1} corresponding to the stretching associated with O-H, C-H and C-O bonds respectively. Analysis of spectra for phenacetin (figure 4.21b) showed specific absorption bands at wave numbers 3286, 2928, 1267 and 838 cm^{-1} corresponding to the stretching associated with N-H, C-H, C-N and C-H respectively. However, infra red spectra for both the physical mix (Figure 4.21c) as well as the solid dispersion for phenacetin (figure 4.21d) showed broadening of peaks at 3286 cm^{-1} associated with N-H in the presence of PEG 8000. The broadening of these peaks (3450 cm^{-1} for PEG associated with O-H) clearly suggests the formation of hydrogen bond (Den et al., 1998) between the lone pair of electrons in the nitrogen atom and the hydrogen atom.

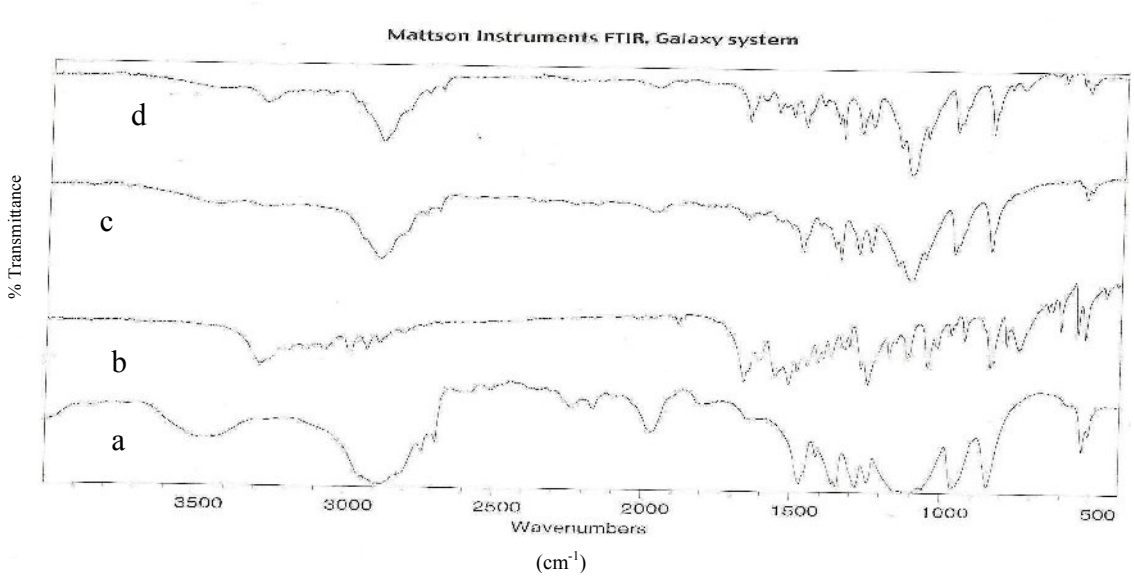

Figure 4.21. Fourier transform infrared spectra of (bottom to top): (a) PEG 8000, (b) phenacetin, (c) physical mixture of PEG 8000 and phenacetin and (d) Solid dispersion of PEG 8000 and phenacetin.

4.3.2.3 FTIR spectra of polymer alone, paracetamol alone, solid dispersion 15% (w/w) (paracetamol-PEG 8000) and physical mixture 15% (w/w) of paracetamol-PEG 8000

The infra red spectra for the polymer (figure 4.22a) was characterised by sharp peaks at 3450, 2891 and 1148 cm^{-1} corresponding to the stretching associated with O-H, C-H and C-O bonds respectively. Analysis of spectra for paracetamol (figure 4.22b) showed specific absorption bands at wave numbers 3324, 3289 and 1225 cm^{-1} corresponding to the stretching associated with O-H, N-H and C-O respectively. However, infra red spectra for the physical mix (figure 4.22c) as well as the solid dispersion for paracetamol (figure 4.22d) showed broadening of peaks at 3450 cm^{-1} associated with O-H group in PEG 8000 and 3289 cm^{-1} associated with N-H group in paracetamol suggesting the formation of hydrogen bond between the two groups (Den et al., 1998).

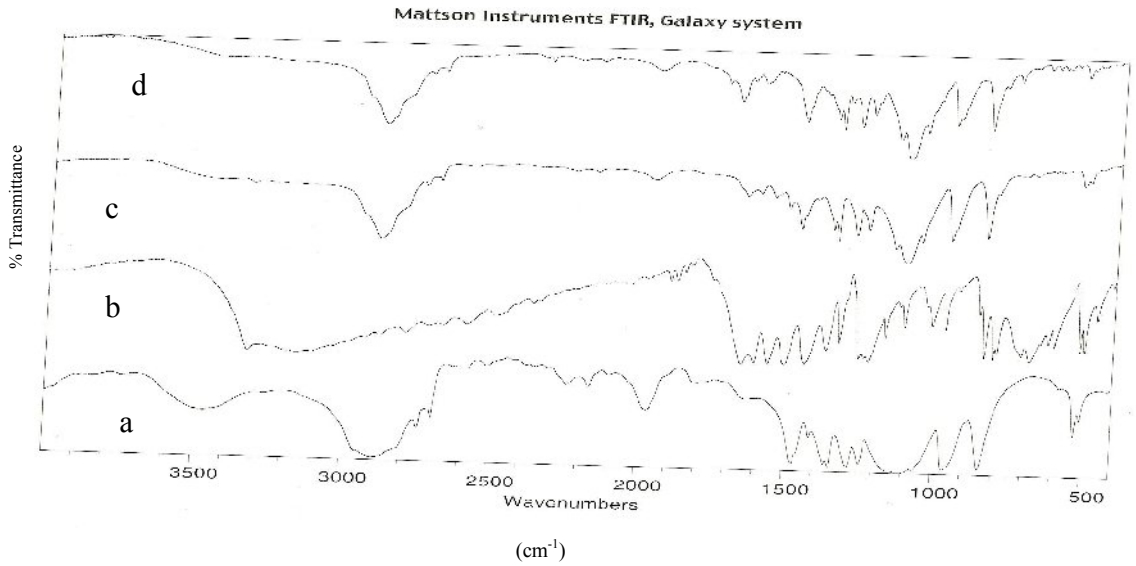

Figure 4.22. Fourier transform infrared spectra of (bottom to top): (a) PEG 8000, (b) paracetamol, (c) physical mixture of PEG 8000 and paracetamol and (d) Solid dispersion of PEG 8000 and paracetamol.

4.3.2.4 FTIR spectra of polymer alone, phenylbutazone alone, solid dispersion 15% (w/w) (phenylbutazone-PEG 8000) and physical mixture 15% (w/w) of phenylbutazone-PEG 8000

The infra red spectra for the polymer (figure 4.23a) was characterised by sharp peaks at 3450, 2891 and 1148 cm^{-1} corresponding to the stretching associated with O-H, C-H and C-O bonds respectively. The IR spectra for phenylbutazone (figure 4.23b) was characterised by sharp transition occurring at 2956, 1752, 1325, 898 and 694 cm^{-1} corresponding to the bond stretching associated with C-H, C=O, C-N, C-H and C-H bonds respectively. Analysis of the spectra for both the physical mixture (figure 4.23c) as well as the solid dispersion of phenylbutazone (figure 4.23d) did not reveal any changes for the specific absorption bands for both the polymer as well as the drug suggesting a lack of interaction between the two moieties.

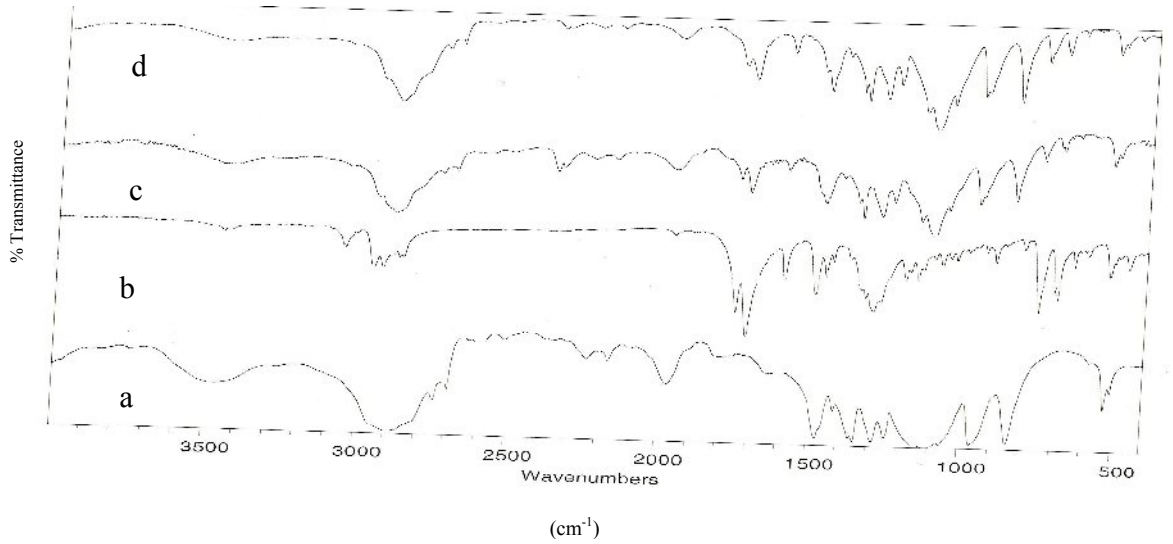

Figure 4.23. Fourier transform infrared spectra of (bottom to top): (a) PEG 8000, (b) phenylbutazone, (c) physical mixture of PEG 8000 and phenylbutazone and (d) Solid dispersion of PEG 8000 and phenylbutazone.

4.3.2.5 FTIR spectra polymer alone, chloramphenicol alone, solid dispersion 15% (w/w) (chloramphenicol-PEG 8000) and physical mixture 15% (w/w) of chloramphenicol- PEG 8000

The infra red spectra for the polymer (figure 4.24a) was characterised by sharp peaks at 3450, 2891 and 1148 cm^{-1} corresponding to the stretching associated with O-H, C-H and C-O bonds respectively. The IR spectra for chloramphenicol (figure 4.24b) was characterised by sharp transition occurring at 3466, 3347, 3259, 1686, 1563, 1348, 1107, 845 and 656 cm^{-1} corresponding to the bond stretching associated with O-H alcohol, N-H amide, N-H, C=O carbonyl, C-C ring, N-O nitro compound, C-N aliphatic amine, C-H aromatic and C-Cl alkyl halide bonds respectively. Analysis of the spectra for both solid dispersion (figure 4.24a) as well as the physical mixture of chloramphenicol (figure 4.24c) did not reveal any changes for the specific absorption bands for both the polymer as well as the drug suggesting that there is no interaction between the two groups.

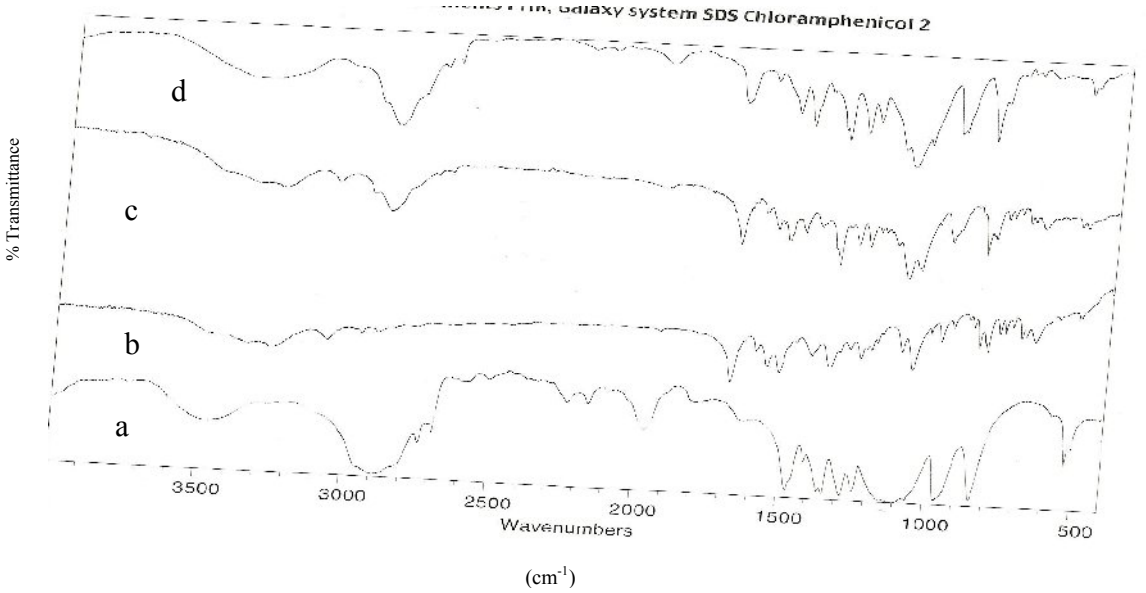

Figure 4.24. Fourier transform infrared spectra of (bottom to top): (a) PEG 8000, (b) chloramphenicol, (c) physical mixture of PEG 8000 and chloramphenicol (d) Solid dispersion of PEG 8000 and chloramphenicol.

4.3.2.6 FTIR spectra of polymer alone, sulphamethoxazole alone, solid dispersion 15% (w/w) (sulphamethoxazole-PEG 8000) and physical mixture 15% (w/w) of sulphamethoxazole-PEG 8000

The infra red spectra for the polymer (figure 4.25a) was characterised by sharp peaks at 3450, 2891 and 1148 cm^{-1} corresponding to the stretching associated with O-H, C-H and C-O bonds respectively. Analysis of spectra for sulphamethoxazole (figure 4.25b) showed absorption bands at wave numbers 3467, 1621, 1596 and 1144 cm^{-1} corresponding to the presence of H-bonding, N-H amine, C-C aromtic ring and N-H aliphatic amine respectively. Analysis of the spectra for both solid dispersion (figure 4.25d) as well as the physical mixture of sulphamethoxazole (figure 4.25c) did not reveal any changes for the specific absorption bands for both the polymer as well as the drug suggesting that there is no interaction between the two groups.

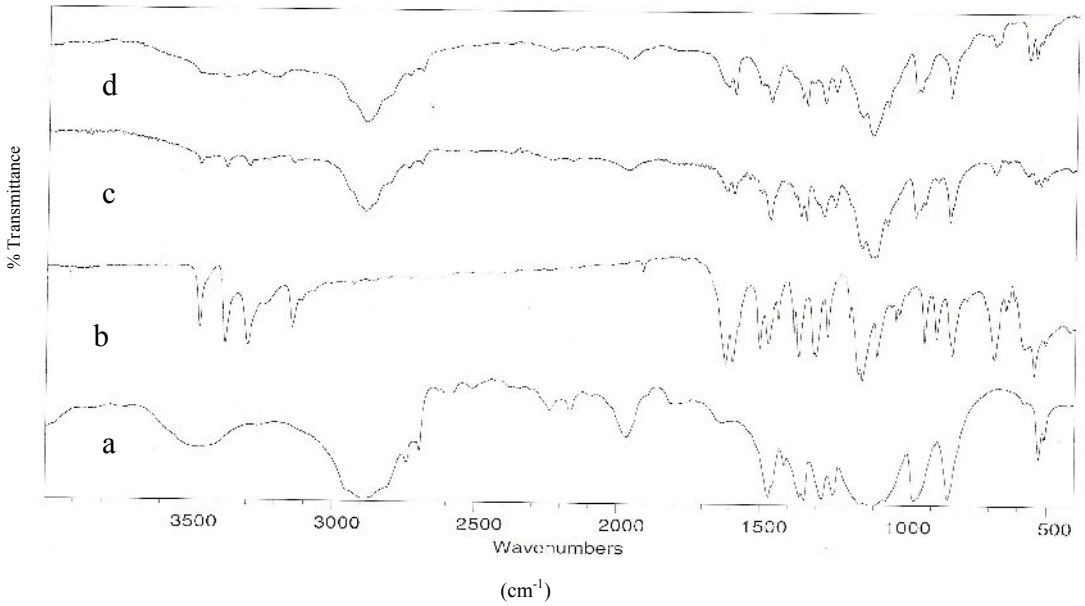

Figure 4.25. Fourier transform infrared spectra of (bottom to top): (a) PEG 8000, (b) sulphamethoxazole, (c) physical mixture of PEG 8000 and sulphamethoxazole (d) Solid dispersion of PEG 8000 and sulphamethoxazole.

4.3.2.7 FTIR spectra of polymer alone, succinylsulphathiazole alone, solid dispersion 15% (w/w) (succinylsulphathiazole-PEG 8000) and physical mixture 15% (w/w) of succinylsulphathiazole-PEG 8000

The infra red spectra for the polymer (figure 4.26a) was characterised by sharp peaks at 3450, 2891 and 1148 cm^{-1} corresponding to the stretching associated with O-H, C-H and C-O bonds respectively. Analysis of spectra for succinylsulphathiazole (figure 4.26b) showed specific absorption bands at wave numbers 3471, 2945 and 842 cm^{-1} corresponding to the stretching associated with H-bonding, O-H and C-H respectively. Analysis of the spectra for both solid dispersion (figure 4.26d) as well as the physical mixture of succinylsulphathiazole (figure 4.26c) did not reveal any changes for the

specific absorption bands for both the polymer as well as the drug suggesting that there is no interaction between the two components.

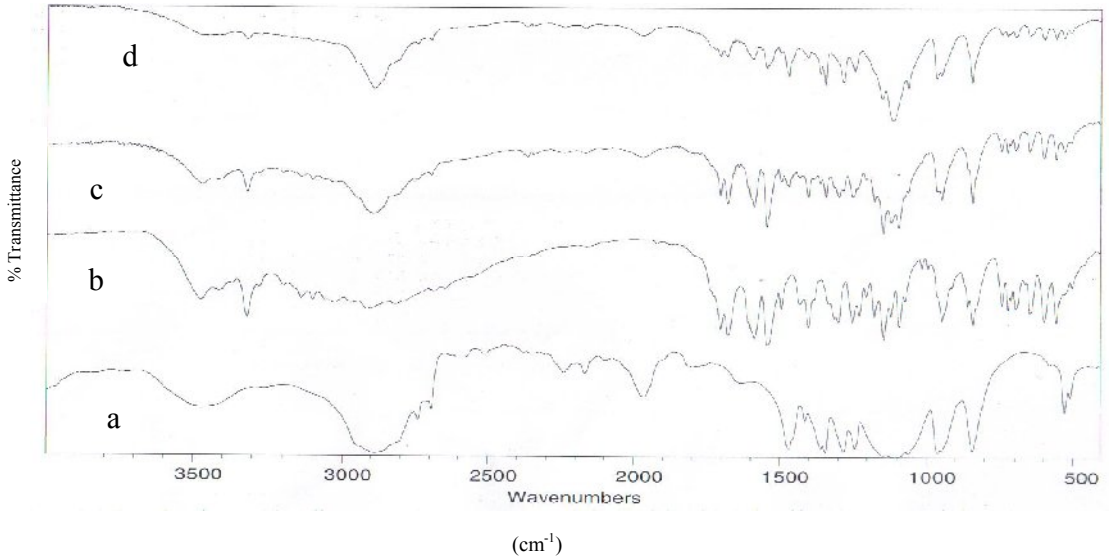

Figure 4.26. Fourier transform infrared spectra of (bottom to top): (a) PEG 8000, (b) succinylsulphathiazole, (c) physical mixture of PEG 8000 and succinylsulphathiazole (d) Solid dispersion of PEG 8000 and succinylsulphathiazole.

The formation of hydrogen bond (Den et al., 1998) between the drug (paracetamol and phenacetin) with the polymer even as a physical mixture could possibly explain the DSC scans reported above. It may be possible that lower temperatures fail to break the strong hydrogen bonding association between the drug and the polymer whereby the mixing of the two components during the heating process of the DSC run is impeded as a result of which two distinct peaks corresponding to the melt of the polymer and the drug were obtained. However, the formulation of solid dispersions of these drugs which is characterised by continuous heating at a temperature above which both the polymer as well as the drug melt and the supplementation of the process with continuous stirring would explain the lack of peak in the DSC scans characteristic of the drug suggesting the drug to be in a dispersed amorphous state.

4.3.3 Scanning electron microscopy

Scanning electron microscopy (SEM) at different magnifications was used for investigating the morphological differences of samples (drugs, PEG 8000, physical mixtures and solid dispersions) and to further explain the DSC results.

4.3.3.1 SEM of PEG 8000

Figure 4.27 reveals that PEG 8000 exists as irregularly shaped particles as previously reported (Badens et al., 2009).

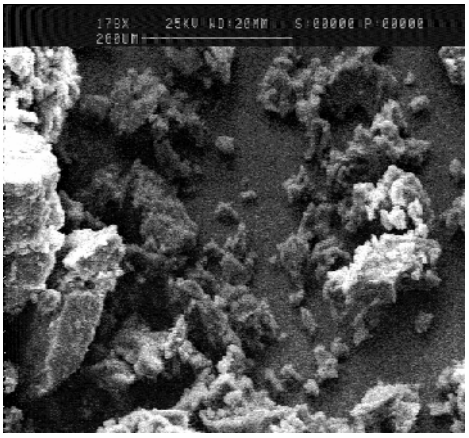

Figure 4.27. Scanning electron microphotograph of PEG 8000

4.3.3.2 SEM of indomethacin alone, solid dispersion 15% (w/w) (indomethacin-PEG 8000) and physical mixture 15% (w/w) of indomethacin-PEG 8000

Figure 4.28 reveals that indomethacin (figure 4.28a) showed plate-like crystals with irregular borders (Bandi et al., 2004). The physical mixture of the indomethacin with PEG 8000 (figure 4.28b) showed the presence of drug attached on the surface of carrier (not dispersed in the carrier completely) which is justified by DSC results in physical mixtures. On the other hand, the photomicrographs of the solid dispersion (figure 4.28c) show that indomethacin might have dispersed in the carrier. It is clear that morphological

differences are seen between indomethacin alone, physical mixture and solid dispersion. These observations show that the determinations from DSC study are justified from SEM studies.

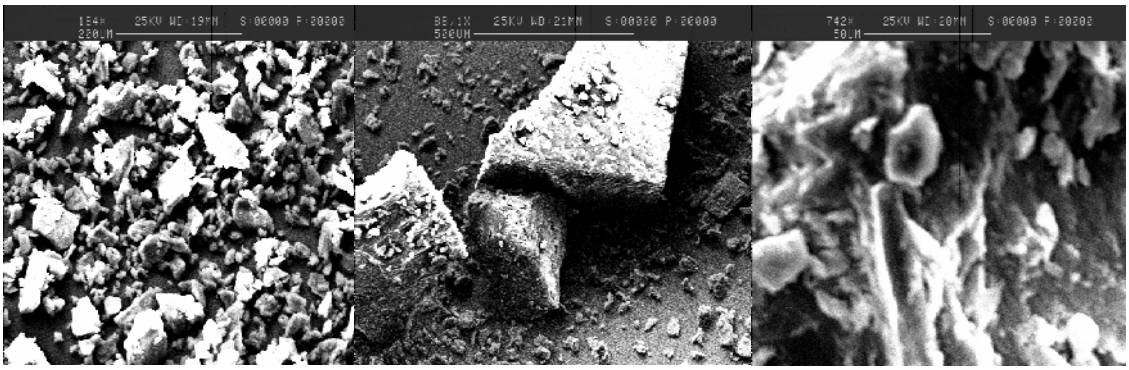

a **b** **c**

Figure 4.28. Scanning electron microphotographs of (a) indomethacin alone; (b) physical mixture of PEG 8000-indomethacin binary systems with 15% (w/w) drug content; (c) solid dispersion of indomethacin binary system with 15% (w/w) drug content.

4.3.3.3 SEM of phenacetin alone, solid dispersion 15% (w/w) (phenacetin-PEG 8000) and physical mixture 15% (w/w) of phenacetin-PEG 8000

Figure 4.29 reveals that phenacetin (figure 4.29a) consists of rod shaped crystals. The physical mixture of phenacetin with the carrier (figure 4.29b) showed that the drug was in crystalline form. On the other hand, the photomicrographs of the solid dispersion (figure 4.29c) showed that phenacetin might have dispersed in the carrier.

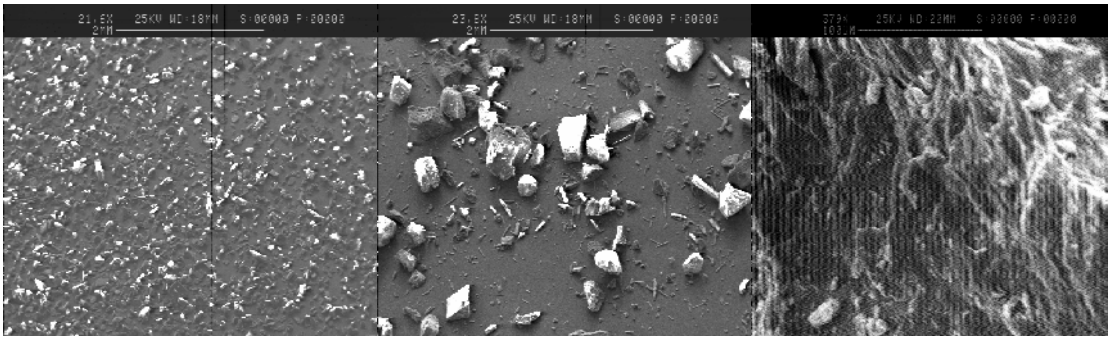

a **b** **c**

Figure 4.29. Scanning electron microphotographs of (a) phenacetin alone; (b) physical mixture of PEG 8000-phenacetin binary systems with 15% (w/w) drug content; (c) solid dispersion of phenacetin binary system with 15% (w/w) drug content.

4.3.3.4 SEM of paracetamol alone, solid dispersion 15% (w/w) (paracetamol-PEG 8000) and physical mixture 15% (w/w) of paracetamol-PEG 8000

Figure 4.30 reveals that paracetamol (figure 4.30a) SEM images were composed of irregular shaped particles and included cumulations of fine particles (Hirokazu et al., 2005). The physical mixture of paracetamol with the carrier (figure 4.30b) showed that the drug was in the crystalline form. However, the photomicrographs of the solid dispersion (figure 4.30c) showed that paracetamol might have dispersed in the carrier.

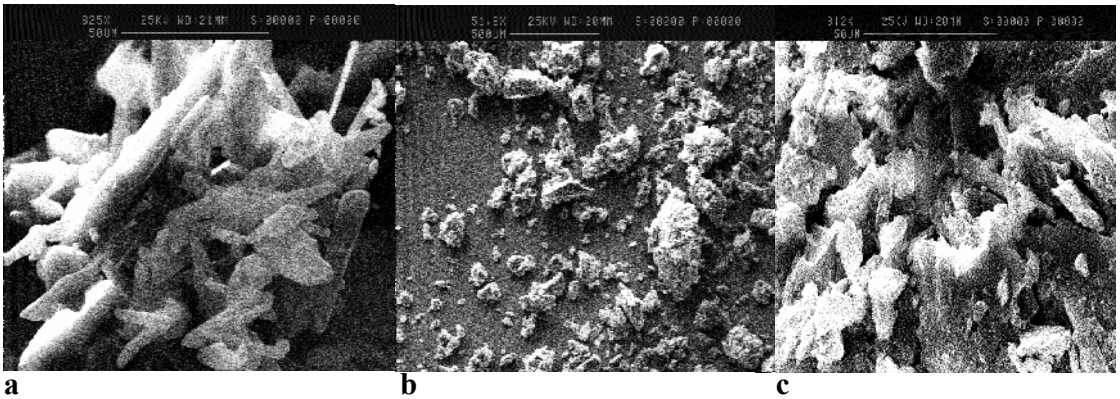

a **b** **c**

Figure 4.30. Scanning electron microphotographs of (a) paracetamol alone; (b) physical mixture of PEG 8000-paracetamol binary systems with 15% (w/w) drug content; (c) solid dispersion of paracetamol binary system with 15% (w/w) drug content.

4.3.3.5 SEM of phenylbutazone alone, solid dispersion 15% (w/w) (phenylbutazone-PEG 8000) and physical mixture 15% (w/w) of phenylbutazone-PEG 8000

Figure 4.31 reveals that phenylbutazone (figure 4.31a) consists of needle shaped crystals (Beretzky et al., 2002). The physical mixture of phenylbutazone with PEG 8000 (figure 4.31b) showed the presence of drug attached on the surface of carrier (not dispersed in the carrier completely) as explained by DSC results of physical mixtures. On the other hand, the photomicrographs of the solid dispersion (figure 4.31c) showed that phenylbutazone might have dispersed within the carrier.

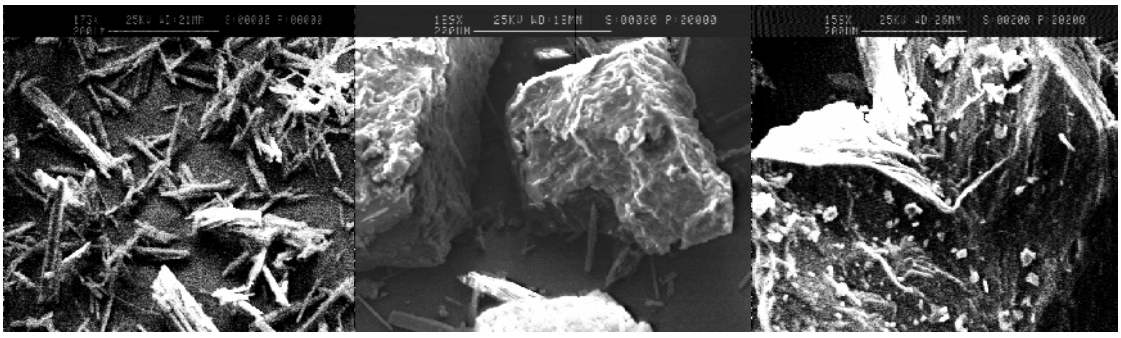

a **b** **c**

Figure 4.31. Scanning electron microphotographs of (a) phenylbutazone alone; (b) physical mixture of PEG 8000-phenylbutazone binary systems with 15% (w/w) drug content; (c) solid dispersion of phenylbutazone binary system with 15% (w/w) drug content.

4.3.3.6 SEM of chloramphenicol alone, solid dispersion 15% (w/w) (chloramphenicol-PEG 8000) and physical mixture 15% (w/w) of chloramphenicol-PEG 8000

Figure 4.32 reveals that chloramphenicol SEM (figure 4.32a) was composed of irregular shaped particles. The physical mixture of chloramphenicol with PEG 8000 (figure 4.32b) showed the presence of drug attached on the surface of the carrier. Solid dispersion

(figure 4.32c) SEM showed that the drug might have dispersed within the carrier matrix which further supported DSC results.

a **b** **c**

Figure 4.32. Scanning electron microphotographs of (a) chloramphencol alone; (b) physical mixture of PEG 8000- chloramphencol binary systems with 15% (w/w) drug content; (c) solid dispersion of chloramphencol binary system with 15% (w/w) drug content.

4.3.3.7 SEM of sulphamethoxazole alone, solid dispersion 15% (w/w) (sulphamethoxazole-PEG 8000) and physical mixture 15% (w/w) of sulphamethoxazole-PEG 8000

Figure 4.33 reveals that sulphamethoxazole (figure 4.33a) consists of rod shaped crystals. The physical mixture of sulphamethoxazole with PEG 8000 (figure 4.33b) showed the presence of drug attached on the surface of carrier. The photomicrographs of solid dispersion (figure 4.33c) showed that sulphamethoxazole might have dispersed in the carrier. SEM images reveal morphological differences between sulphamethoxazole, physical mixture and solid dispersion.

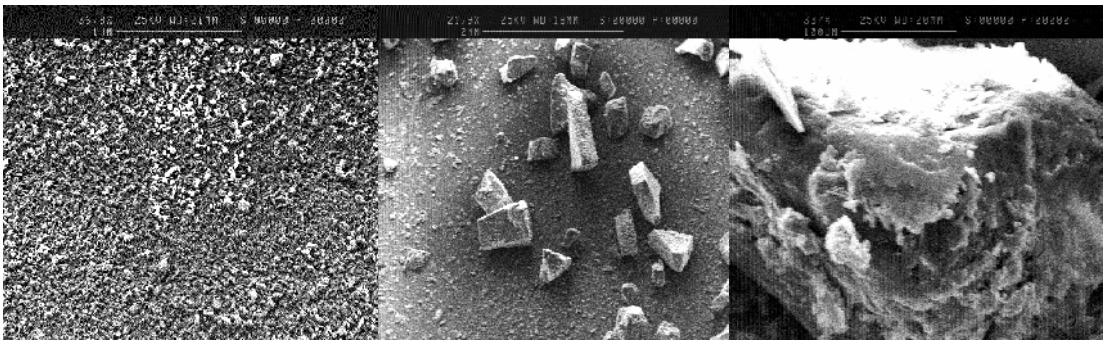

a **b** **c**

Figure 4.33. Scanning electron microphotographs of (a) sulphamethoxazole alone; (b) physical mixture of PEG 8000- sulphamethoxazole binary systems with 15% (w/w) drug content; (c) solid dispersion of sulphamethoxazole binary system with 15% (w/w) drug content.

4.3.3.8 SEM of succinylsulphathiazole alone, solid dispersion 15% (w/w) (succinylsulphathiazole-PEG 8000) and physical mixture 15% (w/w) of succinylsulphathiazole-PEG 8000

Figure 4.34 reveals that succinylsulphathiazole (figure 4.34a) showed plate-like crystals with irregular borders. The physical mixture of the drug with PEG 8000 (figure 4.34b) showed the presence of drug attached on the surface of carrier (not dispersed in the carrier completely) which was justified by DSC results of physical mixtures. On the other hand, the photomicrographs of the solid dispersion (figure 4.34c) show that succinylsulphathiazole might have dispersed in the carrier. These observations show that the results from DSC study are justified from SEM studies.

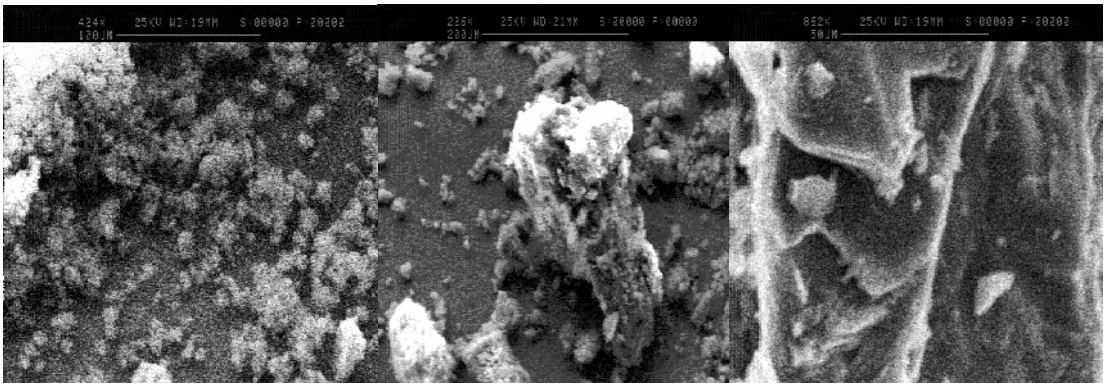

a **b** **c**

Figure 4.34. Scanning electron microphotographs of (a) succinylsulphathiazole alone; (b) physical mixture of PEG 8000- succinylsulphathiazole binary systems with 15% (w/w) drug content; (c) solid dispersion of succinylsulphathiazole binary system with 15% (w/w) drug content.

The physical mixture of paracetamol (figure 4.30b) and phenacetin (figure 4.29b) with the carrier showed that the drug was in crystalline form. Similar results were obtained with indomethacin (figure 4.28b), phenylbutazone (figure 4.31b), chloramphenicol (figure 4.32b), sulphamethoxazole (figure 4.33b) and succinylsulphathiazole (figure 4.34b) with PEG 8000 with the drug attached on the surface of carrier (not dispersed in the carrier completely) which was justified by DSC results in physical mixtures. On the other hand, the photomicrographs of the solid dispersion (figures 4.28c-34c) show that drugs might have dispersed in the carrier. It is clear that morphological differences were seen between different drugs, physical mixtures and solid dispersions. All drug molecules must be dispersed or soluble or particle size reduced in the solid dispersions without crystal formation in order to enhance the dissolution profile (Al-Angary et al., 1996). These observations also exhibit that the results from DSC study are tenable. SEM studies further suggested that the surface properties of all drugs and PEG 8000 were lost during the formation of solid dispersion system by melting and solidification resulting in the dispersion of the drug molecules within the carrier matrix. Furthermore, these results also

substantiate an enhancement in dissolution profile of the drug candidates possibly due to dispersion of the drug molecules and the absence of any crystalline particles characterised by the prominent absence of the endotherm specific to the drug candidate during thermal analysis of solid dispersions using DSC.

4.3.4 Solubility

The solubility of solid dispersions of indomethacin, phenacetin, paracetamol, phenylbutazone, chloramphenicol, sulphamethoxazole and succinylsulphathiazole were compared to physical mixture and pure drug to further evaluate the affect of PEG 8000.

4.3.4.1 Solubility of indomethacin alone, solid dispersion 15% (w/w) (indomethacin-PEG 8000) and physical mixture 15% (w/w) of indomethacin-PEG 8000

The solubility of the indomethacin from solid dispersions, physical mixtures and indomethacin alone were 33.14±0.93 µg/mL, 5.28±1.13 µg/mL and 1.02±0.45 µg/mL in phosphate buffer saline. As expected the solubility was higher in solid dispersion as compared to physical mixture and drug alone. This may be due to the amorphous form of indomethacin or dispersion of the indomethacin in the PEG 8000 resulting in its higher wettability (Teresa et al., 2002). In case of physical mixture higher solubility value (as compared to indomethacin alone) was due the presence of PEG 8000 which enhanced wettability of the drug.

4.3.4.2 Solubility of phenacetin alone, solid dispersion 15% (w/w) (phenacetin-PEG 8000) and physical mixture 15% (w/w) of phenacetin-PEG 8000

The solubility of the phenacetin from solid dispersions, physical mixtures and phenacetin alone were 69.44±2.27 µg/mL, 10.47±0.63 µg/mL and 7.42±0.56 µg/mL in phosphate buffer saline. As expected the solubility was higher in solid dispersion as compared to physical mixture and drug alone. This may be due to the amorphous form of phenacetin in solid dispersion as confirmed by DSC studies. In case of physical mixture higher solubility value (as compared to phenacetin alone) was due the presence of PEG 8000 which enhanced wettability of the drug in the mixtures.

4.3.4.3 Solubility of paracetamol alone, solid dispersion 15% (w/w) (paracetamol-PEG 8000) and physical mixture 15% (w/w) of paracetamol-PEG 8000

The solubility of the paracetamol from solid dispersions, physical mixtures and paracetamol alone were 82.15±4.90 µg/mL, 30.53±4.49 µg/mL and 21.6±3.11 µg/mL in phosphate buffer saline. As expected the solubility was higher in solid dispersion as compared to physical mixture and drug alone. This may be due to the amorphous form of paracetamol in solid dipsersion.

4.3.4.4 Solubility of phenylbutazone alone, solid dispersion 15% (w/w) (phenylbutazone-PEG 8000) and physical mixture 15% (w/w) of phenylbutazone-PEG 8000

The solubility of the phenylbutazone from solid dispersions, physical mixtures and phenylbutazone alone were 44.68±2.7 µg/mL, 9.97±1.24 µg/mL and 6.34±0.68 µg/mL in

phosphate buffer saline. The higher solubility of the solid dispersion may be due to the amorphous form of phenylbutazone or dispersion of the phenylbutazone in the PEG 8000 resulting in its higher wettability. The slight increase in solubility of the physical mixture was possibly due to the presence of PEG 8000 which enhanced wettability of the drug as compared to phenylbutazone alone.

4.3.4.5 Solubility of chloramphenicol alone, solid dispersion 15% (w/w) (chloramphenicol-PEG 8000) and physical mixture 15% (w/w) of chloramphenicol-PEG 8000

The solubility of the chloramphenicol from solid dispersions, physical mixtures and chloramphenicol alone were 75.60±6.23 µg/mL, 27.80±4.78 µg/mL and 15.78±1.18 µg/mL in phosphate buffer saline. The solubility of chloramphenicol was higher in solid dispersion as compared to physical mixture and drug alone. The increase in solubility of chloramphenicol when formulated as a solid dispersion may be due to the amorphous form of the drug.

4.3.4.6 Solubility of sulphamethoxazole alone, solid dispersion 15% (w/w) (sulphamethoxazole-PEG 8000) and physical mixture 15% (w/w) of sulphamethoxazole-PEG 8000

The solubility of the sulphamethoxazole from solid dispersions, physical mixtures and sulphamethoxazole alone were 68.66±4.48 µg/mL, 20.07±0.95 µg/mL and 13.02±0.99 µg/mL in phosphate buffer saline. As expected the solubility was higher in solid dispersion as compared to physical mixture and drug alone. This may be due to the

amorphous form of sulphamethoxazole or dispersion of the sulphamethoxazole in the PEG 8000 resulting in its higher wettability. In case of physical mixture higher solubility value was due the presence of PEG 8000 which enhanced wettability of the drug as compared to sulphamethoxazole alone.

4.3.4.7 Solubility of succinylsulphathiazole alone, solid dispersion 15% (w/w) (succinylsulphathiazole-PEG 8000) and physical mixture 15% (w/w) of succinylsulphathiazole-PEG 8000

The solubility of the succinylsulphathiazole from solid dispersions, physical mixtures and succinylsulphathiazole alone were 60.29±2.27 µg/mL, 10.26±1.22 µg/mL and 5.72±0.53 µg/mL in phosphate buffer saline. The increase in solubility for the solid dispersion may be due to the amorphous form of succinylsulphathiazole or dispersion of the succinylsulphathiazole in the PEG 8000 resulting in its higher wettability. In case of physical mixture higher solubility value was due the presence of PEG 8000 which enhanced wettability of the drug as compared to succinylsulphathiazole alone.

The solubility for solid dispersions of indomethacin, phenacetin, paracetamol, phenylbutazone, chloramphenicol, sulphamethoxazole, succinylsulphathiazole, their physical mixtures (drug-PEG 8000) and drug alone are shown in table 4.2. The solubility of physical mixtures of indomethacin, phenacetin, paracetamol, phenylbutazone, chloramphenicol, sulphamethoxazole and succinylsulphathiazole with PEG 8000 in phosphate buffer saline after 24 hrs was higher than pure drug. This process can be attributed in the physical mixtures to the wettability of all drugs in the presence of PEG

8000 even though the drugs are not dispersed in the carrier nor are in amorphous form. It can be noticed that the solubility of all drugs were enhanced in the solid dispersion followed by physical mixture and pure drug. In case of solid dispersions the increase in solubility is due to the amorphous form of drug or dispersion of the drug in the PEG 8000 resulting in its higher wettability as reported by Teresa et al. (2002). These results are in accordance with those of DSC and SEM data which suggested that solid dispersion of the drug results in loss of crystallinity which enhanced the solubility of the drug.

Table 4.2. Solubility for solid dispersions 15% (w/w) of indomethacin, phenacetin, paracetamol, phenylbutazone, chloramphenicol, sulphamethoxazole, succinylsulphathiazole, their physical mixtures 15% (w/w) (drug-PEG 8000) and drug alone in phosphate buffer saline. Data are expressed as mean±S.D.

Drug	Solid dispersions (µg/mL)±S.D	Physical mixtures (µg/mL)±S.D	Drug alone (µg/mL)±S.D
Indomethacin	33.14±0.93	5.28±1.13	1.02±0.45
Phenacetin	69.44±2.27	10.47±0.63	7.42±0.56
Paracetamol	82.15±4.90	30.53±4.49	21.6±3.11
Phenylbutazone	44.68±2.7	9.97±1.24	6.34±0.68
Chloramphenicol	75.60±6.23	27.80±4.78	15.78±1.18
Sulphamethoxazole	68.66±4.48	20.07±0.95	13.02±0.99
Succinylsulphathiazole	60.29±2.27	10.26±1.22	5.72±0.53

4.3.5 Isothermal titration calorimetry

Isothermal titration calorimetry (ITC) can determine the small changes of heat during reaction of drug and polymer (PEG 8000). The basic aim of using ITC technique was to detect binding of paracetamol and phenacetin to PEG 8000 in a physical mix as suggested from FTIR studies. Further more we tried to use ITC for the PEG 8000/drug interactions in a similar way as protein–protein or carbohydrate–protein interactions. To the best of

our knowledge, this is the first time that PEG 8000/ drugs (paracetamol, phenacetin, chloramphenicol and sulphamethoxazole) interactions have been explored in this way.

4.3.5.1 Thermodynamic analysis of paracetamol using ITC

Figure 4.35 shows the ITC curves of the binding of the PEG 8000 to paracetamol (A) at 25 °C. ITC data are shown in figure 4.35a, while a figure 4.35b shows a plot of the heat flow per mole of the titrant versus the molar ratio of the titrant to drugs for each injection, after subtraction of the background titration. It is observed that the binding of the PEG 8000 to paracetamol is exothermic process. The best fit for the integrated heat was obtained using a one binding site model. The binding constant K ($\times 10^{-3} M^{-1}$) of the paracetamol is -2.46E4±7.47E3. The stoichiometry (N) for the binding of a PEG 8000 monomer paracetamol is 1:1.

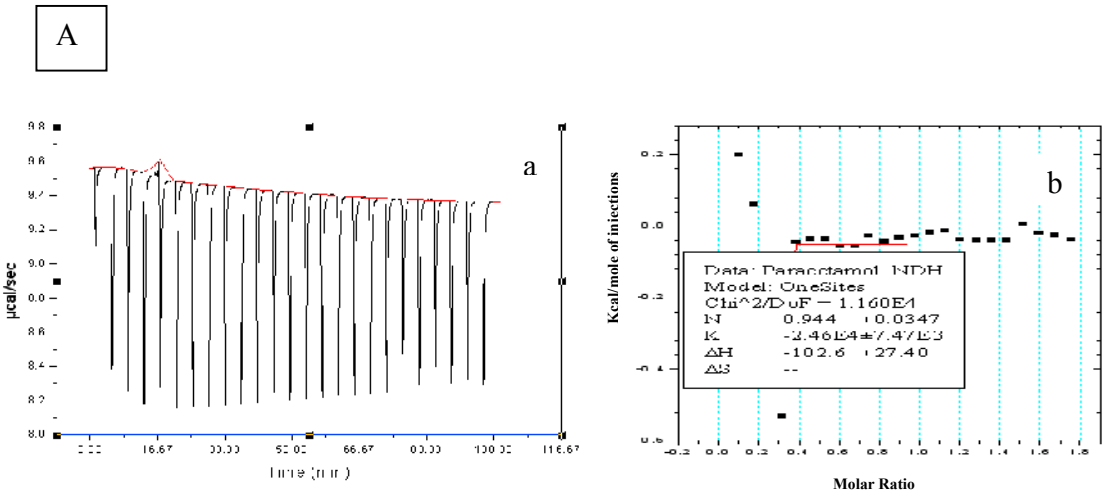

Figure 4.35. ITC data from the titration of 0.25mM paracetamol (A) in the presence of 2.5 mM Polyethylene glycol 8000 (PEG 8000). a: heat flow versus time during 25 injections of (PEG 8000) at 25°C (the first injection 2µL, subsequent ones 10µL each). b: heat evolved per mole of PEG 8000 added against the molar ratio of PEG 8000 to drug for each injection. (The data were fitted to a one- binding site model. ▪: the experimental data; -: the best fit).

4.3.5.2 Thermodynamic analysis of phenacetin using ITC

Figure 4.36 shows the ITC curves of the binding of PEG 8000 to phenacetin (B) at 25 °C. The ITC data are shown in figure 4.36a, while a figure 4.36b shows a plot of the heat flow per mole of the titrant versus the molar ratio of the titrant to drug for each injection, after subtraction of the background titration. As noted for paracetamol, the interaction between phenacetin and polymer was an exothermic process. The binding constant K ($\times 10^{-3}M^{-1}$) of phenacetin was -1.16E4±1. The stoichiometry (N) for the binding of a PEG 8000 monomer to phenacetin was 4:1. The value of N was high. Possible reason for the higher N value is that the PEG 8000 long chain might fold in such a way that its monomers are close enough to allow drug to bind both electrostatically and through H bonding (Helder et al., 2007).

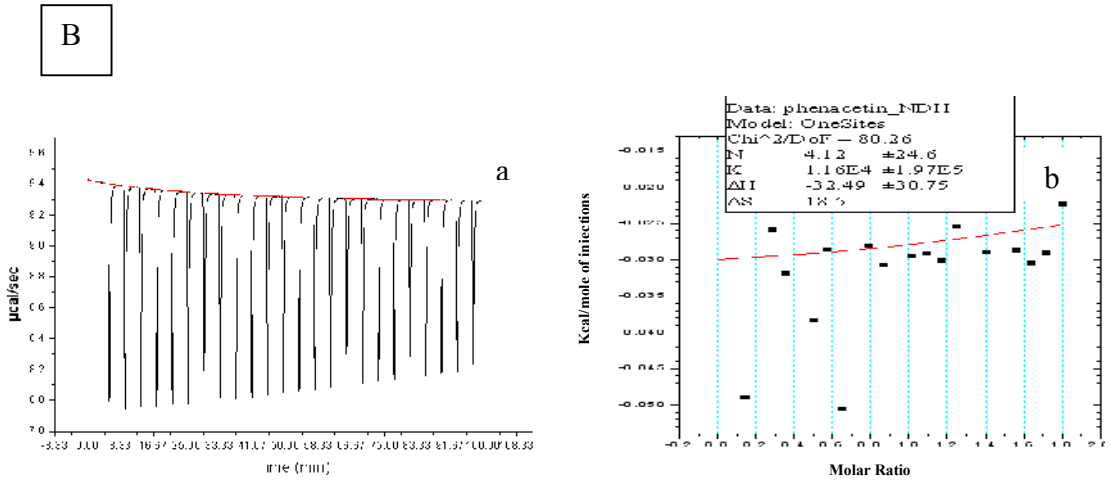

Figure 4.36. ITC data from the titration of 0.25mM phenacetin (B) in the presence of 2.5 mM Polyethylene glycol 8000 (PEG 8000). a: heat flow versus time during 25 injections of (PEG 8000) at 25°C (the first injection 2µL, subsequent ones 10µL each). b: heat evolved per mole of PEG 8000 added against the molar ratio of PEG 8000 to drug for each injection. (The data were fitted to a one- binding site model. ▪: the experimental data; -: the best fit).

4.3.5.3 Thermodynamic analysis of chloramphenicol using ITC

Figure 4.37 shows the ITC curves of the binding of PEG 8000 to chloramphenicol (C) at 25 °C. The ITC data are shown in figure 4.37a, while a figure 4.37b shows a plot of the heat flow per mole of the titrant versus the molar ratio of the titrant to drug for each injection, after subtraction of the background titration. The binding of PEG 8000 with chloramphenicol was exothermic. The binding constant K ($\times 10^{-3}M^{-1}$) of chloramphenicol was 4.48E4±1.53E5. The stoichiometry (N) for the binding of a PEG 8000 monomer to chloramphenicol was 2:1.

C

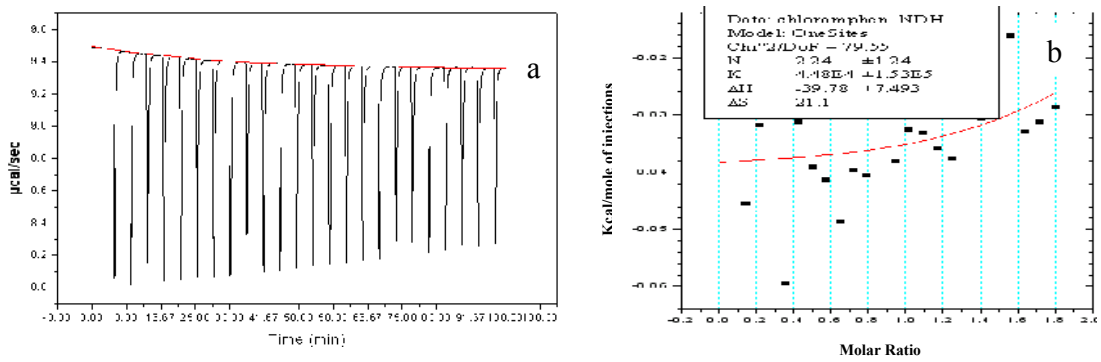

Figure 4.37. ITC data from the titration of 0.25mM chloramphenicol (C) in the presence of 2.5 mM Polyethylene glycol 8000 (PEG 8000). a: heat flow versus time during 25 injections of (PEG 8000) at 25°C (the first injection 2µL, subsequent ones 10µL each). b: heat evolved per mole of PEG 8000 added against the molar ratio of PEG 8000 to drug for each injection. (The data were fitted to a one- binding site model. ▪: the experimental data; -: the best fit).

4.3.5.4 Thermodynamic analysis of sulphamethoxazole using ITC

Figure 4.38 shows the ITC curves of the binding of PEG 8000 with sulphamethoxazole (D) at 25 °C. ITC data are shown in figure 4.38a, while a figure 4.38b shows a plot of the heat flow per mole of the titrant versus the molar ratio of the titrant to drug for each injection, after subtraction of the background titration. It was observed that the binding of

the PEG 8000 to chloramphenicol is exothermic. The binding constant K ($\times 10^{-3}M^{-1}$) of chloramphenicol was -3.20E3±2.11E4. The stoichiometry (N) for the binding of a PEG 8000 monomer to sulphamethoxazole was 1:1.

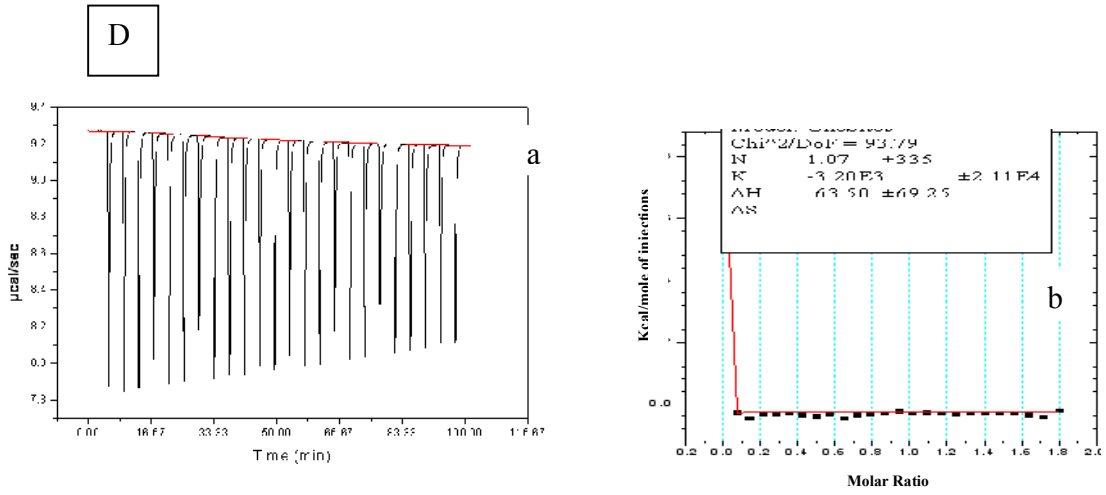

Figure 4.38. ITC data from the titration of 0.25mM sulphamethoxazole (D) in the presence of 2.5 mM Polyethylene glycol 8000 (PEG 8000). a: heat flow versus time during 25 injections of (PEG 8000) at 25°C (the first injection 2µL, subsequent ones 10µL each). b: heat evolved per mole of PEG 8000 added against the molar ratio of PEG 8000 to drug for each injection. (The data were fitted to a one- binding site model. ▪: the experimental data; -: the best fit).

The best fit for the integrated heat was obtained using a one binding site model (table 4.3). Furthermore, the data indicated that the binding of paracetamol is more exothermic (ΔH= −102.6 kcal/mol) than phenacetin, chloramphenicol and sulphamethoxazole (table 4.3). Results show a positive value of ΔS for the drug- PEG 8000 binding (phenacetin and chloramphenicol) indicating that the binding is favoured by conformational entropy.

Table 4.3. Thermodynamic parameters for the binding of PEG 8000 to paracetamol, phenacetin, chloramphenicol and sulphamethoxazole at pH 7.4 (from ITC measurements at 25°C); N: stoichiometry; K: binding constant; ΔH: binding enthalpy; ΔS: entropy change; and ΔG: free energy change.

Parameter	Paracetamol	Phenacetin	Chloramphenicol	Sulphamethoxazole
N	0.944±0.0347	4.12±24.6	2.24±1.24	1.07±335
K ($\times 10^{-3} M^{-1}$)	-2.46E4±7.47E3	1.16E4±1.97E5	4.48E4±1.53E5	-3.20E3±2.11E4
ΔH (kcal/mol)	-102.6±27.40	-32.49±30.75	-39.78±7.493	-63.50±69.25
ΔG (kcal/mol)	-	-38.003	-45.6458	-
ΔS (cal/mol K)	-	0.0185	0.021	-

The binding constants K of the drugs was in the order Kchloramphenicol > Kphenacetin > Kparacetamol > Ksulphamethoxazole. The effective numbers of binding sites per PEG 8000 monomer was in the order Nphenacetin > Nchloramphenicol > Nsulphamethoxazole > Nparacetamol. The stoichiometry (N) for the binding of a PEG 8000 monomer to phenacetin was 4:1, for binding to chloramphenicol was 2:1, sulphamethoxazole was 1:1 and paracetamol was 1:1.

4.3.5.5 Thermodynamic analysis of PEG 8000 using ITC

Figure 4.39 shows the ITC curves of the binding of the PEG 8000 to phosphate buffer (E) and distilled water (F) at 25 °C. The ITC data are shown in figure 4.39. It is clear from ITC experiment that there were large heat changes (heat of dilution) that result when PEG 8000 was added to either phosphate buffer or to water. These mask any possible interaction between PEG 8000 and the drug.

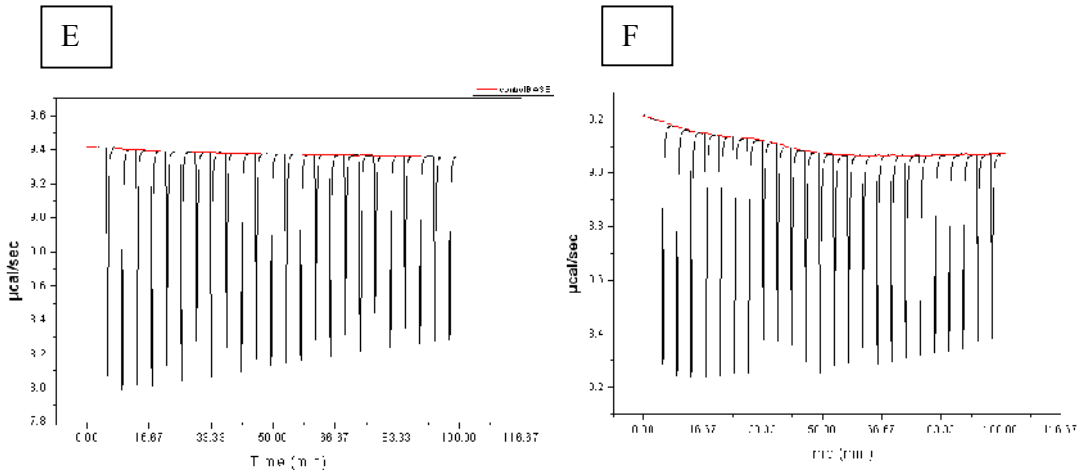

Figure 4.39. ITC data from the titration of 25mM phosphate buffer (E) and distilled water (F) in the presence of 2.5mM PEG 8000 (sample injector). Heat flow versus time during 25 injections of (PEG 8000) at 25°C (the first injection 2µL, subsequent ones 10µL each).

ITC was valuable tool in unravelling the minute differences between the interactions of drug with PEG 8000 under identical conditions. It allowed a quantitative comparison of the heat of interaction between the polymer and drug.

We can possibly hypothesise that the heat changes increases the dissolution of the drug within solid dispersion. We can further explain from ITC that the high energy released when PEG 8000 was titrated with drug in water or phosphate buffer enhanced dissolution rate.

The binding enthalpy of 4 drugs with PEG 8000 was in the order paracetamol > sulphamethoxazole > chloramphenicol > phenacetin and the reaction was exothermic.

4.4 Conclusions

DSC studies showed melting peak for the polymer at around 59 °C with no endothermic peak corresponding to the drug for all solid dispersion. The absence of a melting peak could potentially be assigned to the solubilisation or distribution of the drug within PEG 8000 resulting in the conversion of crystalline drug form into amorphous form in solid dispersions. DSC scans for the physical mixture showed a very interesting profile. Physical mixtures of phenacetin and paracetamol with the PEG 8000 showed two transitions: the first corresponding to the melt of the PEG 8000 and the second due to the melting of the drug (phenacetin and paracetamol). However, physical mixtures of indomethacin, phenylbutazone, chloramphenicol, sulphamethoxazole and succinylsulphathiazole with the PEG 8000 showed single melting endotherm correposnding to the PEG 8000 as seen in the thermograms for the solid dispersion.

In order to further look into the differences in thermal behavior of the physical mixtures (presence and absence of drug endotherms), the samples were subjected to infra red analysis to determine the possibility of functional group interactions between drug and PEG 8000. FTIR spectra for the solid dispersion of all drugs did not reveal any changes for the specific absorption bands for both the PEG 8000 as well as the drug suggesting a lack of interaction between the PEG 8000 and drug. However, in the physical mixture of phenacetin and paracetmol showed the formation of hydrogen bond between the drug (paracetamol and phenacetin) and the PEG 8000 even as a physical mixture could possibly explain the DSC scans reported.

Drugs solubility was enhanced in the solid dispersion followed by physical mixture and pure drug. In case of solid dispersions it was possibly due to the conversion of crystalline drug into amorphous form during the formation of solid dispersion resulting in its higher wettability.

ITC results show that it is a heat change that increases the dissolution of the drug in physical mixture and solid dispersion in PEG 8000 as carrier. It may be due to high energy released when polymer titrated with drug that enhanced dissolution rate as compared to drug alone.

Chapter 5

Stability Studies

5.1 Introduction

One of the problems that must be addressed for the commercial translation of solid dispersion is the instability of the dosage forms where the amorphous form may recrystallise out. In the field of drug targeting and delivery systems little attention is paid to issues related to stability and reproducibility in formulation and performance. Stability testing is carried out to provide evidence on how the quality of pharmaceutical formulation varies with time under the influence of environmental factors such as temperature and humidity. Additionally, product-related factors also influence the stability e.g. the chemical and physical properties of the active substances and the pharmaceutical excipients, the dosage form and its composition, the manufacturing process, the nature of the container-closure system and packaging materials. The quality of the pharmaceutical product has significant role in the safety of patients. The quality and safety of a pharmaceutical product is decreased by the changes in the chemical, pharmacological and toxicological properties of drugs that are caused by impurities and potential degradation products. To ensure delivery of active therapeutics to the patients, drug stability is regarded as the safest method (Ahuja, 1998; FDA, Guidance for Industry: Impurities in Drug Product, Draft guidance, Center for Drug Evaluation and Research (CDER), 1998). Pharmaceuticals are highly sensitive to environmental factors because of their possible composition. Storage conditions should be kept in such a way that the product must remain intact and their activity is maintained.

"Stability is defined as the capacity of a drug substance or drug product to remain within established specifications to maintain its identity, strength, quality, and purity throughout the retest or expiration dating periods". (FDA, Draft Guidance for Industry: Stability Testing of Drug Substances and Drug Products, FDA, Rockville, MD, 1998).

In 1988, World Health Organization (WHO) initiated the stability testing protocols of pharmaceutical products. In 1996 WHO brought the Guidelines on stability testing for well established drug substance in conventional dosage forms on specification of pharmaceutical preparations. In 2000, International Conference on Harmonization (ICH) and WHO agreed to a number of stability tests and conditions employed. The mean kinetic temperature in any part of the world can be derived from climatic data, and the world can be divided into four climatic zones I, II, III and IV (table 5.1). The four zones in the world are differentiated by their characteristic prevalent annual climatic conditions. Information on the stability of the drug substance is an integral part of the systematic approach to stability evaluation.

Table 5.1. Definition and storage conditions for the four climatic zones adopted from (ICH Q1A(R2), 2003).

Climatic zone	Definition	Storage condition
I	temperate climate	21°C/45% RH
II	subtropical and mediterranean climates	25°C/60% RH
III	hot, dry climate	30°C/35% RH
IV	hot, humid climate	30°C/70% RH

General case

Table 5.2. General case with storage condition and duration adopted from (ICH Q1A(R2), 2003).

Study	Storage condition	Duration
Long term	25°C±2°C/60%RH±5%RH or 30°C±2°C/65%RH±5%RH	12 months
Intermediate	30°C±2°C/65%RH±5%RH	6 months
Accelerated	40°C±2°C/75%RH±5%RH	6 months

The formulation to be tested should be packaged in the same containers and packing that is proposed for the marketing of the final product. The stability study should cover those characteristics susceptible to change during storage conditions and likely to influence the quality, safety and efficacy of the formulation. Test parameters to be measured in a stability trial are determined by the dosage form/formulation type and may include physical properties of the product, drug content (active ingredient content), moisture content and any chemical interaction.

5.2 Aim of the study

The main purpose of the current study was to investigate the qualitative and quantitative changes of drug (recrystallisation of drug, drug-excipient interaction, drug content and moisture absorption) in the formulations with time under influence of temperature and humidity. The solid dispersion based tablets for all the drugs studied were prepared and packed in aluminum foil wrapping to simulate the blister packaging of the final product. Differential scanning calorimetry (DSC), fourier transform infrared spectroscopy (FTIR), drug content and thermogravimetric analysis (TGA) were carried out as part of the quality assessment criterion for all the formulations. All the studies and characterisation reported were carried out in triplicate from three independently prepared batches.

5.3 Results and Discussion

5.3.1 Differential scanning calorimetry (DSC)

Representative DSC curves of solid dispersions of paracetamol, sulphamethoxazole, phenacetin, indomethacin, chloramphenicol, phenylbutazone and succinylsulphathiazole with PEG 8000 after 3 months at accelerated conditions and 12 months at room temperature of storage are shown in table 5.3. Depending on the storage conditions, the DSC measurements reveal changes of three characteristics:

(1) Change of the melting peak of PEG 8000,
(2) The melting point of the drug and
(3) Recrystallisation of drug.

The main observation that can be made from these curves is that the melting behavior of PEG 8000 changed as a function of time and recrystallisation of drugs in accelerated conditions. Examination of peak temperature of PEG 8000 in the solid dispersions stored at accelerated storage condition (40°C±2°C/75%RH±5%RH) indicated a slight decrease in the peak temperature of PEG 8000 and recrystallisation of drug except indomethacin and phenacetin as illustrated from figures 5.1, 5.3, 5.5, 5.7, 5.9, 5.11 and 5.13. On the other hand, there were no marked differences between samples stored at room

temperature. There was no influence of storage time as well as storage conditions on the peak temperatures of these drugs in the solid dispersions stored at room temperature.

5.3.2 Fourier transform infrared spectroscopy (FTIR)

It was interesting to observe that the amorphous state of drug in solid dispersions with PEG 8000 was maintained throughout the storage period at room temperature for 12 months. The spectra were identical and almost all the characteristic features of the drug were observed in every sample, showing that the lapse of the storage time had no influence on the appearance of the FTIR spectra at room temperature. However, in accelerated storage conditions (40°C±2°C/75%RH±5%RH) certain changes were noticed, for example, the lost or broadening or shortening or presence of some new functional group were shown in the FTIR spectra of solid dispersions.

5.3.3 Drug Content

In order to evaluate the effect of storage conditions on the chemical properties of the solid dispersions under investigation, their drug content behavior was studied. The data shows (table 5.4) a significant reduction of the percentage of drug content at accelerated storage conditions (40°C±2°C/75%RH±5%RH).

5.3.4 Thermogravimetric Analysis (TGA)

Thermogravimetric Analysis (TGA) is a type of testing that is performed on samples to determine changes in weight in relation to change in temperature. Its primary use includes measuring the thermal stability of a material. The effect of moisture content on product execution on stability should be evaluated by TGA. The moisture content of solid dispersion as shown in table 5.5 at room temperature after storage for 12 months was unchanged or remained same but in case of accelerated storage conditions (40°C±2°C/75%RH±5%RH) it absorbed the moisture which caused the recrystallisation of drug demonstrated by DSC and change in the functional group as suggested by FTIR studies.

5.3.5 Stability studies of paracetamol

5.3.5.1 Stability studies of paracetamol solid dispersion by DSC

The onset temperature for solid dispersion of paracetamol (figure 5.1) was 59 °C (a) and after 12 months storage at room temperature (c) stayed the same as no changes were observed in onset indicating the absence of any crystalline paracetamol. However, samples stored under accelerated stability conditions (b) for 3 months revealed four thermal events at 52 °C, 143 °C, 160 °C and 183 °C. The 52 °C melt possibly relates to the melting of the carrier which was lower than the onset temperature for solid dispersion

and this might be due to humidity and high temperature in accelerated conditions. The peak at 143 °C and 160 °C might be the drug onset which suggested that paracetamol reverted to other polymorphic forms and drug recrystallised at 183 °C. This might also be due to moisture content and exposure to high temperature which suggested that solid dispersion of paracetamol is unstable at accelerated conditions.

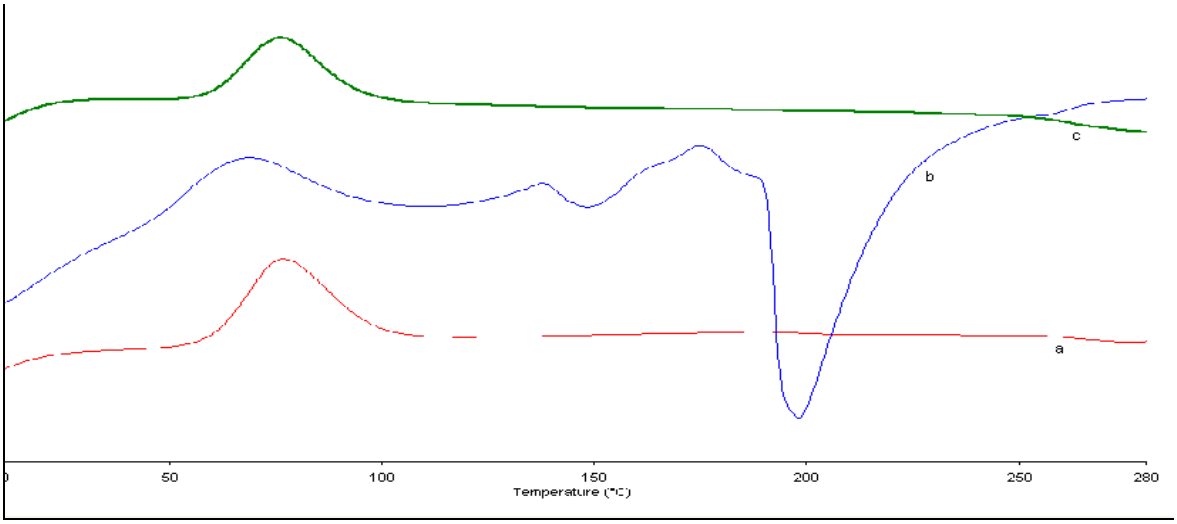

Figure 5.1. DSC traces of solid dispersion of paracetamol with PEG 8000 (a, t=0), stored at 40°C±2°C/75%RH±5%RH (b, t=3) and at room temperature (c, t=12). t represents storage time (months).

5.3.5.2 Stability studies of paracetamol solid dispersion by FTIR

Analysis of spectra for paracetamol solid dispersion (figure 5.2) showed specific absorption bands at wave numbers 3500, 3291, 2888, 1267, 1250, 1243, 1149 and 700 cm^{-1} corresponding to the stretching associated with O-H, N-H O-H, C-H, C-C, C-O, C-O

and C-C respectively. Spectra for paracetamol solid dispersion did not reveal any changes for the specific absorption bands at room temperature for 12 months suggesting a lack of interaction which was further justified by DSC studies. However, changes were observed at wave numbers 3500 and 2888 cm^{-1} when stored under accelerated storage conditions. This might be due to moisture content and high temperature exposed at accelerated conditions.

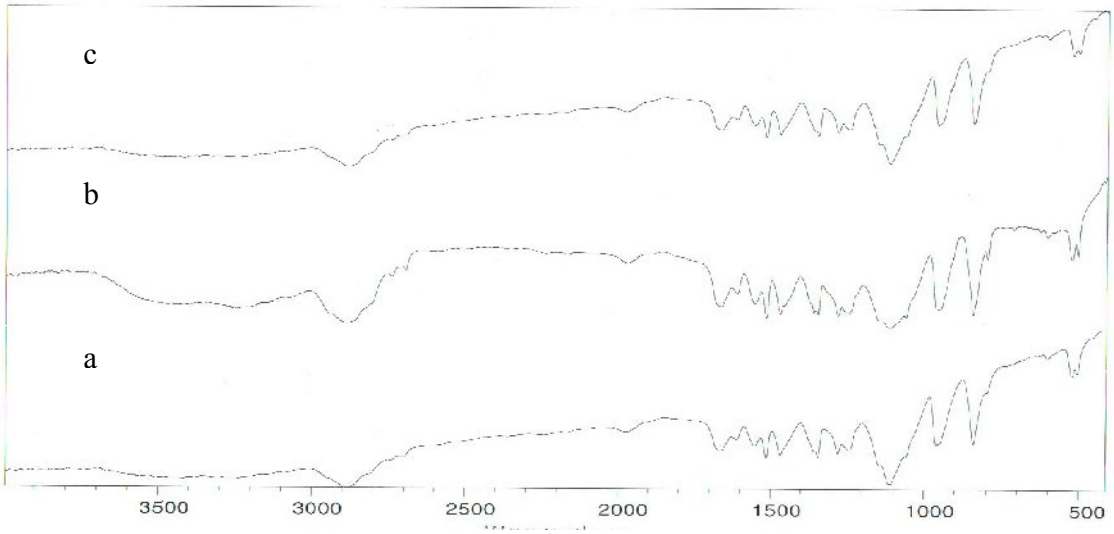

Figure 5.2. FTIR of solid dispersion of paracetamol with PEG 8000 (a, t=0), stored at 40°C±2°C/75%RH±5%RH (b, t=3) and at room temperature (c, t=12). t represents storage time (months).

5.3.5.3 Stability studies of paracetamol solid dispersion by drug content

The drug content of paracetamol solid dispersion was 99% at time point zero but after 3 months at accelerated storage conditions (40°C±2°C/75%RH±5%RH), the drug content

was down to 27%. However, at room conditions the content of paracetamol was 97% which further suggested that the drug was intact in an amorphous form in the solid dispersion formulation. The reduction in the drug content at accelerated storage conditions suggests that there was a change in the physical structure of the amorphous drug/PEG 8000 dispersions. These differences are similar to that observed from DSC and FTIR.

5.3.5.4 Stability studies of paracetamol solid dispersion by TGA

The moisture content of paracetamol solid dispersion was less than 1% at the start of the stability studies but after 3 months at accelerated storage condition (40°C±2°C/75%RH±5%RH), the moisture content was up to 10%. Formulations stored at room conditions showed similar results after 12 months as that observed at the initial time point suggesting minimum absorption of moisture. The enhancement in the moisture content at accelerated storage condition suggests that there was a change in the physical structure of the amorphous drug/PEG 8000 dispersions, which was further justified from drug content studies. However, these differences were also observed by the data obtained from DSC and FTIR suggesting that moisture absorption at higher humidity results in conversion of amorphous form into crystalline form.

5.3.6 Stability studies of sulphamethoxazole

5.3.6.1 Stability studies of sulphamethoxazole solid dispersion by DSC

The onset temperature for solid dispersion of sulphamethoxazole (figure 5.3) was 61 °C (a) and was found to be exactly the same at room temperature (c) after 12 months storage time since no difference was noticed in its onset temperature neither was sulphamethoxazole recrystallised within the solid dispersion. Three thermal events at 46 °C, 160 °C and 173 °C were recorded when exposed under accelerated stability conditions (b) after storage for three months. The 46 °C melt possibly relates to the carrier, where humidity and high temperature (accelerated conditions) to which the drug is exposed have caused the decrease in the onset temperature of solid dispersion. While the peaks at 160 °C and 173 °C are possibly due to the recrystallisation of drug suggesting the instability of solid dispersion of sulphamethoxazole at accelerated conditions.

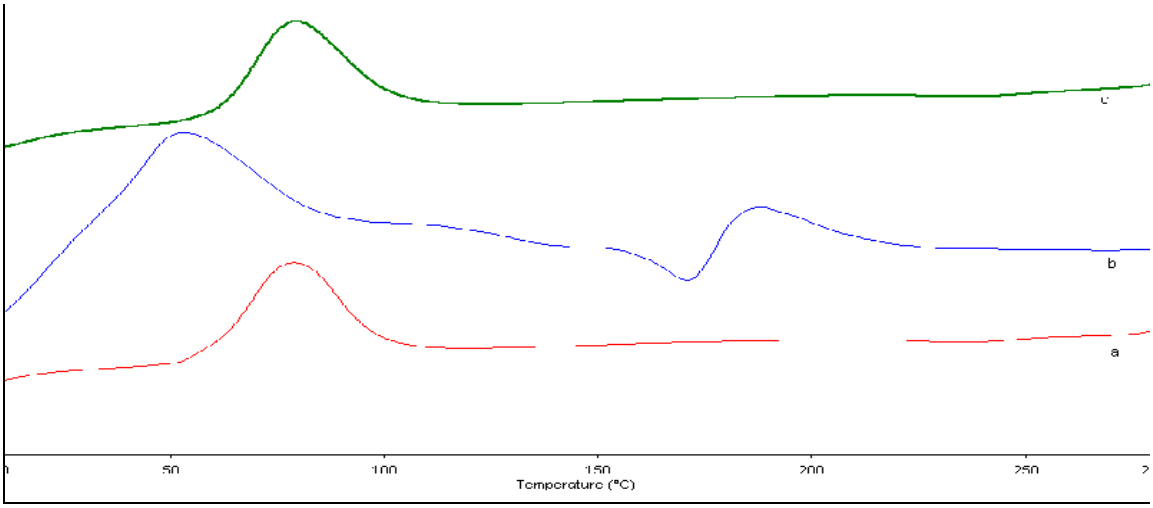

Figure 5.3. DSC traces of solid dispersion of sulphamethoxazole with PEG 8000 (a, t=0), stored at 40°C±2°C/75%RH±5%RH (b, t=3) and at room temperature (c, t=12). t represents storage time (months).

5.3.6.2 Stability studies of sulphamethoxazole solid dispersion by FTIR

FTIR spectra for sulphamethoxazole solid dispersion (figure 5.4) exhibited absorption bands at wave numbers 3475, 3374, 2889, 1620, 1596, 1467 and 1150 cm^{-1} corresponding to the stretching associated with O-H, N-H, C-H, N-H, C-C, C-H and C-O respectively. Spectra for sulphamethoxazole solid dispersion showed the loss of absorption band at wave number 3475 cm^{-1} (O-H) at accelerated storage conditions. However, formulations at room temperature exhibited no change for specific absorption bands of sulphamethoxazole solid dispersion for 12 months as was further justified by DSC studies.

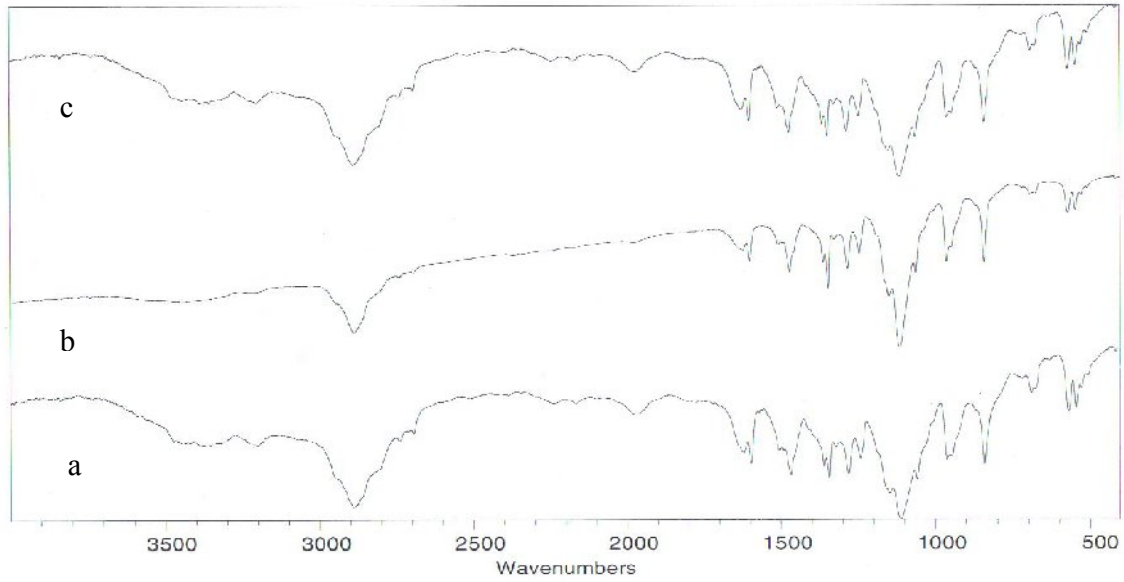

Figure 5.4. FTIR of solid dispersion of sulphamethoxazole with PEG 8000 (a, t=0), stored at 40°C±2°C/75%RH±5%RH (b, t=3) and at room temperature (c, t=12). t represents storage time (months).

5.3.6.3 Stability studies of sulphamethoxazole solid dispersion by drug content

The drug content of sulphamethoxazole solid dispersion was 98% at time point zero and remained the same at room conditions when stored at room temperature conditions. In contrast, the drug content was found to be 47% when exposed to accelerated storage conditions (40°C±2°C/75%RH±5%RH) after three months. This decline in the drug content suggests that a change in the physical structure of the amorphous drug/PEG 8000 dispersions had occurred, as suggested by DSC and FTIR studies above. It may be due to the recrystallisation of the amorphous drug in the carrier matrix which decreases drug content in the solid dispersion of sulphamethoxazole.

5.3.6.4 Stability studies of sulphamethoxazole solid dispersion by TGA

The moisture content of sulphamethoxazole solid dispersion was found to be less than 1% at the start of the studies. It can be said that sulphamethoxazole was stable within the solid dispersion throughout the time period of 12 months as the moisture content was again observed to be less than 1% at room temperature conditions. However, moisture content increased to 6% after 3 months when accelerated storage conditions were applied (40°C±2°C/75%RH±5%RH). It is likely that during accelerated storage conditions the moisture absorption in the dispersion changes the stable and amorphous sulphamethoxazole into crystalline form as demonstrated from DSC results. In addition to this FTIR and drug content studies revealed results demonstrating similar differences.

5.3.7 Stability studies of phenacetin

5.3.7.1 Stability studies of phenacetin solid dispersion by DSC

The onset temperature of 59 °C (a) was observed for solid dispersion of phenacetin (figure 5.5) which was found to be unaltered after 12 months storage at room temperature (c) as recrystallisation of phenacetin in the solid dispersion was not found. In case of accelerated stability conditions (b) thermal event at 52 °C was observed after 3 months storage.

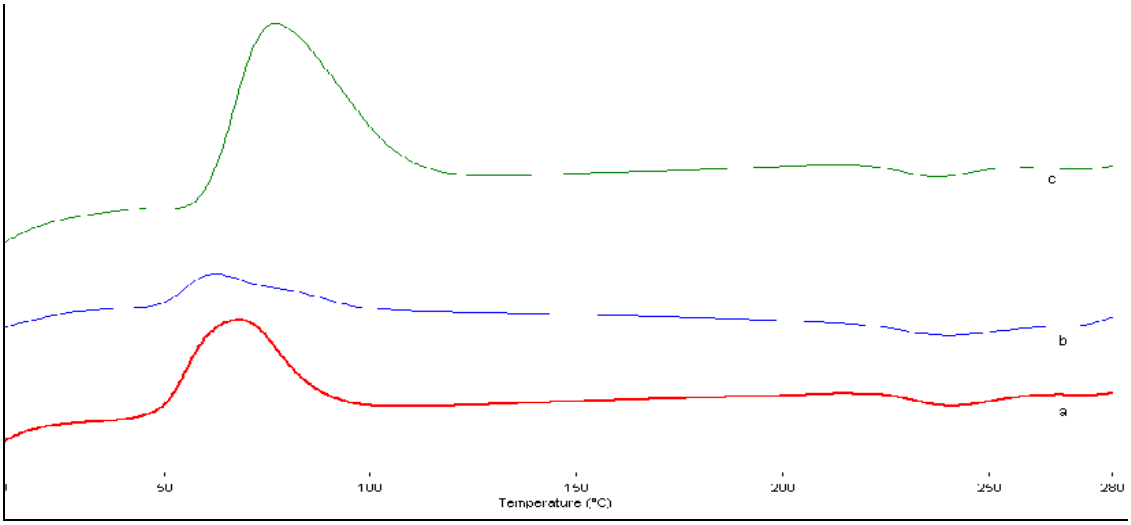

Figure 5.5. DSC traces of solid dispersion of phenacetin with PEG 8000 (a, t=0), stored at 40°C±2°C/75%RH±5%RH (b, t=3) and at room temperature (c, t=12). t represents storage time (months).

5.3.7.2 Stability studies of phenacetin solid dispersion by FTIR

Spectral analysis for phenacetin solid dispersion (figure 5.6) demonstrated absorption bands at wave numbers 3283, 2889, 1468, 1243, 1150 and 842 cm^{-1} associated with N-H, C-H, C-H, C-N, C-O and C-H respectively. No variation was displayed in the spectra for phenacetin solid dispersion for the specific absorption bands at room temperature for 12 months suggesting a lack of interaction which was explained by DSC studies, while accelerated storage conditions altered the spectra showing an absorption band at wave numbers 3283 and 2889 cm^{-1} associated with N-H and C-H.

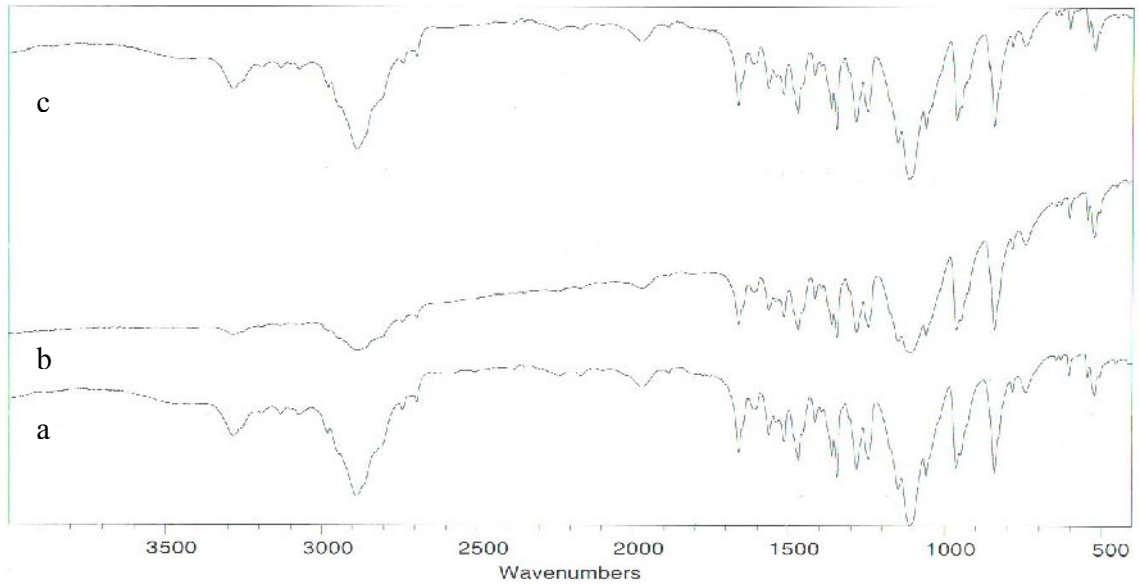

Figure 5.6. FTIR of solid dispersion of phenacetin with PEG 8000 (a, t=0), stored at 40°C±2°C/75%RH±5%RH (b, t=3) and at room temperature (c, t=12). t represents storage time (months).

5.3.7.3 Stability studies of phenacetin solid dispersion by drug content

Analysis of drug content for phenacetin solid dispersion when subjected to accelerated storage conditions (40°C±2°C/75%RH±5%RH) showed that 74% of the initial amount of drug was recovered after 3 months when compared to a 97% recovery at the start of the study. Interestingly, formulations stored at room temperature conditions resulted in 96% drug recovery suggesting that lower temperature did not have any significant affect on drug stability. These results can further be substantiated with DSC as well as FTIR data where no changes were observed upon storage at room temperature conditions for 12 months.

5.3.7.4 Stability studies of phenacetin solid dispersion by TGA

The moisture content of phenacetin solid dispersion when exposed to accelerated storage conditions was 2% over a period of 3 months when compared to start of the study and samples stored at room temperature (1%).

5.3.8 Stability studies of indomethacin

5.3.8.1 Stability studies of indomethacin solid dispersion by DSC

The onset temperature for solid dispersion of indomethacin (figure 5.7) was 64 °C (a) and after 12 months storage at room temperature (c) remained unaltered as no difference was found either in the onset and the recrystallisation of indomethacin in the solid dispersion or its melting point. However, (b) after 3 months of storage at accelerated conditions, thermal event at 50 °C was noticed.

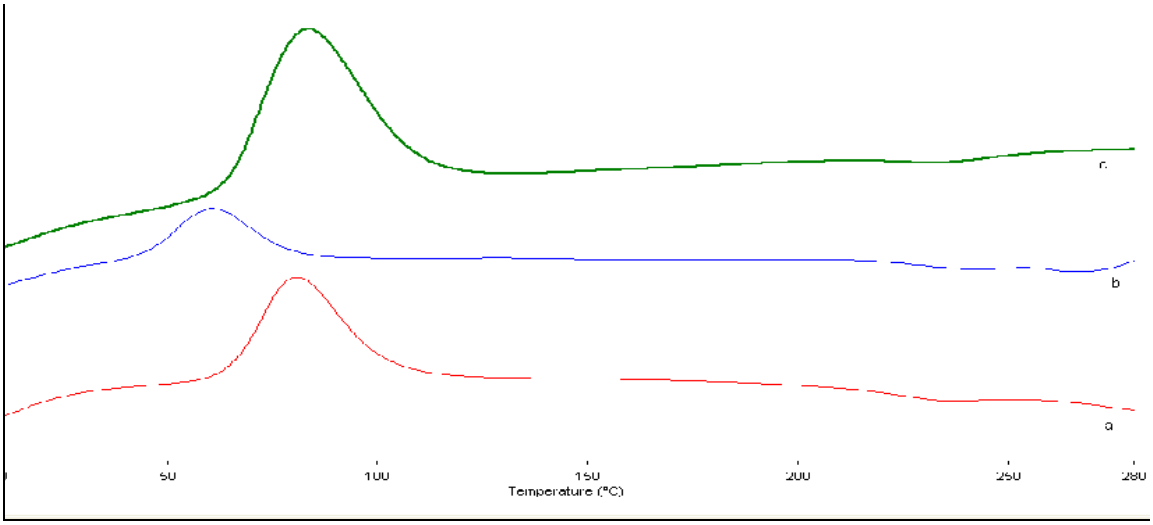

Figure 5.7. DSC traces of solid dispersion of indomethacin with PEG 8000 (a, t=0), stored at 40°C±2°C/75%RH±5%RH (b, t=3) and at room temperature (c, t=12). t represents storage time (months).

5.3.8.2 Stability studies of indomethacin solid dispersion by FTIR

Analysis of spectra for indomethacin solid dispersion (figure 5.8) demonstrated specific absorption bands at wave numbers 3394, 2945, 2890, 1702,1468,1343, 1242, 1149 and 842 cm^{-1} associated with O-H, O-H, C-H, C=C, C-C, C-H, C-O, C-O and C-H respectively. Spectra for indomethacin solid dispersion did not reveal any changes for the specific absorption bands at room temperature for 12 months thus indicating a lack of interaction as supported by DSC. However, at accelerated storage conditions variations were seen in absorption band at wave numbers 3394 and 1702 cm^{-1}.

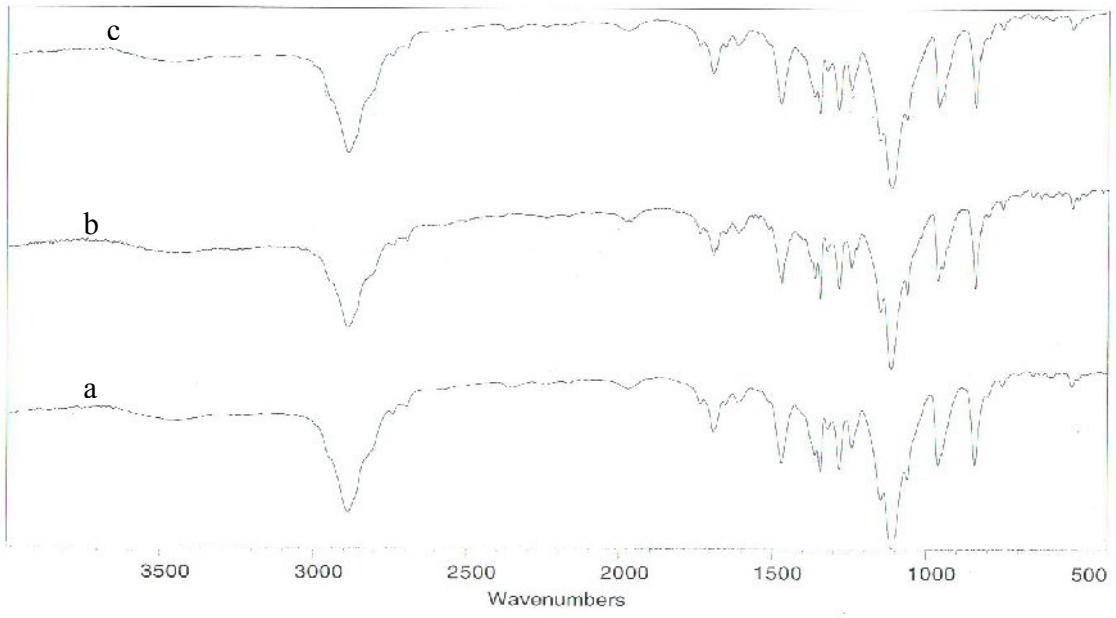

Figure 5.8. FTIR of solid dispersion of indomethacin with PEG 8000 (a, t=0), stored at 40°C±2°C/75%RH±5%RH (b, t=3) and at room temperature (c, t=12). t represents storage time (months).

5.3.8.3 Stability studies of indomethacin solid dispersion by drug content

The drug content of indomethacin solid dispersion at the start of the experiment was 99% but after 3 months of storage at accelerated conditions, it was reduced to 70%. However, for samples stored at room temperature conditions the content of indomethacin was 99% which evidently proved that the drug was intact in an amorphous form within the solid dispersion. As compared to paracetamol solid dispersion indomethacin drug content was more from indomethacin solid dispersion; this may be due to the factor that drug was an amorphous form in the solid dispersion as suggested by DSC. The thermogram of

indomethacin solid dispersion shows the onset change from 64 °C to 50 °C and also that no recrystallisation of drug has taken place during accelerated storage conditions.

5.3.8.4 Stability studies of indomethacin solid dispersion by TGA

The moisture content of indomethacin solid dispersion was less than 1% but after 3 months at accelerated storage conditions, the moisture content increased to 3%. Although at room conditions after 12 months the moisture content of indomethacin was found to be less than 1% suggesting that the drug was present in amorphous form in the solid dispersion. The enhancement in the moisture content at accelerated storage conditions suggests a change in the physical structure of the amorphous drug/PEG 8000 dispersions, which can also be seen from drug content studies. However, these differences were also observed by the results obtained from DSC and FTIR.

5.3.9 Stability studies of chloramphenicol

5.3.9.1 Stability studies of chloramphenicol solid dispersion by DSC

The onset temperature for solid dispersion of chloramphenicol (figure 5.9) was 59 °C (a) and after 12 months storage at room temperature (c) remained constant as no changes were observed in onset temperature and recrystallisation of chloramphenicol. However, two thermal events at 50 °C and 203 °C were displayed over the time period of (b) 3

months when subjected to accelerated stability conditions. The 50 °C melt possibly relates to the carrier which was lower than onset temperature for chloramphenicol solid dispersion and drug recrystallised at 203°C. The reasons for this might be high moisture content and exposure to high temperature at accelerated conditions.

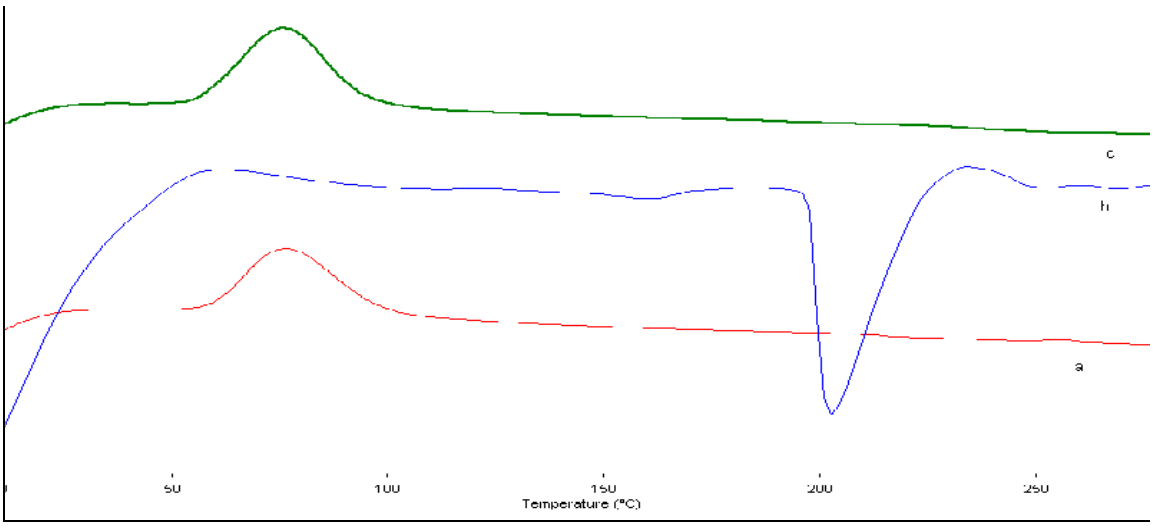

Figure 5.9. DSC traces of solid dispersion of chloramphenicol with PEG 8000 (a, t=0), stored at 40°C±2°C/75%RH±5%RH (b, t=3) and at room temperature (c, t=12). t represents storage time (months).

5.3.9.2 Stability studies of chloramphenicol solid dispersion by FTIR

Analysis of spectra for chloramphenicol solid dispersion (figure 5.10) showed specific absorption bands at wave numbers 3376, 3357, 2889, 1701, 1580, 1468, 1360, 1149, 1113, and 842 cm^{-1} corresponding to the stretching associated with O-H, N-H, C-H, C=O, C-C, C-H, N-O, C-O, C-N and C-H respectively. No variation was exhibited by the spectra for chloramphenicol solid dispersion for the specific absorption bands at room

temperature conditions during the 12 months storage time. However, formulations subjected to accelerated storage conditions revealed alterations for absorption band at wave numbers 1580 cm^{-1} and loss of functional group at wave number 3375 cm^{-1} associated with O-H.

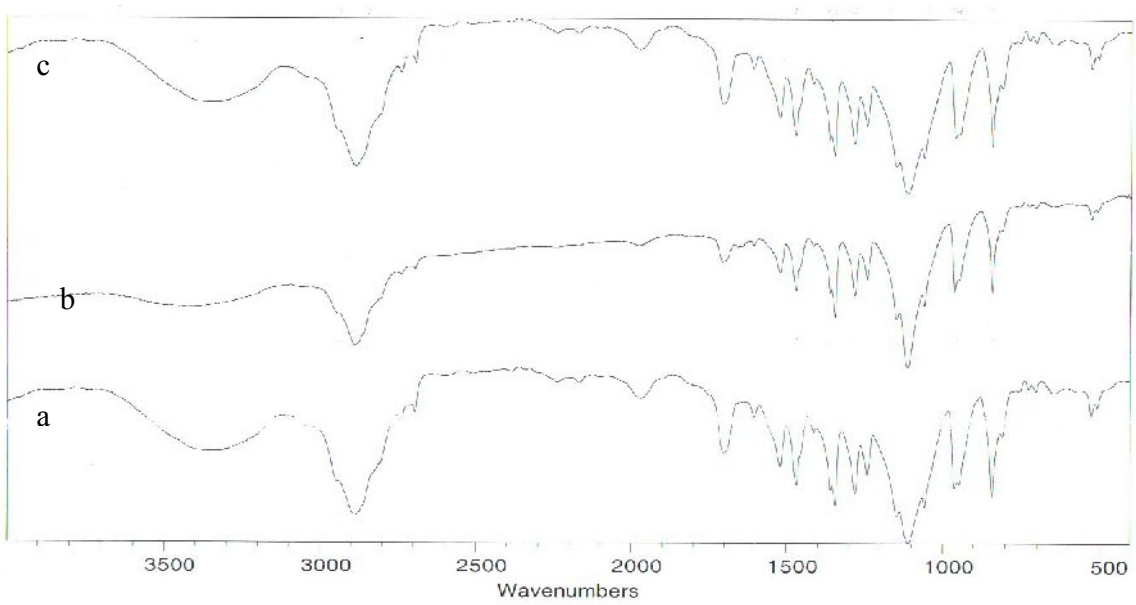

Figure 5.10. FTIR of solid dispersion of chloramphenicol with PEG 8000 (a, t=0), stored at 40°C±2°C/75%RH±5%RH (b, t=3) and at room temperature (c, t=12). t represents storage time (months).

5.3.9.3 Stability studies of chloramphenicol solid dispersion by drug content

The drug content of chloramphenicol solid dispersion at the start of the experiment was 98% but with the passage of 3 months at accelerated storage conditions, the drug content was reduced to 62%. While at normal room temperature conditions the content of

chloramphenicol was found to be 96% stating that the drug remained intact in its amorphous form within the solid dispersion. The reduction in the drug content when exposed to accelerated storage conditions suggests that the physical structure of the amorphous drug/PEG 8000 dispersions had changed. Moreover, these differences were also observed in the data obtained from DSC and FTIR. Recrystallisation of the amorphous drug is the key factor for this in the solid dispersion.

5.3.9.4 Stability studies of chloramphenicol solid dispersion by TGA

The moisture content of chloramphenicol solid dispersion was found to be less than 1% whereas, after 3 months at accelerated storage conditions, the moisture content was 6%. On the other hand, for samples tested after 12 months duration at room temperature conditions, the moisture content of chloramphenicol was shown to be less than 1% which further implies that the drug was present in amorphous form in the solid dispersion.

5.3.10 Stability studies of phenylbutazone

5.3.10.1 Stability studies of phenylbutazone solid dispersion by DSC

The onset temperature for solid dispersion of phenylbutazone (figure 5.11) was 61 °C (a) and no difference was seen in the onset tempereature of phenylbutazone in the solid dispersion even after 12 months storage at room temperature (c). But during accelerated

stability conditions (b) two thermal events were detected after storage for 3 months; 50 °C and 212 °C. The 212 °C indicates that this might be the recrystallisation (breakdown) or conversion into different polymorphic form of phenylbutazone in the solid dispersion, whereas, 50 °C melt relates to the carrier. Moisture content and high temperature could possibly explain changes in the onset temperature and breakdown/conversion into different polymorphic form of phenylbutazone at accelerated stability conditions.

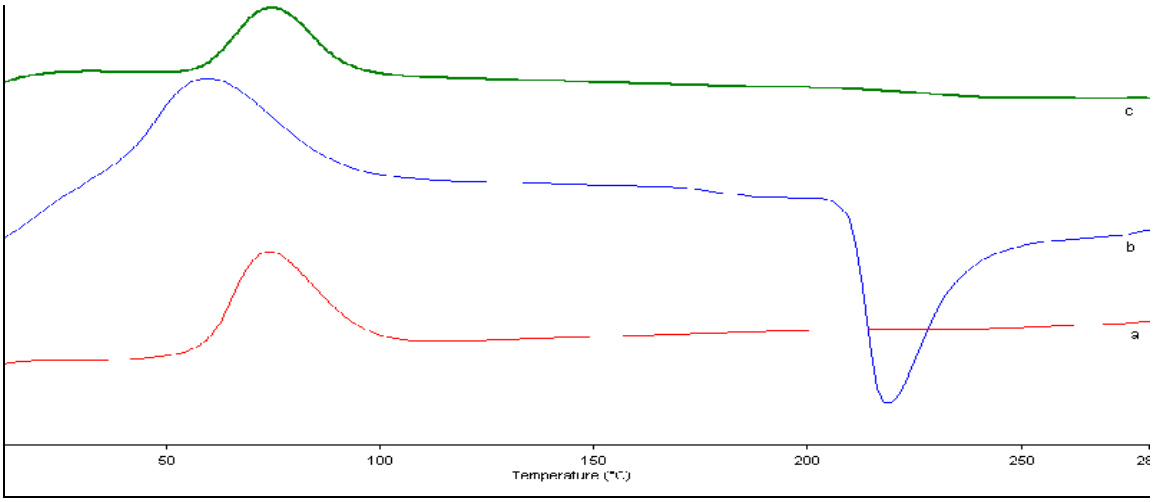

Figure 5.11. DSC traces of solid dispersion of phenylbutazone with PEG 8000 (a, t=0), stored at 40°C±2°C/75%RH±5%RH (b, t=3) and at room temperature (c, t=12). t represents storage time (months).

5.3.10.2 Stability studies of phenylbutazone solid dispersion by FTIR

Analysis of spectra for phenylbutazone solid dispersion (Fig. 5.12) showed specific absorption bands at wave numbers 3450, 2947, 1753, 1468, 1281, 1150 and 842 cm^{-1}

corresponding to the stretching associated with O-H, C-H, C=O, C-H, C-N, C-O and C-H respectively. Although no variations were exhibited by the spectra for phenylbutazone solid dispersion for the specific absorption bands after storage for 12 months at room temperature, absorption bands at wave numbers 2947, 1753 cm^{-1} and loss of functional group at wave number 3450 cm^{-1} associated with O-H were detected for the samples stored at accelerated conditions.

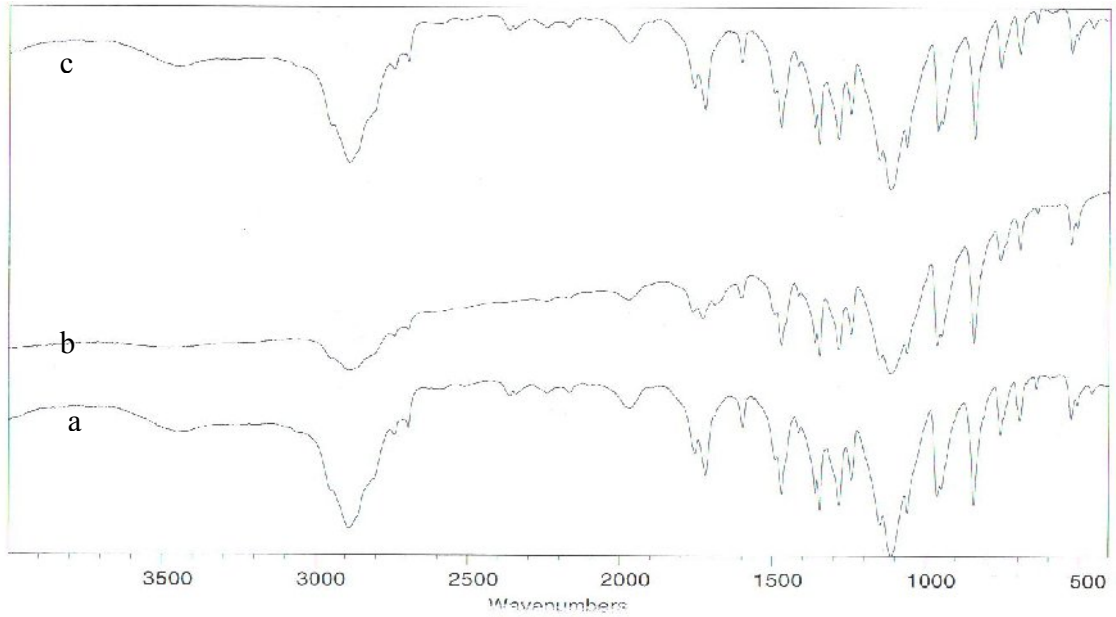

Figure 5.12. FTIR of solid dispersion of phenylbutazone with PEG 8000 (a, t=0), stored at 40°C±2°C/75%RH±5%RH (b, t=3) and at room temperature (c, t=12). t represents storage time (months).

5.3.10.3 Stability studies of phenylbutazone solid dispersion by drug content

The drug content of phenylbutazone solid dispersion was found to be 98% but was reduced to 61% after exposure to accelerated storage conditions over the period of 3 months. However, the content of phenylbutazone when stored at room temperature was shown to be 97% implying that the drug was in an amorphous form in the solid dispersion.

5.3.10.4 Stability studies of phenylbutazone solid dispersion by TGA

Phenylbutazone solid dispersion had less than 1% moisture content which increased to be 4% at accelerated storage conditions when examined after 3 months. On the contrary formulations stored at room temperature for 12 months duration, revealed low moisture content around 1% as that observed at the start of the study indicating the presence of amorphous form in the solid dispersion as evident from DSC, FTIR and drug content studies. However, the amorphous form of phenylbutazone solid dispersion is not retained as can be clearly seen from DSC results when subjected to accelerated storage conditions. Drug content studies also supported the same change. Moreover, similar differences were also observed by the results obtained from FTIR studies.

5.3.11 Stability studies of succinylsulphathiazole

5.3.11.1 Stability studies of succinylsulphathiazole solid dispersion by DSC

The onset temperature for solid dispersion of succinylsulphathiazole (figure 5.13) was 61 °C (a) and stayed constant after 12 months storage at room temperature (c) as no recrystallisation of succinylsulphathiazole in the solid dispersion was observed. Furthermore, no changes were found in the onset temperature. However, formulations exposed to accelerated stability conditions (b) presented three thermal events at 51 °C, 200 °C and 218 °C after 3 months. The accelerated conditions have high humidity and high temperature which possibly causes the dispersion to melt at 51 °C that relates to the carrier to be lower than onset temperature of solid dispersion (61 °C). The peak at 200 °C might be the drug onset and drug recrystallised at onset 218 °C.

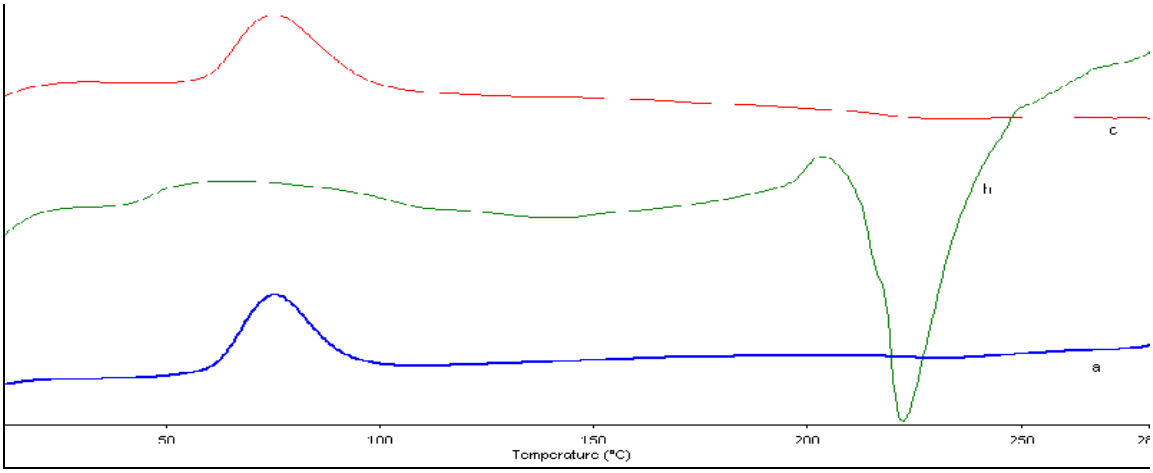

Figure 5.13. DSC traces of solid dispersion of succinylsulphathiazole with PEG 8000 (a, t=0), stored at 40°C±2°C/75%RH±5%RH (b, t=3) and at room temperature (c, t=12). t represents storage time (months).

5.3.11.2 Stability studies of succinylsulphathiazole solid dispersion by FTIR

Analysis of spectra for succinylsulphathiazole solid dispersion (figure 5.14) indicated peaks at wave number 3472, 3448, 2890, 1467, 1149 and 842 cm^{-1} corresponding to the stretching associated with O-H, O-H, C-H, C-H, C-O and C-H respectively. A lack of interaction can rightly be deduced as zero variations were observed by spectra for succinylsulphathiazole solid dispersion for the specific absorption bands at room temperature conditions for 12 months which was also supported by DSC studies. However, in case of samples stored at accelerated conditions, changes were observed which included loss of an absorption band at wave number 3448 cm^{-1} associated with O-H.

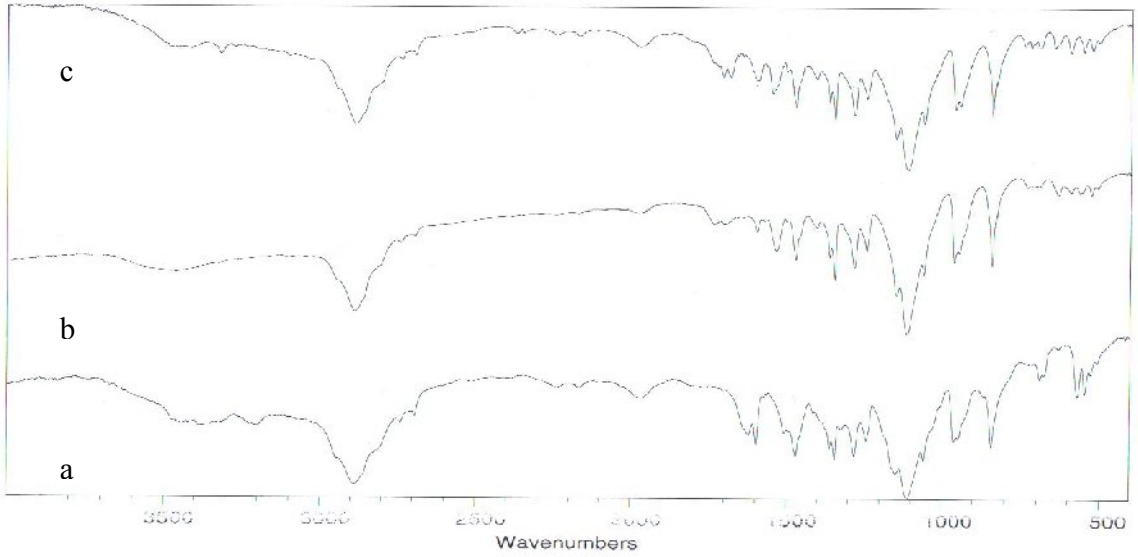

Figure 5.14. FTIR of solid dispersion of succinylsulphathiazole with PEG 8000 (a, t=0), stored at 40°C±2°C/75%RH±5%RH (b, t=3) and at room temperature (c, t=12). t represents storage time (months).

5.3.11.3 Stability studies of succinylsulphathiazole solid dispersion by drug content

Drug content observed for succinylsulphathiazole solid dispersion was 96% at the start of the experimental set up. The moisture content was 94% at room temperature conditions suggesting that succinylsulphathiazole was present in the amorphous form within the solid dispersion. When exposed to accelerated storage conditions, the drug content was reduced to 46% over the time period of 3 months. The accelerated storage conditions cause a decrease in the drug content showing that the amorphous form of succinylsulphathiazole within the solid dispersions had changed and resulted in drug degradation.

5.3.11.4 Stability studies of succinylsulphathiazole solid dispersion by TGA

When the moisture content of succinylsulphathiazole was studied within the solid dispersion, it was found to be less than 1% at the start of the studies. After 3 months time period when subjected to accelerated storage conditions, the moisture content increased to 7%. However, the moisture content of succinylsulphathiazole after 12 months was less than 1% at room temperature conditions. It suggests that the succinylsulphathiazole was present in an amorphous form in the solid dispersion. The enhanced moisture content when exposed to high humidity and temperature possibly indicates that amorphous form of succinylsulphathiazole underwent a change at accelerated storage conditions, which can be additionally proved from DSC, FTIR and drug content studies.

From the DSC curves of solid dispersions (table 5.3) it could be observed that the melting behavior (onset) of the carrier and drug recrystallisation significantly changed as a function of storage conditions at 40°C±2°C/75%RH±5%RH. But on other hand solid dispersion for all drugs were stable at room temperature conditions for 12 months.

Table 5.3. Summary of DSC results for all solid dispersions at (t=0), stored at 40°C±2°C/75%RH±5%RH (t=3) and at room temperature (t=12). t represents storage time (months).

S.No	15% solid dispersion (w/w)	DSC (onset To±S.D, recrystallisation Tr±S.D (time point 0 month) °C	DSC (onset To±S.D, recrystallisation Tr±S.D (accelerated studies 3 months) °C	DSC (onset To±S.D, recrystallisation Tr±S.D (room temperature studies 12 months) °C
1	Paracetamol	59±2	52±2,143±11,160, 183±9	59±2
2	Sulphamethoxazole	61±1	46±5,160±4,173±3	60±2
3	Phenacetin	59±5	52±1	59±2
4	Indomethacin	64±1	50±0.5	64±0.5
5	Chloramphenicol	59±1	50±2, 203±6	59±2
6	Phenylbutazone	60±0	50±2, 212±24	61±1
7	Succinylsulphathiazole	61±1	51±5, 200±18, 218±5	61±2

From the drug content of solid dispersions (table 5.4) it could be observed that the drug content significantly changed as a function of storage conditions at 40°C±2°C/75%RH±5%RH. But on other hand solid dispersion for all drugs remained same at room temperature conditions for 12 months.

From the moisture content of solid dispersions (table 5.5) it could be observed that the moisture content significantly increased as a function of storage condition at accelerated storage conditions (40°C±2°C/75%RH±5%RH). But on other hand solid dispersion for all drugs remain same at room temperature for 12 months.

Table 5.4. Summary of drug content for all solid dispersions at (t=0), stored at 40°C±2°C/75%RH±5%RH (t=3) and at room temperature (t=12). t represents storage time (months).

S.No	15% solid dispersion (w/w)	Drug contents mean%±S.D (time point 0 month)	Drug contents mean%±S.D (accelerated studies 3 months)	Drug contents mean%±S.D (room temperature studies 12 months)
1	Paracetamol	99±5	27±5	97±3
2	Sulphamethoxazole	98±7	47±6	98±2
3	Phenacetin	97±4	74±5	96±4
4	Indomethacin	99±4	70±6	99±2
5	Chloramphenicol	98±8	62±9	96±3
6	Phenylbutazone	98±3	61±4	97±3
7	Succinylsulphathiazole	96±6	46±2	94±6

Table 5.5. Summary of moisture content for all solid dispersions at (t=0), stored at 40°C±2°C/75%RH±5%RH (t=3) and at room temperature (t=12). t represents storage time (months).

S.No	15% solid dispersion (w/w)	TGA mean%±S.D (time point 0 month)	TGA mean%±S.D (accelerated studies 3 months)	TGA mean%±S.D (room temperature studies 12 months)
1	Paracetamol	0.54±0.29	9.76±0.42	0.48±0.20
2	Sulphamethoxazole	1.57±1.42	6.47±0.60	1.20±0.93
3	Phenacetin	0.30±0.182	1.93±0.25	0.29±0.16
4	Indomethacin	0.72±0.64	2.63±0.45	0.71±0.65
5	Chloramphenicol	0.23±0.07	6.07±0.55	0.23±0.09
6	Phenylbutazone	0.56±0.47	3.9±0.44	0.62±0.40
7	Succinylsulphathiazole	0.64±0.95	6.77±0.45	0.45±0.40

The formation of solid dispersions often leads to the conversion of a crystalline drug into the amorphous state (a higher energy state). Thermodynamically, this high energy state is metastable and can in the course of time, be reconverted into the stable crystalline state (Fukuoka et al., 1986; Izutsu et al., 1994; Yoshioka et al., 1995). The dimensional arrangements of atom which exist in the crystalline form are absent in the amorphous form. When the storage condition i.e. temperature increases, the movement of molecules also increases, providing quicker crystallisation of the amorphous state. The movement of molecules in an amorphous state is related to chemical reactivity has been presented by Yoshioka and Aso (2007) and Craig et al. (1999) in which enhancing movement of molecules resulted in increased chemical decomposition of amorphous states. Exposure of metastable systems to high humidity may induce changes resulting in a decrease in their dissolution properties, melting point, FTIR spectra and drug content. Solid dispersions tend to absorb a higher amount of moisture this may lead to the induction of crystallisation (Takeuchi et al., 2000).

New peaks were observed in the FTIR spectra of the solid dispersions after storage under 40 °C; these conditions indicated the drug in the matrix system underwent phase change, the kinetics of the reaction increase and the physico-chemical properties of the drug-excipient are changed. Also, shift in the peak positions was observed indicating interaction between the drug and the polymeric matrix during accelerated storage

conditions. Furthermore, significant change in peak intensities corresponding to solid dispersions stored at 40 °C suggests that there is significant increase in the amount of crystalline drug in the matrix system after 3 months. Because the DSC studies have indicated that the drug is in the crystalline form in the matrix, it is not surprising to see significant changes of FTIR spectra. Storage at higher temperature speeds up and enhances recrystallisation process (Chieng et al., 2008). The FTIR spectra of the solid dispersions showed no loss or addition of bands, indicating the essential chemical and physical stability of the dispersion at room temperature conditions during the period of 12 months study. All solid dispersions have high moisture content and lower drug content at accelerated conditions. The solid dispersion has the tendency to absorb higher amount of moisture which causes the recrystallisation of drug. This recrystallised drug in the solid dispersion affects the drug content. We get a similar trend for all solid dispersions having high moisture content and lower drug content except chloramphenicol at accelerated stability conditions.

Stability studies show that solid dispersions were unstable at accelerated storage conditions. This might be due to high temperature which enhances the molecules movement causing decomposition and conversion of drug into crystalline form. The solid dispersions were more sensitive to moisture and during accelerated storage it absorbs moisture which causes the recrystallisation of drug. The recrystallised drugs had low drug

content as compared to an amorphous drug form. This might be the reason for its effect on the dissolution, solubility and bioavailability because the amorphous state shows enhanced dissolution, solubility and bioavailability (Yu, 2001).

On the other hand, solid dispersions stored at room temperature conditions were stable after 12 months. There can be two possible explanations for this: Firstly, the temperature remained low at room (25 °C) as compared to temperature at accelerated storage (40 °C), and secondly the moisture content was controlled by silica gel. The hygroscopic nature of PEG 8000 results in the recrystallisation of the amorphous drug in the carrier matrix. In addition, the visual observation from our study showed that the solid dispersions were sticky due to moisture uptake of the polymer, which is also reflected from DSC, FTIR, drug content and TGA results. For stable solid dispersion formulations kept the temperature low to decrease the molecules movement to stop the chemical decomposition. Recrystallisation of drug in the solid dispersion was prevented by controlling the moisture content using silica gel.

5.4 Conclusions

Stability studies were carried out for all solid dispersions under investigation at room conditions and accelerated conditions to determine the stability of drugs in the solid dispersions.

Accelerated stability studies (40°C±2°C/75%RH±5%RH) indicated that the solid dispersion for all seven drugs were unstable as shown by DSC, FTIR, drug content and TGA analysis. However, solid dispersions stored at room temperature conditions (controlled moisture using silica gel) were stable for 12 months. Temperature and moisture are the two major factors that can rightly be said to have affected the stability of solid dispersions.

Chapter 6

Permeability Studies

6.1 Introduction

The process by which drug is taken from the site of administration to the site of action within the body has been defined as absorption (Rowland & Tozer, 1995). Oral drug absorption is often referred to as drug transfer across the apical membrane of the enterocyte, as the apical membrane is considered to be the rate limiting step for permeation through the membrane (Fagerholm & Lennernas, 1995). Permeability is a general term describing how readily the drug is transferred through a membrane. The specific permeability characteristics of a drug are dependent on its physicochemical properties, including lipophilicity, charge, pH, size and polar surface area (Rowland & Tozer, 1995; Lipinski et al., 2001). The rate of absorption is dependent on permeability, surface area and concentration gradient across the membrane. The concentration gradient is the driving force for passive diffusion, the most common mechanism for drug membrane transport.

The intestinal pH is an important factor for drug permeability as unionized molecules will pass the intestinal barrier most readily (Shore et al., 1957). As many drugs have a pKa in the physiological pH range, the permeability might vary with the degree of ionization of the compound according to the Henderson-Hasselbalch equation (Rowland & Tozer, 1995). The lumenal pH in the fasted state of the gastro-intestinal tract varies from one intestinal region to another. In the stomach, it has been shown that the pH is approximately 2, in duodenum it is 6.0, from the jejunum to the ileum, it lies in the interval 6.5-7.5 and in colon it is 7.0 (Evans et al., 1988; Dressman et al., 1990). Consequently, there could also be a pH gradient across the intestinal membrane as the pH

of the blood is constant. This gradient could affect the drug permeability and is, therefore, often applied in *in vitro* permeability screening (Yamashita et al., 2000).

The small intestinal epithelium is a highly dynamic system, being spatially classified into proliferative, differentiating, and functional cells in the lower and upper crypt parts and on the villi, respectively. Therefore, dynamics during absorption has been studied in experimental animals (Kedinger et al., 1987; Evans et al., 1994) or human colon cancer cell lines (Rousset, 1986). Animal models offer limited information about absorption in humans; for example, major differences in an intestinal cell differentiation in humans and rodents have been detected (Simon-Assman et al., 1994).

Because *in vivo* studies performed with humans and laboratory animals are expensive, time consuming and often even unethical, *in vitro* methods, as accurate as possible, are needed in the screening of new formulations. Immortalized, often of cancer origin, animal and human cell cultures have been used for the estimation and prediction of human drug absorption. Several possible *in vitro* human cell models are available for this purpose, one of which is the Caco-2 cell model, a well characterised cell line. The Caco-2 cell line is widely used in *in vitro* system for predicting gastro-intestinal absorption (Artursson et al., 1996). Caco-2 cells are derived from human colorectal carcinoma (Fogh et al., 1977) and differentiated spontaneously in culture into polarised cell monolayers with microvilli and tight junctions (Hidalgo et al., 1989). They differentiate spontaneously in culture and exhibit structural and functional differentiation patterns characteristic of mature enterocytes (Pinto et al., 1983). Caco-2 cells reach confluency

within 3-6 days and reach the stationary growth phase after 10 days in culture (Braun et al., 2000). Twenty days time period is required for complete differentiation (Pinto et al., 1983). These cells when differentiated possess very high levels of different enzymes such as alkaline phosphatase, sucrase isomaltase and aminopeptidase activity characteristic to enterocyte brush border microvilli. Polarization of the monolayer after confluency is in correlation with the structural and functional differentiation of the microvilli. The tight junctions produced during the differentiation indicate the presence of structural polarity. Barrier function is shown by monolayers as characterised by high transepithelial electrical resistance (TEER) values (200-600 Ωcm^2, grown on polycarbonate filters). Fully differentiated Caco-2 cells form an epithelial membrane with a barrier function similar to the human colon (Artursson et al., 1993). Caco-2 cell monolayers have been used for studying mechanisms of passive paracellular (Artursson et al., 1993; Artursson et al., 1996) and passive transcellular permeability (Artursson, 1990), carrier mediated absorptive transport of amino acids (Thwaites et al., 1995b), amino acid analogues (Hu and Borchardt, 1990; Thwaites et al., 1995a), oligopeptides (Thwaites et al., 1993), ß-lactam antibiotics and ACE-inhibitors (Inui et al., 1992), and peptidomimetic thrombin inhibitors (Walter et al., 1995). Carrier mediated efflux of several drugs has been intensively studied over the last years (Benet et al., 1999; Collett et al., 2004). Many enzymes (e.g. Cytochrome P450 (CYP), UDP-glucuronosyltransferase (UGT), sulphotransferases) and transporters (e.g. monocarboxylic acid transporter, P-glycoprotein (P-gp) present in the small intestine are expressed in Caco-2 cells, though in different quantities than in the small intestine (Hidalgo et al., 1989; Konishi et al., 2002). Caco-2 cells nevertheless share many properties with the absorptive cells in human

intestine, and several studies have demonstrated excellent correlation between Caco-2 permeability and intestine absorption in humans (Artursson and Karlsson, 1991; Yamashita et al., 2000). According to Biopharmaceutics Classification System (BCS) and FDA approval, Caco-2 cells can be used as a screening method for new drug candidates during drug discovery and development (Rubas et al., 1996; Artursson and Borchardt, 1997; Guidance for Industry, FDA 2000).

P-gp is a phosphoglycoprotein belonging to the ATP (adenosine triphosphate)-binding cassette (ABC) transporter super-family. ABC transporters have a highly conserved ATP binding region, which is characteristic for these transporters. Over 200 ABC transporters are known and they exist in a wide variety of species, ranging from bacteria to humans, and are found in association with import or export of nutrients such as amino acids, sugars, peptides or hydrophobic substances (Higgins, 1992). The P-gp, (Pgp/ABCB1), can transport compounds with a broad range of chemical structure out of a cell through the consumption of energy. This phenomenon has been referred to as multidrug resistance (MDR) (Hunter & Hirst, 1997). Humans have one gene for multidrug resistance, the MDR1. One determinant for interaction with P-gp is the relative hydrophobicity of the interacting molecule. Substrates for P-gp have a partition coefficient (octanol/ water) of approximately +1 or greater (Hunter & Hirst, 1997). P-gp transports large hydrophobic, uncharged or slightly positively charged molecules (Sarkadi and Muller, 1997; Stein, 1997). It was reported that P-gp was expressed not only in tumor cells but in many normal cells in various organs such as the liver, kidney, intestine and brain in humans and animals (Fojo et al., 1987; Thiebaut et al., 1987;

Cordon- Cardo et al., 1990). It has been suggested that the function of P-gp is to protect the body and important organs, such as the brain, from naturally occurring toxic substances. The contribution of P-gp in the blood-brain barrier (BBB) has been shown using knockout mice lacking the MDR gene, and drugs such as ivermectin and loperamide exhibited a much higher degree of brain toxicity when P-gp was absent (Schinkel et al., 1994; Schinkel et al., 1996). The function of P-gp in the intestine in not fully understood but it has been suggested that intestinal efflux transport by P-gp and other efflux proteins can affect the rate and extent of drug absorption and metabolism in rat and human intestine (Gan et al., 1996; Terao et al., 1996; Lown et al., 1997). Intestinal transporters, such as P-gp, could also cause drug-drug interactions due to changes in drug pharmacokinetics (Lin and Yamazaki, 2003). It could also be possible to increase the bioavailability after oral administration and transport across the BBB for some drugs and to further understand drug-drug interactions.

Rhodamine123 is considered a permeant cationic fluorescent probe (Johnson et al., 1981). Rhodamine123 is a substrate for P-gp and used as a marker for P-gp activity in cells, including Caco-2 cells. Rhodamine123 was used to study processes such as uptake, carrier-mediated studies (Cho et al., 2000), enhanced oral bioavailability of paclitaxel by d-α-tocopheryl polyethylene glycol 400 succinate (Hoa et al., 2008), permeability (Jung et al., 2006) and modulation of P-glycoprotein-mediated efflux (Rupa et al., 2006).

6.2 Aims of the study

The aim of this study was to study permeability of four drugs (indomethacin, phenacetin, paracetamol, phenylbutazone and their solid dispersions) and to establish any potential correlation with dissolution studies during permeation across Caco-2 cell monolayers. Indomethacin and phenylbutazone are carrier-controlled drugs whereas paracetamol and phenacetin are drug-controlled drugs. Indomethacin is a P-gp inhibitor and paracetamol is a P-gp substrate. Cell uptake studies were performed using rhodamine123 to further explore the effect and role of PEG 8000 in the permeability of these drugs.

6.3 Results and Discussion

6.3.1 Calibration curve of indomethacin

Figure 6.1 shows the calibration curves of indomethacin by HPLC in Hank's balanced salt solution (HBSS) at 264 nm. A calibration range of 2–10 µg/mL was established with good linearity over the entire working range (Coefficient of Determination $R^2 = 0.99$).

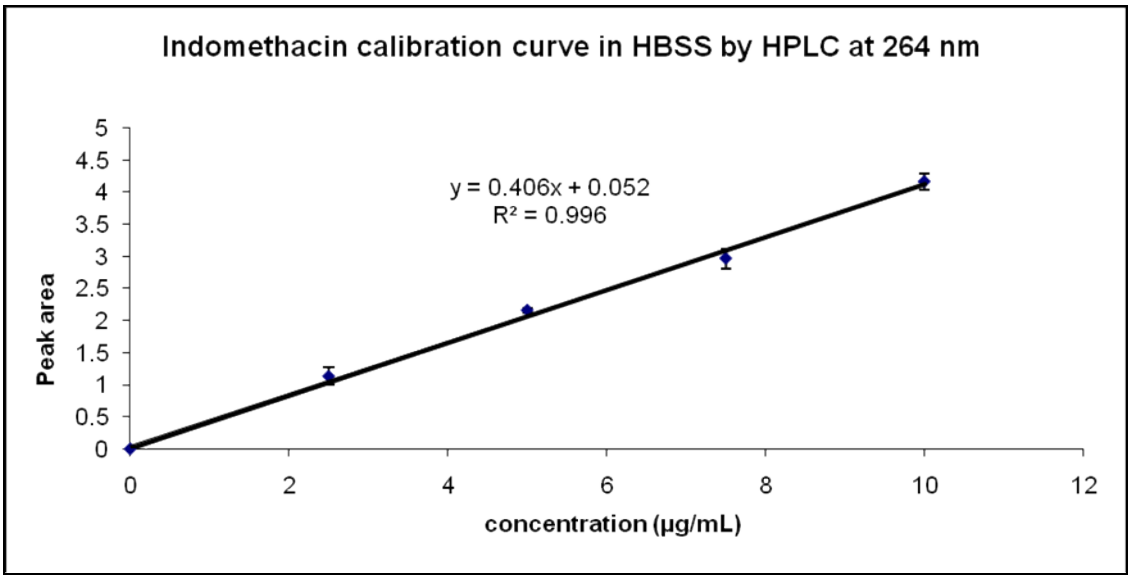

Figure 6.1. Calibration curve of indomethacin in Hank's balanced salt solution (HBSS) at 264 nm using HPLC (n=3±S.D).

6.3.2 Calibration curve of phenacetin

Figure 6.2 shows the calibration curves of phenacetin by HPLC in Hank's balanced salt solution (HBSS) at 244 nm. A calibration range of 2–10 µg/mL was established with good linearity over the entire working range (Coefficient of Determination $R^2 = 0.99$).

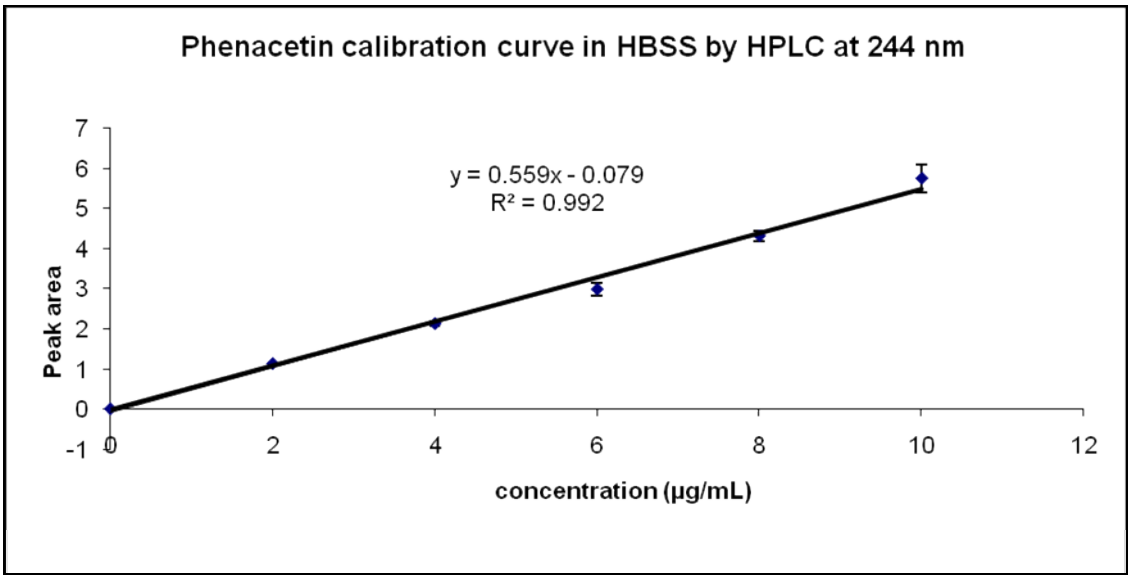

Figure 6.2. Calibration curve of phenacetin in Hank's balanced salt solution (HBSS) at 244 nm using HPLC (n=3±S.D).

6.3.3 Calibration curve of paracetamol

Figure 6.3 shows the calibration curves of paracetamol by HPLC in Hank's balanced salt solution (HBSS) at 240 nm. A calibration range of 2–10 µg/mL was established with good linearity over the entire working range (Coefficient of Determination $R^2 = 0.99$).

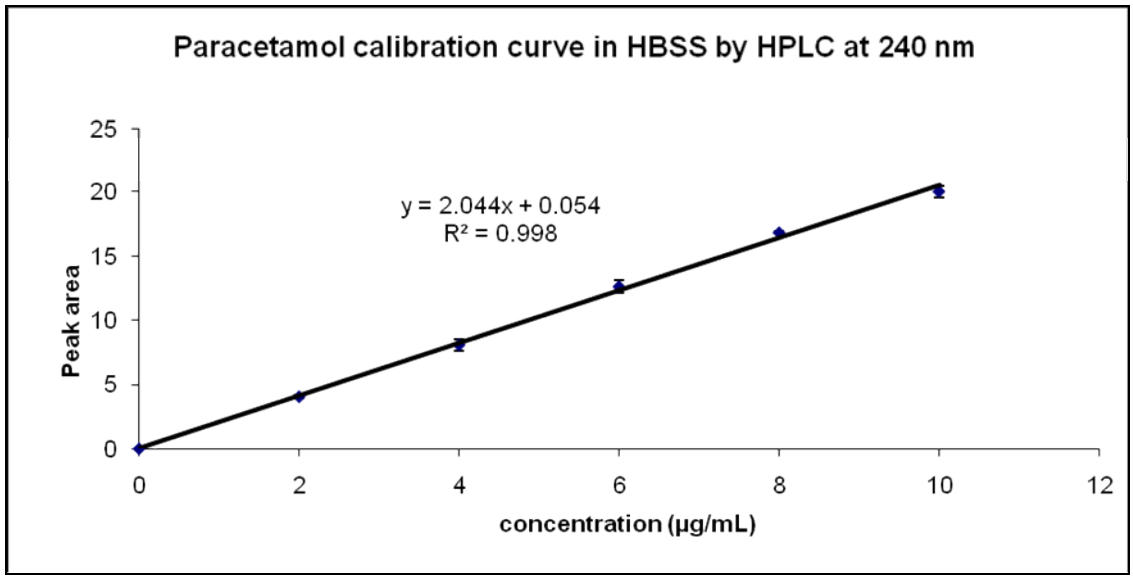

Figure 6.3. Calibration curve of paracetamol in Hank's balanced salt solution (HBSS) at 240 nm using HPLC (n=3±S.D).

6.3.4 Calibration curve of phenylbutazone

Figure 6.4 shows the calibration curves of phenylbutazone by HPLC in Hank's balanced salt solution (HBSS) at 236 nm. A calibration range of 3–15 µg/mL was established with good linearity over the entire working range (Coefficient of Determination $R^2 = 0.99$).

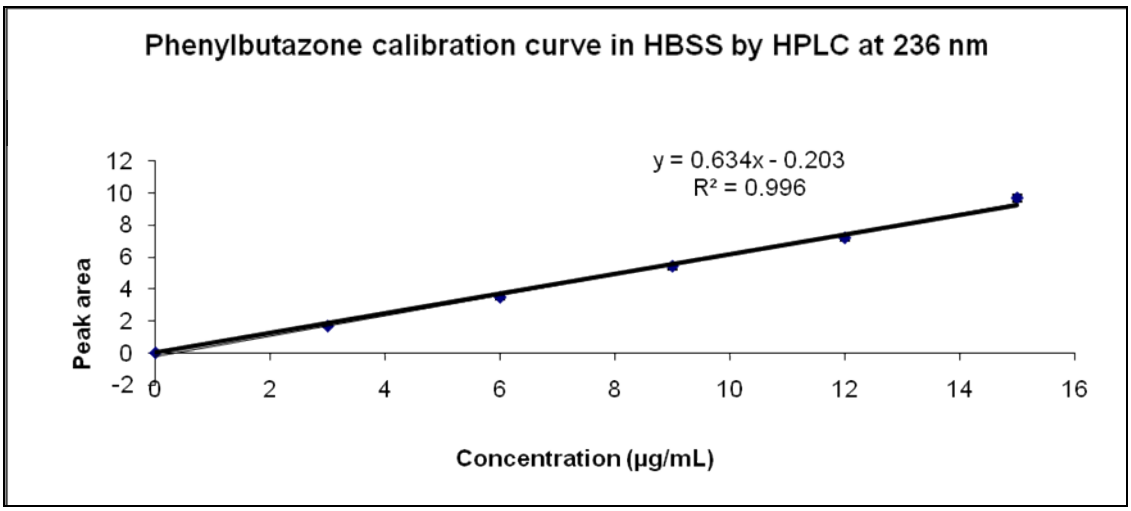

Figure 6.4. Calibration curve of phenylbutazone in Hank's balanced salt solution (HBSS) at 236 nm using HPLC (n=3±S.D).

6.3.5 Transepithelial electrical resistance and Recovery of drug (s)

6.3.5.1 Transepithelial electrical resistance (TEER)

The transepithelial electrical resistance (TEER) of the Caco-2 monolayers measured at the start (t= 0 min) and end (t= 60 mins) of the experiment. The TEER values in the Caco-2 monolayers did not change during the course of the experiment (60 mins) (with all drugs and solid dispersions) which showed that tight junction of the Caco-2 monolayers were intact throughout the study (table 6.1).

Table 6.1. Transepithelial electrical resistance (TEER) of the Caco-2 monolayers measured at the start (t= 0 min) and end (t= 60 min) of the experiment. The TEER values are represented as mean±S.D (*n* =3).

Formulation (s)	Before experiment TEER ohms (Ω)cm^2 ±S.D. (n=3)	After experiment TEER ohms (Ω)cm^2 ±S.D. (n=3)
Indomethacin	562±35	527±27
Solid dispersion of indomethacin	551±42	537±41
Phenacetin	564±32	547±29
Solid dispersion of phenacetin	562±24	538±29
Paracetamol	556±29	537±31
Solid dispersion of paracetamol	570±21	563±17
Phenylbutazone	549±36	533±35
Solid dispersion of phenylbutazone	555±30	543±23

The differentiation of Caco-2 monolayers is completed within 20 days (Pinto et al., 1983). Enzymes like alkaline phosphatase, sucrase isomaltase and aminopeptidase are found in these differentiated cells in high levels characteristic to enterocyte brush border microvilli. The structural and functional differentiation of the microvilli is associated with the polarization of the monolayer after confluency. The structural polarity is evident from the tight junctions, which are formed during the differentiation. The monolayers exhibit a barrier function as judged by high TEER values 200-600 ohms (Ω)cm^2. Figure 6.5 showed the effect of (21) days in culture on the transepithelial electrical resistance of

Caco-2 monolayers grown on 6 transwell inserts. Cells were used in experiments at the age of 21–27 days (Khan et al., 2003; Khan et al., 2004; Tammela et al., 2004; Laitinen et al., 2007).

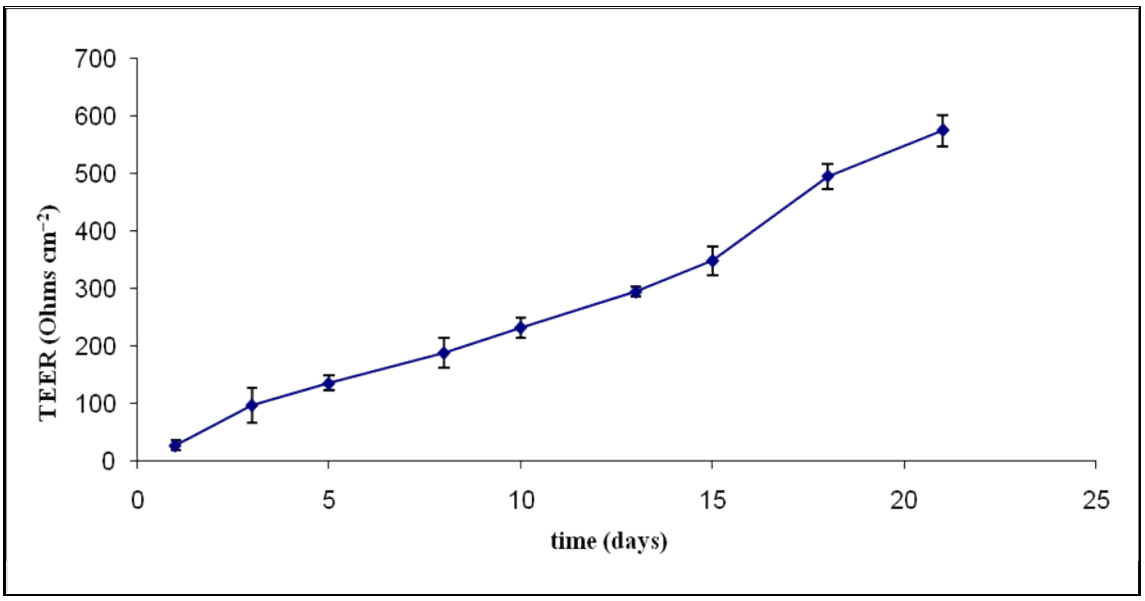

Figure 6.5. The effect of (21) days in culture on the transepithelial electrical resistance of Caco-2 monolayers grown on transwell inserts. Each point is the mean ±S.D (n=6).

6.3.5.2 Recovery of Drug(s)

The calculated recoveries remained >70% for the entire range of drugs and solid dispersions investigated. An acceptable recovery value at the end of the Caco-2 experiment is critical for the predictive value of the Caco-2 experiment. Indeed, if a low adsorption to the device surface), this could result in an erroneous estimation of the transport rate of the compound. Our result suggested that there was good recovery of drug after transport experiment and was more than 70% (shown in table 6.2) and no significant non-specific adsorption of drug to the plastic transwells was found at 37 °C suggesting that the drug was present in the cell monolayer (Neuhoff et al., 2005).

Table 6.2. Recovery values (%) for the Apical-to-Basal transport experiment of the all drugs and solid dispersions. The values represent the average value of three experiments ±S.D(n =3).

Formulations	Recovery (%)±S.D (n=3)
Indomethacin	83±10
Solid dispersion of indomethacin	90±4
Phenacetin	92±2
Solid dispersion of phenacetin	85±15
Paracetamol	70±3
Solid dispersion of paracetamol	76±3
Phenylbutazone	74±4
Solid dispersion of phenylbutazone	95±5

The permeability coefficients (Papp) were calculated and are tabulated in table 6.3.

Table 6.3. Shows the permeability coefficients (Papp) value calculated from solid dispersion and drug alone (n = 7)

Drug (s)	The permeability coefficients (Papp) x 10^{-6} cm/s (solid dispersion) ±S.D.	The permeability coefficients (Papp) x 10^{-6} cm/s (drug alone) ±S.D.
Indomethacin	3.92±0.37	1.12±0.08
Phenacetin	42.52±5.97	29.37±4.12
Paracetamol	7.09±3.76	5.12±0.76
Phenylbutazone	15.98±0.99	10.04±0.30

6.3.6 Permeability Studies

6.3.6.1 Indomethacin

Figures 6.6-7 shows HPLC scan from permeability studies across Caco-2 monolayers at different time points of indomethacin and solid dispersion of indomethacin.

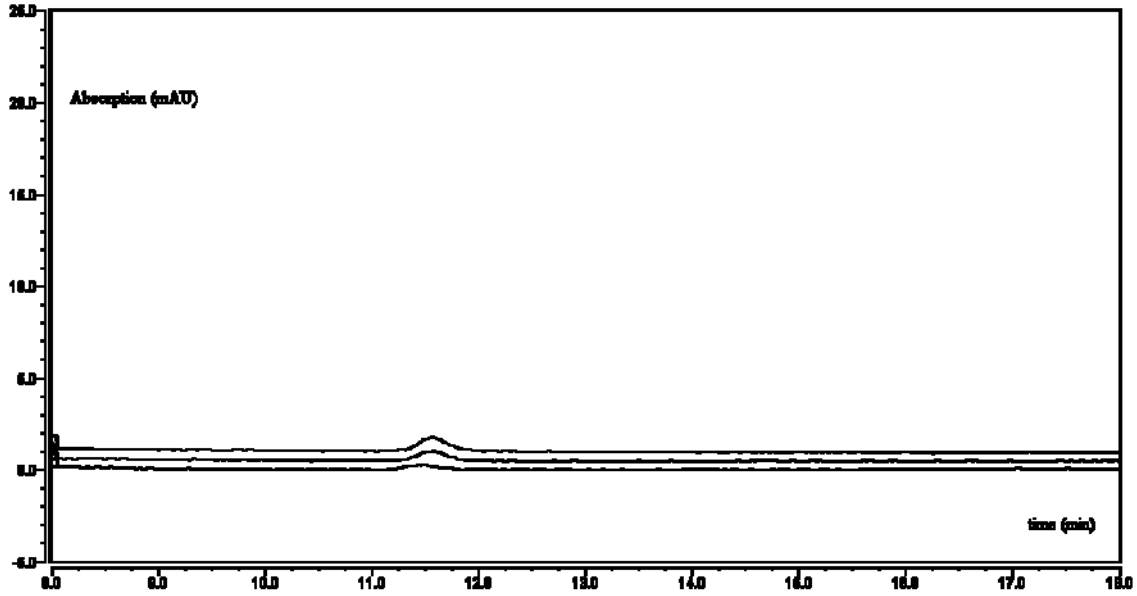

Figure 6.6. HPLC analysis of indomethacin alone from permeability studies at 5, 20, 60 mins time points (bottom to top).

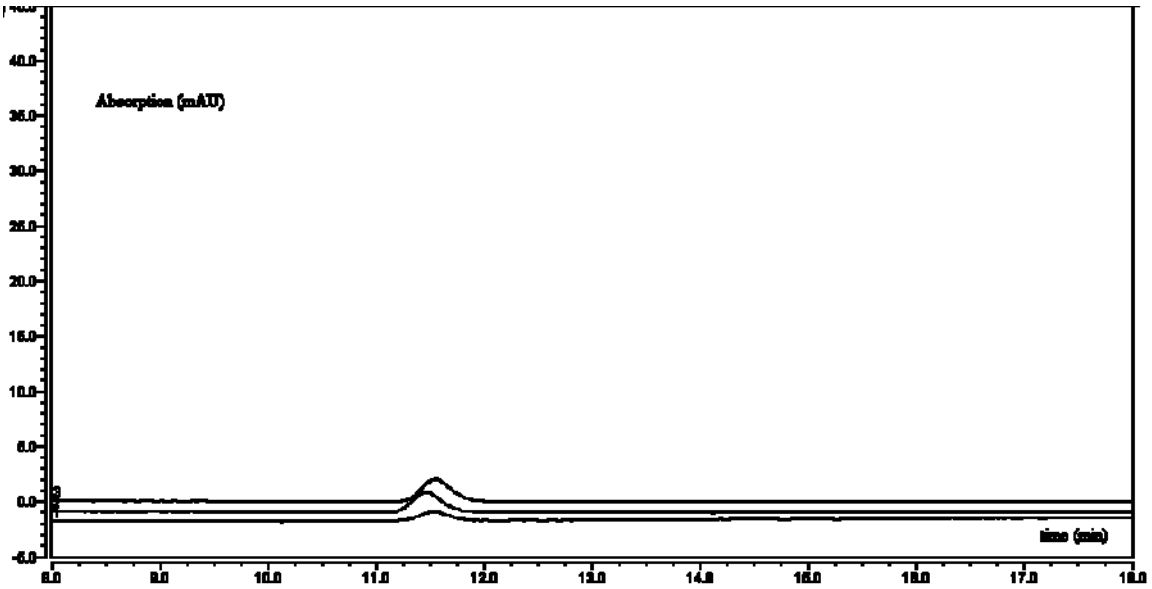

Figure 6.7. HPLC analysis of solid dispersion of indomethacin from permeability studies at 5, 20, 60 mins time points (bottom to top).

Figure 6.8 shows the amount of indomethacin transferred (μg) across Caco-2 monolayer at different time points for both drug alone and solid dispersion.

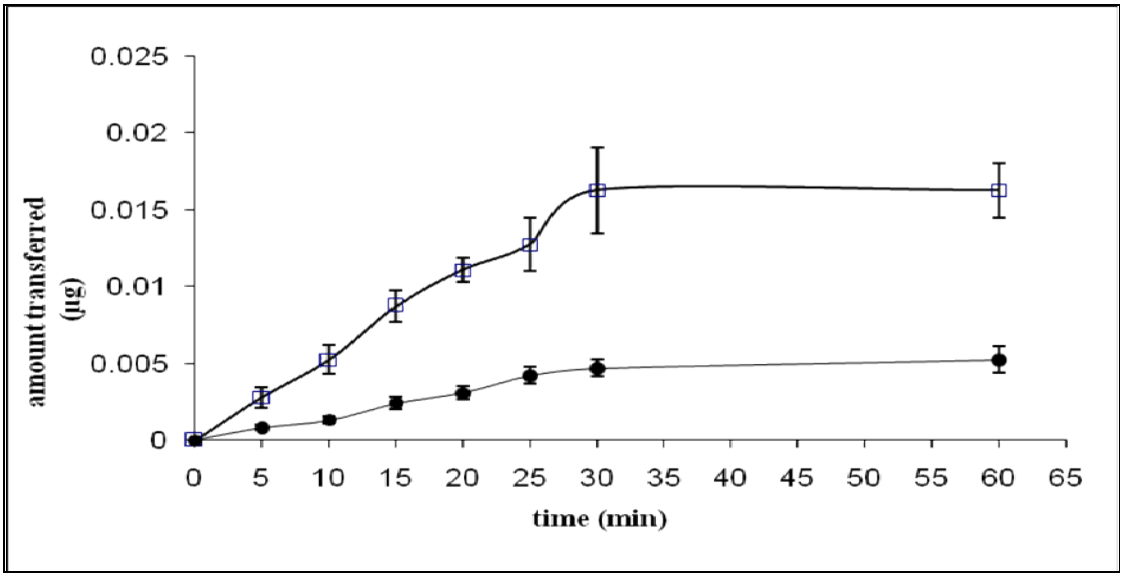

Figure 6.8. HPLC analysis of samples from Caco-2 cell studies evaluating the absorption of solid dispersion (□) of indomethacin in PEG 8000 as a carrier and indomethacin alone (•). Data are expressed as mean±S.D (*n* = 3).

Figure 6.9 shows the cumulative % transferred of indomethacin from apical to basal per transwell (µg/2.5 mL) across Caco-2 monolayer at different time point for both drug alone and solid dispersion.

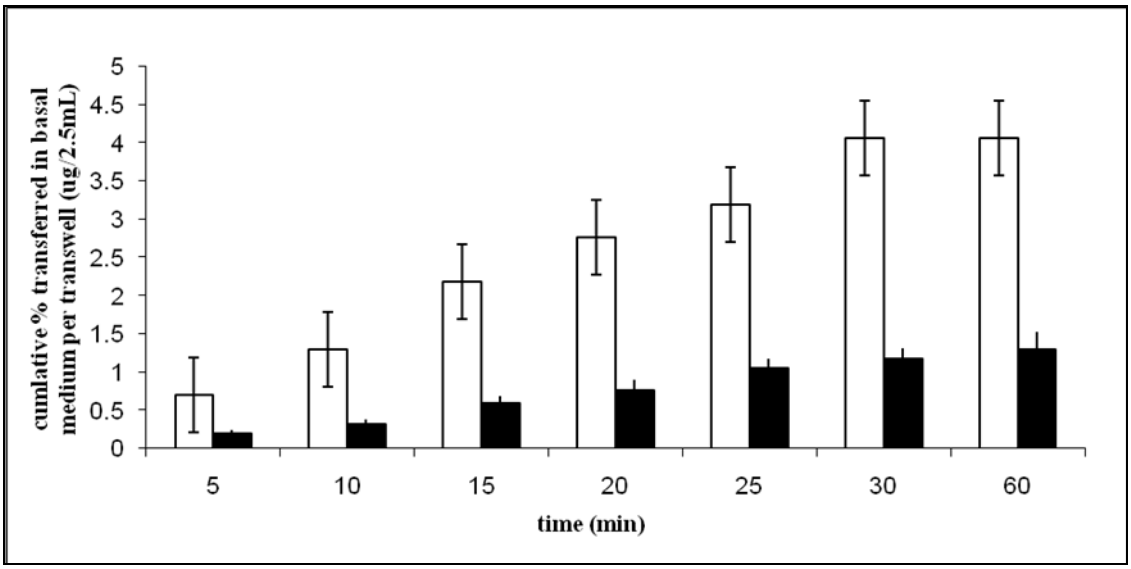

Figure 6.9. Apical-to-basal permeability of solid dispersion of indomethacin (□) and indomethacin alone (■) across Caco-2 monolayers. Each column indicates mean±S.D (n=3).

Figure 6.10 shows the rate transferred of indomethacin from apical to basal across Caco-2 monolayer for first 20 mins for drug alone, solid dispersion and difference in rate transfer from solid dispersion to drug alone.

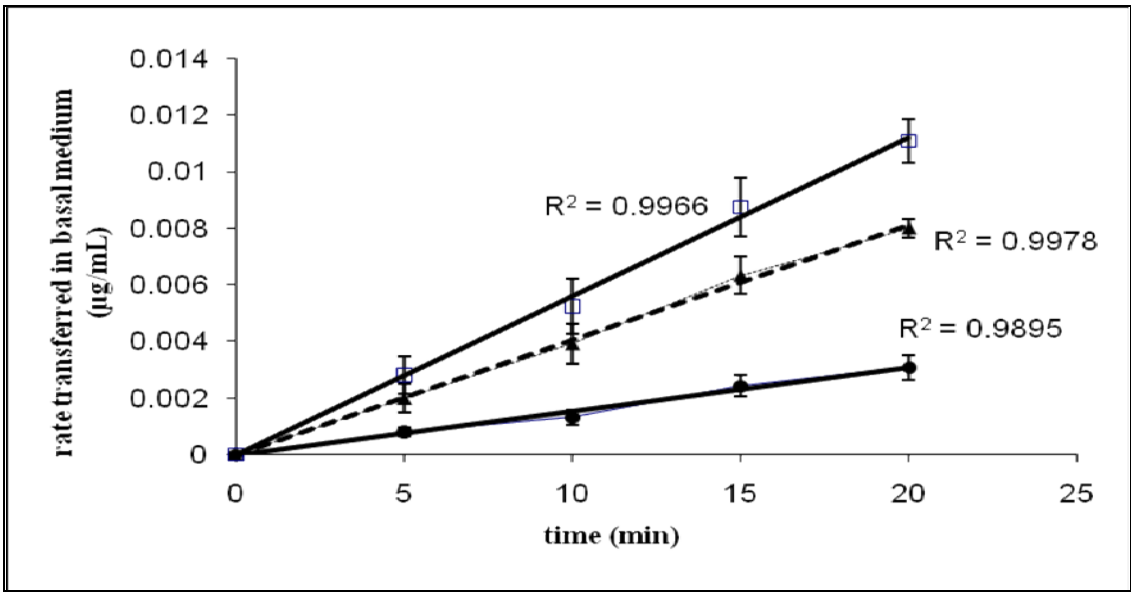

Figure 6.10. Rate transferred of indomethacin across Caco-2 cell monolayers in basal medium by HPLC analysis. (Best linear fit for the apical to basolateral transport of solid dispersion and drug alone across Caco-2 cell monolyers was found over the first 20 mins) : Solid dispersion of indomethacin (□),indomethacin alone (●) and difference between amount transferred (µg) of solid dispersion to indomethacin alone (▲) with R^2 value. Data are expressed as mean±S.D (*n* = 3).

Figure 6.11 shows the apparent permeability coefficients (Papp) of indomethacin at different time points for both drug alone and solid dispersion across Caco-2 monolayers.

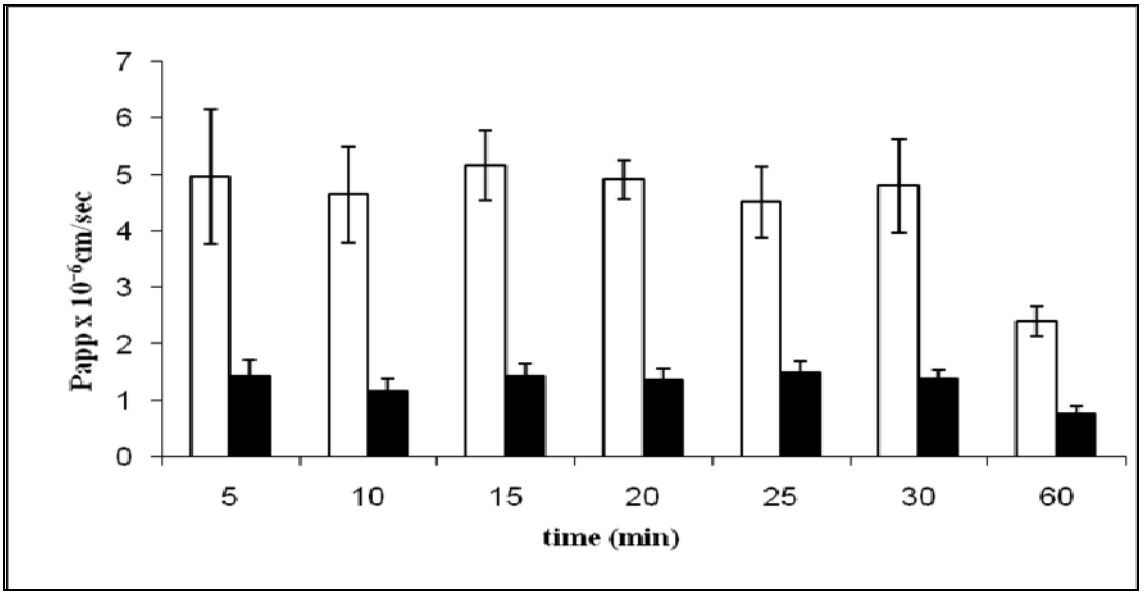

Figure 6.11. The apparent permeability coefficients (Papp) of solid dispersion containing indomethacin (□) compared to the indomethacin alone (■).Each column indicates mean±S.D (n=3).

6.3.6.2 Phenacetin

Figures 6.12-13 show HPLC analysis from permeability studies across Caco-2 monolayers at different time points of phenacetin alone and solid dispersion of phenacetin.

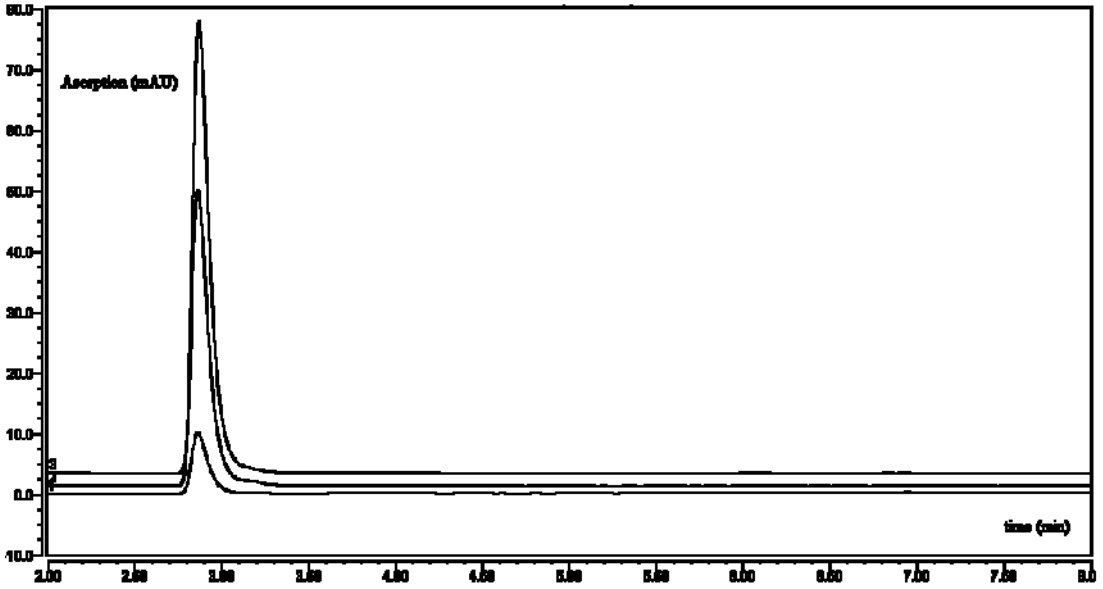

Figure 6.12. HPLC analysis of phenacetin alone from permeability studies at 5, 20, 60 mins time points (bottom to top).

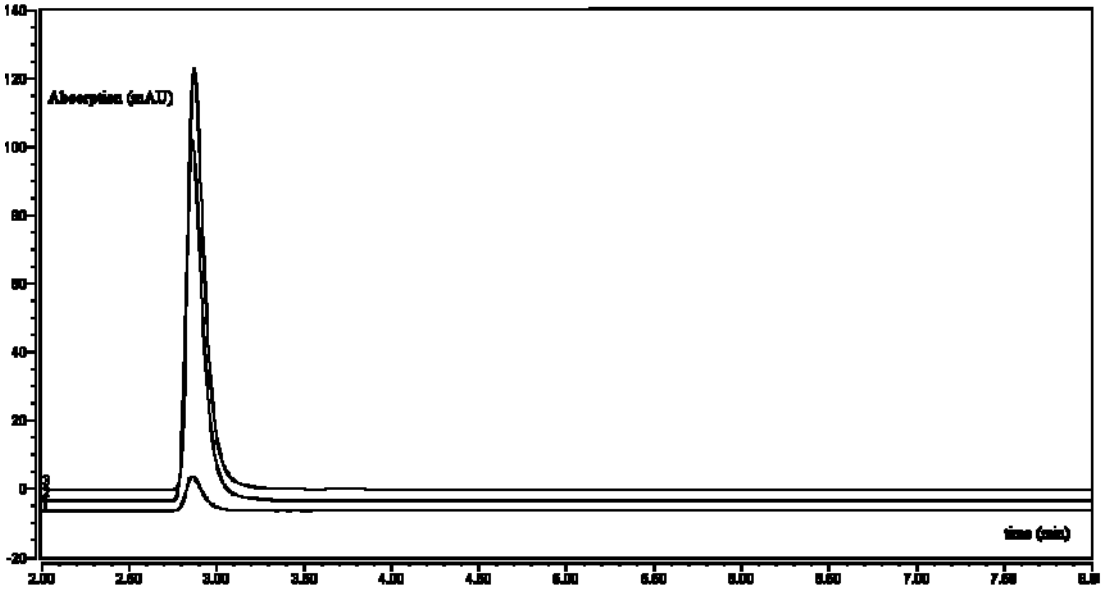

Figure 6.13. HPLC analysis of solid dispersion of phenacetin from permeability studies at 5, 20, 60 mins time points (bottom to top).

Figure 6.14 shows the amount of phenacetin transferred (μg) across Caco-2 monolayer at different time points for both drug alone and solid dispersion.

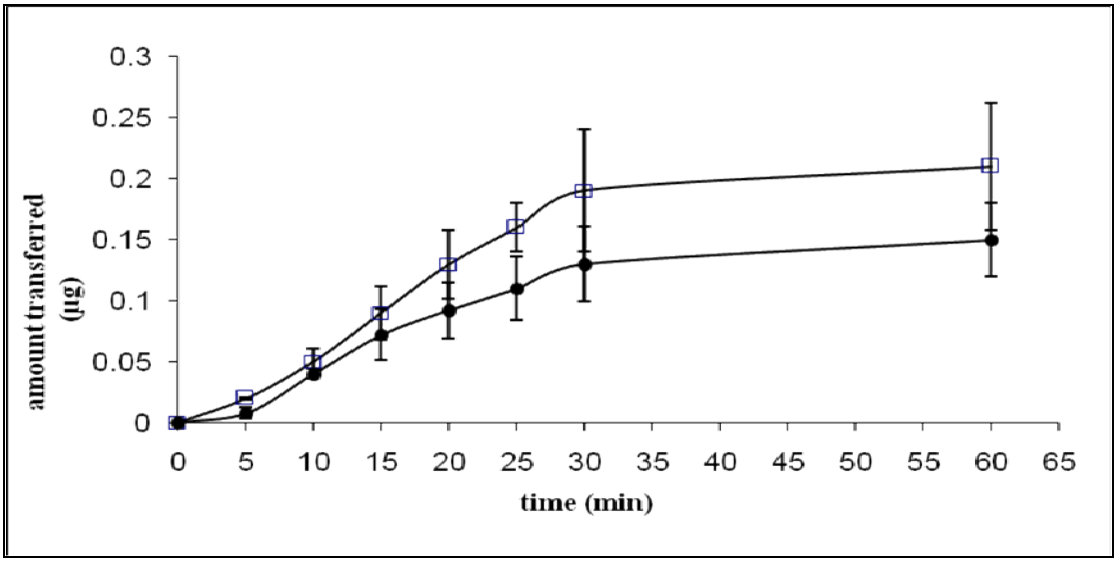

Figure 6.14. HPLC analysis of samples from Caco-2 cell studies evaluating the absorption of solid dispersion (□) of phenacetin in PEG 8000 as a carrier and phenacetin alone (●). Data are expressed as mean±S.D (*n* = 3).

Figure 6.15 shows the cumulative % transferred of phenacetin from apical to basal per transwell (µg/2.5 mL) across Caco-2 monolayer at different time points for both drug alone and solid dispersion.

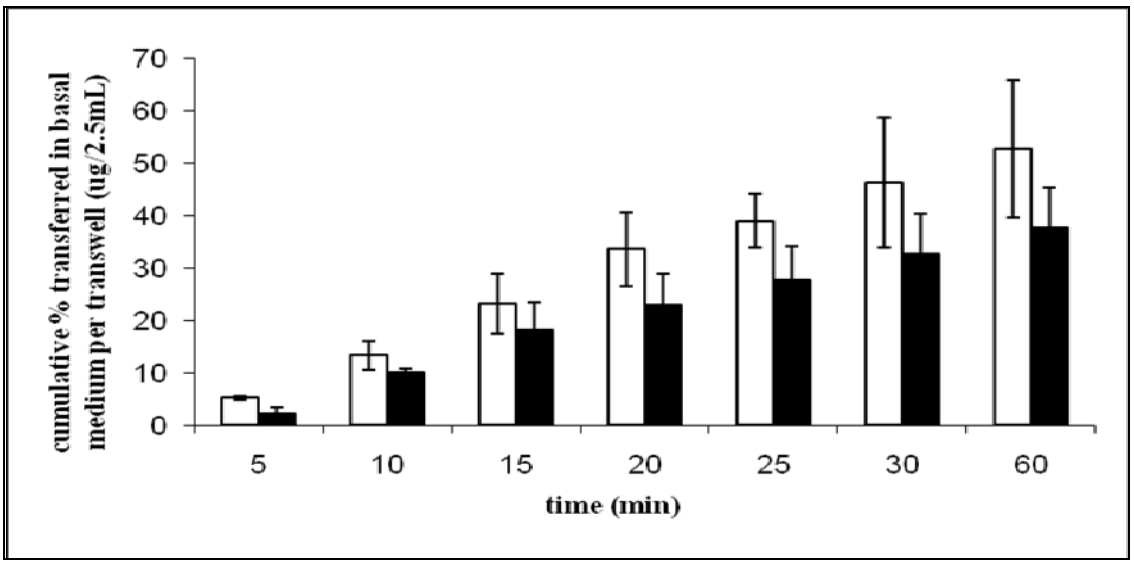

Figure 6.15. Apical-to-basal permeability of solid dispersion of phenacetin (□) and phenacetin alone (■) across Caco-2 monolayers. Each column indicates mean±S.D (n=3).

Figure 6.16 shows the rate transferred of phenacetin from apical to basal across Caco-2 monolayer for first 20 mins for drug alone, solid dispersion and difference in rate transfer from solid dispersion to drug alone.

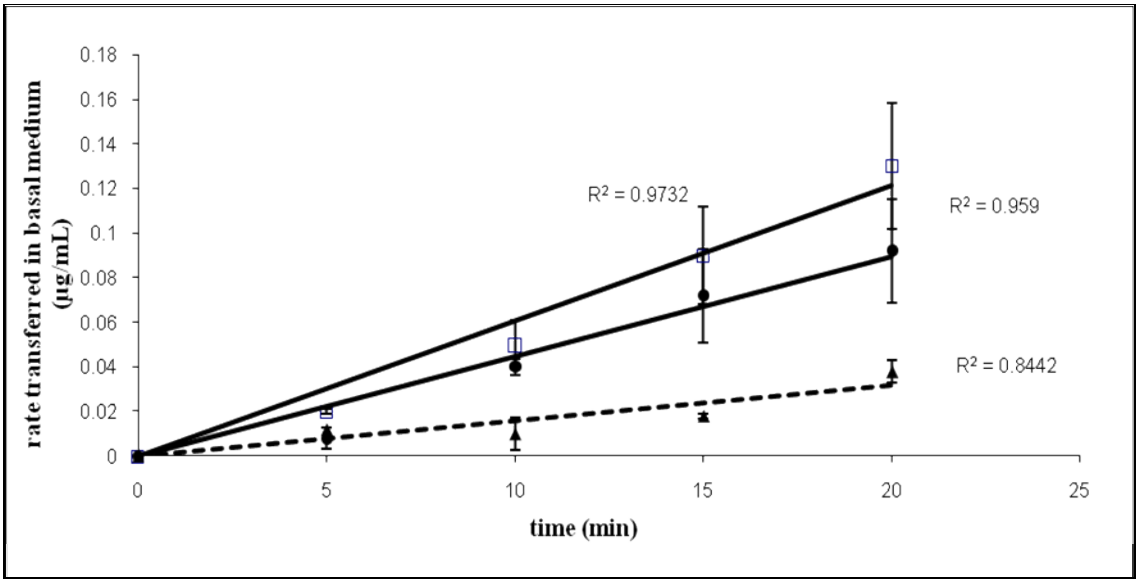

Figure 6.16. Rate transferred of phenacetin across Caco-2 cell monolayers in basal medium by HPLC analysis (Best linear fit for the apical to basolateral transport of solid dispersion and drug alone across Caco-2 cell monolyers was found over the first 20 mins): Solid dispersion of phenacetin (□),phenacetin alone (●) and difference between amount transferred (µg) of solid dispersion to phenacetin alone (▲) with R^2 value. Data are expressed as mean±S.D (*n* = 3).

Figure 6.17 shows the apparent permeability coefficients (Papp) of phenacetin at different time points for both drug alone and solid dispersion across Caco-2 monolayers.

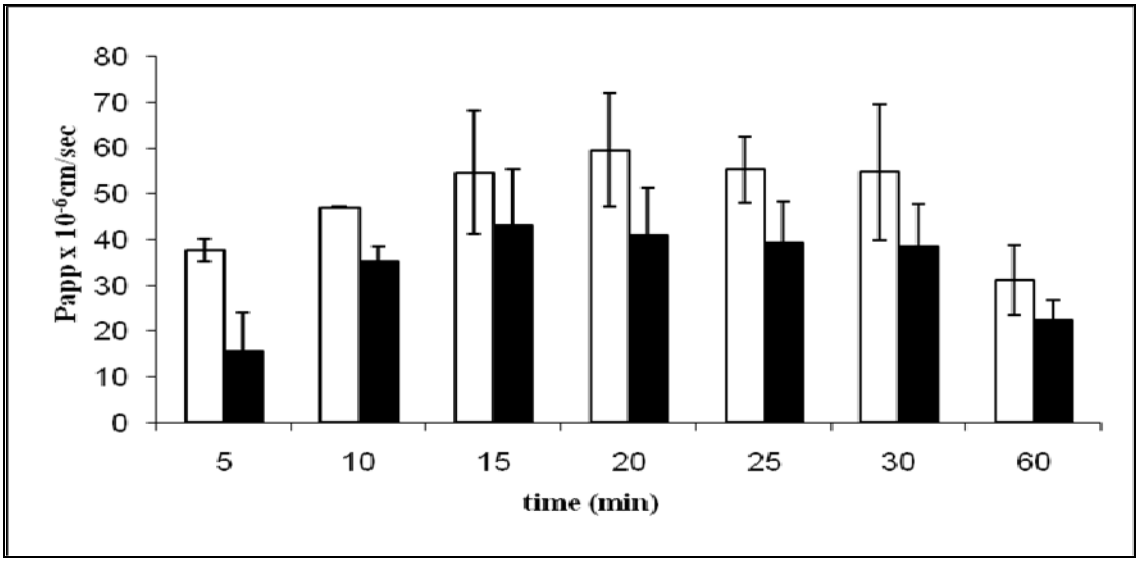

Figure 6.17. The apparent permeability coefficients (Papp) of solid dispersion containing phenacetin (□) compared to the phenacetin alone (■).Each column indicates mean±S.D (n=3).

6.3.6.3 Paracetamol

Figures 6.18-19 shows HPLC analysis from permeability studies across Caco-2 monolayers at different time points of paracetamol alone and solid dispersion of paracetamol.

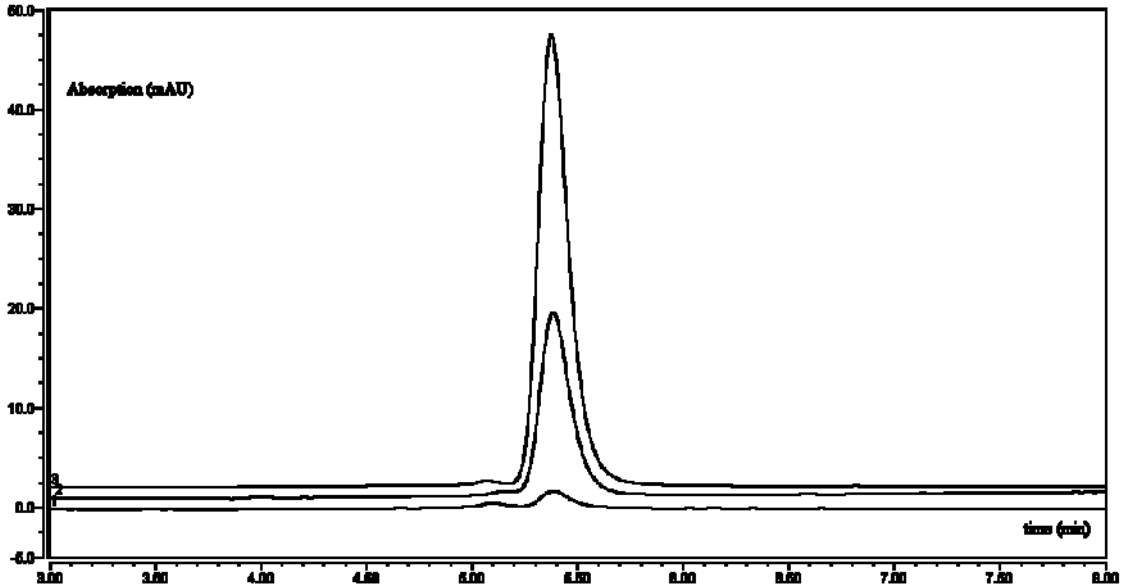

Figure 6.18. HPLC analysis of paracetamol alone from permeability studies at 5, 20, 60 mins time points (bottom to top).

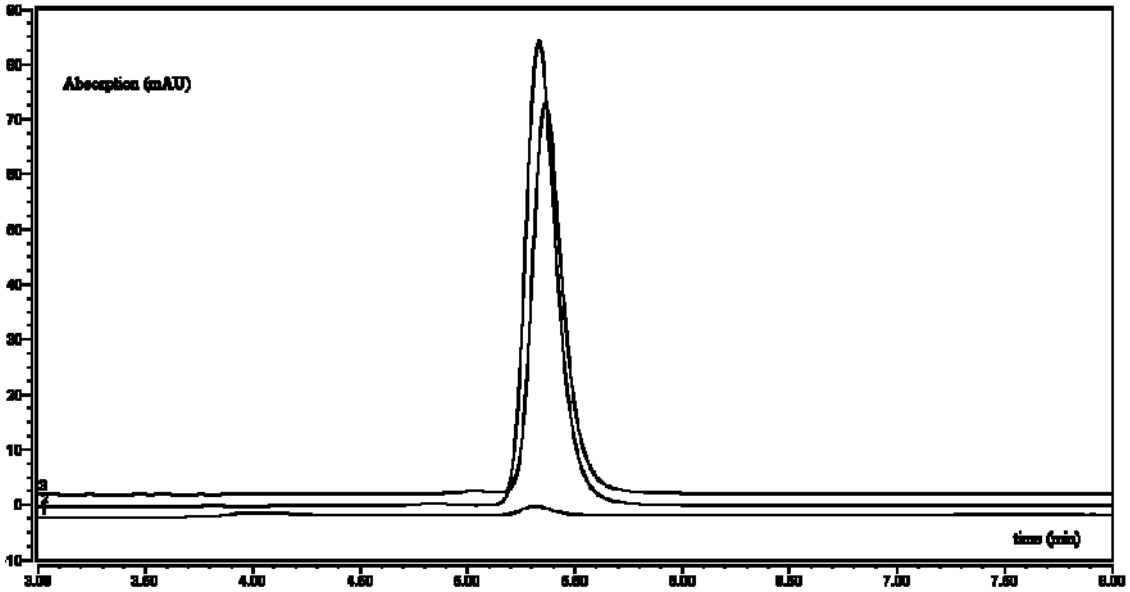

Figure 6.19. HPLC analysis of solid dispersion of paracetamol from permeability studies at 5, 20, 60 mins time points (bottom to top).

Figure 6.20 shows the amount of paracetamol transferred (μg) across Caco-2 monolayer at different time points for both drug alone and solid dispersion.

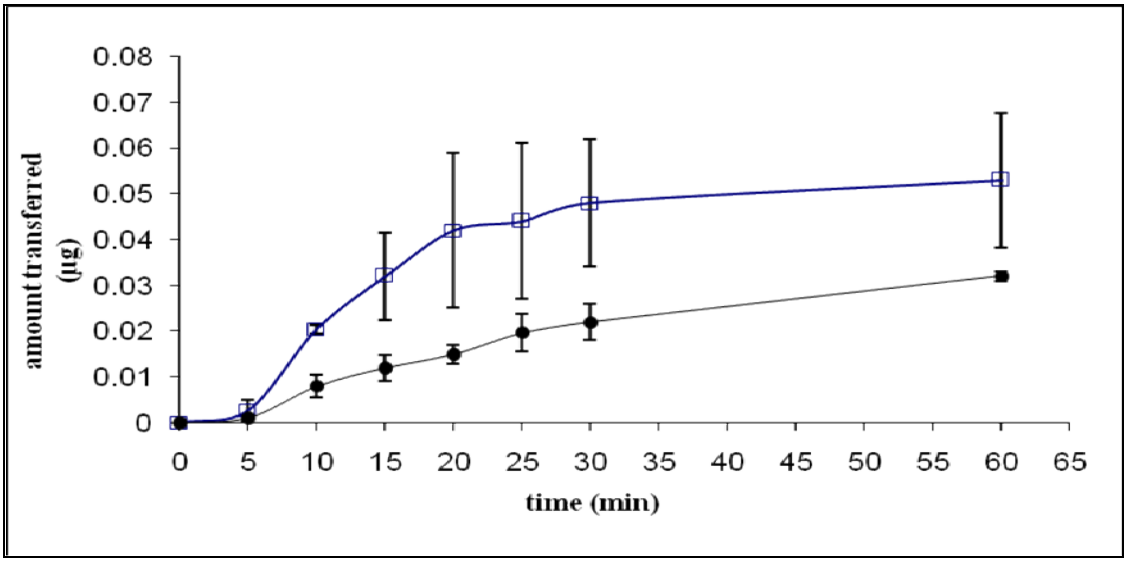

Figure 6.20. HPLC analysis of samples from Caco-2 cell studies evaluating the absorption of solid dispersion (□) of parcetamol in PEG 8000 as a carrier and paracetamol alone (●). Data are expressed as mean±S.D (*n* = 3).

Figure 6.21 shows the cumulative % transferred of paracetamol from apical to basal per transwell (µg/2.5 mL) across Caco-2 monolayer at different time point for both drug alone and solid dispersion.

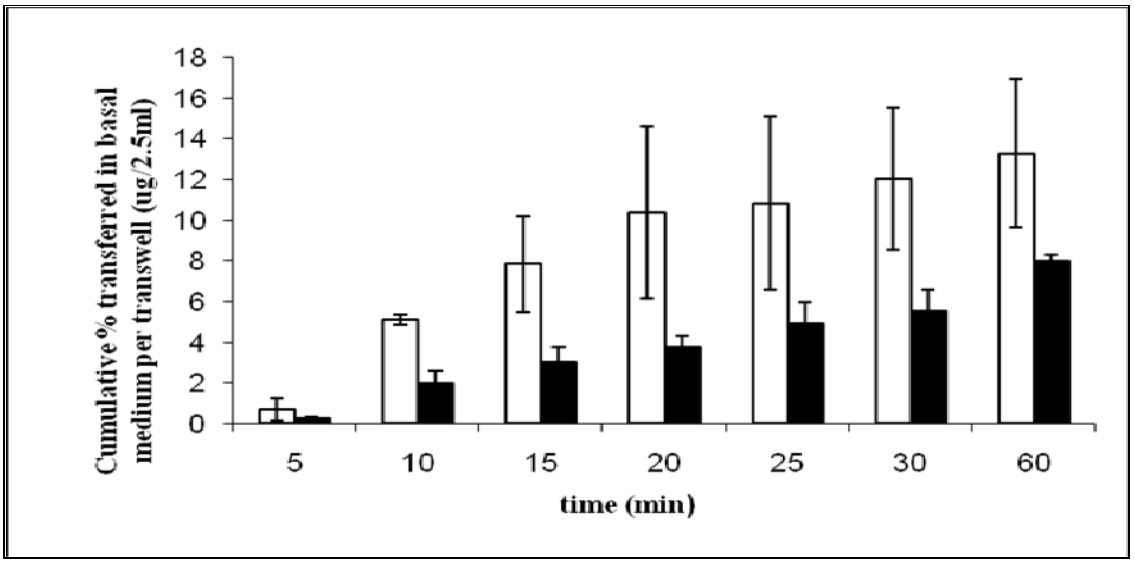

Figure 6.21. Apical-to-basal permeability of solid dispersion of paracetamol (□) and paracetamol alone (■) across Caco-2 monolayers. Each column indicates mean±S.D (n=3).

Figure 6.22 shows the rate transferred of paracetamol from apical to basal across Caco-2 monolayer for first 20 mins for drug alone, solid dispersion and difference in rate transfer from solid dispersion to drug alone.

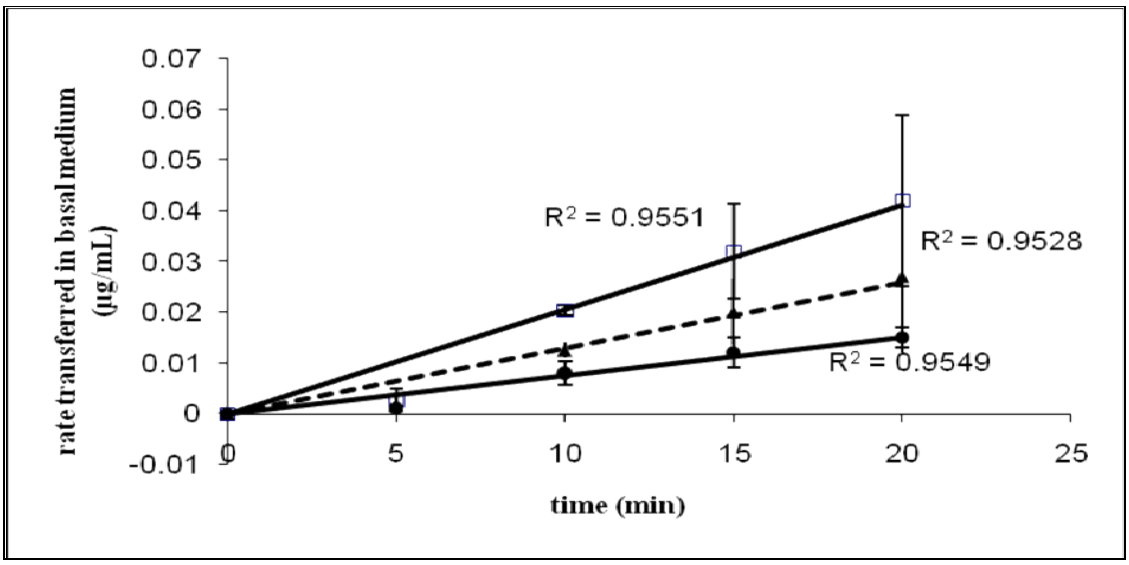

Figure 6.22. Rate transferred of paracetamol across Caco-2 cell monolayers in basal medium by HPLC analysis: (Best linear fit for the apical to basolateral transport of solid dispersion and drug alone across Caco-2 cell monolyers was found over the first 20 mins). Solid dispersion of parcetamol (□), paracetamol alone (•) and difference between amount transferred (µg) of solid dispersion to paracetamol alone (▲) with R^2 value. Data are expressed as mean±S.D (*n* = 3).

Figure 6.23 shows the apparent permeability coefficients (Papp) of paracetamol at different time points for both drug alone and solid dispersion across Caco-2 monolayers.

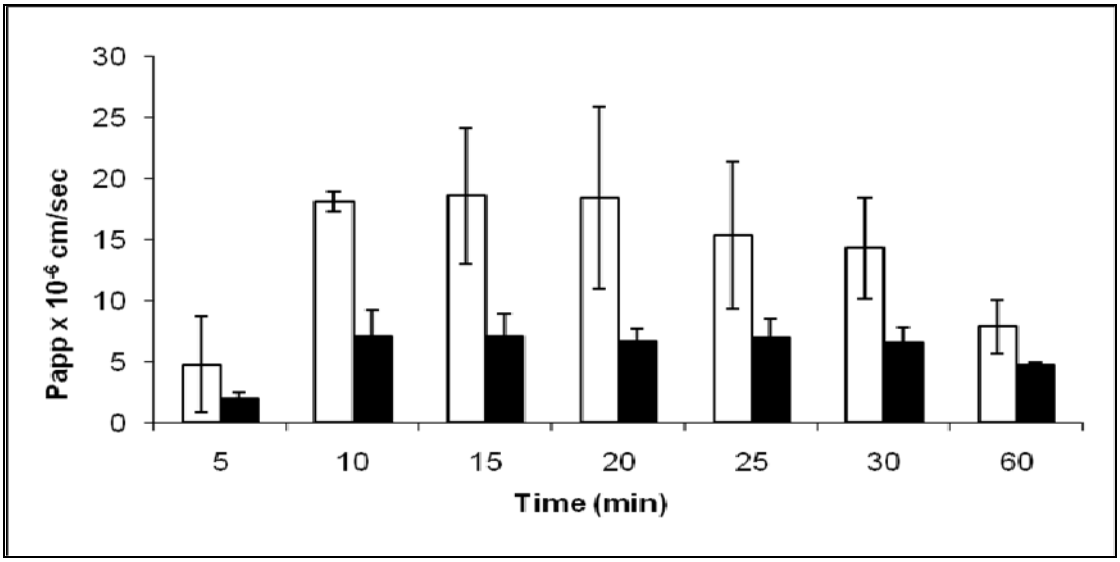

Figure 6.23. The apparent permeability coefficients (Papp) of solid dispersion containing paracetamol (□) compared to the paracetamol alone (■).Each column indicates mean±S.D (n=3).

6.3.6.4 Phenylbutazone

Figures 6.24-25 show HPLC analysis from permeability studies across Caco-2 monolayers at different time points of phenylbutazone alone and solid dispersion of phenylbutazone.

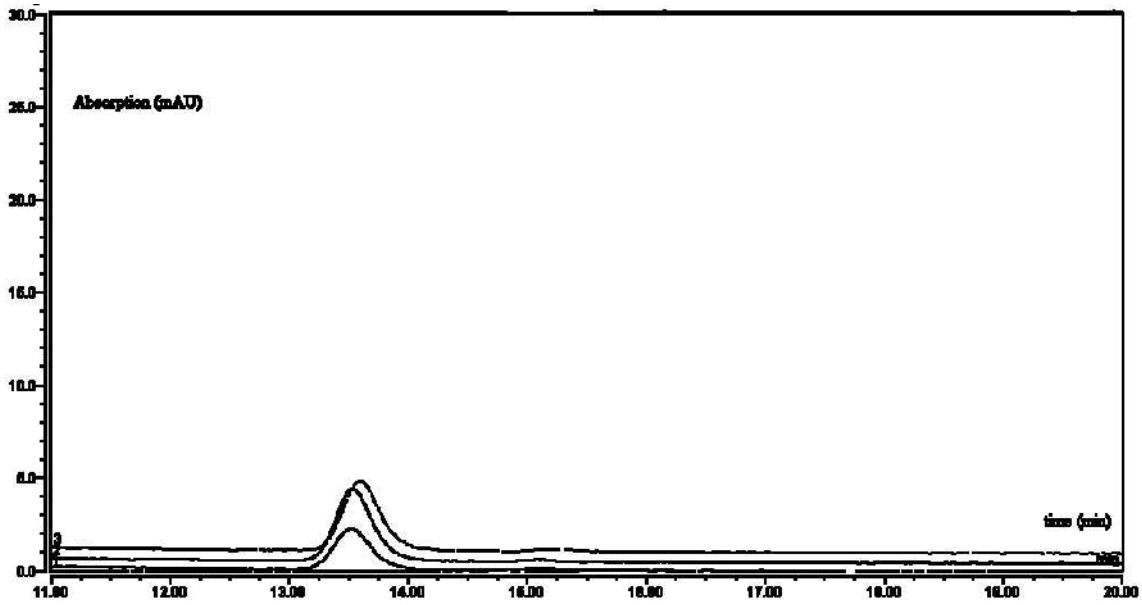

Figure 6.24. HPLC analysis of phenylbutazone alone from permeability studies at 5, 20, 60 mins time points (bottom to top).

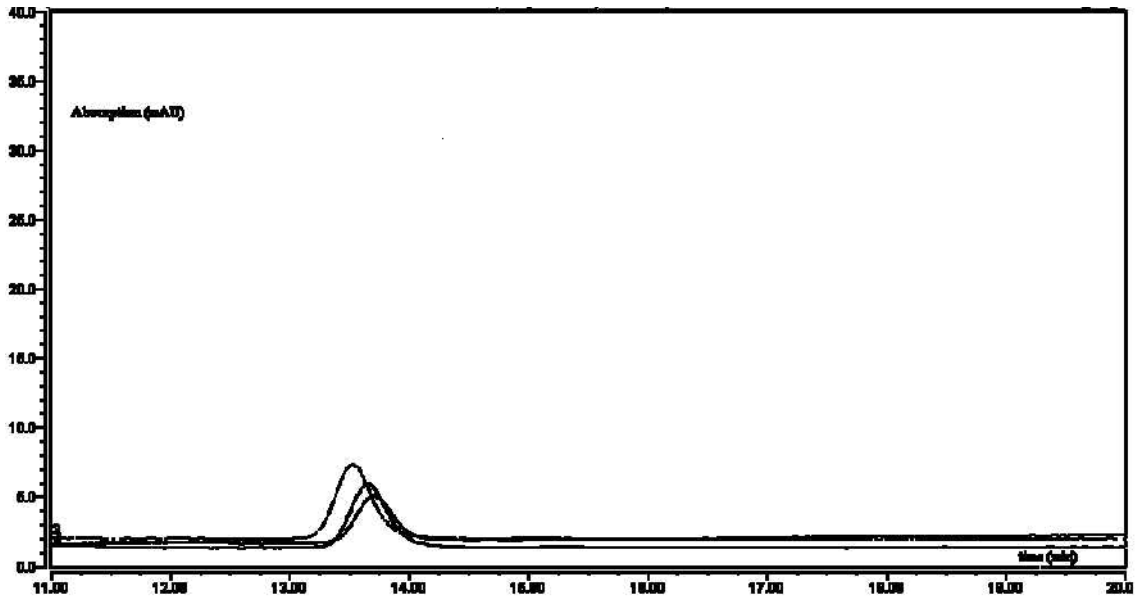

Figure 6.25. HPLC analysis of solid dispersion of phenylbutazone from permeability studies at 5, 20, 60 mins time points (bottom to top).

Figure 6.26 shows the amount of phenylbutazone transferred (μg) across Caco-2 monolayer at different time points for both drug alone and solid dispersion.

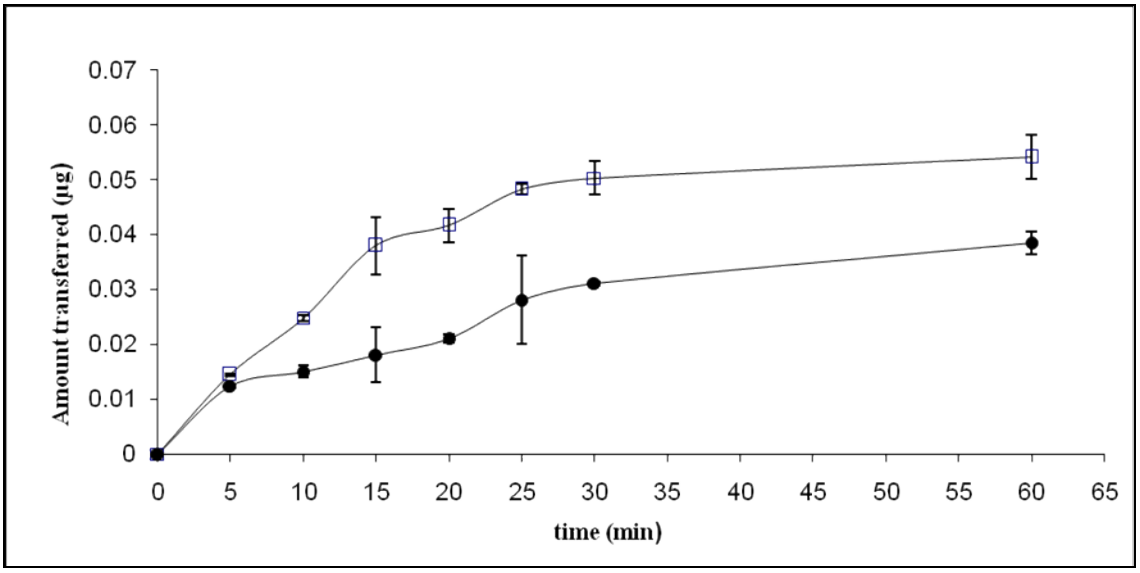

Figure 6.26. HPLC analysis of samples from Caco-2 cell studies evaluating the absorption of solid dispersion (□) of phenylbutazone in PEG 8000 as a carrier and phenylbutazone alone (•). Data are expressed as mean±S.D. (*n* = 3).

Figure 6.27 shows the cumulative % transferred of phenylbutazone from apical to basal per transwell (µg/2.5 mL) across Caco-2 monolayer at different time point for both drug alone and solid dispersion.

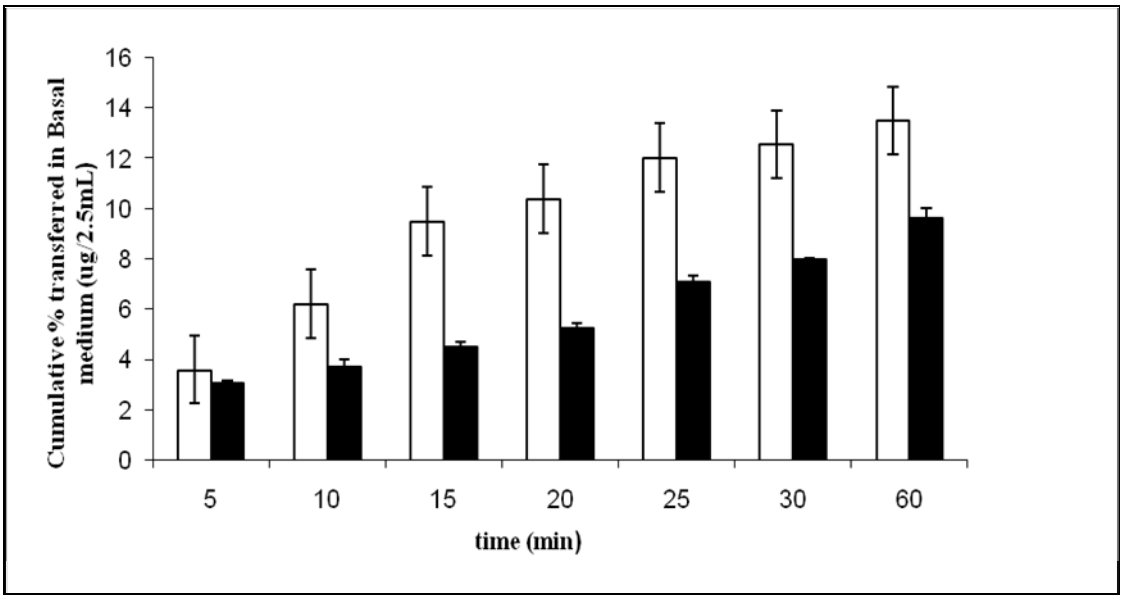

Figure 6.27. Apical-to-basal permeability of solid dispersion of phenylbutazone (□) and phenylbutazone alone (■) across Caco-2 monolayers. Each column indicates mean±S.D (n=3).

Figure 6.28 shows the rate transferred of phenylbutazone from apical to basal across Caco-2 monolayer for first 20 mins for drug alone, solid dispersion and difference in rate transfer from solid dispersion to drug alone.

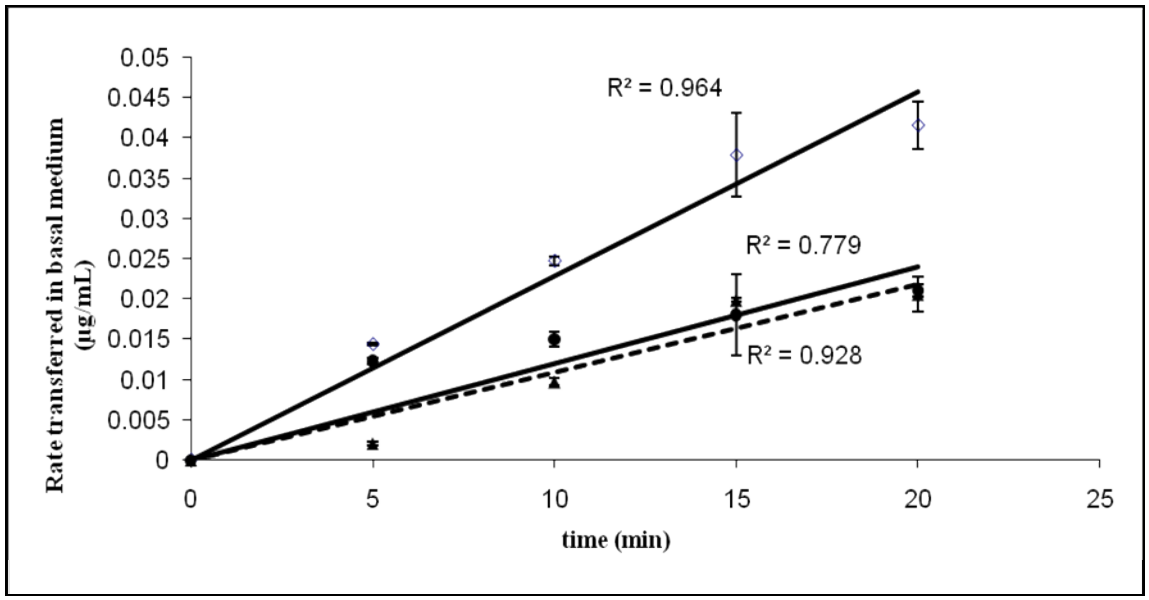

Figure 6.28. Rate transferred of phenylbutazone across Caco-2 cell monolayers in basal medium by HPLC analysis: (Best linear fit for the apical to basolateral transport of solid dispersion and drug alone across CaCo-2 cell monolyers was found over the first 20 mins). Solid dispersion of phenylbutazone (◊), phenylbutazone alone (●) and difference between amount transferred (µg) of solid dispersion to phenylbutazone alone (▲) with R^2 value. Data are expressed as mean±S.D (*n* = 3).

Figure 6.29 shows the apparent permeability coefficients (Papp) of phenylbutazone at different time points for both drug alone and solid dispersion across Caco-2 monolayers.

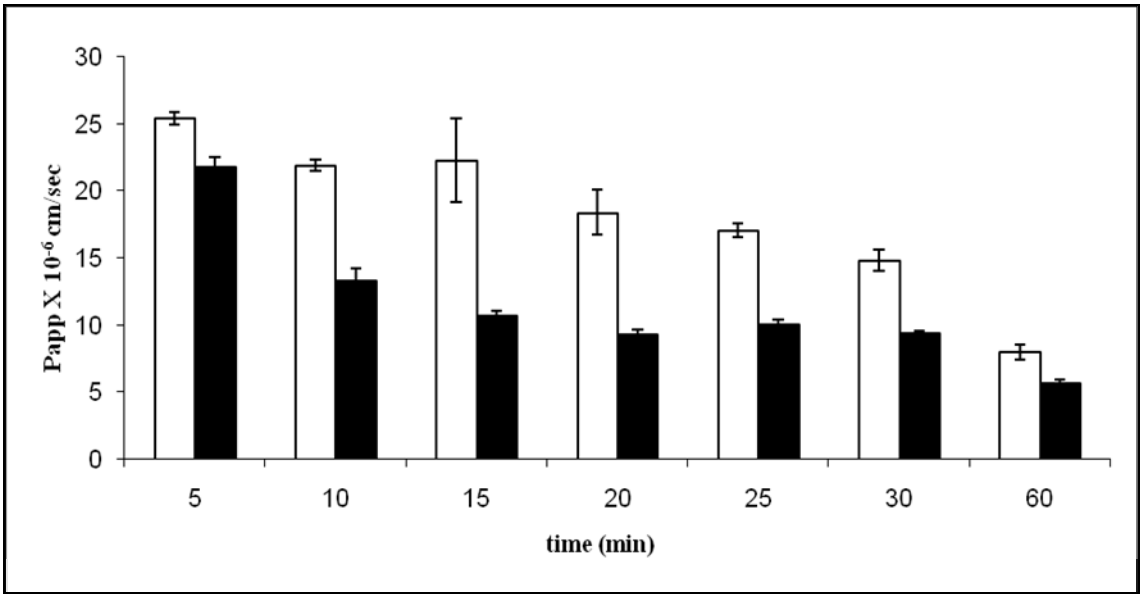

Figure 6.29. The apparent permeability coefficients (Papp) of solid dispersion containing phenylbutazone (□) compared to the phenylbutazone alone (■).Each column indicates mean±S.D (n=3).

The transport of each drug through Caco-2 monolayers was more from the respective solid dispersions as shown in figures 6.8, 6.14, 6.20 and 6.26. All solid dispersions of the four drugs demonstrated a higher rate and extent of permeation than the drug alone. It gives the best linear fit for the apical to basal transport of drug, solid dispersion and difference rate of transfer solid dispersion to drug alone over the first 20 mins with R^2 value as shown in figures 6.10, 6.16, 6.22 and 6.28. Unpaired *t* test results using Gradpad software showed that the difference were considered to be statistically significant in case of indomethacin (P value equals 0.0378) while in case of phenylbutazone (P value equals 0.0922), paracetamol (P value equals 0.1392) and phenacetin (P value equals 0.5425) the difference were not considered to be statistically significant. It can be concluded that the amount of transfer of drug in figures 6.8, 6.14, 6.20 and 6.26 show similar trend over time as shown by the dissolution studies (figures 3.19, 3.23, 3.25 and 3.29). The Papp at different time points for all solid dispersions and drug alone showed

two different trends for carrier and drug-controlled release drugs. The Papp of carrier-controlled release drugs (indomethacin and phenylbutazone) did not change and remained constant for 30 mins as shown in figures 6.11 and 6.29. But in case of drug-controlled released drugs (paracetamol and phenacetin) the Papp were increased first (maximum at 20 mins time point) and then decreased as shown in figures 6.17 and 6.23. The cumulative % transferred in basal medium from carrier and drug-controlled also showed some interesting profiles. In case of carrier-controlled release indomethacin and phenylbutazone the cumulative % transferred in basal medium tends to increase with time as shown in figures 6.9 and 6.27. But in case of drug-controlled release paracetamol and phenacetin the cumulative % transferred in basal medium remained constant as shown in figures 6.15 and 6.21.

The pattern of absorption followed the *in vitro* dissolution behavior of the solid dispersion reinforcing the role of PEG 8000 as a solubiliser for the drug in formulation. This observation was anticipated since the presentation of the drug at the site of absorption is dependent on the carriers. The solubilising effect of PEG 8000 allows the drug to quickly associate into the aqueous surrounding possibly by molecular complexation. This enables the solubilised drug to be absorbed quicker than the drug presented at the site of absorption without any carriers (Prabhu et al., 2005). Nanoparticles to the size range of 230.95±38.97 nm are formed by PEG 8000 which might increase the uptake and also enhance the permeability of hydrophobic drugs as suggested by permeability (rhodamine123 cell uptake studies section 6.3.7) and dissolution studies. As shown from dissolution studies of pure drug (figures 3.19, 3.23,

3.25 and 3.29), the dissolution of drug alone was extremely poor in the phosphate buffer saline media as compared to solid dispersion. Poor solubility can be attributed to its hydrophobic nature and poor wettability. The dissolution rate increased significantly when PEG 8000 was added. The addition of PEG 8000 to the drug afforded a greater solubilising effect thus enhancing the dissolution rate (Alonso et al., 1988; Frances et al., 1991; Al-Angary et al., 1996; Tantishaiyakul et al., 1999). The presence of PEG creates a better micro-environment for the dissolution of the drug (Weuts et al., 2005) which is further supported by permeability studies. Scanning electron microscopy suggests that drugs are dispersed in the carrier (PEG 8000) within the solid dispersions. Moreover, drugs are in amorphous form within the solid dispersions as was further reinforced by differential scanning calorimetry, which in turn enhances permeability (figures 6.8, 6.14, 6.20 and 6.26.) and dissolution as compared to crystal or rod shape of drug alone. It can be suggested that drug is present in an amorphous form within the solid dispersions which improves the permeability of drugs.

The permeability coefficients (Papp) were calculated and are tabulated in table 6.2. Studies reported by Yee (1997) categorised the permeability coefficient (Papp) as low Papp ($<1 \times 10^{-6}$ cm/s), moderate Papp ($=1\text{-}10 \times 10^{-6}$ cm/s), or high Papp ($>10 \times 10^{-6}$ cm/s) corresponding to poor, moderate, and well-absorbed compounds, respectively. Based on this categorisation, the overall trend of absorption for all the four drugs suggests that the drug is absorbed more from the Caco-2 monolayers using PEG 8000 as a carrier in solid dispersion as compared to drug alone (table 6.3). However, as seen from table 6.3 phenacetin and phenylbutazone solid dispersion, tend towards the higher range of

absorption suggesting a high absorption behavior as compared to indomethacin and paracetamol which can be categorised as moderately absorbed systems. The drug absorbed from solid dispersion across Caco-2 monolayers for indomethacin is approximately 4 fold when compared to drug alone. In case of phenacetin, paracetamol and phenylbutazone solid dispersion the permeability coefficients are 1.5 fold as compared to drug alone across Caco-2 monolayers from apical to basal. These differences can be possibly explained as indomethacin is an inhibitor of a P-gp (Draper et al., 1997) which reduces the efflux of drug. However, paracetamol (Manov et al., 2007) which is the P-gp substrate possibly undergoes from drug efflux. The permeability data also shows similar trend toward the solubility of drug except paracetamol. The higher soluble drugs have higher permeability when administered as both solid dispersion and drug alone and are in order of phenacetin>phenylbutazone >indomethacin (solubility data shown in table 6.4).

Table 6.4. Solubility of solid dispersions and drug alone in phosphate buffer saline. Data are expressed as mean±S.D.

Drugs	Solid dispersions (µg/mL)±S.D	Drug alone (µg/mL)±S.D
Phenacetin	69.44±2.27	7.42±0.56
Phenylbutazone	44.68±2.7	6.34±0.68
Indomethacin	33.14±0.93	1.02±0.45
Paracetamol	82.15±4.90	21.6±3.11

Recently, it was reported that some excipients, which are commonly added to pharmaceutical formulations, could inhibit the function of P-gp in the intestine. These excipients, which are added to formulations, are considered to be non-toxic and inert. To achieve an increase in drug transport by P-gp inhibition, the presence of polyoxyethylene groups is required (Cornaire et al., 2004). The possible explanation for the increase in

permeability across Caco-2 monolayers within the solid dispersions is the presence of PEG (Choi and Jo, 2004) which is inhibitor of a P-gp (Shen, et al., 2006), which improved the solubility of drug (Betageri and Makarla, 1995) and form nanoparticle which modulate the permeability (Chiu et al., 2003; Johnson et al., 2002; Collnot et al., 2006). It is suggested that PEG may have reduced P-gp activity by interfering with the structure of the apical membrane and thereby affecting either directly or indirectly the function of the transporter (Johnson et al., 2002). The data for PEG 8000 in the solid dispersion which implies that PEG increases the absorption and enhances permeability as compared to drug alone are shown (figures 6.8, 6.14, 6.20 and 6.26). It is further postulated for the carrier like PEG which is an inhibitor of a P-gp that it increases the absorption (Shen et al., 2006) and permeability of drug when used in the formulation.

6.3.7 Cell Uptake Studies

The aim of the work was to set up a proof of concept study to illustrate the uptake of hydrophobic drug in Caco-2 cell line. Rhodamine123 is a lipophilic fluorescent dye as a drug that has been found to be relatively non-toxic (Johnson and Walsh, 1980; Johnson and Walsh, 1981). Being a hydrophobic dye, rhodamine123 (Chawla et al., 2002; Liang et al., 2005) was efficiently loaded in the PEG 8000. Rhodamine123 is a substrate for P-gp and can, therefore, be used as a marker for P-gp activity in cells. 4', 6-diamidino-2-phenylindole (DAPI) treatment confirmed that the cells had remained completely viable assuring that the PEG 8000 did not induce any cytotoxicity (figures 6.30 and 6.32).

6.3.7.1 Caco-2 cells treated with PEG 8000

The figure 6.30 shows Caco-2 cells treated with PEG 8000 and remained unclear because PEG 8000 is non-fluorescent. It also demonstrated that the nuclei of Caco-2 cells remain intact and cells were viable when treated with PEG 8000 as shown in figure 6.30. To get clear vision of uptake, superimposed PEG 8000 with stain nuclei of PEG 8000 treated Caco-2 cells. It is not possible to differentiate in case of PEG 8000 because of non-florescent nature.

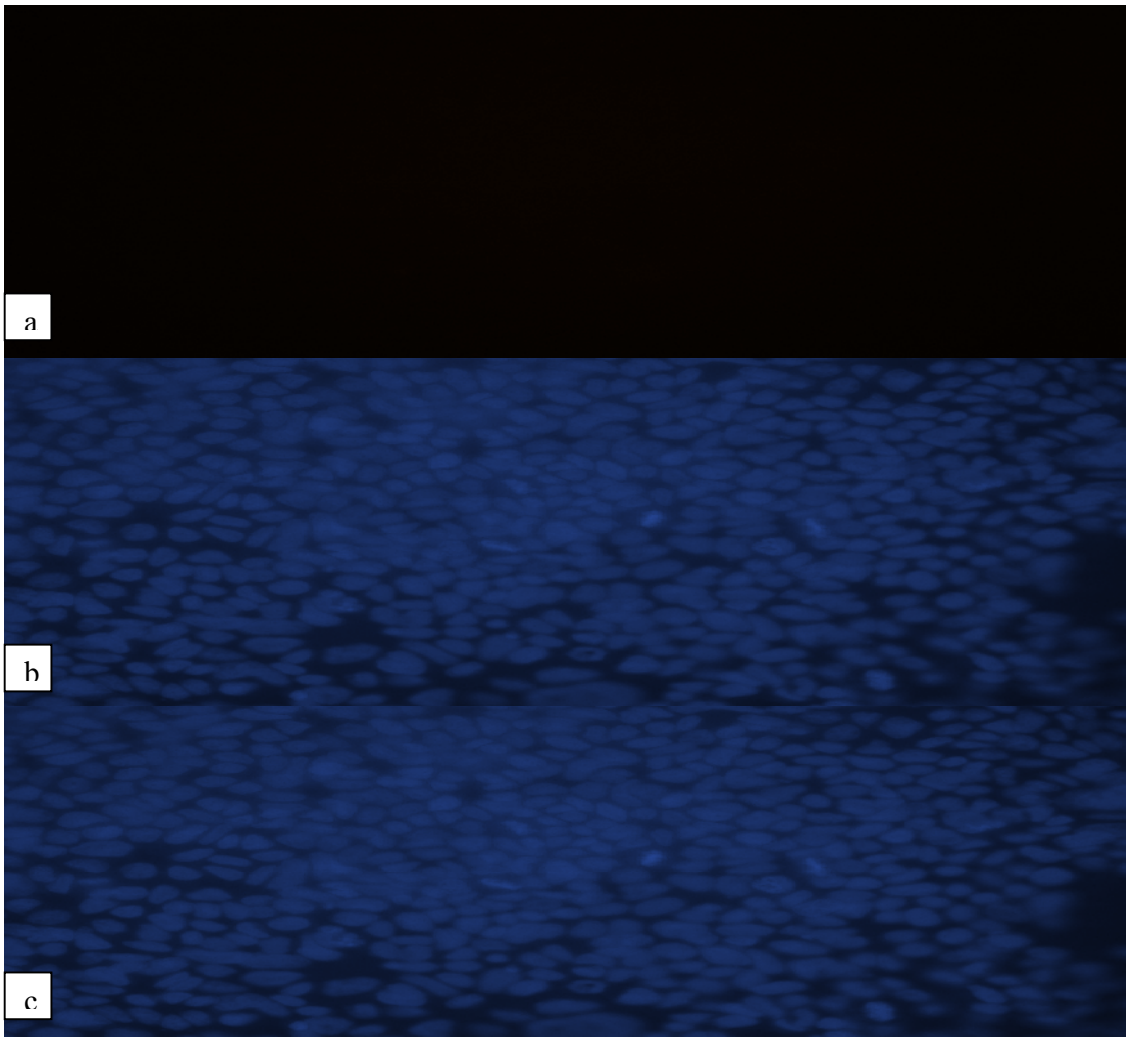

Figure 6.30. Caco-2 cells were grown on 6 Transwell plates and treated with PEG 8000 The images were taken by Fluorescence microscopy after 1h showing PEG 8000 alone (a), PEG 8000 alone nuclei (b) and superimposed PEG 8000 alone with nuclei (c).

6.3.7.2 Caco-2 cells treated with rhodamine123

The figure 6.31 shows Caco-2 cells treated with rhodamine123 are less fade. It also demonstrated that the nuclei of Caco-2 cells remained intact and cells were viable when treated with rhodamine123 as shown in figure 6.31. To further understand the uptake of rhodamine123, superimposed the rhodamine123 with stain nuclei of rhodamine123 treated Caco-2 cells and clearly seen the rhodamine123 in figure 6.31c.

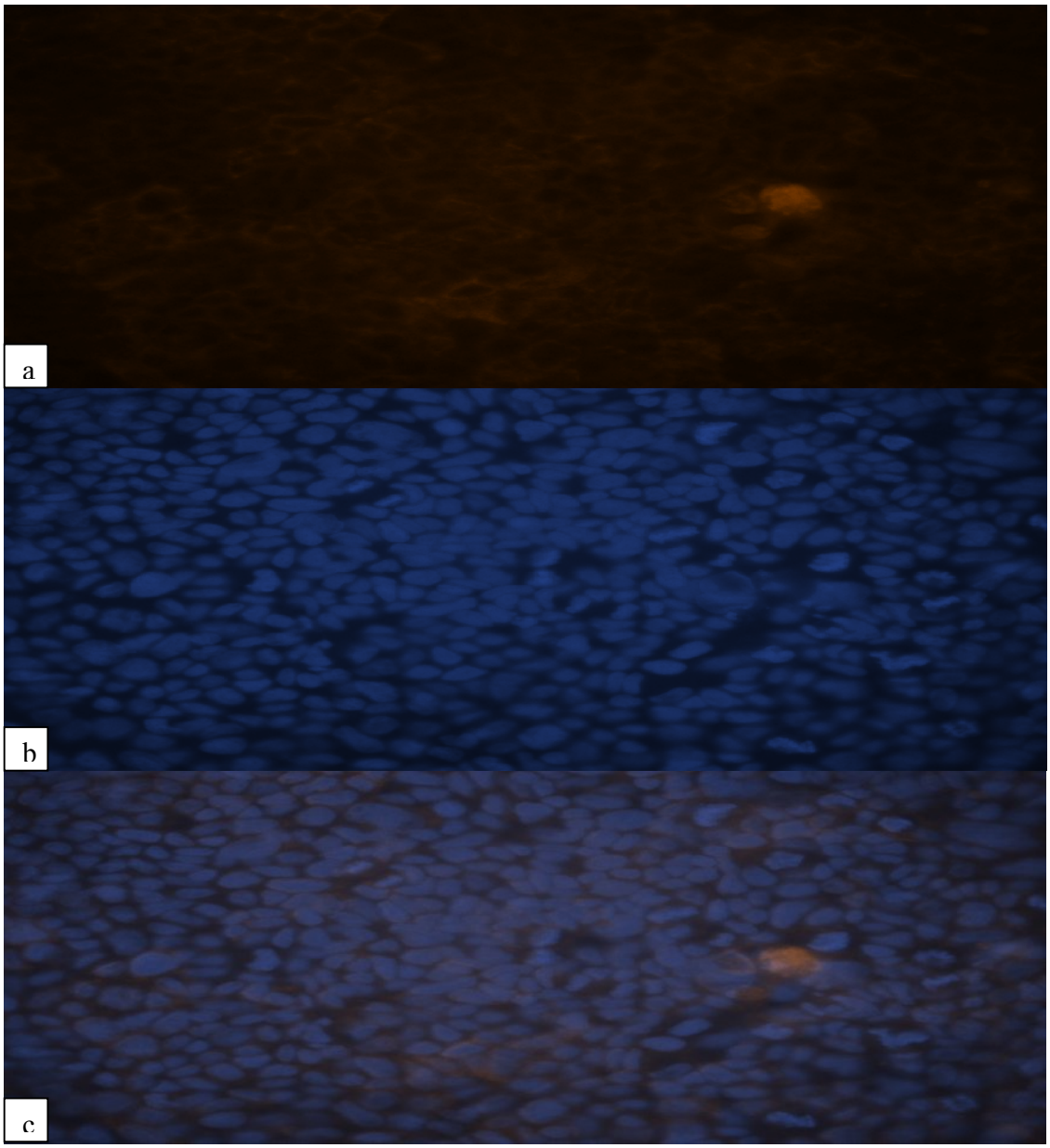

Figure 6.31. Caco-2 cells were grown on 6 Transwell plates and treated with rhodamine 123. The images were taken by Fluorescence microscopy after 1h showing rhodamine 123 alone (a), rhodamine123 alone nuclei (b) and superimposed rhodamine123 alone with nuclei (c).

6.3.7.3 Caco-2 cells treated with rhodamine123-PEG 8000

The figure 6.32 shows Caco-2 cells treated with rhodamine123-PEG (rhodamine123-PEG) 8000. It is clear that PEG 8000 enhanced the uptake of rhodamine123 as shown in figure 6.32 as compared to rhodamine123 alone (figure 6.31).It also demonstrated that the nuclei of Caco-2 cells remain intact and cells were viable when treated with rhodamine123-PEG 8000 as shown in figure 6.32.

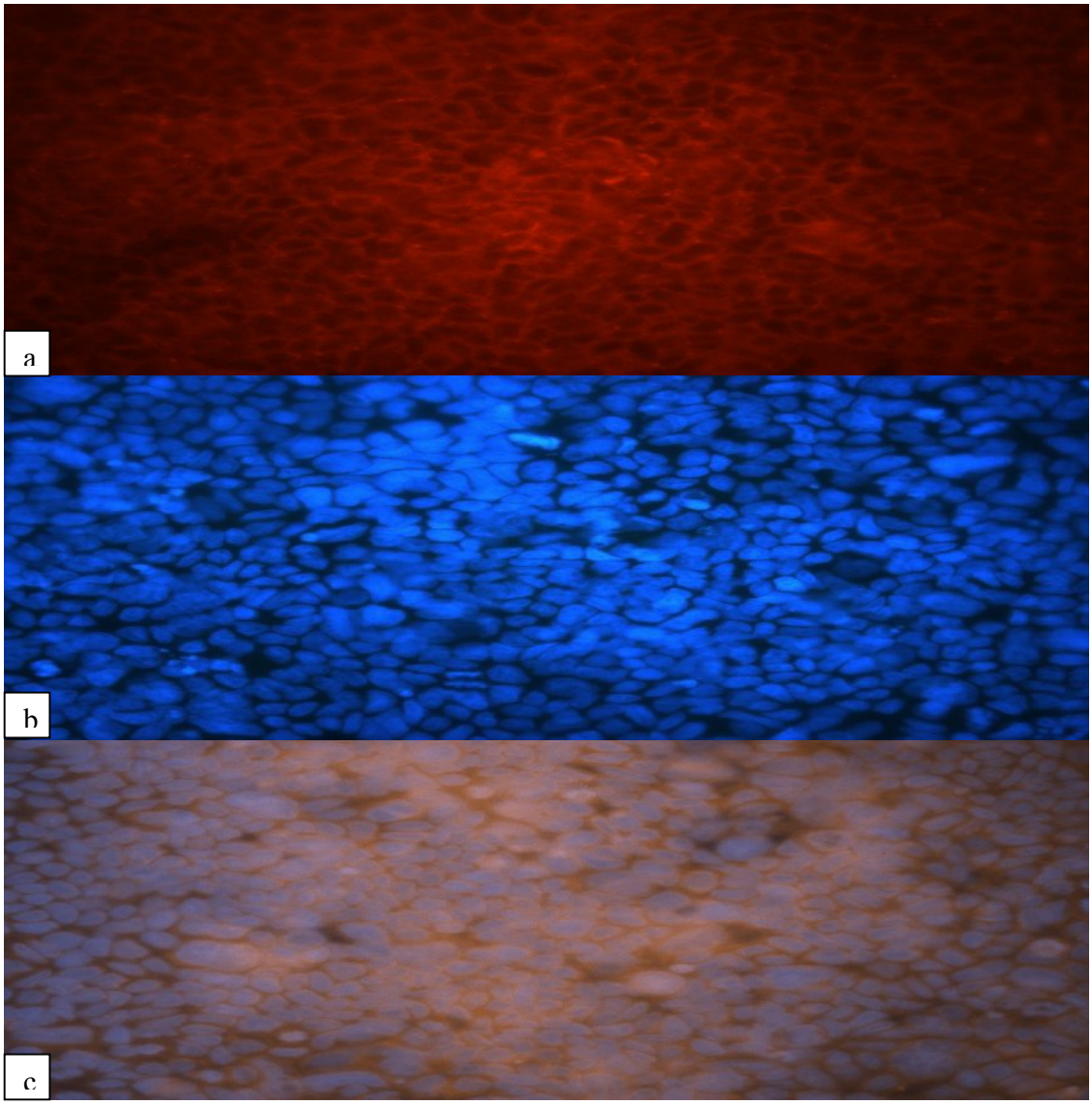

Figure 6.32. Caco-2 cells were grown on 6 Transwell plates and treated with rhodamine123-PEG 8000. The images were taken by Fluorescence microscopy after 1h showing rhodamine123-PEG 8000 (a), rhodamine123-PEG 8000 nuclei (b) and superimposed rhodamine123-PEG 8000 with nuclei (c).

The intensity of rhodamine123 in rhodamine123-PEG 8000 is more as compared to rhodamine123 alone. The uptake level was increased approximately 4 times in the presence of PEG 8000 as shown in figure 6.33.

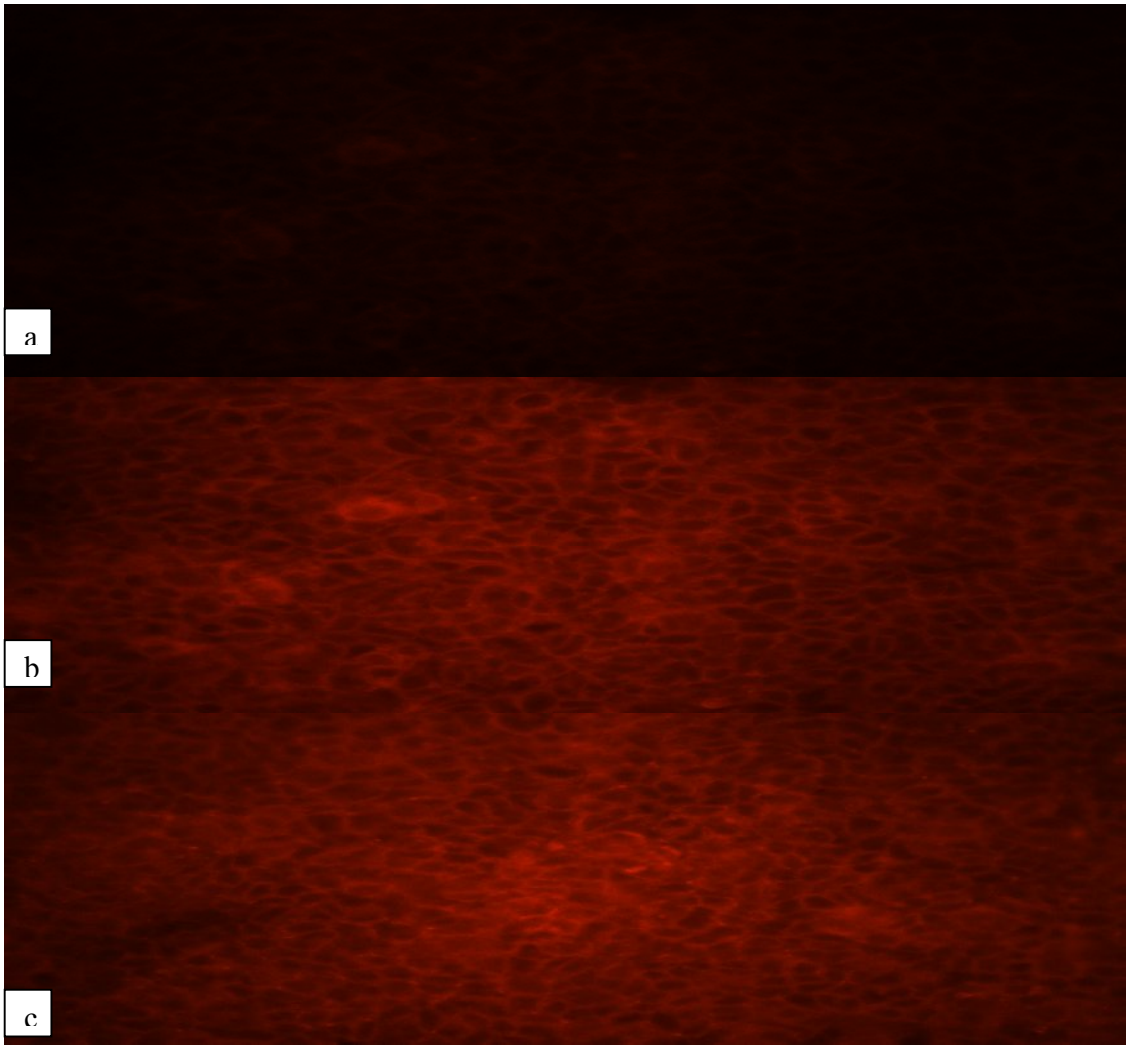

Figure 6.33. Fluorescence microscopy of Caco-2 cells after incubation with rhodamine-123 solution in the absence of PEG 8000 exposed at 529 ms(a); in the presence of PEG 8000 exposed at 529 ms (b) and in the absence of PEG 8000 exposed at 2121 ms(c).

It also suggests a more pronounced qualitative increase in rhodamine123 accumulation when treated with PEG 8000 as compared to rhodamine123 alone. To get the same florescence and intensity the rhodamine123 alone treated Caco-2 cells were exposed at 2121 ms as compared to rhodamine123-PEG 8000 which was exposed at 529 ms as shown in figure 6.33.

The uptake of rhodamine123 was significantly increased by PEG 8000 as compared to rhodamine123 alone as shown in figure 6.32. We have determined that significantly higher accumulation of rhodamine123 in Caco-2 cells was observed in cells treated rhodamine123-PEG 8000 as compared to rhodamine123 alone treated cells evidently by PEG 8000. The most evident explanation for this phenomenon is that PEG 8000 increased solubility, permeability and formation of nanoparticles which enhanced the uptake of rhodamine123. As suggested by various researchers (Johnson et al., 2002; Chiu et al., 2003; Collnot et al., 2006) PEG 8000 modulated the uptake of rhodamine123 possibly due to the formation of nanoparticles by PEG 8000. This study demonstrated that cells were intact after treated with rhodamine123-PEG 8000.

To further explain the permeability results and transport mechanism, microarray studies for indomethacin (carrier-controlled release) which is P-gp inhibitor and paracetamol (drug-controlled release) which is P-gp substrate, were carried out.

6.4 Conclusions

It can be concluded from the permeability studies of four drugs under investigation; indomethacin, phenacetin, phenylbutazone and paracetamol that permeability was higher from solid dispersions as compared to drug alone. In case of indomethacin solid dispersion the permeability was as high as 4 times when compared with indomethacin alone. In solid dispersions of paracetamol, phenactin and phenylbutazone, the permeability was approximately twice than pure drug treatment. From the cell uptake studies it has been shown that PEG 8000 enhanced the rhodamine123 uptake. From the above study the viability of Caco-2 cells can also be concluded when treated with PEG 8000.

Chapter 7

Gene expression analyses during drug permeability

7.1 Introduction

Genomics is the field that deals with the study of genes and their function. The development of bioinformatics and the new emerging advanced technologies like microarray analysis has increased the knowledge of molecular mechanisms forming the basis of normal and dysfunctional biological processes.

It is now possible to analyse and measure thousands of genes in a single RNA sample by using microarray analysis, also known as Gene expression profiling. This task can be achieved with the variety of the recently developed microarray platforms and the main concept for every sample is same: An array is spotted with DNA fragments or oligonucleotides that indicate particular gene coding regions. RNA after purification is labeled either fluorescently or radioactively and then hybridised to the slide/membrane. Hybridisation is also carried out simultaneously with reference RNA as it provides an opportunity to compare data of many experiments.

Microarray has gained great popularity in recent years and is a routine work in laboratories. In almost every cancer related conference, microarray data is presented. Microarray was used to demonstrate the heterogeneous nature of breast cancer in a paper published in 2000 (Perou et al., 2000). This approach was already introduced but it was the first microarray publication to explain corresponding results. It was found for the first time by clinicians that it is possible to represent a patient-specific molecular signature by using microarray analysis which assists in selecting appropriate treatments from various options as well as in suggesting their consequences.

7.1.1. Types of microarray

The expression of tens of hundreds of genes can be analysed simultaneously with the help of microarray. It also enables identification of genes which when arranged under certain conditions in specific tissues, for instance the induction of drugs or growth related changes can measure gene expression changes. This technique can also be employed to clinical procedures, like, establishing gene expression profiles in tumours by comparing patients that suffered a relapse to those sensitive to a drug (Folgueira, 2005; Jansen, 2005). Microarrays have been classified into DNA and RNA microarrays, tissue microarrays and protein and antibody arrays.

7.1.2 DNA and RNA microarrays

The genetic profile of DNA greatly influences the basic principle of microarray technology. DNA or RNA, the starting material, should be of high quality and also the experimental replicates should be provided in adequate number in order to carry out the experiment successfully. To keep RNA intact, fresh tissue should either be snap frozen or kept in a proprietary RNA preservation reagent for subsequent storage in liquid nitrogen, since RNA degrades because it is a highly labile molecule. In the process of microarray manufacture thousands of 'probe' DNAs/RNAs, each of these are complementary to a certain gene transcript, are attached by applying various methods to a solid surface. DNA (target) is produced by reverse transcriptase of experimental RNA obtained from two different sources. DNA is labelled in this process with fluorescent dyes, such as green cyanine 3 and red cyanine 5 dyes (if single array is used for hybridisation of two samples). This in turn produces images and unprocessed raw data (figure 7.1). It is

possible to obtain targeted genotyping either by using the whole genome chips or by custom synthesis of the arrays. The difference of genes between the two samples is identified through the information obtained as a result of the molecular signature that is produced by applying bioinformatics.

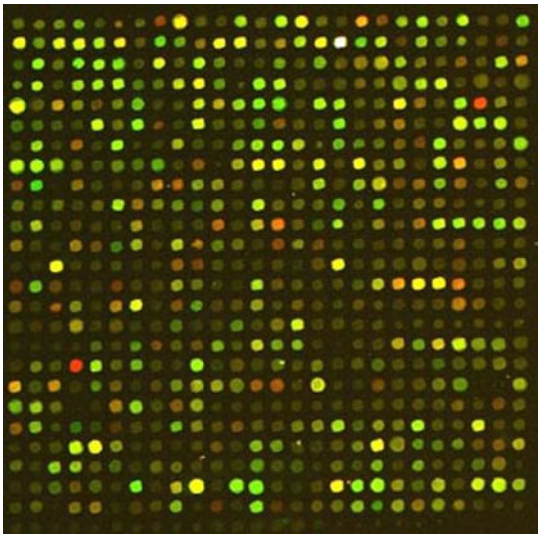

Figure 7.1. Exemplar of microarray hybridisation. A representative portion from the 38K genome reveals the differential signals from two RNA samples.

7.2 Aim of the study

The aim of the work presented in this chapter was to understand any gene expression changes that take place during the process of drug permeability. Emphasis was laid on analysing the expression changes in the transporter network system (ATP binding cassette) and solute carrier transporter during permeability studies at different time points when treated with drug alone or the solid dispersion of the drug.

Two drugs, indomethacin and paracetamol were studied. Indomethacin was chosen as it an inhibitor for PgP expression whereas paracetamol is a popular substrate.

7.3 Results and Discussion

7.3.1 RNA concentration measurement of control and PEG treated cells

RNA concentrations of control (untreated Caco-2 cells), PEG 8000, paracetamol, paracetamol solid dispersion, indomethacin and indomethacin solid dispersion treated Caco-2 cells were determined using a spectrophotometer.

RNA concentration of control (untreated Caco-2 cells) was measured at three different time intervals using spectrophotometer: initial time point being at 15 mins (1.89, 1.80, and 1.87), second at 30 mins (1.80, 1.87, and 1.8) and last at 60 mins (1.81, 1.80 and 2). RNA quantification was studied by measuring absorbance at 260 nm and 280 nm. Absorbance ratio for RNA was observed to be about 1.80-2.0 (table 7.1) suggesting that nucleic acid preparations did not contain any protein contamination for downstream experiments.

Measurement of RNA concentration for PEG 8000 (table 7.1) treated Caco-2 cells at three different time intervals using spectrophotometer showed absorbance values at 260 nm and 280 nm to be in the range of 1.8-2.16. The recorded absorbances at 15 mins (1.96, 2.16 and 1.84), at 30 mins (1.85, 2 and 2.00) and at 60 mins (1.97, 1.90 and 2.06) showed that the extracted RNA was free from any protein contamination.

7.3.2 RNA concentration measurement of paracetamol aone and paracetamol solid dispersion treated Caco-2 cells

RNA concentration measurement of paracetamol alone treated Caco-2 cells was measured via spectrophotometer at three time intervals of 15 mins (1.97, 1.94 and 1.95), 30 mins (1.94, 1.85 and 2.04) and 60 mins (1.83, 1.83 and 2). Absorbance at 260 nm and 280 nm were used for RNA quantification. It displayed absorbance ratio of approximately 1.83-2.04 (table 7.1) revealing that nucleic acid preparations have no protein contamination for downstream experiments.

Analyses of RNA concentration of the solid dispersion of paracetamol treated Caco-2 cells at three different time events revealed the absorbance ratio in the region of 1.8-2.04 (table 7.1).

7.3.3 RNA concentration measurement of indomethacin alone and indomethacin solid dispersion treated Caco-2 cells

RNA concentration was noted for indomethacin alone (table 7.1) treated Caco-2 cells through spectrophotometer at three time periods i-e 15 mins (1.84, 1.96 and 1.9), 30 mins (2.04, 1.88 and 1.85) and 60 mins (1.87, 2.03 and 1.95). RNA was quantified by applying absorbance at 260 nm and 280 nm. The absorbance ratio approximately was in the region of 1.84-2.04.

RNA concentration measurement of indomethacin solid dispersion treated Caco-2 cells (table 7.1) showed the ratio of absorbance (260 nm/280 nm) was approximately 1.82-2.14.

Table 7.1 shows the summary of RNA absorbance value at 260 nm and 280 nm for control (untreated Caco-2 cells), PEG 8000, paracetamol, paracetamol solid dispersion, indomethacin and indomethacin solid dispersion treated Caco-2 cells.

Table 7.1 RNA concentrations of control (untreated Caco-2 cells), PEG 8000, paracetamol, paracetamol solid dispersion, indomethacin and indomethacin solid dispersion were measured using a spectrophotometer. Absorbance at 260 nm and 280 nm (absorbance ratios: 260 nm/280 nm) were used for quantification of RNA.

	15mins			30mins			60mins		
Sample(s)	260nm	280nm	Absorbance ratio	260nm	280nm	Absorbance ratio	260nm	280nm	Absorbance ratio
Control	0.053	0.028	1.89	0.06	0.0332	1.80	0.069	0.038	1.81
	0.065	0.036	1.80	0.055	0.029	1.87	0.074	0.041	1.80
	0.062	0.033	1.87	0.072	0.04	1.8	0.054	0.027	2
PEG 8000	0.059	0.03	1.96	0.052	0.028	1.85	0.0612	0.031	1.97
	0.056	0.026	2.16	0.056	0.028	2	0.0611	0.032	1.90
	0.059	0.032	1.84	0.062	0.031	2.00	0.062	0.03	2.06
Paracetamol	0.075	0.038	1.97	0.066	0.034	1.94	0.077	0.042	1.83
	0.096	0.049	1.95	0.089	0.048	1.85	0.065	0.0354	1.83
	0.068	0.035	1.94	0.086	0.042	2.04	0.076	0.038	2
Paracetamol solid dispersion	0.184	0.102	1.80	0.096	0.045	2.13	0.084	0.041	2.04
	0.181	0.098	1.84	0.091	0.048	1.89	0.079	0.04	1.97
	0.165	0.088	1.87	0.183	0.091	2.01	0.0786	0.042	1.87
Indomethacin	0.061	0.033	1.84	0.098	0.048	2.04	0.107	0.057	1.87
	0.055	0.028	1.96	0.096	0.051	1.88	0.13	0.064	2.03
	0.095	0.05	1.9	0.087	0.047	1.85	0.096	0.049	1.95
Indomethacin solid dispersion	0.056	0.03	1.86	0.062	0.032	1.93	0.071	0.038	1.86
	0.067	0.035	1.93	0.071	0.039	1.82	0.096	0.051	1.88
	0.061	0.032	1.90	0.067	0.0312	2.14	0.075	0.039	1.92

7.3.4 Gel electrophoresis

Gel electrophoresis is a technique mostly used in biochemistry and molecular biology for RNA molecules separation by size. Negatively charged nucleic acid molecules move towards positive charged electrode through an agarose matrix in an applied electric field. RNA of control (untreated Caco-2 cells), PEG 8000, paracetamol, paracetamol solid dispersion, indomethacin and indomethacin solid dispersion treated Caco-2 cells were run on gel electrophoresis to determine their integrity.

7.3.4.1 Gel electrophoresis of control RNA

RNA of untreated Caco-2 cells run on gel electrophoresis showed rRNA (ribosomal Ribonucleic Acid) bands for 28 S and 18 S. This implies that RNA did not degrade. Before the formation of cDNA (complementary Deoxyribonucleic Acid), the quality of RNA was proved from these bands. Figure 7.2 shows samples of control RNA at three different time intervals using gel electrophoresis.

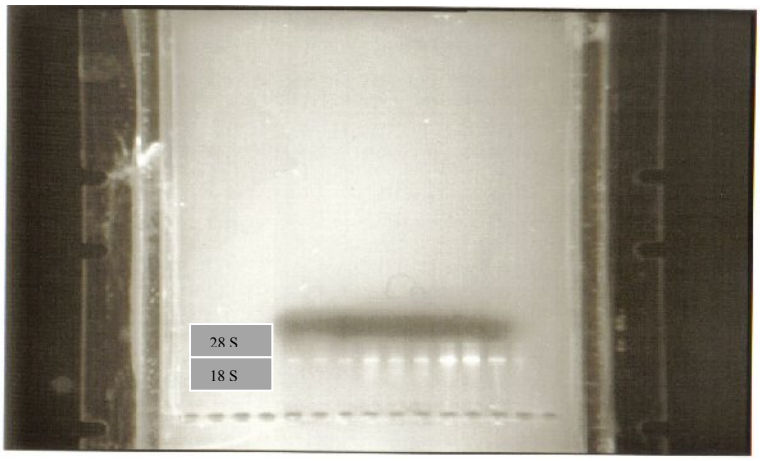

Figure 7.2. Gel electrophoresis of RNA untreated Caco-2 cells showing bands for 28 S and 18 S rRNA. First 3 samples represent 15 mins time point followed by next 3 samples for 30 mins time point and last 3 samples for 60 mins time point (from left to right).

7.3.4.2 Gel electrophoresis of Caco-2 cells RNA treated with PEG 8000

rRNA bands of 28 S and 18 S were seen by running RNA of Caco-2 cell treated with PEG 8000 on a gel electrophoresis. These bands suggest that RNA remained intact. Partially degraded RNA possessed a smeared appearance. Figure 7.3 shows samples of PEG 8000 treated RNA of Caco-2 cells at three different time intervals using gel electrophoresis. The quality of RNA was confirmed before cDNA was synthesised through the gel electrophoresis as is evident from rRNA bands that RNA was intact.

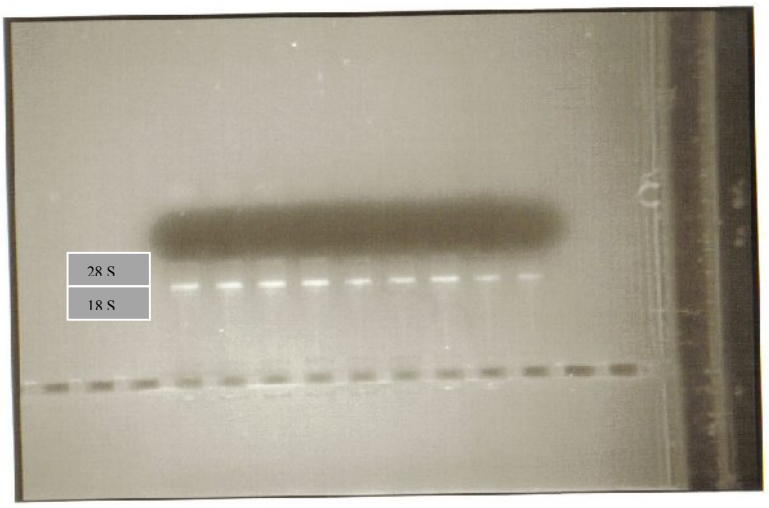

Figure 7.3. Gel electrophoresis of PEG 8000 treated Caco-2 cells RNA showing bands for 28 S and 18 S rRNA. First 3 samples represent 15 mins time point followed by next 3 samples for 30 mins time point and last 3 samples for 60 mins time point (from left to right).

7.3.4.3 Gel electrophoresis of Caco-2 cells RNA treated with paracetamol

RNA of Caco-2 cells treated with paracetamol run on gel electrophoresis showed rRNA bands for 28 S and 18 S. Figure 7.4 shows samples of paracetamol treated RNA of Caco-2 cells at three different time intervals using gel electrophoresis. Similarly, Caco-2 cells

treated with solid dispersion showed intact RNA bands as shown in figure 7.5 suggesting that the quality of RNA was not compromised during experimental procedures.

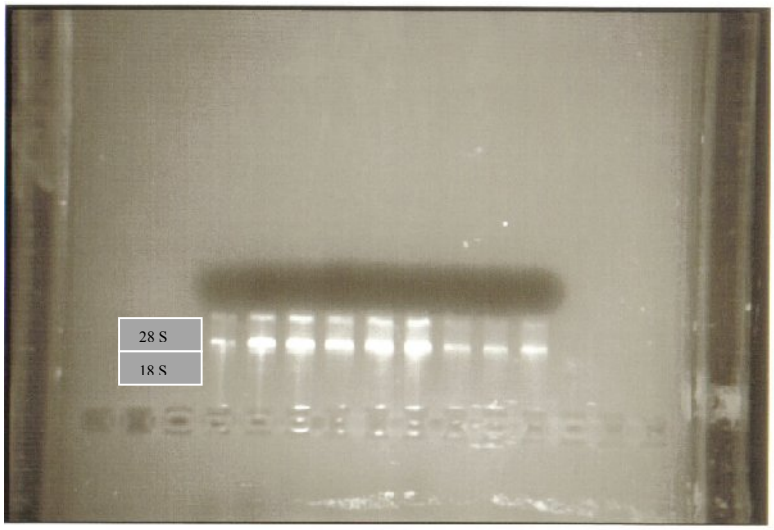

Figure 7.4. Gel electrophoresis of Caco-2 cells RNA treated with paracetamol showing bands for 28 S and 18 S rRNA. First 3 samples represent 15 mins time point followed by next 3 samples for 30 mins time point and last 3 samples for 60 mins time point (from left to right).

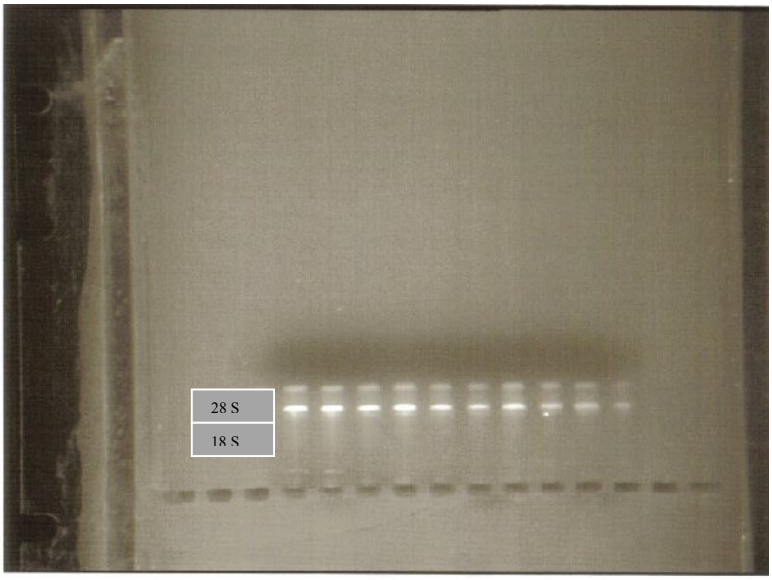

Figure 7.5. Gel electrophoresis of Caco-2 cells RNA treated with paracetamol solid dispersion showing bands for 28 S and 18 S rRNA. First 3 samples represent 15 mins time point followed by next 3 samples for 30 mins time point and last 3 samples for 60 mins time point (from left to right).

7.3.4.4 Gel electrophoresis of Caco-2 cells RNA treated indomethacin

RNA of Caco-2 cells treated with indomethacin run on gel electrophoresis have rRNA bands for 28 S and 18 S. These bands signify the intactness of RNA. Figure 7.6 show samples of indomethacin treated RNA of Caco-2 cells at three different time intervals using gel electrophoresis. Similar results were obtained upon treatment with solid dispersion of indomethacin (figure 7.7).

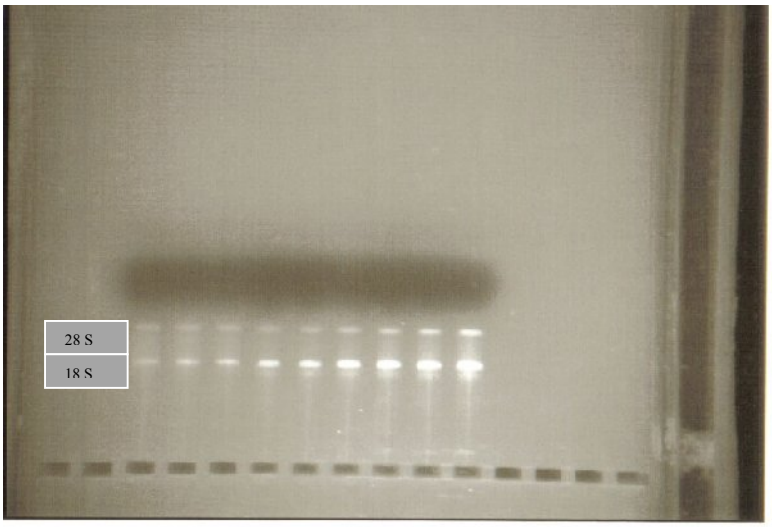

Figure 7.6. Gel electrophoresis of Caco-2 cells RNA treated with indomethacin showing bands for 28 S and 18 S rRNA. First 3 samples represent 15 mins time point followed by next 3 samples for 30 mins time point and last 3 samples for 60 mins time point (from left to right).

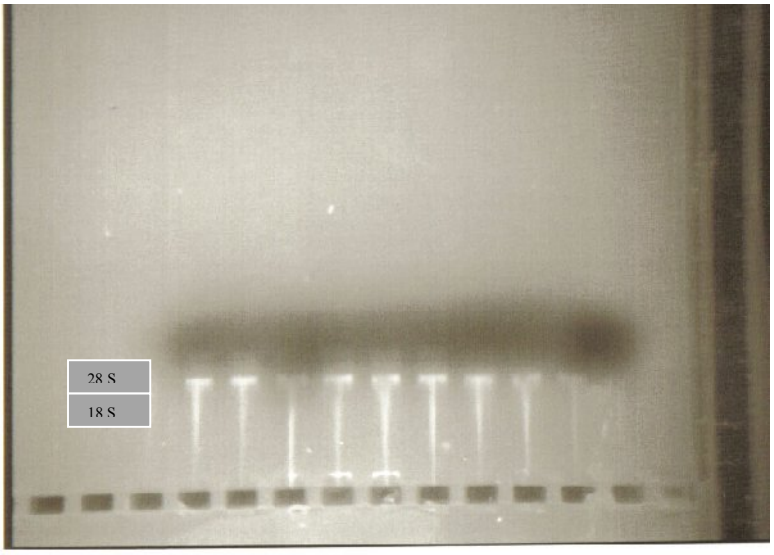

Figure 7.7. Gel electrophoresis of Caco-2 cells RNA treated with indomethacin solid dispersion showing bands for 28 S and 18 S rRNA. First 3 samples represent 15 mins time point followed by next 3 samples for 30 mins time point and last 3 samples for 60 mins time point (from left to right).

7.3.5 Data clustering and normalisation

The data set obtained was normalised using the TMEV software. This was done to eliminate any deviations due to the introduction of any systematic errors such as differential labelling efficiency of the two fluorescent dyes, differences in starting amount of mRNA prior to cDNA synthesis and hybridisation. Total intensity normalisation was carried out as the amount of RNA for the various experiments was same.

Various methods are employed to analyse microarray data (Claverie, 1999). It is an extremely difficult task for biologists to interpret highly complex and vast dimensional experimental results. In order to make the dimension of the data less extensive and also to distinguish and recognise useful patterns, various computational and statistical approaches are required. Out of these the most commonly used method is clustering (i.e. unsupervised learning) which enable to unfold and investigate coordinated expression patterns in a group of microarrays (Eisen et al., 1998; Tibshirani et al., 1999; Getz et al., 2000). The fundamental purpose in carrying out interpretation of huge data from cDNA array experiments is to extract the basic gene expression patterns which gives knowledge about the underlying biology of given sample. Genes having identical expression patterns in different circumstances can contribute in similar signal pathway or are co-regulated. Data is usually collected in the form of heat maps, with rows and columns, representing a different gene and an individual sample respectively. There are distinct areas that are predominantly green, representing down regulated genes in multiple samples while the red represents up regulated genes. Shade differences indicate the level of up or down

regulation between tumours and black areas relate to genes whose expression between samples remains unaltered.

Data clustering was carried out for the different data sets. The results showed that when clustering for the controls was carried out, all the different data sets were grouped together suggesting that little or minimal variation in gene expression profiling was observed throughout the entire duration of the experimental set up. Hierarchical agglomerative clustering was used to group different data sets into bigger clusters. As the results from the control clustering analysis showed that there was very little variation observed over the time course of the experimental analysis, a single mean value was used for clustering when comparison with other data sets (formulation treated and PEG treated) was carried out.

Furthermore, when multi class significant analysis of microarrays (SAM) was performed on the gene set of the control samples, it was observed that at a false discovery rate (FDR) of 12%, accounting for approximately 1000 out of the total 38000 genes significantly changing between the control samples at the three different times.

When SAM analysis was carried out on data sets comparing control, PEG treated, indomethacin alone treated and solid dispersion of indomethacin treated cells, there were 47% of the total genes showing variations at an FDR of 1%. Similar analyses for paracetamol based data showed that there were 25% of the total genes exhibiting variations at an FDR of 1%.

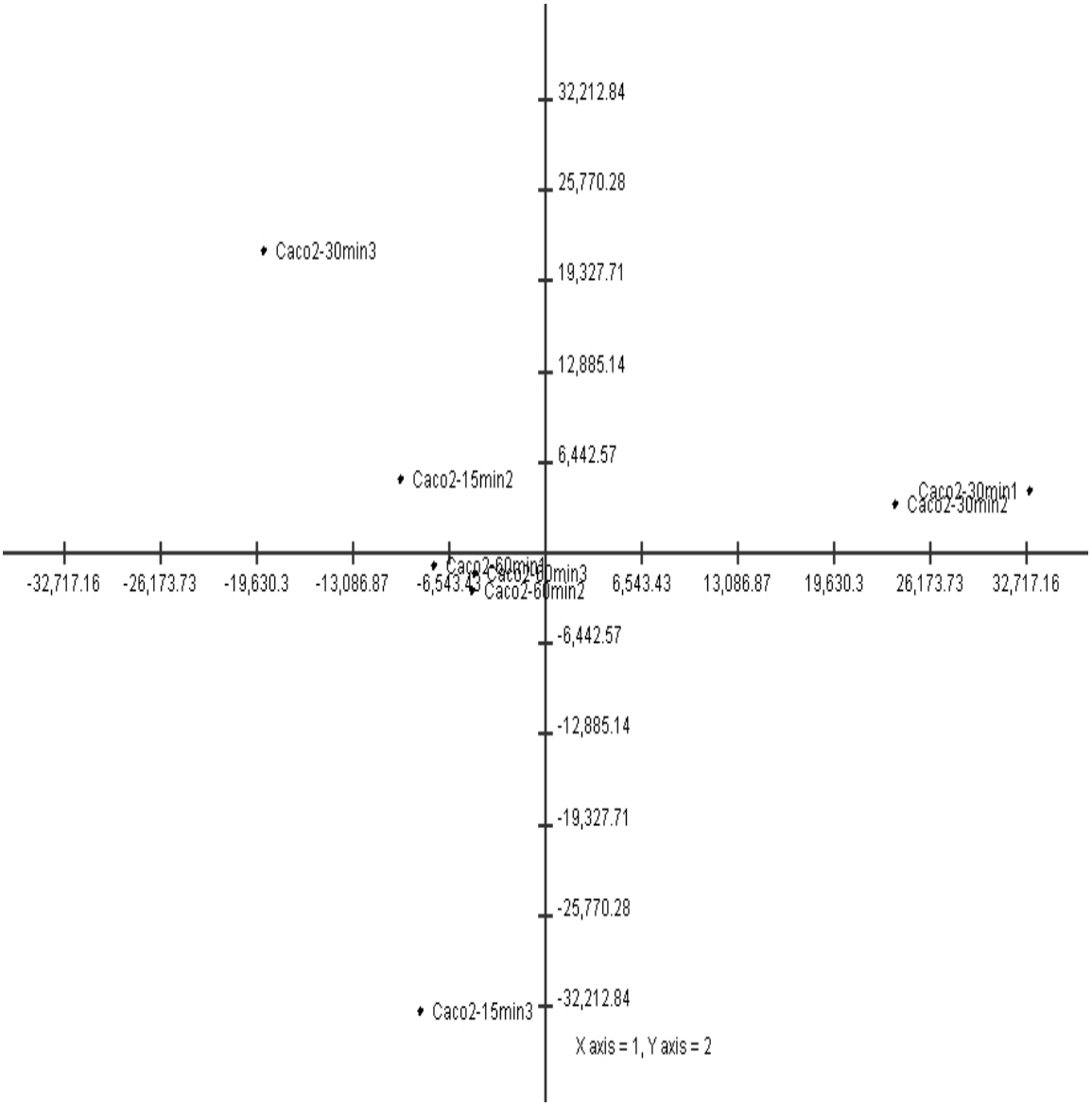

Figure 7.8. Principal component analysis performed on the transcriptional time course data of the control samples (Caco-2 only). Samples were tested at 15 mins, 30 mins and 60 mins.

Principle component analysis (PCA) was carried out on the control samples studies over the duration of the study (15 mins, 30 mins and 60mins). The results (figure 7.8) show that majority of the samples tested clustered together around the origin on the PCA plot suggesting that minimal variation in gene expression over the time course analysis of the experiment. However, single data set for time point 15 as well as 30 mins showed minor variability across the second component. Additionally, two sample sets (Caco-2 30 mins 1 and 2) were shown to have higher degree of variability as they were separated from the rest of the centrally clustered samples across the first principle component. These differences for the outliers can potentially be attributed to the experimental as well as biological sample variations. Research has shown that variability's beyond 20% can be expected due to changes in physical conditions of the experimental set up such as variation of temperature, pH, changes in biological processes and sampling errors.

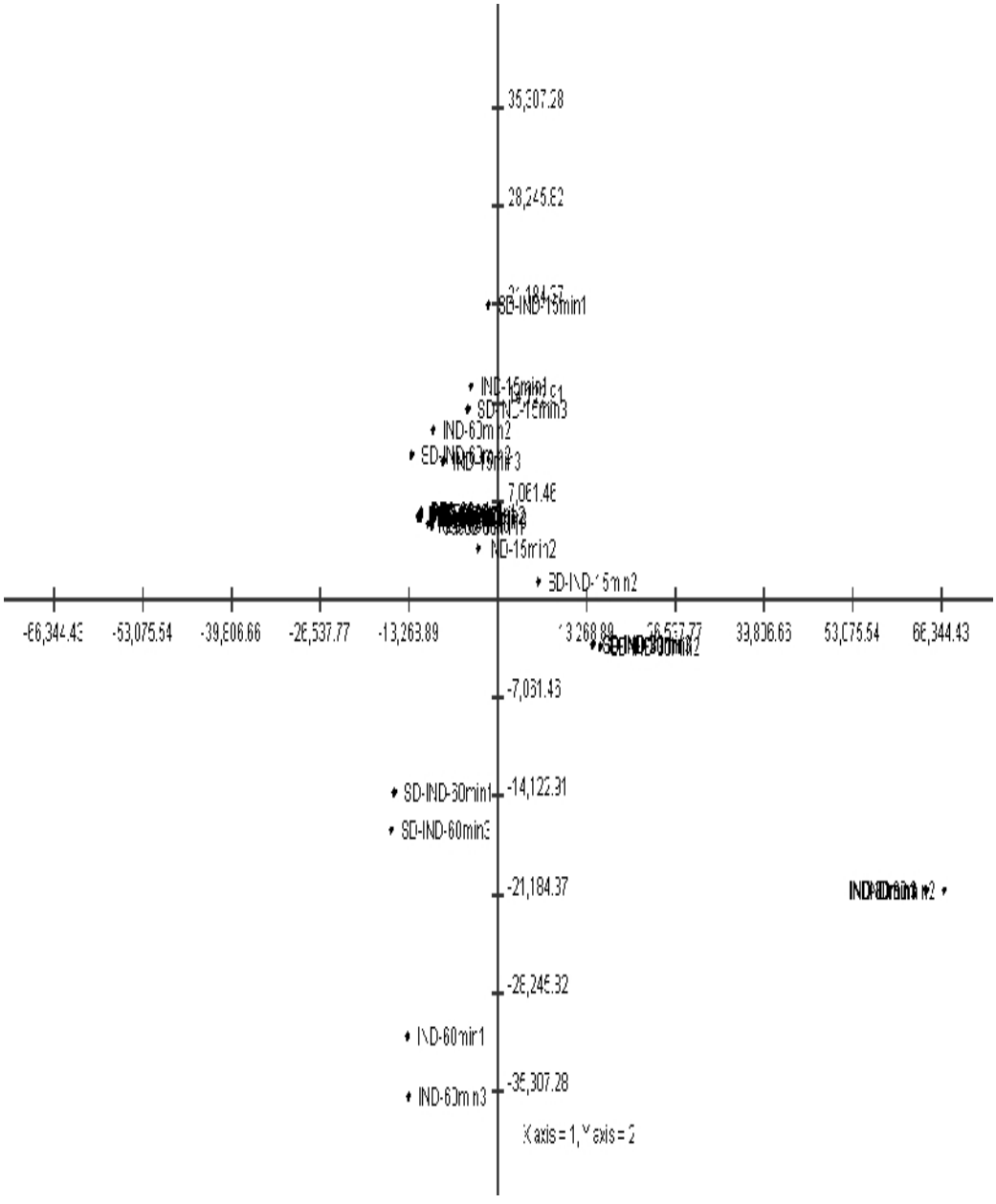

Figure 7.9. Principal component analysis on the transcriptional time course for indomethacin (IND) alone and solid dispersion of indomethacin (SD-IND). The number represents the time points. The plot represents the data for all the individual data sets.

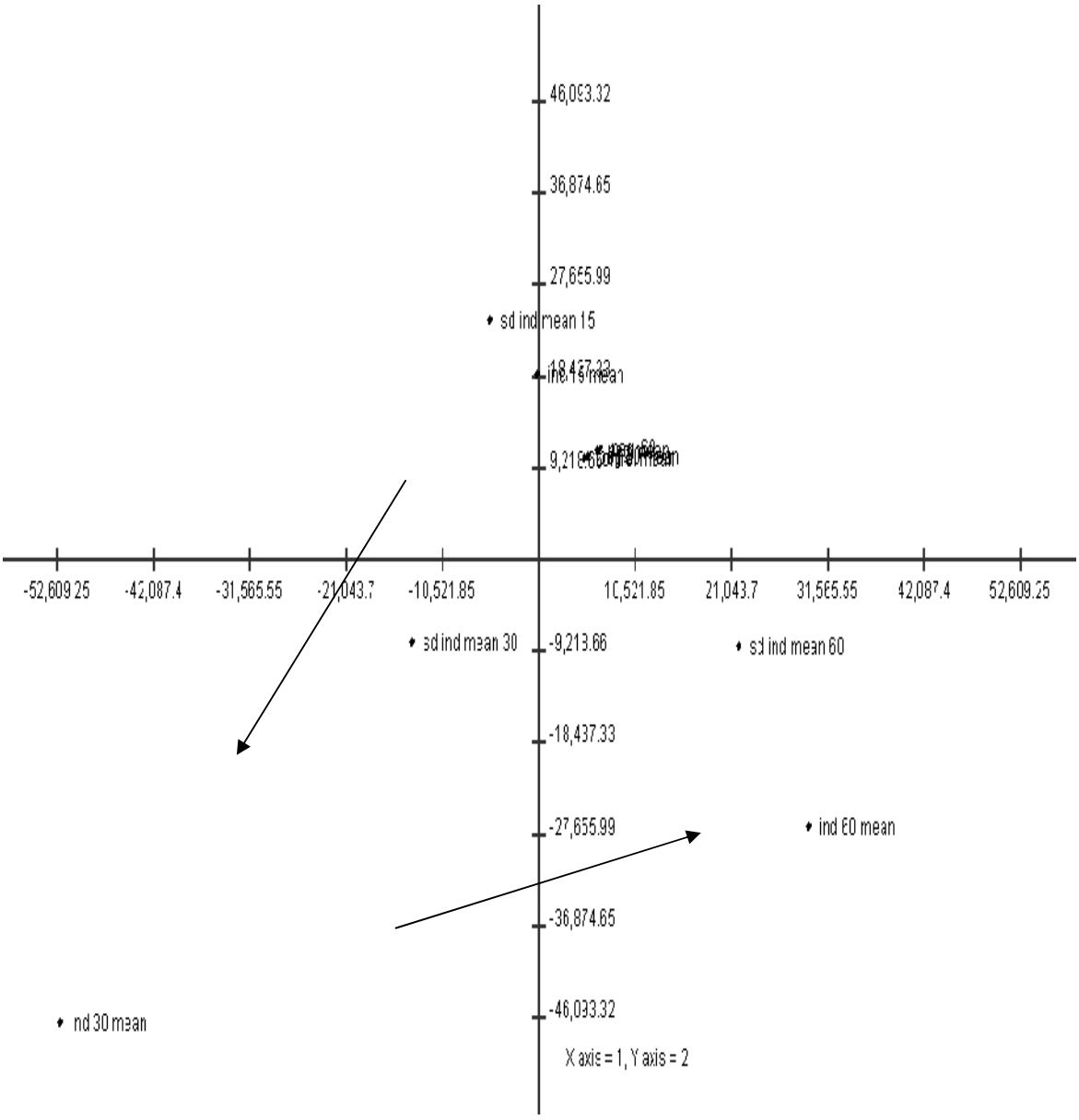

Figure 7.10. Principal component analysis on the transcriptional time course for indomethacin (IND) alone and solid dispersion of indomethacin (SD-IND). The number represents the time points. The plot represents the data for the mean values at each time point.

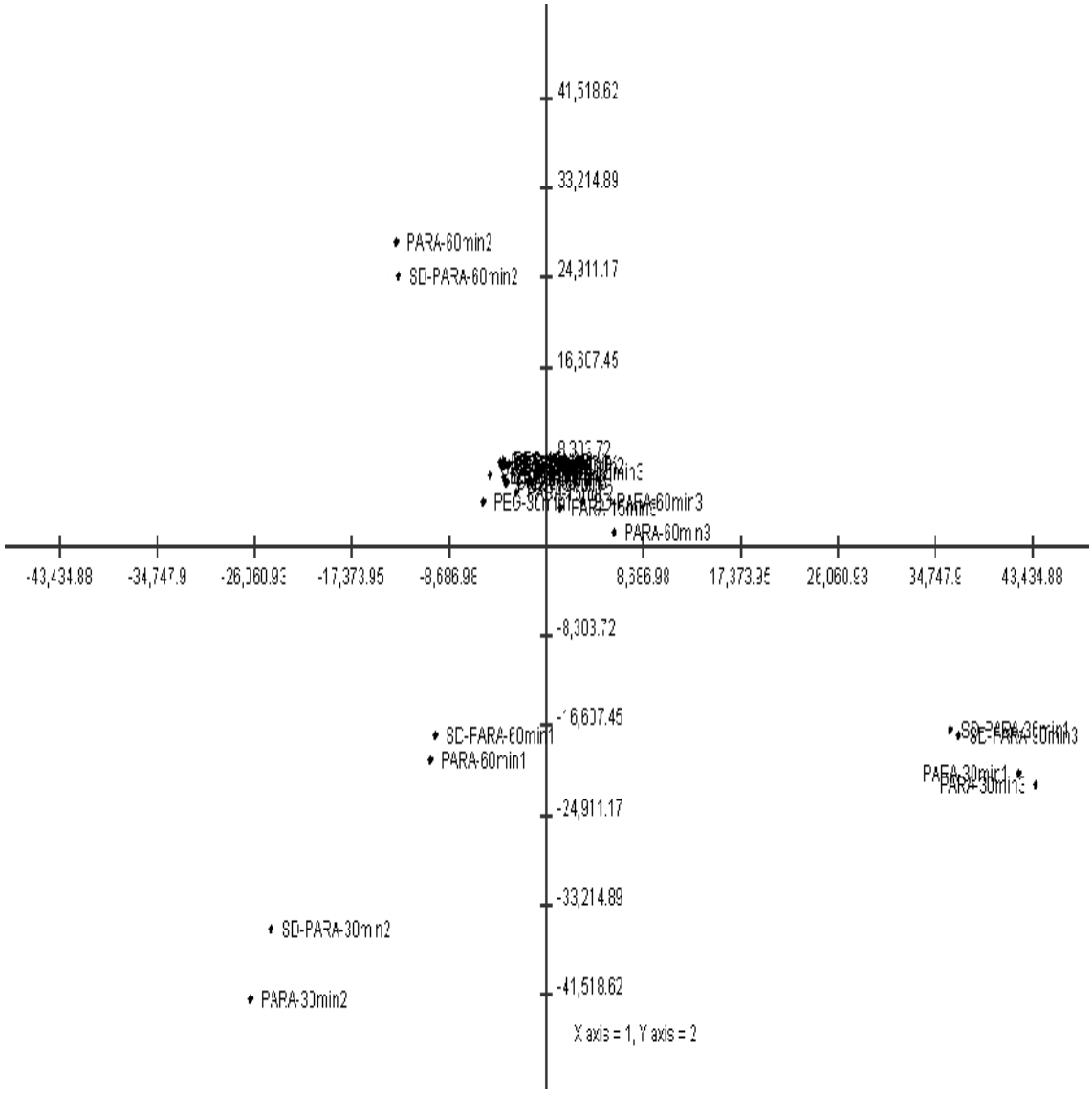

Figure 7.11. Principal component analysis on the transcriptional time course for paracetamol (PARA) alone and solid dispersion of paracetamol (SD-PARA). The number represents the time points. The plot represents the data for the individual values at each time point.

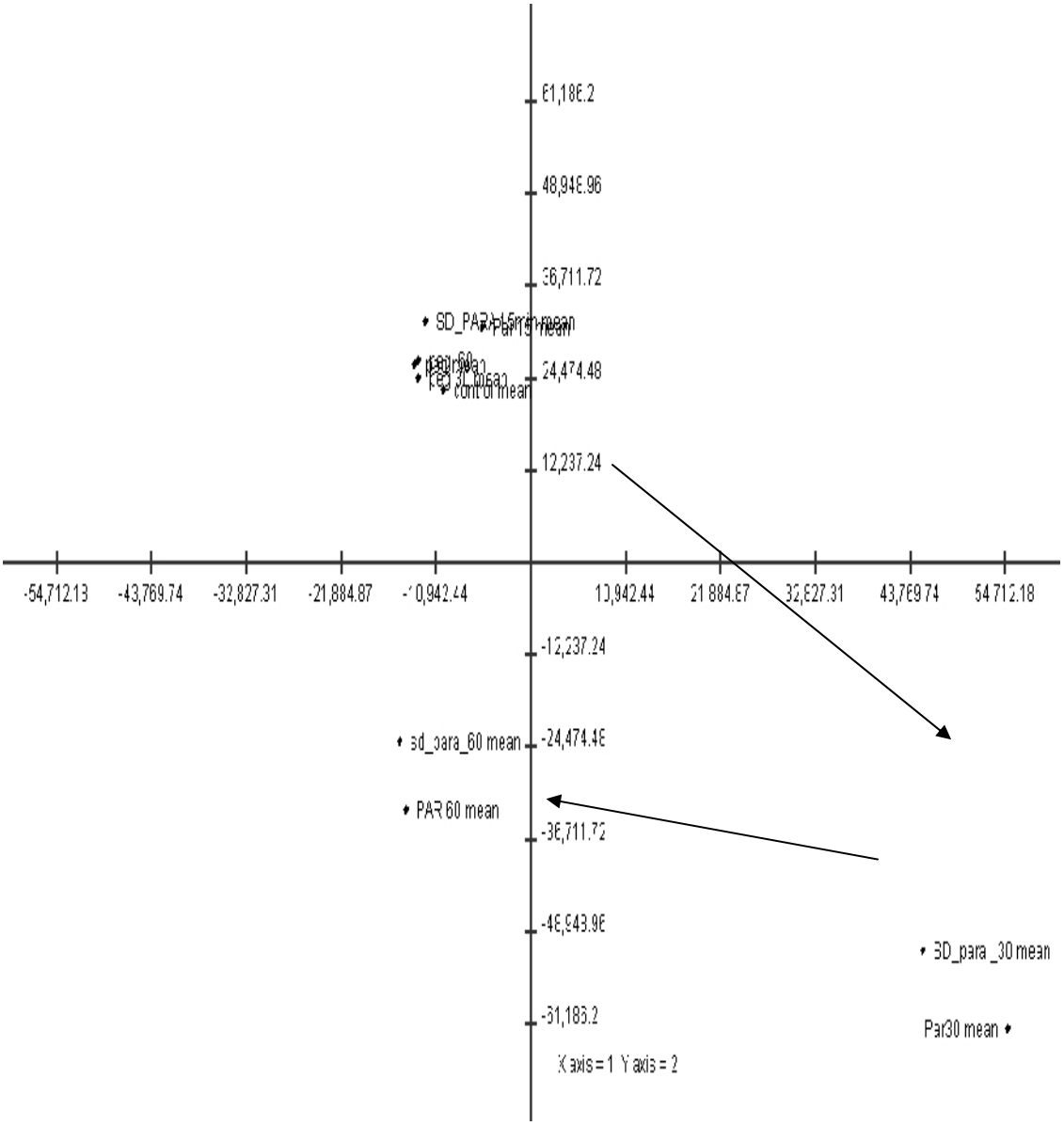

Figure 7.12. Principal component analysis on the transcriptional time course for paracetamol (PARA) alone and solid dispersion of paracetamol (SD-PARA). The number represents the time points. The plot represents the data for mean values at each time point.

Principal component analysis was carried out on the averaged normalised data for both indomethacin (figures 7.9 and 7.10) as well as paracetamol (figures 7.11 and 7.12) treated samples. Principal component 1 and principal component 2 were used to describe the molecular state of the cell and to determine dynamic trends during drug permeability.

The PCA plot in figure 7.9 represents the data for individual data sets at each time. For clarity, mean values at each time point were taken and PCA plot was obtained as illustrated in figure 7.10. The PCA plot in figures 7.9 and 7.10 show that the response of indomethacin permeability was minimum during the first 15 mins. This could possibly be due to the time required for DNA transcription and mRNA synthesis. However, at 30 mins, indomethacin alone treated cells exhibited maximum variability across the first principal component when compared to solid dispersion. Solid dispersion exposed cells cluster around the centre representing relatively lower gene expression changes when compared to their control counterparts. The molecular state of gene expression following exposure to indomethacin follows a circular trajectory as the gene cluster at 60 mins moves close to the origin. PCA analysis also suggests that maximum variability in gene expression was observed when exposed to drug alone when compared to its solid dispersion counterpart. This observation highlights an important finding that drug permeability increase (as reported in the chapter on drug permeability) is not necessarily followed by an increase in overall gene expression profile and the presence of other excipients (PEG 8000) can be used as a tool to optimise and deliver drug across the gastro-intestinal barrier.

The PCA plot in figures 7.11 and 7.12 for paracetamol reveals a different trend. The trajectory was clockwise when compared to the anticlockwise profile for indomethacin. Secondly, both the drug as well as solid dispersion treated cells show similar changes and follow the same path. Maximum variability in gene expression profile was obtained after 30 mins of drug permeability and the changes revert back to the original cluster after 60 mins of treatment.

7.3.6 Data analyses of genes controlling transporter network systems

7.3.6.1 Selection of polyethylene glycol

The number of poorly soluble drugs has increased sharply especially after the introduction of high through put screening to drug development cycle. It is now a challenge to improve the solubility of such poorly soluble compounds. Many techniques have been adapted to improve the drug solubility by using physical modifications (drug micronisation, use of cyclodextrins or use of surfactants), chemical modifications (salt formation and prodrugs) and solid dispersions (Leuner and Dressman, 2000).

Solid dispersions were first discussed by Sekiguchi et al. 1964 when it was suggested that the preparation of eutectic mixture could improve the drug solubility and in turn its bioavailability.

Polyethylene glycol (PEG) is one of the most common carriers used to prepare solid dispersions (Leuner and Dressman, 2000).

A study conducted by Hugger et al. 2002 suggested that PEG has an effect on the efflux transporter activity in Caco-2 cell monolayer. The study suggested that PEG 300 is capable of inhibiting the efflux transporter (MRP/P-gp) activity in Caco-2 cell monolayer and the reason for this could be the changes in the microenviroment of P-gp such as change in membrane fluidity; as a result the transporter lose its ability to efflux substrates such as taxol and doxorubicin.

In this study PEG was used to formulate a solid dispersion of poorly water soluble drugs (namely indomethacin and paracetamol) in order to improve the drug solubility and inhibit the efflux mechanism of the transporters and hence improve the overall bioavailability.

This study also evaluated the gene expression of different transporters (including ABC and SLC transporters) on Caco-2 cells monolayer.

7.3.7 Effect of Indomethacin and paracetamol dispersion systems on transporter gene expression

7.3.7.1 ATP- binding cassette (ABC)

The small intestine is considered as the main absorption site for any ingested material including dietary, therapeutic and toxic compounds. Oral administration is one of the most popular routes of administration as the oral dosage forms are non-invasive and convenient. However, intestinal enterocytes form a barrier to xenobiotics and drugs; as

such this barrier is created by a specific membrane transport system and metabolising enzymes.

The largest transporter gene family is ATP- binding cassette (ABC) also known as traffic ATPase. ABC is a diverse class of transporter proteins which utilise ATP hydrolysis energy to translocate solute across biological membranes. Members of ABC family are involved in large number of processess including signal transduction, presenting genes, uptaking nutrients and resisting drugs and xenobiotic (Higgins, 1992).

Different members of ABC family were identified in bacterial, archaea and eukrya. Therefore, it could be considered as an ancient proteinaceous device to transport solute against its concentration gradient across lipid bilayer (Schneider and Hunke, 1998).

ABC transporters consist of a pair of ATP-binding domains which is known as nucleotide binding folds (NBF), two sets of transmembrane (TM) domains. The former consists of 3 conserved domains; walker A, B and signature (C) motif. Signature C is characteristic for ABC transporters and differentiates them from other ATP-binding proteins. ABC are organised as either full transporters containing two TM and two NBF or half transporter containing one of each domain (Dean et al., 2001). ABC mechanism of action is not yet fully understood although many studies have tried to evaluate how ABC maintains these broad, distinct substrate specifications.

The results for the current study suggest that the level of differentially expressed genes varies with the type of drug, formulation and time. In the case of indomethacin exposed

cells, there were 26 genes that were over expressed after half an hour when compared to 1 gene that was suppressed (figure 7.13A). However, exposure of solid dispersion of indomethacin for the same duration resulted in 23 genes that were over expressed and three remained unaltered (figure 7.13B).

In the case of paracetamol exposed cells, there were 13 genes that were over expressed after 30 mins and two remained unchanged (figure 7.14A). However, exposure of solid dispersion of paracetamol for the same duration showed 13 genes that were over expressed and two remained unaltered (figure 7.14B).

Investigation of the results for paracetamol reveals that the total number of genes exhibiting variations was similar for both drug alone as well as solid dispersion after exposure for 30 mins (figures 7.15 and 7.16) with differences being apparent in the type of genes involved.

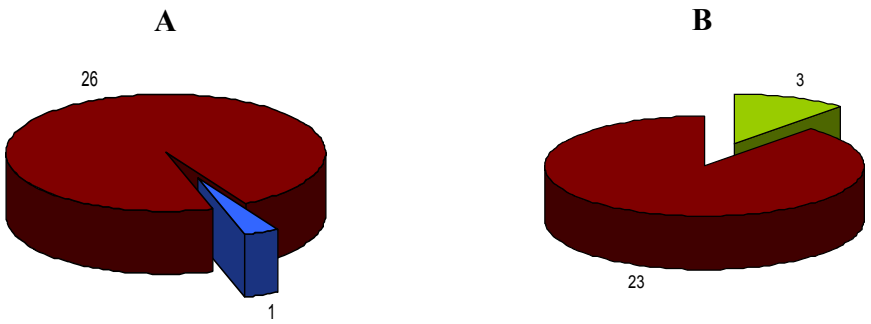

Figure 7.13. Total number of ABC genes over-expressed ( ) and suppressed ( ) after 30 mins of exposure to indomethacin (7.13A), Total number of ABC genes over-expressed( ) and unchanged ( ) after 30 mins of exposure to indomethacin-PEG solid dispersion (7.13B).

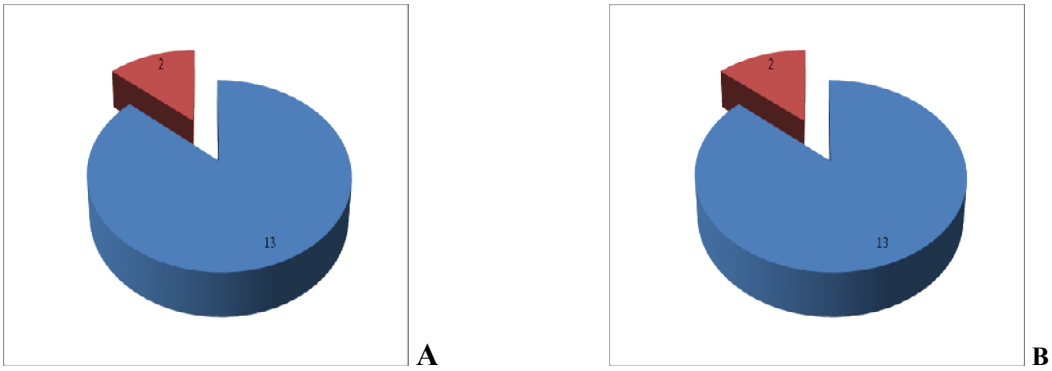

Figure 7.14. Total number of ABC genes over-expressed (13 genes) (□) and unchanged (2 genes) (■) after 30 mins of exposure to paracetamol (7.14A), Total number of ABC genes over-expressed (13 genes) (□) and unchanged (2 genes) (■) after 30 mins of exposure to solid dispersion of paracetamol (7.14B).

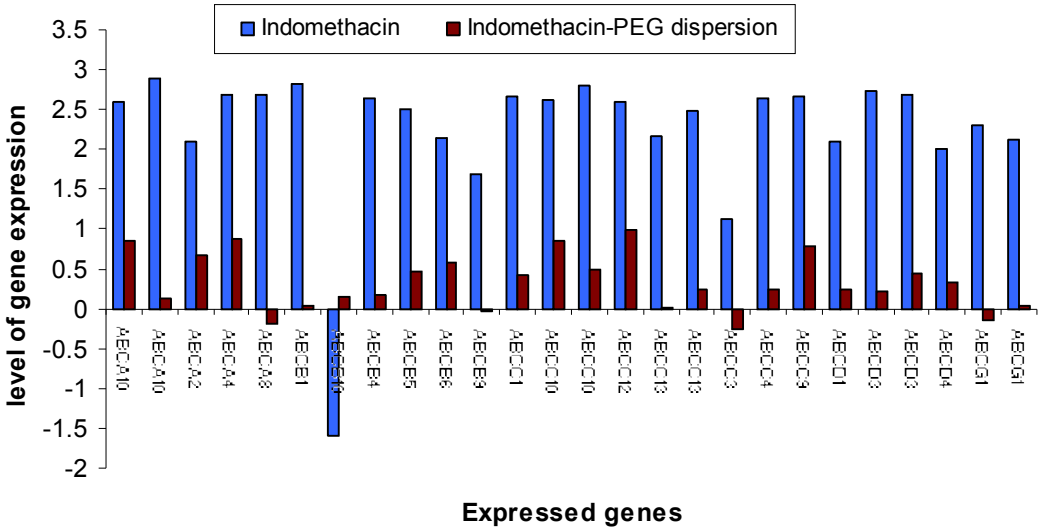

Figure 7.15. Gene expression of ABC transporters on Caco-2 cells after 30 mins of exposure to indomethacin(□) and indomethacin-PEG solid dispersion(■). (n=3).

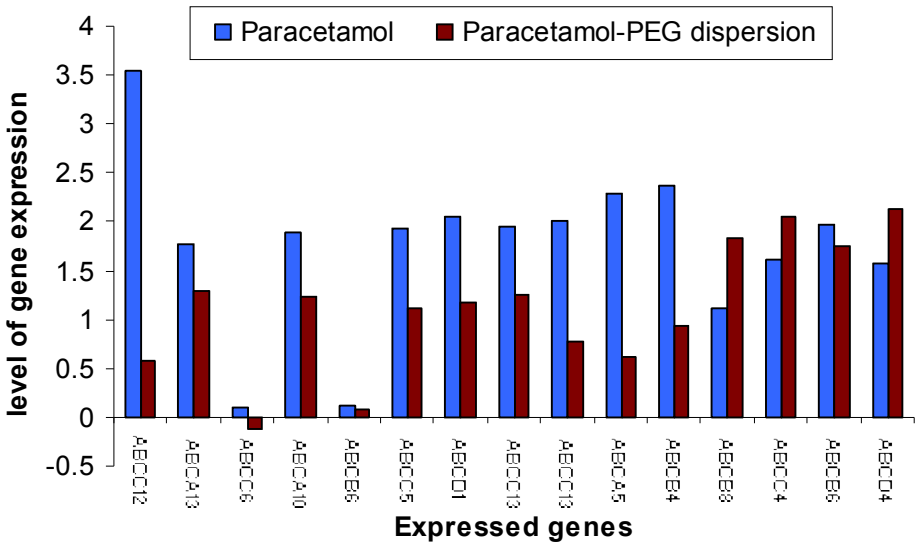

Figure 7.16. Gene expression profiles of ABC transporters on Caco-2 cells after 30 mins of exposure to paracetamol( ) and paracetamol-PEG solid dispersion( ). (n=3).

7.3.7.2 ABCA10

It is a member of ABCA6-like ABC transporters. ABCA10 expression is induced by cholesterol efflux in human macrophages and inhibited by cholesterol influx, therefore, ABCA10 is believed to play a role in lipid trafficking (Wenzel et al., 2003).

Addition of PEG causes only a slight decrease on ABCA10 expression over 15 mins, 30 mins and 60 mins, while exposure to indomethacin alone caused a significant increase (2.6±0.68) in ABCA10 expression only after 30 mins of Caco-2 cells exposure to the drug (figure 7.15). However, exposure of Caco-2 cells to indomethacin-PEG solid dispersion system resulted in a slight increase in ABCA10 expression when compared to indomethacin alone (0.85±0.51). This could be attributed to the low permeability coefficient of indomethacin and in turn indomethacin remains in contact with the genes on the apical cells for longer time and hence increased the expression of large number of

genes. On the other hand, indomethacin-PEG solid dispersion has higher permeability coefficient (almost 4 times of indomethacin alone) (figures 6.8 and 6.9). This might result in less contact time with genes of apical cells and hence less gene expression. Similarly, studying the effect of paracetamol and paracetamol-PEG dispersion system on ABCA10 gene expression has showed a significant increase in the expression from 0.47 (basal state) to (1.88±1.9) for paracetamol alone and (1.23±0.96) for paracetamol dispersion system (figure 7.15).

7.3.7.3 ABCA2

It is the largest known mammalian ABC transporter which consists of 2436 amino acids with apparent molecular weight of Mr 270,000 (Vuleric, 2001). ABCA2 shares highest homology with cholesterol responsive transporter ABCA1 (50%) and it is believed that ABCA2 has a potential role in neural development and microphage lipid metabolism (Kaminiski et al., 2001).

Similar trend as ABCA10, PEG has no effect on the gene expression profile, while indomethacin causes a sharp increase in ABCA2 expression (2.09±2.17) after 30 mins of Caco-2 cells exposure to the drug. Such this expression was reduced (0.67±0.94) when the solid dispersion system of indomethacin-PEG was added.

7.3.7.4 ABCA4

It is also known as ABCR or rim protein and expressed highly and intensively in retina. ABCA4 is linked with stargardt macular degeneration and retinal degenerative disease which causes severe vision loss in affected individuals (Molday, 2007).

ABCA4 actively transport N-retinylidene-phosphotidyl ethanol amine from lumen to cytoplasmic side of disc membrane such this transport ensures that retinoids do not accumulate in disc membrane. Mutation of ABCA4 which could result in diminished transport activity and hence accumulation of N-retinyldene PE in disc membrane and react to preduce A2E precursors, causing RPE cell death and photoreceptor degradation and finally loss of vision (Molday, 2007).

Indomethacin-PEG dispersion system increase ABCA4 gene expression from -0.47 to 0.87±0.05) which in turn ensures the transport of N-retinylidene PE and prevents it accumulation on the disc, thus avoids stargardt macular degeneration.

7.3.7.5 ABCA8

It is located in the ABCA transporter cluster of genes on chromosome 17q24 and was isolated from human brain libraries (Nagase et al., 1998; Dean et al., 2001). It mainly functions as a lipid transporter.

Exposure of the cells to indomethacin resulted in a 2.5 fold increase in the expression after 30 mins whereas reformulation as solid dispersion suppressed its expression.

7.3.7.6 ABCB1/ P-gp

It is also known as phosphoglycoprotein (P-gp) originally discovered in tumor cell (Juliano and Ling, 1976). ABCB1 was involved in development of tumor resistance to many chemotherapeutic agents. Also played a role in transporting wide range of hydrophobic and amphipathic drugs for instance cardioglycosides (like digoxin), analgesics (morphine), epileptic drugs (phenytoin).

Recently, ABCB1 was identified in normal tissues such as liver, kidney, intestine and adrenal and was reported to play a role in limiting the absorption and facilitating the excretion of xenobiotics.

Indomethacin acts as a specific inhibitor ABCB1 but its permeability is inhibited by efflux mechanism, this could be demonstrated by the increase of P-gp expression from -0.53 to (2.8±0.29) upon exposing the Caco-2 cells to indomethacin. On the contrary, the solid dispersion system resulted in suppression of P-gp expression (0.037±0.003) which possibly accounts as one of the reasons for increase in its influx/permeability when compared to indomethacin alone.

7.3.7.7 ABCB10

ABCB10 is also known as ABC-me (ABC-mitochondrial erythroid). It possesses a long 105 amino acid mitochondrial targeting presequence (mTP). ABCB10 is embedded in mitochondrial inner membrane homodimerizes and homo-oligomerizes.

AMC-me overexpression enhances haemoglobin synthesis in erythroleukemia cells and also participates in diverse physiological processes by coupling ATP hydrolysis to substrate transport across the cell membranes (Shirihai, 2000)

Interestingly, indomethacin alone was found to decrease the expression of ABCB10 from 0.239 to (-1.58±0.31) after 30 mins, while indomethacin-PEG solid dispersion has no significant effect on ABCB10 expression during 30 mins (0.15±0.12) and started to decrease the gene expression after 60 mins.

7.3.7.8 ABCB4

Adenosine triphosphate-binding cassette, subfamily B, member 4 which encodes the phosphatidyl choline translocator across canalicular membrane, homozygous and heterozygous mutation in ABCB4 are responsible for progressive intrahepatic cholethesis type 3 (Jacquemai et al., 2001).

Fracchia et al. 2001 suggested that ABCB4 gene defects in peculiar forms of cholelithiasis (e.g intrahepatic gallstone disease).

During the basal state of Caco-2 cells, ABCB4 expression was -0.5 and this expression slightly decreased upon adding PEG. However, adding indomethacin alone, ABCB4 expression increased drastically to 2.64, while indomethacin-PEG dispersion system increased the expression to 0.166 only. In a similar way, ABCB4 gene expression was

increased to (2.36±1.5) and (0.93±0.61) for paracetamol and paracetamol-PEG dispersion respectively.

7.3.7.9 ABCC12

Also known as MRP9 and consists of 29 exons; oriented tail to head on human chromosome 16q12.1 (Yabucchi et al., 2001).

No physiological function is known for ABCC12 but it is believed to play a role in a genetic disease in infancy known as paroxysmal kinesigenic choreoathetosis PKC (Shimizu et al., 2003). It is suggested that ABCC12 plays a role in detoxification system and could be involved in transporting endogenous substances in testis.

Both indomethacin and paracetamol caused an increase in ABCC12 expression from (-0.37 at basal state) to 2.6 and 3.54 respectively. However, the solid dispersion of these drugs resulted in a slight increase in ABCC12 expression (0.98±0.31) for indomethacin-PEG and (0.579±0.99) for paracetamol-PEG solid dispersion.

7.3.7.10 ABCC13

ABCC13 was first identified by (Yabuuchi et al., 2002) and it spans ~70 Kb on human chromosome 21q11.2 and possesses 14 exons. ABCC13 is expressed highly in fetal liver (20 times than adult liver). Also human leukaemia K562 were found to express ABCC13 and this expression decrease during cell differentiation induced by TPA.

The results were similar for both indomethacin as well as paracetamol exposed cells. In both the cases, the expression was nearly 2.5 fold higher when exposed to drug alone as compared to their solid dispersion counterparts.

7.3.7.11 ABCB5

(MDR/TAP) is a new human ABC transporter which encode on 7p15.3 chromosome. It maintains the membrane hyperpolarisation and acts as a determinant of membrane potential and regulator of cell fusion in physiological skin progenitor cells.

Study conducted by (Frank et al., 2005) identified ABCB5 as a novel drug transporter and chemoresistance mediator in human malignant melanoma.

Indomethacin alone exposed cells showed a 2.5 fold increase in its expression when compared to solid dispersion suggesting that the drug could be a substrate resulting in resistance.

7.3.7.12 ABCB6

ABCB6 has multiple functions such as iron homeostasis (as it transfers heme or iron-related compounds from mitochondrial matrix into cytosol), porphrin transport and cytotoxic agents resistance.

A study conducted by Paterson et al. 2007 demonstrated that ABCB6 has two distinct molecular weight forms and is localised at the plasma membrane and outer mitochondrial

membrane. Another study conducted by Masashi et al. 2008 found that ABCB6 is localised in the endoplasmic reticulum; mainly golgi apparatus rather than the mitochondria.

Indomethacin exposed cells showed approximately 2.3 fold increase in its expression when compared to their solid dispersion counter parts. However, there was no change observed in the extent of expression in the case of paracetamol exposed cells.

7.3.7.13 ABCB9

It is a member of transporter associated with antigen processing TAP-like (TAPL) and translocates a large number of solutions across membranes.

According to mRNA level, TAPL is highly expressed in testes and moderately in brain and spinal cord but expressed at low levels in other tissues (Wolters et al., 2005).

ABCB9 also forms a homodimeric complex which acts as a specific and ATP-dependent peptide transporter (i.e vacuum cleaner removing peptides from cytosol).

There was a two fold increase in its expression when exposed to indomethacin alone after 30 mins as compared to its solid dispersion. This possibly suggests that indomethacin is a substrate for ABCB9.

7.3.7.14 ABCC10

It is a member of multidrug resistance protein (MRP) known as (MRP-7). Yet, its protein structure has the lowest degree of structure resemblance to other MRPs. On the basis of amono acid alignment (~34-26%), MRP7 showed resistance to natural anticancer agent including Texans, vinca alkaloids and anthracyclins. It exhibits its highest activity against docetaxel (9-13 folds) (Hopper-Borge et al., 2004).

Indomethacin alone exposed cells resulted in approximately 2.5 fold increase in the expression of ABCC10 when compared to their solid dispersion counterparts. This was expected as ABCC10 is a member of MRP and would therefore play a vital role in the efflux of indomethacin. The result also suggests that reformulation of MRP substrates and inclusion of excipients (in this case PEG 8000) can be a simple tool to overcome drug resistance.

7.3.7.15 ABCC1

Known as 190 kDa multidrug resistance protein 1 (MRP1) and was first discovered in lung cancer cells. It is a primary transporter of glucuronate, sulphate conjugate and unconjugated organic anions and GSH (Lesile et al., 2001). MRP1 plays a role in efflux of several xenobiotics such as vinca alkaloids, methotrexate and arsenic and antimonal oxyanions (Cole et al., 1994).

Similar results were obtained as that seen with ABCC10. There was approximately 3 fold increase in the expression of ABCC1 when subjected to drug alone (indomethacin) when compared to solid dispersion.

7.3.7.16 ABCC3

It is a member of MRP family and known as MRP3. It shares the highest amino acid sequence identity with MRP1 (58%); it also localised at basolateral membrane of polarised cells. Human adrenal glands and intra-hepatic bile ducts are the highest organs to express MRP3 followed by small intestine, kidney and pancreas (Kool et al., 1997).

A study conducted by Hiroshashi et al. 1999 suggests that MRP3 plays a role in organic anions detoxification from liver.

Zelcer et al. 2001 concluded that ABCC3 resist the transportation of etoposide and teniposide in cancer cells. Moreover, ABCC3 transport bile salt plays a role in enteolepatic circulation of these salts.

Exposure of indomethacin alone resulted in a 2 fold increase in its expression when compared to solid dispersion.

7.3.7.17 ABCC4

Known as MRP4 and is localised to proximal tubule apical membrane kidney. A study conducted by Van Aubel et al. (2002) suggested that MRP4 is a novel apical organic

anion transporter which acts as an efflux pump for cGMP and cAMP in proximal tubules of human kidney.

Another study conducted by (Chen et al., 2002) concluded that MRP4 is a resistance factor for methotrxate and it acts as an energy dependent efflux system for methotrexate and physiological factors along with MRP1 and MRP2.

The results show that exposure of indomethacin alone caused a three folds increase in its expression when compared to solid dispersion. This was expected as ABCC4 has been shown to act as an efflux pump in the removal of hydrophobic anti cancer compounds. Exposure of indomethacin alone resulted in a higher level of its expression with reformulation enabling its suppression.

On the other hand, the results for paracetamol suggest that the expression of ABCC4 was higher in solid dispersion when compared to drug alone.

7.3.7.18 ABCC9

It is a sulsonyl urea receptor (SUR2) and is a member of c-branch adenosine triphosphate superfamily. ABCC9 produces two isoforms namely SUR2A and SUR2B, the former plays a role in assembling KATP channels in cardiac and skeletal muscles while the later participates in maintaining of vascular tone (Bryan et al., 2007).

Exposure of indomethacin alone resulted in nearly 1.5 times higher levels of expression when compared to solid dispersion.

7.3.8 Solute carrier transporters (SLC)

Another superfamily of membrane proteins is solute carrier transporters (SLC). SLC transporters play numerous roles in physiological process such as transporting nutrients, metabolites and neurotransmitters.

Around 43 SLC families with 300 SLC genes have been established. Each family has specific substrate like, monocarboxylic acids, organic anions, cations and sugars.

SLC transporters have broad substrate selectivity as they confer sensitivity to multiple drugs with different structures. Yet some SLC possess drug chemosensitivity properties. Moreover, SLC transporters could be used as an analysis tool for polymorphism associated with therapeutic response and toxicity of anticancer drugs (Huang et al., 2007).

Figures 7.17, 7.18 and 7.19 show total number of SLC genes over-expressed and unchanged after 30 mins of exposure both drugs and dispersion.

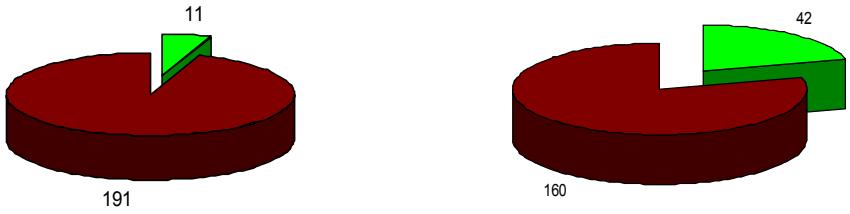

A **B**

Figure 7.17. Total number of SLC genes over-expressed ( ) and unchanged ( ) after 30 mins of exposure to indomethacin (7.17A), Total number of SLC genes over-expressed( ) and unchanged( ) after 30 mins of exposure to solid dispersion indomethacin (7.17B).

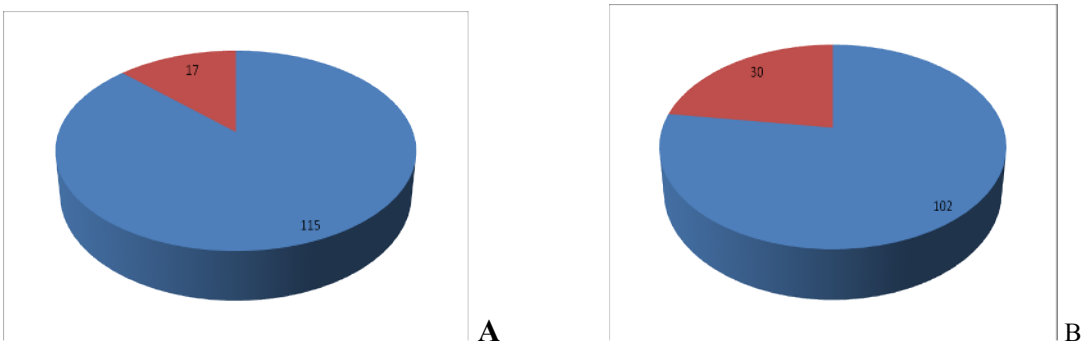

A B

Figure 7.18. Total number of SLC genes over-expressed ( ) and unchanged( ) after 30 mins of exposure to paracetamol (7.18A), Total number of SLC genes over-expressed( ) and unchanged( ) after 30 mins of exposure to solid dispersion of paracetamol (7.18B).

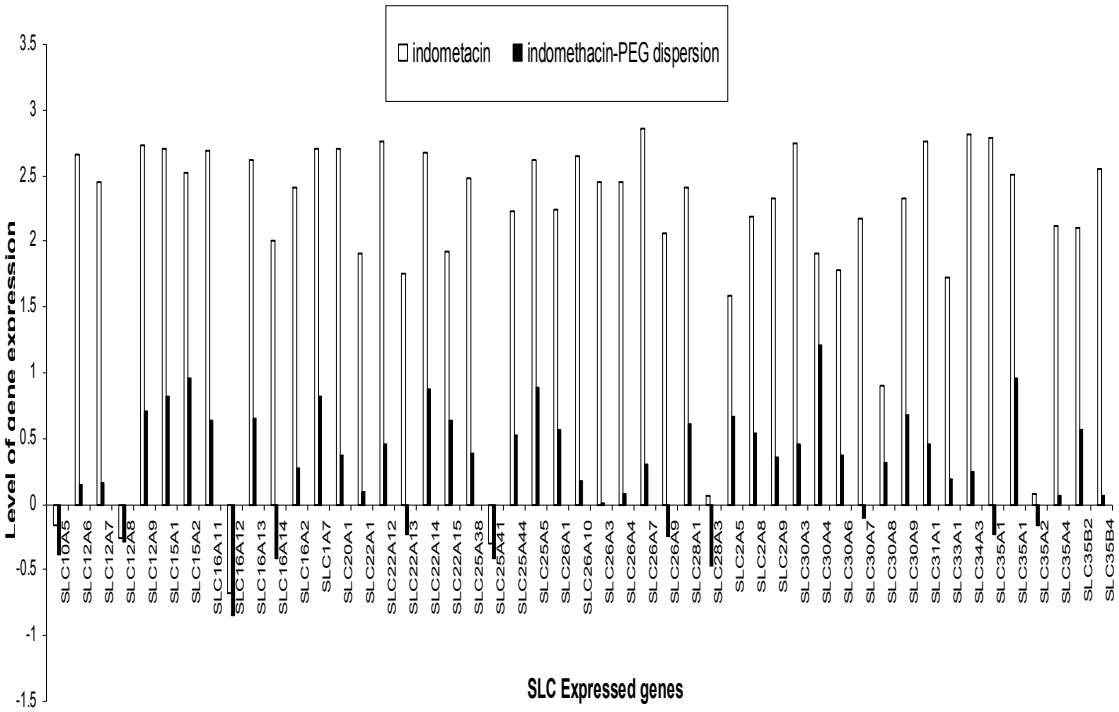

Figure 7.19. Gene expression of SLC transporters on Caco-2 cells after 30 minutes of exposure to indomethacin(□) and indomethacin-PEG solid dispersion(■). (n=3).

7.3.8.1 SLC12A6

It is a K^+ Cl^- cotransporters (KCC3) which belongs to electroneutral cation-chloride cotransporters family. KCCs play a major role in swelling activated K+ efflux in erythrocytes. KCCs are not affected by membrane potential. However, they are sensitive for loop diuretics such as furosamide and bumetamide (Mount et al., 1999).

Indomethacin was found to affect SLC12A6 expression in Caco-2 cells and increased its expression from -0.637 to 2.66. However, indomethacin dispersion system had slightly increased this expression to 0.144.

7.3.8.2 SLC16A13

It is a member of monocarboxylate cotansporter (MCT) family; which consists of 14 members. MCT 13 is expressed on 17p13.1 gene and distributed mainly in breast, bone marrow and stem cells. Up till now no information is available on their functions and properties (Halestrap and Meredith, 2004).

MCT13 expression was increased by indomethacin and reached 2.62±0.63 after half an hour of exposure to indomethacin alone. Yet the solid dispersion system increased the expression slightly by (0.64±0.3). The expression of other MCT members such as MCT11, MCT14, MCT3 and MCT2 increased as well and only MCT12 was depressed.

Both paracetamol and paracetamol-PEG SD were found to affect the gene expression of MCT13. Interestingly, paracetamol-PEG SD had over expressed MCT 13 more than the drug alone; 1.86±0.85 and 1.36±0.1 respectively.

7.3.8.3 SLC22A12

It acts as a urate-anion exchanger in human kidney (Iwai et al., 2004). Mutation of SLC22A12 which could result in inactivating gene causes renal idiopathic hypouricemia. The genetic variation of SLC22A12 affects the urate levels in general population and contribute to hypo or hyperuricemia.

The result suggests that SLC22A12 expression is affected by indomethacin as its expression increases to (2.75±0.217), while the indomethacin-PEG SD caused a slight increase in its expression (0.45±0.05).

7.3.8.4 SLC6A6

It belongs to Na+ and Cl- dependent neurotransporters family. It plays a major role in γ-amino butyric acid (GABA) transportation. It also known as taurine transporter (Taut) which is expressed in retinal capillary endothelial cells and mediates taurine transporting. Tomi et al. (2008) established that SLC6A6 is involved in transporting GABA across blood retinal barrier (BRB).

The basal expression of SLC6A6 in Caco-2 cells was -0.49 and increased sharply to (2.69±0.97) upon adding indomethacin alone for 30mins into cell culture. On the other hand, indomethacin solid dispersion system had a slight increase (0.51±0.23) in the SLC6A6 expression. The expression of SLC6A8, SLC 6A9 and SLC6A18 were similar to that of SLC6A6.

7.3.8.5 SLC25A26/ SAMC

S-adenosylmethionine carrier (SAMC) belongs to a mitochondrial carrier family of proteins (SLC25). Members of this family have different functions, but they had related sequences. S-adenosylmetionine is essential for mitochondrial metabolism especially protein synthesis. S-adenosylmetionine also plays a role in methylation of various types of nucleic acid in mitochondria such as DNA. Moreover, it takes part in post-transitional

modification of some proteins. S-adenosylmetionine is synthesised in the cytosol and is required in mitochondria; this transportation is catalysed by SAMC in exchange for internal substrates (Agrimi et al., 2004).

Paracetamol was found to increase the expression of SAMC gene from -0.36 in basal state of Caco-2 cells to (3.58±0.36) after 30 mins of exposure to paracetamol. On the other hand, paracetamol-PEG solid dispersion had a slight effect on SAMC genes expression (0.18±0.001).

7.3.8.6 SLC38A4/ATA3

It is a member of amino acid transporter system A gene family and known as ATA3. It is expressed mainly in liver and skeletal muscle. ATA3 mediates the uptake of aliphatic, neutral, short chain amino acids.

Both paracetamol and parcetamol-PEG SD raised ATA3 gene expression. ATA3 gene was expressed to (3.5±0.52) by paracetamol alone and only expressed to (0.737±0.14) by the solid dispersion.

7.3.8.7 SLC6A2

SLC6A2 is a human norepinephrine transporter (hNET) and is a member of Na+/Cl-dependent GAT (GABA transporter)/NET transporter family. Bruss et al. 1993 suggested that hNET is a single copy of gene located on chromosome 16. Mutation which results in

inactivation or dysfunction of SLC6A2 could cause many diseases such as cardiovascular disorders, fatal arrhythmias and orthostatic intolerance disorder (Hahn et al., 2003).

SLC6A2 expression was increased by paracetamol (3.08±0.175), whereas, paracetamol-PEG SD increased the gene expression to (1.1±0.8).

7.4 Conclusions

Gene expression profiles analysing the expression changes in the transporter network system ABC (ATP binding cassette) and solute carrier transporter when treated with drug alone (paracetamol alone and indomethacin alone) or the solid dispersion of the drug (solid dispersion of paracetamol and solid dispersion of indomethacin).

The Caco-2 cells exposed to indomethacin solid dispersion lead in a slight increase in ABCA10 expression when matched to indomethacin alone. This could be attributed to the low permeability coefficient of indomethacin and higher permeability coefficient of indomethacin solid dispersion. The indomethacin alone contacts with the genes on the apical Caco-2 cells for longer time as compared to indomethacin solid dispersion and so changed the expression of large number of genes. Indomethacin acts as a substrate on ABCB1 but its permeability is reduced by efflux mechanism, this increase of P-gp expression upon treating the Caco-2 cells to indomethacin alone. On the contrary, the solid dispersion of indomethacin resulted in a slight increase in P-gp expression. Thus its permeability is higher than indomethacin alone. Indomethacin decreases the expression of ABCB10 while indomethacin solid dispersion has no significant effect on ABCB10 gene expression during 30 mins and started to decrease the gene expression after 60 mins. Indomethacin alone and indomethacin solid dispersion increases the expression of ABCB4.

Paracetamol and paracetamol solid dispersion on ABCA10 gene expression has demonstrated a significant increase in the expression. In a case of paracetamol and

paracetamol solid dispersion, ABCB4 gene expression was increased. Both indomethacin and paracetamol made an increase in ABCC12 gene expression. However, the solid dispersions for both drugs showed in a slight increase in ABCC12 expression.

Indomethacin alone was resulted to effect SLC12A6 gene expression and increased its expression. However, indomethacin solid dispersion had slightly increased the expression. MCT13 gene expression was increased by indomethacin alone and solid dispersion of indomethacin. SLC22A12 and SLC6A6 gene expression were increased by indomethacin alone while indomethacin solid dispersion resulted in a slight increase in its expression.

Both paracetamol and solid dispersion of paracetamol were found to effect the gene expression of MCT13. Paracetamol alone resulted increase the expression of SAMC gene. While in case of paracetamol solid dispersion had a slight effect on SAMC genes expression. Both paracetamol and parcetamol solid dispersion increased SLC6A2 and ATA3 gene expression.

Conclusions

Solid dispersions in water-soluble carriers are regarded as highly effective means of increasing the dissolution rate which in turn enhances bioavailability of various drugs like paracetamol, sulphamethoxazole, phenacetin, indomethacin, chloramphenicol, phenylbutazone and succinylsulphathiazole. Solid dispersions increase the solubility of drug due to the conversion of the drug's crystal lattice into amorphous form, decrease in the particle size and increase in wettability caused by hydrophilic polymer. Current study suggests the suitability of PEG 8000 as a carrier for solid dispersions for all seven drugs studies. It has been shown that PEG 8000 used as a carrier within the solid dispersions increase the dissolution rate. The physical mixtures displayed higher dissolution rates in all seven drugs as compared to pure drugs which can rightly be attributed to the wettability of drug caused by the presence of PEG 8000. Moreover, solid dispersions exhibited higher dissolution rates than those of physical mixtures and drug alone which is possibly due to increase in drug wettability caused by polymer used as carrier. Maximum dissolution rate was shown by solid dispersions containing 5% (w/w) drug loading implying that high carrier concentration increases the dissolution rate. Microviscometry has been shown to be a suitable technique for determining the dissolution of the PEG 8000 within the solid dispersions.

Theories presented for the mechanisms governing release of drug from solid dispersions depends on the dissolution behavior of either drug or polymer. Paracetamol, sulphamathoxazole and phenacetin demonstrated faster release rate than PEG 8000 while PEG 8000 released faster than other drugs of the study, like, indomethacin,

chloramphenicol, phenylbutazone and succinylsulphathiazole in solid dispersions. Some formulations such as indomethacin, chloramphenicol, phenylbutazone and succinylsulphathiazole showed carrier-controlled release with the release rate being controlled by the dissolution of the polymer while solid dispersions of paracetamol, sulphamathoxazole and phenacetin displayed that the properties of the drug are the controlling factor in the release rate.

Characterisation studies were performed to gain an insight into the possible explanation as how solid dispersions enhance the dissolution of drugs as compared to physical mixtures and drug alone. DSC studies revealed that melting peak of the polymer was 59 °C with the absence of endothermic peak relating to the drug for all solid dispersions. This lack of a melting peak could potentially be due to the distribution or solubilisation of the drug within PEG 8000 which leads to the conversion of drug's crystals into amorphous form within the solid dispersions. DSC scans for the physical mixture presented highly distinguishing profile. Two transitions were displayed by the physical mixtures of phenacetin and paracetamol with PEG 8000 in which the first melt corresponds to the melt of PEG 8000 while the second relates to the melting of the drug (phenacetin and paracetamol). Whereas, a single melting endotherm was noticed for the physical mixtures of indomethacin, phenylbutazone, chloramphenicol, sulphamethoxazole and succinylsulfathiazole with the PEG 8000 that relates to the PEG 8000 as is given by the thermograms for the solid dispersion.

To further investigate the difference in thermal behavior of the physical mixtures (presence and absence of drug endotherms) infra red analysis of the samples was carried out to detect any possibility of functional group interactions between drug and PEG 8000. FTIR spectra revealed the absence of any interaction between the drug and PEG 8000 for the solid dispersion of all drugs as no variations in the specific absorption bands for both the PEG 8000 as well as the drug were observed. However, the physical mixture of phenacetin and paracetmol showed the formation of hydrogen bond between the drug and the polymer.

Scanning electron microscopy (SEM) was used at different magnifications to determine the morphological differences of solid dispersions. SEM studies showed that the surface properties of all drugs and PEG 8000 were lost in the process of preparing the solid dispersion system by melting and solidification causing the drug to be molecularly dispersed within the carrier matrix.

Solubility of the drug increased in the solid dispersion followed by physical mixture and pure drug. The increased solubility in solid dispersions is potentially due to the conversion of crystalline drug into amorphous form during the formation of solid dispersion which leads to higher wettability. ITC results revealed that heat change causes an increase in the dissolution of the drug in physical mixture and solid dispersion with PEG 8000 as a carrier. The high energy released while polymer is titrated with drug enhances the dissolution rate as compared to drug alone.

Stability studies were performed at room temperature conditions and accelerated conditions (40°C±2°C/75%RH±5%RH). Accelerated stability studies showed that the paracetamol, sulphamethoxazole, phenacetin, indomethacin, chloramphenicol, phenylbutazone and succinylsulphathiazole were unstable as suggested by DSC, FTIR, drug content and TGA analysis. Solid dispersions stored at room temperature (controlled moisture using silica gel) were stable for 12 months for all seven drugs. Temperature and moisture can affect the stability of solid dispersions.

Permeability of indomethacin, phenacetin, phenylbutazone and paracetamol was higher for solid dispersions as compared to pure drugs across Caco-2 cell monolayers. In case of indomethacin solid dispersion the permeability was 4 times higher than indomethacin alone. In solid dispersions of paracetamol, phenactin and phenylbutazone, the permeability was twice as compared to drug alone treatment. Cell uptake studies shows that PEG 8000 enhanced the rhodamine123 uptake which may have increased the permeability of indomethacin, phenacetin, phenylbutazone and paracetamol in solid dispersions across Caco-2 cell monolayers.

Gene expression profiles analysing the expression changes in the transporter network system ABC (ATP binding cassette) and solute carrier transporter during permeability studies at three different time points (15 mins, 30 mins and 60 mins) when treated with drug alone (paracetamol alone and indomethacin alone) or the solid dispersions of the drug (solid dispersion of paracetamol and solid dispersion of indomethacin).

The exposure of Caco-2 cells to indomethacin solid dispersion led to a little increase in ABCA10 expression when matched to indomethacin alone. This could be ascribed to the low permeability coefficient of indomethacin and contact with the genes on the apical Caco-2 cells for longer duration and hence changed the expression of large number of genes. In case of indomethacin solid dispersions, a higher permeability coefficient was observed. This might cause in less contact time with apical cells gene and hence results in less gene expression. Paracetamol and paracetamol solid dispersion on ABCA10 gene expression has shown a significant increase in the expression.

Indomethacin acts as a specific substrate on ABCB1 but its permeability is repressed by efflux mechanism, this could be shown by the increase of P-gp expression upon treating the Caco-2 cells with indomethacin alone. Contrary to this, the solid dispersions of indomethacin ensued in a slight increase in P-gp expression. Hence, the permeability of solid dispersions of indomethacin is higher than indomethacin alone.

Indomethacin alone causes the expression of ABCB10 to decrease after 30 mins, while indomethacin solid dispersion has no significant effect on ABCB10 expression during 30 mins and tends to limit the gene expression after 60 mins.

Indomethacin alone increases the expression of ABCB4 to 2.64, while indomethacin solid dispersion increased the expression of the same to 0.166. In a case of paracetamol

(2.36±1.5) and paracetamol solid dispersion (0.93±0.61), ABCB4 gene expression was shown to have increased.

Both indomethacin and paracetamol made significant increase in ABCC12 gene expression. However, the solid dispersions for both drugs showed a minor increase in ABCC12 expression.

Results showed that indomethacin alone effect SLC12A6 gene expression and increased its expression from -0.637 to 2.66. However, indomethacin solid dispersion had slightly increased this expression to 0.144.

MCT13 gene expression was increased by indomethacin alone (2.62±0.63) after 30 mins of exposure. But the solid dispersion of indomethacin increased the gene expression slightly (0.64±0.3). Both paracetamol (1.36±0.1) and solid dispersion of paracetamol (1.86±0.85) were found to effect the gene expression of MCT13.

SLC22A12 gene expression was increased by indomethacin alone as its expression increases (2.75±0.217), while indomethacin solid dispersion resulted in a slight increase in its expression (0.45±0.05). SLC6A6 gene expression was increased by indomethacin sharply (2.69±0.97) for 30 mins into cell culture. On the other hand, indomethacin solid dispersion had a slight increase (0.51±0.23) in the SLC6A6 expression.

Paracetamol alone resulted in an increased expression of SAMC gene. While in case of paracetamol solid dispersion, it did not have any significant effect on SAMC gene expression. Both paracetamol (3.5±0.52) and parcetamol solid dispersion (0.737±0.14) increased ATA3 gene expression. SLC6A2 expression was increased by paracetamol (3.08±0.175) whereas paracetamol solid dispersion increased the gene expression slightly (1.1±0.8).

References

Abdul-Fattah, A.M., Bhargava, H.N., 2002. Preparation and in vitro evaluation of solid dispersions of halofantrine. Int. J. Pharm. 235, 17-33.

Agrimi, G., DiNoia, M. A., Marobbio, C. M. T., Fiermonte, G., Lasorsa, F.M., Palmieri, F., 2004. Identification of the human mitochondrial S adenosylmethionine transporter: bacterial expression, reconstitution, functional characterization and tissue distribution, Biochem. J. 379, 183–190.

Ahuja, N., Katare, O.P., Singh, B., 2007. Studies on dissolution enhancement and mathematical modeling of drug release of a poorly water-soluble drug using water-soluble carriers. Eur. J. Pharm. Biopharm. 65, 26–38.

Ahuja, S., 1998. Impurities Evaluation of Pharmaceuticals, Marcel Dekker, Inc., New York, USA.

Akbua, J., 1993. The effect of the physicochemical properties of a drug on its release from chitosonium malate matrix tablets. Int. J. Pharm. Vol 100. Issues 1-3, 257-261.

Al-Angary, A.A., A1-Meshal, M.A., Bayomi, M.A., Khidr, S.H., 1996. Evaluation of liposomal formulations containing the antimalarial agent, arteether. Int. J. Pharm. 128, 163-168.

Albert, A., 1958. Chemical aspects of selective toxicity. Nature. 182, 421-422.

Alonso, M.J., Maincent, P., Garcie-Arias, T., Vila-Jato, J.L., 1988. A comparative biopharmaceutical study of fresh and ageing tolbutamide-polyethylene glycol solid dispersions. Int. J. Pharm. 42, 27–33.

Alsaidan, S.M., Alsughayer, A.A., Eshra, A.G., 1998. Improved dissolution rate of indomethacin by adsorbents. Drug Dev. Ind. Pharm. 24, 389–394.

Amidon, G. L., 1981. Drug derivatization as a means of solubilization: Physiochemical and biochemical strategies. In: Techniques of solubilization of drugs, Marcel Dekker, New York, Yalkowsky. S. H. Ed. 183-211.

Amidon, G., Lennernäs, H., Shah, V., Crison, J., 1995. A theoretical basis for a Biopharmaceutics Drug Classification: the correlation of in vitro drug product dissolution and *in vivo* bioavailability. Pharm. Res. 12, 413–420.

Anderson, B. D., 1985. Prodrugs for improved formulation properties. In: Design of Prodrugs, Elsevier, Amsterdam, Bundgaard. H. Ed. 243-270.

Artursson, P., Borchardt, R.T., 1997. Intestinal drug absorption and metabolism in cell cultures: Caco-2 and beyond. Pharm. Res. 14, 1655-1658.

Artursson, P., Karlsson, J., 1991. Correlation between oral drug absorption in humans and apparent drug permeability coefficients in human intestinal epithelial (Caco-2) cells. Biochem. Biophys. Res. Com. 175, 880–885.

Artursson, P., Palm, K., Luthman, K., 1996. Caco-2 monolayers in experimental and theoretical predictions of drug transport. Adv. Drug Dev. Rev. 22, 67-84.

Artursson, P., Ungell, A-L., Lofroth, J-E., 1993. Selective paracellular permeability in two models for intestinal absorption: cultured monolayers of human intestinal epithelial cells and rat intestinal segments. Pharm. Res. 10, 1123-1129.

Asker, A.F., Whitworth, C.W., 1975. Dissolution of acetylsalicylic acid from acetylsalicylic acid-polyethylene glycol 6000 coprecipitates. Pharmazie. 30, 530-531.

Atkinson, R.M., Bedford, C., Child, K.J., Tomich, E.G., 1962. The effect of griseofulvin particle size on blood levels in man. Antibiot. Chemother. 12, 232–238.

Badens , E., Majerik, V., Horvath, G., Szokonya, L., Bosc, N., Teillaud, E., Charbit, G., 2009. Comparison of solid dispersions produced by supercritical antisolvent and spray-freezing technologies. Int. J. Pharm. 377(1-2), 25-34.

Bandi, N., Wei, W., Roberts, C.B., Kotra, L.P., Kompella, U.B., 2004. Preparation of budesonide– and indomethacin–hydroxypropyl-β-cyclodextrin (HPBCD) complexes using a single-step, organic-solvent-free supercritical fluid process. Eur. J. Pharm. Sci. 23(2), 159-168.

Benet, L.Z., Izumi, T., Zhang, Y., Silverman, J.A., Wacher, V.J., 1999. Intestinal MDR transport proteins and P-450 enzymes as barriers to oral drug delivery. J. Contl. Rel. 62, 25-31.

Beretzky, A., Kasa Jr, P., Pintye-Hodi, K., Bajdik, J., Szabo-Revesz , P., Eros, I., 2002. Pelletization of Needle-Shaped Phenylbutazone crystals. J. Ther. Anal. Calorim. 69(2), 529–539.

Berge, S. M., Bighley, L. D., Monkhouse, D. C., 1977. Pharmaceutical salts. J. Pharm. Sci. 66, 1-19.

Betageri, G.V., Makarla, K.R., 1995. Enhancement of dissolution of glyburide by solid dispersion and lyophilization techniques. Int. J. Pharm. 126, 155-160.

Blais, A., Bissonnette, P., Berteloot, A., 1987. Common characteristics for 1 Na -dependent sugar transport in Caco-2 cells and human fetal colon. J. Membr. Biol. 99, 113–125.

Blohm, D.H., Guiseppi-Elie, A., 2001. New developments in microarray technology. Curr. Opin. Biotech. 12, 41-47.

Bogdanova, S., Bontcheva, E., Avramova, N., 2007. Phase characterization of indomethacin in adsorbates onto hydroxyl-ethylcellulose. Drug Dev. Ind. Pharm. 33, 900–906.

Bogdanova, S., Pajeva, I., Nikolova, P., TsakovskaI., Muller, B., 2005. Interactions of poly(vinylpyrrolidone) with ibuprofen and naproxen experimental and modelling studies. Pharm. Res. 22, 806–815.

Borges, O., Borchard, G., Verhoef, J. C., Sousa, A., Junginger, H. E., 2005. Preparation of coated nanoparticles for a new mucosal vaccinedelivery system. Int. J. Pharm. 299(1–2), 155–166.

Braun, A., Hämmerle, S., Suda, K., Rothen-Rotishauser, B., Günther, M., Krämer, S., Wunderli-Allenspach, H., 2000. Cell cultures as tools in biopharmacy. Eur. J. Pharm. Sci. 11, 51-60.

Bruss, M., Kunz, J., Lingen, B., Bonisch, H., 1993. Chromosomal mapping of the human gene for the tricyclic antidepressant-sensitive noradrenaline transporter. Hum. Genet. 91, 278–280.

Bryan, J., Muñoz, A., Zhang, X., Düfer, M., Drews, G., Krippeit-Drews, P., Aguilar-Bryan, L., 2007. ABCC8 and ABCC9: ABC transporters that regulate K+ Channels. Eur. J. Physiol. 453, 703–718.

Chawla, J.S., Amiji, M.M., 2002. Biodegradable poly (epsilon-caprolactone) nanoparticles for tumor-targeted delivery of tamoxifen. Int. J. Pharm. 249, 127–138.

Chee, M., Yang, R., Hubbell, E., Berno, A., Huang, X.C., Stern, D., Winkler, J., Lockhart, D.J., Morris, M.S., Fodor, S.P., 1996. Accessing genetic information with high-density DNA arrays. Sci. 274, 610-614.

Chen, J., Zhu, Y., Hu, M., 1994. Mechanisms and kinetics of uptake and efflux of L-methionine in an intestinal epithelial model (Caco-2). J. Nutr. 124, 1907–1916.

Chen, Y., E. Dougherty., Bittner, M., 1997. Ratio-based decisions and the quantitative analysis of cDNA micro-array images. J. Biomed. Optics. 2, 364.

Chen, Z., Lee, K., Walther, S., Raftogianis, R.B., Kuwano, M., Zeng, H., Kruh, G. D., 2002. Analysis of Methotrexate and Folate Transport by Multidrug Resistance Protein 4 (ABCC4): MRP4 Is a Component of the Methotrexate Efflux System1. Cancer Res. 62, 3144–3150.

Chieng, N., Rades, T., Saville, D., 2008. Formation and physical stability of the amorphous phase of ranitidine hydrochloride polymorphs prepared by cryo-milling. Eur. J. Pharm. Biopharm. 68, 771–780.

Chiou, W. L., Reigelman, S., 1971. Pharmaceutical applications of solid dispersion systems. J. Pharm. Sci. 60, 1281-1302.

Chiou, W.L., and Riegelman, S., 1969. Preparation and dissolution characteristics of several fast-release solid dispersions of griseofulvin. J. Pharm. Sci. 58, 1505–1510.

Chiu, Y.Y., Higaki, K., Neudeck, B.L., Barnett, J.L., Welage, L.S., Amidon, G.L., 2003. Human jejunal permeability of cyclosporin A: influence of surfactants on P-glycoprotein efflux in Caco-2 cells. Pharm. Res. 20, 749–756.

Cho, C.W., Liu, Y., Yan, X., Henthorn, T., Ng, K.U., 2000. Carrier-Mediated Uptake of Rhodamine 123: Implications on Its Use for MDR. Res. Biochem. Biophys. Res. Com. 279, 124–130.

Choi, J.S., Jo, B.W., 2004. Enhanced paclitaxel bioavailability after oral administration of pegylated paclitaxel prodrug for oral delivery in rats. Int. J. Pharm. 280, 221–227.

Chong, S., Dando, S.A., Soucek, K.M., Morrison, R.A., 1996. In vitro permeability through Caco-2 cells is not quantitatively predictive of in vitro absorption for peptide-like drugs absorbed via the dipeptide transporter system. Pharm. Res. 13, 120–123.

Christensen, F. N., Davis, S. S., Hardy, J. G., Taylor, M. J., Whalley, D. R., Wilson, C. G., 1985. The use of gamma scintigraphy to follow the gastrointestinal transit of pharmaceutical formulations. J. Pharm. Pharmaco. 37(2), 91-95.

Claverie, J., 1999. Computational methods for the identification of differential and coordinated gene expression. Hum. Mol. Genet. 8, 1821-1832.

Cole, S.P.C., Sparks, K.E., Fraser, K., Loe, D.W., Grant, C.E., Wilson, G.M., Deeley, R.G., 1994. Pharmacological characterization of multidrug resistant MRP-transfected human tumor cells. Cancer Res. 54, 5902–5910.

Collett, A., Tanianis-Hughes, J., Carlson, G.L., Harwood, M.D., Warhurst, G., 2005. Comparison of P-glycoprotein-mediated drug-digoxin interactions in Caco-2 with human and rodent intestine: Relevance to in vivo prediction. Eur. J. Pharm. Sci. 26, 386-393.

Collnot, E.M., Baldes, C., Wempe, M.F., Hyatt, J., Navarro, L., Edgar, K.J., Schaefer, U.F., Lehr, C.M., 2006. Influence of vitamin E TPGS poly (ethylene glycol) chain length on apical efflux transporters in Caco-2 cell monolayers. J. Contl. Rel. 111, 35–40.

Cordon-Cardo, C., O'Brien, J.P., Boccia, J., Casals, D., Bertino, J.R., Melamed, M.R., 1990. Expression of the multidrug resistance gene product (P-glycoprotein) in human normal and tumor tissues. J. Histochem. Cytochem. 138, 1277–1287.

Cornaire, G., Woodley, J., Hermann, P., Cloarec, A., Arellano, C., Houin, G., 2004. Impact of excipients on the absorption of P-glycoprotein substrates in vitro and in vivo. Int. J. Pharm. 278, 119–131.

Corrigan, O.I., 1985. Mechanisms of dissolution of fast release solid dispersions. Drug Dev. Ind. Pharm.11, 697-724.

Corrigan, O.I., 1986. Retardation of polymeric carrier dissolution by dispersed drugs: factors influencing the dissolution of solid dispersions containing polyethylene glycol. Drug Dev. Ind. Pharm. 12, 1777-1793.

Craig, D.Q.M, Newton, J.M., 1992. The dissolution of nortryptiline HCl from polyethylene glycol solid dispersions. Int. J. Pharm. 78, 175–182.

Craig, D.Q.M., 1990. Polyethylene glycols and drug release. Drug Dev. Ind. Pharm. 16, 2501-2527.

Craig, D.Q.M., 2002. The mechanisms of drug release from solid dispersions in water soluble polymers. Int. J. Pharm. 231, 131-144.

Craig, D.Q.M., Newton, J.M., 1991. Characterisation of polyethylene glycols using differential scanning calorimetry. Int. J. Pharm. 74, 33–41.

Craig, D.Q.M., Royall, P.G., Kett, V.L., Hopton, M.L., 1999. The relevance of the amorphous state to pharmaceutical dosage forms: glassy drugs and freeze dried systems. Int. J. Pharm. 179, 179–207.

Curtis, H., Barnes, S., 1994.Invitation to Biology. New York; Worth., 5th Edition, 529.

Damian, F., Blaton, N., Naesens, L., Balzarini, J., Kinget, R., Augustijns, P., Van den Mooter, G., 2000. Physicochemical characterization of solid dispersions of the antiviral agent UC-781 with polyethylene glycol 6000 and Gelucire 44/14. Eur. J. Pharm. Sci. 10, 311-322.

Dantzig, A.H., Bergin, L., 1990. Uptake of the cephalosporin, cephalexin, by a dipeptide transport carrier in the human intestinal cell line, Caco-2. Biochem. Biophys. Acta. 1027, 211–217.

Davis, S. S., Hardy, J. G., Fara, J. W., 1986. Transit of pharmaceutical dosage forms through the small intestine. Gut. 27, 886-92.

Davis, S. S., Norring-Christensen, F., Khosla, R., Feely, L. C., 1988. Gastric emptying of large single unit dosage forms. J. Pharm. Pharmaco. 40, 205-207.

Dean,M., Hamon,Y., Chimini,G., 2001. The human ATP-binding cassette (ABC) transporter superfamily, Journal of Lipid Research Volume 42, 1007-1017.

Den, V.M.G., Augustijns, P., Blaton, N., Kinget, R., 1998. Physicochemical characterization of solid dispersions of temazepam with polyethylene glycol 6000 and PVP K30. Int. J. Pharm. 164, 67-80.

DeRisi, J., Penland, L., Brown, P.O., Bittner, M.L., Meltzer, P.S., Ray, M., Chen, Y., Su, Y.A., Trent, J.M., 1996. Use of a cDNA microarray to analyse gene expression patterns in human cancer. Nat. Genet.14, 457–460.

DeRisi. J., Vishwanath, R.L., Brown, P.O., 1997. Exploring the metabolic and genetic control of gene expression on a genomic scale. Sci. 278, 680–6.

Dordunoo, S. K., Ford, J. L., Rubinstein, M. H., 1997. Physical stability of solid dispersions containing triamterene or temazepam in polyethylene glycols. J. Pharm. Pharmaco. 59, 390-396.

Dordunoo, S.K., Ford, J.L., Rubinstein, M.H., 1991. Preformulation studies on solid dispersions containing triamterene or temazepam in polyethylene glycols or Gelucire 44/14 for liquid filling of hard gelatin capsules. Drug Dev. Ind. Pharm. 17, 685-1713.

Draper, M.P., Martell, R.L., Levy, S.B., 1997. Indomethacin-mediated reversal of multidrug resistance and drug efflux in human and murine cell lines overexpressing MRP, but not P-glycoprotein. Br. J. Cancer. 75(6), 810–815.

Dressman, J., Berardi, R., Dermentzoglou, L., Russel, T., Schmaltz, S., Barnett, J., Jarvenpaa, K., 1990. Upper gastrointestinal pH in young, healthy men and women. Pharm. Res. 7, 756–761.

Dubois, J., Ford, J.L., 1985. Similarities in the release rates of different drugs from polyethylene glycol 6000 solid dispersions. J. Pharm. Pharmaco. 37, 494-496.

Eisen, M.B., Spellman, P.T., Brown, P.O., 1998 Cluster Analysis and Display of Genome-Wide Expression Patterns. Proc. Natl. Acad. Sci. USA, 95, 14863-14868.

El-Zein, H., Riad, L., Elbary, A.A., 1998. Enhancement of carbamazepine dissolution -in vitro and in vivo evaluation. Int. J. Pharm. 168, 209-220.

Esnaashari, S., Javadzadeh, Y., Hannah, K., Batchelor and Barbara., Conway, R., 2005. The use of microviscometry to study polymer dissolution from solid dispersion drug delivery systems. Int. J. Pharm. 292(1-2), 227-230.

Etman, M.A., Nada, A.H., 1999. Hydrotropic and cosolvent solubilisation of indomethacin. Acta. Pharm. 49, 291–298.

Evans, D. F., Pye, G., Bramley, R., Clark, A. G., Dyson, T. G., Hardcastle, J. D., 1988. Measurement of gastrointestinal pH profiles in normal ambulant human subjects. Gut. 29, 1035-1041.

Evans, G.S., Flint, N., Potten, C.S., 1994. Primary cultures for studies of cell regulation and physiology in intestinal epithelium. Annu. Rev. Physiol. 56, 399-417.

Fagerholm, U., Lennernäs, H., 1995. Experimental estimation of the effective unstirred water layer thickness in the human jejunum, and its importance in oral drug absorption. Eur. J. Pharm. Sci. 3(5), 247-253.

Fawaz, F., Bonini, F., Guyot, M., Bildet, J., Maury, M., Lagueny, A.M., 1996. Bioavailability of norfoxacin from PEG 6000 solid dispersion and cyclodextrin inclusion complexes in rabbits. Int. J. Pharm. 132, 271-275.

FDA., 1998. Draft Guidance for Industry: Stability Testing of Drug Substances and Drug Products, FDA, Rockville, MD.

FDA., 1998. Guidance for Industry: Impurities in Drug Product, Draft guidance, Center for Drug Evaluation and Research (CDER).

Fernandez, M., Margarit, M.V., Rodriguez, I.C., Cerezo, A., 1993. Dissolution kinetics of piroxicam in solid dispersions with polyethylene glycol-4000. Int. J. Pharm. 98, 29-35.

Ferrer-Dufol, A., Menao-Guillen, S., 2009. Toxicogenomics and clinical toxicology: An example of the connection between basic and applied sciences Toxicology Letters. Toxicogen. Clin. Toxico. 186(1), 2-8

Finia, A., Moyano, J.R., Gines, J.M., Perez-Martinez, J.I., Rabasco, A.M., 2005. Diclofenac salts, II. Solid dispersions in PEG6000 and Gelucire 50/13. Eur. J. Pharm. Biopharm. 60, 99–111.

FIP, 2008. Federation International Pharmaceutical. http://www.fip.org/www2/, accessed August 2008.

Florence, A.T. and Attwood, D., 1988. Physicochemical principles in pharmacy. Basingstoke UK. Macmillan. Press. 115-130.

Fogh, J., Fogh, J.M., Orfeo, T., 1977. One hundred and twenty seven cultured human tumor cell lines producing tumors in nude mice. J. Natl. Cancer. Inst. 59, 221-226.

Fojo, A.T., Ueda, K., Slamon, D.J., Poplack, D.G., Gottesman, M.M., Pastan, I., 1987. Expression of a multidrug-resistance gene in human tumors and tissues. Proc. Natl. Acad. Sci. USA. 84, 265–269.

Folgueira, M.A., Carraro, D.M., Brentani, H., Patrao, D.F., Barbosa, E.M., Netto, M.M., et al., 2005. Gene expression profile associated with response to doxorubicin-based therapy in breast cancer. Clin. Cancer. Res. 11, 7434–43.

Ford, J. L., Rubinstein, M. H., 1980. Formulation and aging of tablets prepared from indomethacin-polyethylene glycol 6000 solid dispersions. Pharm. Acta Helv. 55, 1-7.

Ford, J.L., Stewart, A.F., Dubois, J.L., 1986. The properties of solid dispersions of indomethacin or phenylbutazone in polyethylene glycol. Int. J. Pharm. 28, 11-22.

Ford, J.L., 1986. The current status of solid dispersions. Pharm. Acta Helv. 61, 69-88.

Ford, J.L., Rubinstein, M.H., 1978. Phase equilibria and dissolution rate of indomethacin-polyethylene glycol 6000 solid dispersions. Pharm. Acta. helv. 53, 327-332.

Fracchia, M., Pellegrino, S., Secreto, P., Gallo, L., Masoero, G., Pera, A., Galatola, G., 2001. Biliary lipid composition in cholesterol microlithiasis. Gut. 48, 702–706.

Frances, C., Veiga, M.D., Espafiol, O.M., Cadorniga, R., 1991. Preparation, characterisation and dissolution of ciprofloxacin/PEG 6000 binary systems. Int. J. Pharm. 77, 193-198.

Franco, M., Trapani, G., Latrofa, A., Tullio, C., Provenzano, M. R., Serra, M., Muggironi, M., Biggio, G., Liso, G., 2001. Dissolution properties and anticonvulsant activity of phenytoin-polyethylene glycol 600 and -polyvinylpyrrolidone K-30 solid dispersions. Int. J. Pharm. 225, 63-73.

Frank, N.Y., Margaryan, A., Huang, Y., Schatton, T., Waaga-Gasser, A.M., Gasser, M, et al., 2005. ABCB5-mediated doxorubicin transport and chemoresistance in human malignant melanoma, Cancer. Res. 65(10), 4320–4333.

Friedrich, H., Fussnegger Kolter, B.K., Bodmeier, R., 2006. Dissolution rate improvement of poorly water soluble drugs obtained by absorbing solutions of drugs in hydrophilic solvents onto high surface area carriers. Eur. J. Pharm. Biopharm. 62, 171–176.

Fukuoka, E., Makita, M., Yamamura, S., 1986. Some physicochemical properties of glassy indomethacin. Chem. Pharm. Bull. 34, 4314-4321.

Gan, L-S.L., Moseley, M.A., Khosla, B., Augustijns, P.F., Bradshaw, T.P., Hendren, R.W., Thakker, D.R., 1996. CYP3A-Like cytochrome P450-mediated metabolism and polarized efflux of cyclosporin A in Caco-2 cells: interaction between the two biochemical barriers to intestinal transport. Drug. Metab. Dispos. 24, 344–349.

Getz, G., Levine. E., Domany. E., 2000. Coupled two-way clustering analysis of gene microarray data. Proc. Natl. Acad. Sci. 97, 12079–12084.

Gines, J.M., Arias, M.J., Moyano, J.R., Sanchezsoto, P.J., 1996. Thermal investigation of crystallization of polyethylene glycols in solid dispersions containing oxazepam. Int. J. Pharm. 143, 247-253.

Goldberg, A. H., Gibaldi, M., Kanig, J. L., 1965. Increasing dissolution rates and gastrointestinal absorption of drugs via solid solutions and eutectic mixtures I- theoretical considerations and discussions of the literature. J. Pharm . Sci. 54, 1145-1148.

Goldberg, A. H., Gibaldi, M., Kanig, J. L., 1966a. Increasing dissolution rates and gastrointestinal absorption of drugs via solid solutions and eutectic mixtures II. Experimental evaluation of a eutectic mixture: Urea-Acetaminophen system. J. Pharm. Sci. 55, 482-487.

Goldberg, A. H., Gibaldi, M., Kanig, J. L., Mayersohn, M., 1966b. Increasing dissolution rates and gastrointestinal absorption of drugs via solid solutions and eutectic mixtures. IV. Chloramphenicol-Urea system. J. Pharm. Sci. 55, 581-3.

Grudzien, M., Krol, A., Paterek, G., Stępien, K., Plucinski, F., Mazurek, A, P., 2009. The structure–bioavailability approach in antifungal agents. Eur. J. Med. Chem. 44(5), 1978-1981.

Guidance for Industry. Waiver of In vivo Bioavailability and Bioequivalence studies for immediate-release solid oral dosage forms based on a Biopharmaceutics Classification system, 2000. US Depart-ment of Health and Human Services, Food and Drug Administration, Center for Drug Evaluation and Research (CDER).

Gupta, M. K., Tseng, Y. C., Goldman, D., Bogner, R. H., 2002. Hydrogen bonding with adsorbent during storage governs drug dissolution from solid-dispersion granules. Pharm. Res. 19, 1663-1672.

Guyot, M., Fawaz, F., Bildet, J., Bonini, F., Lagueny, A.M., 1995. Physicochemical characterization and dissolution of norfloxacin:cyclodextrin inclusion compounds and PEG solid dispersions. Int. J. Pharm. 123, 53–63.

Hahn, M. K., Robertson, D., Blakely,R. D., 2003. A Mutation in the Human Norepinephrine Transporter Gene (SLC6A2) Associated with Orthostatic Intolerance Disrupts Surface Expression of Mutant and Wild-Type Transporters. J. Neurosci. 23(11), 4470–4478.

Halestrap, A. P., David Meredith, D., 2004. The SLC16 gene family—from monocarboxylate transporters (MCTs) to aromatic amino acid transporters and beyond. Eur. J. Physiol. 447, 619–628.

Hancock, B.C., Parks, M., 2000. What is the true solubility advantage for amorphous pharmaceuticals? Pharm. Res. 74, 397–404.

Haq, I., Jenkins, T.C., Chowdhry, B.Z., Ren, J., Chaires, J.B., 2000. Parsing free energies of drug-DNA interactions. Methods. Enzymol. 323, 373-405.

Hasegawa, S. et al., 2005. Effects of water content in physical mixture and heating temperature on crystallinity of troglitazone-PVP K30 solid dispersions prepared by closed melting method. Int. J. Pharm. 302, 103–112.

Helder, A., Santos, Jose, A., Manzanares, Murtomaki, L., Kontturi, K., 2007. Thermodynamic analysis of binding between drugs and glycosaminoglycans by isothermal titration calorimetry and fluorescence spectroscopy Eur. J. Pharm. Sci. 32, 105–114.

Heller, R.A., Schena, M., Chai, A., Shalon. D., Bedilion, T., Gilmore, J., Woolley, D.E., Davis, R.W., 1997. Discovery and analysis of inflammatory disease-related genes using cDNA microarray. Proc. Natl. Acad. Sci. USA. 94, 2150–2155.

Hidalgo, I.J., Borchardt, R.T., 1990. Transport of a large neutral amino acid(phenylalanine) in a human intestinal epithelial cell line: Caco-2. Biochem. Biophys. Acta. 1028, 25–30.

Hidalgo, I.J., Raub, T.J., Borchardt, R.T., 1989. Characterization of the human colon carcinoma cell line (Caco-2) as a model system for intestinal epithelial permeability. Gastroenterology. 96, 736-749.

Higgins, C. F., 1992. ABC transporters: from microorganisms to man. Annu. Rev. Cell Bio. 8, 67-113.

Higuchi, T., Ikeda, M., 1974. Rapidly dissolving forms of digoxin-hydroquinone Complex. J. Pharm. Sci. 63, 809-811.

Higuchi, W. I., Mir, N. A., Desai, D. J., 1965. Dissolution rate of polyphase mixtures. J. Pharm. Sci. 54, 1405-1410.

Higuchi, W.I., 1967. Diffusional models useful in biophamaceutics. J. Pharm. Sci. 56, 315-324.

Hilgers, A.R., Conradi, R.A., Burton, P.S., 1990. Caco-2 cell monolayers as a model for drug transport across the intestinal mucosa. Pharm. Res. 7, 902–910.

Hilton, J. E., Summers, M. P., 1986. The effect of wetting agent on the dissolution of indomethacin solid dispersion systems. Int. J. Pharm. 31, 157-164.

Hirasawa, N., Ishise, S., Miyata, H., Danjo, K., 2003. Physicochemical characterization and drug release studies of nilvadipine solid dispersions using water-insoluble polymer as a carrier. Drug Dev. Ind. Pharm. 29, 339–344.

Hirohashi, T., Suzuki, H., Sugiyama, Y., 1999. Characterization of the Transport Properties of Cloned Rat Multidrug Resistance-associated Protein 3 (MRP3). J. Biol. Chem. 274, 15181–15185.

Hirokazu, T., Richer, C., Hirokazu, O., Kazumi, D., 2005. Acetaminophen Particle Design Using Chitosan and a Spray-Drying Technique. Chem. Pharm. Bull. 53(1), 37-41.

Hoa, P.Y., Yeha, T.K., Yaoa, H.T., Lina, H.L., Wua, H.Y., Loa, Y.K., Changa,Y.W., Chianga, T.H., Wub, S.H.W., Chaoa, Y.S., Chen, C.T., 2008. Enhanced oral bioavailability of paclitaxel by d-_-tocopheryl polyethylene glycol 400 succinate in mice. Int. J. Pharm. 359, 174–181.

Hopper-Borge, E., Chen, Z. S., Shchaveleva,I., Belinsky, M, G., Kruh,G.D.,2004. Analysis of the Drug Resistance Profile of Multidrug Resistance Protein 7 (ABCC10): Resistance to Docetaxel. Cancer Res. 64, 4927–4930.

Horter, D., Dressman, J.B., 2001. Influence of physicochemical properties on dissolution of drugs in the gastrointestinal tract. Adv. Drug Dev. Rev. 56, 75–87.

Huang, Y., 2007. Pharmacogenetics/genomics of membrane transporters in cancer chemotherapy. Cancer Metastasis Rev. 26, 183-201.

Hugger, E, D., Audus, K. L., Borchardt, R.T., 2002. Effects of poly (ethylene glycol) on efflux transporter activity in Caco-2 cell monolayers, J. Pharm. Sci**.** 91**,** 1980–1990.

Hughes, T.R., Shoemaker, D.D., 2001. DNA microarrays for expression profiling. Curr. Opin. Chem. Biol. 5, 21-25.

Hunter, J., Hirst, B.H., 1997. Intestinal secretion of drugs. The role of P-glycoprotein and related drug efflux systems in limiting oral drug absorption. Adv. Drug Deliv. Rev. 5, 129–157

ICH., 2003.Q1A (R2) Stability Testing of New Drug Substances and Products.1.1, 16-31

Inui, K., Miyamoto, M., Saito, H., 1992. Transepithelial transport of oral cephalosporins by monolayers of intestinal epithelial cell line Caco-2; Specific transport systems in apical and basolateral membranes. J. Pharmaco. Exp. Ther. 261, 195-201.

Iwai, N., Mino, Y., Hosoyamada, M., Tago, N., Kokubo,Y., Endou, H., 2004. A high prevalence of renal hypouricemia caused by inactive SLC22A12 in Japanese. Kidney Int. 66, 935–944.

Izutsu, K., Yoshioka, S., Terao, T., 1994. Effect of mannitol crystallinity on the stabilization of enzymes during freeze-drying. Chem. Pharm. Bull. 42, 5–8.

Jachowicz, R., 1987. Dissolution rates of partially water-soluble drugs from solid dispersion systems. II. Phenytoin. Int. J. Pharm. 35, 7- 12.

Jachowicz, R., Nurnberg, E., Hoppe, R., 1993. Solid dispersions of oxazepam. Int. J. Pharm. 99, 321-325.

Jacquemin, E., De Vree, M., Cresteil, D., Sokal, E., Sturm, E., Dumont, M., Scheffer, G., Paul, M., Burdelski, M., Bosma, P., Bernard, O., Hadchouel, M., Oude Elferink, R., 2001. The wide spectrum of multidrug resistance 3 deficiency: from neonatal cholestasis to cirrhosis of adulthood. Gastroenterology. 120, 1448–1458.

Jansen, M.P., Foekens, J.A., van Staveren, I.L., Dirkzwager-Kiel, M.M., Ritstier, K., Look, M.P., et al., 2005. Molecular classification of tamoxifenresistant breast carcinomas by gene expression profiling. J. Clin. Oncol. 23, 732–40.

Johnson, B.M., Charman, W.N., Porter, C.J., 2002. An in vitro examination of the impact of polyethylene glycol 400, Pluronic P85, and vitamin E d-alpha-tocopheryl polyethylene glycol 1000 succinate on P-glycoprotein efflux and enterocyte-based metabolism in excised rat intestine. AAPS. Pharm. Sci. 4, 40.

Johnson, L. V., Walsh, M. L., Bockus, B. J. Chen, L. B., 1981. Monitoring of relative mitochondrial membrane potential in living cells by fluorescene microscopy. J. Cell. Biol. 88, 526-535.

Johnson, L.V., Walsh, M.L., Chen, L.B., 1980. Localization of mitochondria in living cells with rhodamine 123. Proc. Natl. Acad. Sci. USA. 77, 339-401.

Juliano, R. L., Ling, V., 1976. A surface glycoprotein modulating drug permeability in Chinese hamster ovary cell mutants. Biochim. Biophys. Acta. 455,152–162.

Jung, S.J., Choi, S.O., Uma, S.Y., Kima, J., Park Choob,H.Y., Choi, S.Y., Chung, S.Y., 2006. Prediction of the permeability of drugs through study on quantitative structure–permeability relationship. J. Pharm. Bio. Anal. 41, 469–475.

Kabasakalian, P., Katz, M., Rosenkrantz, B., Townley, E., 1970. Parameters affecting absorption of griseofulvin in a human subject using urinary metabolite excretion. Data. J. Pharm. Sci. 59, 595-600.

Kaminski, W. E., Piehler, A., Pullmann, K., Porsch-Ozcurumez, M., Duong, C., Bared, G. M., Buchler, C., Schmitz, G., 2001. Complete coding sequence, promoter region, and genomic structure of the human ABCA2 gene and evidence for sterol-dependent regulation in macrophages. Biochem. Biophys. Res. Commun., *281*, 249 –258.

Kanig, J.L., 1964. Properties of fused mannitol in compressed tablets. J. Pharm. Sci. 53, 188–192.

Kassem, A.A., Zaki, S.A., Mursi, N.M., Tayel, S.A., 1979. Chloramphenicol solid dispersion system. I. Pharm. Ind. 41, 390-393.

Kedinger, M., Haffen, K., Simon-Assmann, P., 1987. Intestinal tissue and cell culture. Differentiation. 36(1), 71-85.

Khalafallah, N., Gouda, M.W., Khahl, S.A., 1975. Effect of surfactants on absorption through membranes: IV. Effects of dioctylsulfosuccinate on absorption of a poorly absorbable drug in human. J. Pharm. Sci. 64, 991–994.

Khan, G.M., Zhu, J.B., 1998. Preparation, characterization, and dissolution studies of ibuprofen solid dispersions using polyethylene glycol (peg), talc, and peg-talc as dispersion carriers. Drug Dev. Ind. Pharm. 24, 455-462.

Khan, N., Craig, D.Q.M., 2003. The influence of drug incorporation on the structure and release properties of solid dispersions in lipid matrices. J. Contl. Rel. 93, 355–368.

Khan, S.I., Abourashed, E.A., Khan, I.A., Walker, L.A., 2003. Transport of parthenolide across human intestinal cells (Caco-2). Planta. Med. 69, 1009–1012.

Khan, S.I., Abourashed, E.A., Khan, I.A., Walker, L.A., 2004. Transport of harman alkaloids across Caco-2 cell monolayers. Chem. Pharm. Bull. 52, 394–397.

Konishi, Y., Hagiwara, K., Shimizu, M., 2002. Transepithelial transport of fluorescein in Caco-2 cell monolayers and use of such transport in *in vitro* evaluation of phenolic acid availability. Biosci. Biotech. Biochem. 66, 2449-2457.

Kool, M., de Haas, M., Scheffer, G. L., Scheper, R. J., van Eijk, M. J., Juijn, J. A., Baas, F., and Borst, P., 1997. Cancer Res. 57, 3537–3547.

Korsmeyer, R.W., Buri, P., Doelker, E., Gurney, R., Peppas, N.A., 1983. Mechanism of release from porous hydrophilic polymers. Int. J. Pharm. 15, 25–35.

Kramer, W.G., Rensimer, E.R., Ericsson, C.D., Pickering, L.K., 1984. Comparative bioavailability of intravenous and oral chloramphenicol in adults. J. Clin. Pharmacol. 24, 181–186.

Krasowska, H., 1980. Effect of micellar solubilization on the gastrointestinal absorption of indomethacin in the rate. Int. J. Pharm. 7, 137–143.

Ku.M., 2008. Use of the Biopharmaceutical Classification System in early drug development. AAPS J. 10, 208–212.

Laitinen, L., Takala, E., Vuorela, H., Vuorela, P., Kaukonen, A.M., Marvola, M., 2007. Anthranoid laxatives influence the absorption of poorly permeable drugs in human intestinal cell culture model (Caco-2). Eur. J. Pharm. Biopharm. 66(1), 135-145.

Leavitt, S., Freire, E., 2001. Direct measurement of protein binding energetics by isothermal titration calorimetry. Curr. Opin. Struct. Biol. 11(5), 560-566.

Lennernas, H., Abrahamsson, B., 2005. The use of biopharmaceutic classification of drugs in drug discovery and development: current status and future extension. J. Pharm. Pharmaco. 57, 273–285.

Lettieri, T., 2006. Recent applications of DNA microarray technology to toxicology and ecotoxicology. Environ. Health. Perspect.114 (1), 4-9.

Lennernas, H., Palm, K., Fagerholm, U., Artursson, P., 1996. Comparison between active and passive drug transport in human intestinal epithelial (Caco-2) cells in vitro and human jejunum in vivo. Int. J. Pharm. 127, 103–107.

Leslie, E. M., Deeley, R.G., Cole S.P.C., 2001. Toxicological relevance of the multidrug resistance protein 1, MRP1 (ABCC1) and related transporters. Toxicology. 167, 3–23.

Leuner, C., Dressman, J., 2000. Improving drug solubility for oral delivery using solid dispersions. Eur. J. Pharm. Biopharm. 50, 47-60.

Levy, G., 1963. Effect of particle size on dissolution and gastrointestinal absorption rates of pharmaceuticals. Amer. J. Pharm. Sci. Support Public Health. 135, 78–92.

Lheritier, J., Chauvet, A., Abramovici, B., Masse, J., 1995. Improvement of the dissolution kinetics of SR 33557 by means of solid dispersions containing PEG 6000. Int. J. Pharm. 123, 273-279.

Liang, H.F., Yang, T.F., Huang, C.T., Chen, M.C., Sung, H.W., 2005. Preparation of nanoparticles composed of poly(g-glutamic acid)-poly(lactide) block copolymers and evaluation of their uptake by HepG2 cells. J. Contl. Rel. 105, 213–225

Lin, C.W., Cham, T.M., 1996. Effect of particle size on the available surface area of nifedipine from nifedipine-polyethylene glycol 6000 solid dispersions. Int. J. Pharm. 127, 261-272.

Lin, J.H., Yamazaki, M., 2003. Role of p-glycoprotein in pharmacokinetics: clinical implications. Clin Pharmacokinet. 42, 59-98.

Lipinski, C.A., Lombardo, F., Dominy, B.W., Feeney, P.J., 2001. Experimental and computational approaches to estimate solubility and permeability in drug discovery and development settings.Adv. Drug Dev. Rev. 46, 3–26.

Lloyd, G.R. et al., 1999. A calorimetric investigation into the interaction between paracetamol and polyethlene glycol 4000 in physical mixes and solid dispersions. Eur. J. Pharm. Biopharm. 48, 59–65.

Lobenberg, R., Amidon, G.L., 2000. Modern bioavailability, bioequivalence and biopharmaceutics classification system; new scientific approaches to international regulatory standards. Eur. J. Pharm. Biopharm. 50, 3–12.

Lown, K.S., Mayo, R.R., Leichtman, A.B., Hsiao, H.L., Turgeon, D.K., Schmiedlin-Ren, P., Brown, M.B., Guo, W., Rossi, S.J., Benet, L.Z., Watkins, P.B., 1997. Role of intestinal P-glycoprotein (mdr1) in interpatient variation in the oral bioavailability of cyclosporine. Clin. Pharmaco. Ther. 62, 248–260.

Maillols, H., Acquier, R., Laget, J. P., Keita, A. A., Delonca, H., 1982. Characterizing the particle size analysis of a powder: Influence on the dissolution kinetics. J. Pharm. Belg. 37, 241-248.

Majerik, V. et al., 2007. Bioavailability enhancement of an active substance by supercritical antisolvent precipitation. J. Supercrit. Fluids. 40, 101–110.

Manov, I., Bashenko, Y., Hirsh, M., Iancu, T.C., 2006. Involvement of the Multidrug Resistance P-Glycoprotein in Acetaminophen-Induced Toxicity in Hepatoma-Derived HepG2 and Hep3B Cells. Basic. Clin. Pharmaco. Toxicol. 99(3), 213-24.

Mantsch, H.H., Chapman, D., 1996. Infrared spectroscopy of biomolecules. Wiley-Liss, New York.

Margarit, M.V., Rodriguez, I.C., Cerezo, A., 1994. Physical characteristics and dissolution kinetics of solid dispersions of ketoprofen and polyethylene glycol 6000. Int. J. Pharm. 108, 101-107.

Marton, M.J., 1998. Drug target validation and identification of secondary drug target effects using DNA microarrays. Nature. Med. 4, 1293–1301.

Masashi, T., Yoshikazu, E., Yuichiro, K, Masao, S., 2008. Human ABC transporter isoform B6 (ABCB6) localizes primarily in the Golgi apparatus. Biochem. Biophys. Res. Commun. 369, 369–375.

Miller-Chou, B.A., Koenig, J.L., 2003. A review of polymer dissolution. Prog. Polym. Sci. 28, 1223–1270.

Molday, R.S., 2007. ATP-binding cassette transporter ABCA4: molecular properties and role in vision and macular degeneration. J. Bioenerg. Biomembr. 39, 507–517.

Mount, D. B., Mercado, A., Song, L., Xu, J., George, A, L., Delpire, J, E., Gamba, G., 1999. Cloning and Characterization of KCC3 and KCC4, New Members of the Cation-Chloride Cotransporter. Gene Family.274, (23), 16355–16362.

Mura, P., Faucci, M.T., Manderioli, A., Bramanti, G., Parrini, P., 1999. Thermal behavior and dissolution properties of naproxen from binary and ternary solid dispersions. Drug Dev. Ind. Pharm. 25, 257-264.

Nagase, T., Ishikawa, K., Suyama, M., Kikuno R., Hirosawa, M., Miyajima, N., Tanaka, A., Kotani, H., Nomura, N., Ohara, O., 1998. Prediction of the coding sequences of unidentified human genes. XII. The complete sequences of 100 new cDNA clones from brain which code for large proteins in vitro. DNA Res. 5, 355–364.

Nernst, W., 1904. Theorie der reaktionsgeschwindigkeit in heterogenen systemen. zeitschrift für physikalische chemie. 47, 52-55.

Neuhoff, S., Ungell, A.L., Zamora, I., Arturrson, P., 2005. pH-dependent passive and active transport of acidic drugs across Caco-2 cell monolayers. Eur. J. Pharm. Sci. 25, 211–220.

Noyes, A. A., Whitney, W. R., 1897. The rate of solution of solid substances in their own solution. J. Amer. Chem. Society. 19, 930-934.

Okonogi, S., Yonemochi, E., Oguchi, T., Puttipipatkhachorn, S., Yamamoto, K., 1997. Enhanced dissolution of ursodeoxycholic acid from the solid dispersion. Drug Dev. Ind. Pharm. 23, 1-7.

Paraira, M., Llovet, X., Sufio, J.M., 1994. Granulometric characterization and study of ibuprofen lysinate by means of an image processor. Drug Dev. Ind. Pharm. 20, 259-278.

Paterson, J. K., Shukla, S., Black, C.M., Tachiwada, T., Garfield, S., Wincovitch, S., Ernst, D.N., Agadir, A., Li, X., Ambudkar, S.V., Szakacs, G., Akiyama, S., Gottesman, M.M., 2007. Human ABCB6 localizes to both the outer mitochondrial membrane and the plasma membrane. Biochemistry. 46(33), 9443-52.

Peppas, N.A., 1985. Analysis of Fickian and non-Fickian drug release from polymers, Pharm. Acta Helv. 60 (4), 110–111.

Perng, C.Y., Kearney, A.S., Patel, K., Palepu, N.R., Zuber, G., 1998. Investigation of formulation approaches to improve the dissolution of SB-210661, a poorly water soluble 5-lipoxygenase inhibitor. Int. J. Pharm. 176, 31-38.

Perou, C.M., Sorlie, T., Eisen, M.B., van de Rijn, M., Jeffery, S.S., Rees, C.A., Pollack, J.R., Ross, D.T., Johnsen, H., Akslen, L.A., et al., 2000. Molecular portraits of human breast tumours. Nature. 406, 747-752.

Pietu, G., Alibert, O., Guichard, V., Lamy, B., Bois, F., Leroy, E., Mariage-Samson, R., Houlgatte. R., Soularue, P., Auffray, C., 1996. Novel gene transcripts preferentially expressed in human muscles revealed by quantitative hybridization of a high-density cDNA array. Genome. Res. 6, 492–503.

Pijpers, F.J., Mathot, V.B.F., Goderis, B., Scherrenberg, R.L., van der Vegte, E.W., 2002. High-speed calorimetry for the study of the kinetics of (de)vitrification, crystallisation, and melting of macromolecules. Macromolecules. 35(9)**,** 3601–3613.

Pinto, M., Robine-Leon, S., Appay, M.-D., Kedinger, M., Triadou, N., Dussaulx, E., Lacroix, B., Simon-Assmann, P., Haffen, K., Fogh, J., Zweibaum, A., 1983. Enterocyte-like differentiation and polarization of the human colon carcinoma cell line Caco-2 in culture. Bio. Cell. 47, 323-330.

Pitha, J. and Pitha, J., 1985. Amorphous water soluble derivatives of cyclodextrins: nontoxic dissolution enhancing excipients. J. Pharm. Sci. 74, 987-990.

Prabhu, S., Ortega, M., Ma, C., 2005. Novel lipid-based formulations enhancing the in vitro dissolution and permeability characteristics of a poorly water-soluble model drug, piroxicam. Int. J. Pharm. 301(1-2), 209-216.

Price, J.C., 1994, Polyethylene glycol, in: A. Wade, P.J. Weller (Eds.), Handbook of Pharmaceutical Excipients, American Pharmaceutical Association/The Pharmaceutical Press, Washington, DC/London. 355-361.

Ramadan. M. A, Tawashi. R., 1990. Effect of surface geometry and morphic feature on the flow characteristics of microsphere suspensions. J. Pharm. Sci. 79, 929–933.

Ribeiro, A. J., Silva, C., Ferreira, D., Veiga, F., 2005. Chitosanreinforced alginate microspheres obtained through the emulsification/ internal gelation technique. Eur. J. Pharm. Sci. 25(1), 31–40.

Ritger, P.L., Peppas, N.A., 1987. A simple equation for description of solute release II. Fickian and anomalous release from swellable devices. J. Contl. Rel. 5, 37–42.

Rodier, E. et al., 2005. A three step supercritical process to improve the dissolution rate of Eflucimibe. Eur. J. Pharm. Sci. 26, 184–193.

Rodriguez, F., Krasicky, P.D., Groele, R.J., 1985. Dissolution rate measurements. Solid State Technol. 28(5), 125–131.

Rousset, M., 1986. The human colon carcinoma cell lines HT-29 and Caco-2: Two *in vitro* models for the study of intestinal cell differentiation. Biochemie. 68(9), 1035-1040.

Rowland, M., Tozer, T.N., 1995. Clinical Pharmacokinetics, Concepts and Applications. Williams & Wilkins, Baltimore.

Rubas, W., Cromwell, M.E., Shahrokh, Z., Villagran, J., Nguyen, T.N., Wellton, M., Nguyen, T.H., Mrsny, R.J., 1996. Flux measurements across Caco-2 monolayers may predict transport in human large intestinal tissue. J. Pharm. Sci. 85, 165-169.

Rubas,W., Jezyk, N., Grass, G.M., 1993. Comparison of the permeability characteristics of human colonic epithelial (Caco-2) cell line to colon of rabbit, monkey, and dog intestine and human drug absorption. Pharm. Res. 10, 113–118.

Rupa, D. D., Rishikesh, M. S., Dimitriy, A.M., Padma, V. D., Vladimir, P. T., 2006. Polyethylene glycol phosphatidylethanolamine conjugate (PEG–PE)-based mixed micelles: Some properties, loading with paclitaxel, and modulation of P-glycoprotein-mediated efflux. Int. J. Pharm. 315(1-2), 148-157.

Saeed, A. I., Sharov, V., White, J., Li, J., Liang, W., Bhagabati, N., Braisted, J., Klapa, M., Currier, T., Thiagarajan, M., Sturn, A., Snuffin, M., Rezantsev, A., Popov, D., Ryltsov, A., Kostukovich, E., Borisovsky, I., Liu, Z., Vinsavich, A., Trush, V. and Quackenbush, J. (2003). TM4: a free, open-source system for microarray data management and analysis. Biotechniques 34, 374-378.

Sarkadi, B., Müller, M., 1997. Search for specific inhibitors of multidrug resistance in cancer. Semin. Cancer. Biol. 8(3), 171–182.

Schena, M., 1996. Genome analysis with gene expression microarrays. Bioassays.18, 427–431.

Schena, M., Shalon, D., Davis, R.W., Brown, P.O., 1995. Quantitative monitoring of gene expression patterns with a complementary DNA microarray. Sci. 270, 467–470.

Schinkel, A.H., Smit, J.J., van Tellingen, O., Beijnen, J.H., Wagenaar, E., van Deemter, L., Mol, C.A., van der Valk, M.A., Robanus-Maandag, E.C., te Riele, H.P., Berns, A.J.M., Borst, P., 1994. Disruption of the mouse mdr1a P-glycoprotein gene leads to a deficiency in the blood–brain barrier and to increased sensitivity to drugs. Cell. 7, 491–502.

Schinkel, A.H., Wagenaar, E., Mol, C.A., van Deemter, L., 1996. P-glycoprotein in the blood-brain barrier of mice influences the brain penetration and pharmacological activity of many drugs. J. Clin. Investig. 97, 2517*–2524.*

Schneider, E., Hunke, S., 1998. ATP-binding-cassette (ABC) transport systems:Functional and structural aspects of the ATP-hydrolyzing subunits/domains. FEMS. Microbiol. Rev. 22, 1–20.

Sekiguchi, K., Obi, N., 1961. Studies on absorption of eutectic mixtures. I. A comparison of the behavior of eutectic mixtures of sulphathiazole and that of ordinary sulphathiazole in man. Chem. Pharm. Bull. 9, 866–872.

Sekiguchi, K., Obi, N., 1964. Studies on absorption of eutectic mixture. Ii. Absorption of fused conglomerates of chloramphenicol and urea in rabbits. Chem. Pharm. Bull. 12, 134–144.

Serajuddin, A. T. M., 1999. Solid dispersion of poorly water-soluble drugs: Early promises, subsequent problems, and recent breakthroughs. J. Pharm. Sci. 88, 1058-1066.

Sertsou, G., Butler, J., Scott, A., Hempenstall, J., Rades, T., 2002. Factors affecting incorporation of drug into solid solution with HPMCP during solvent change co-precipitation. Int. J. Pharm. 245, 99-108.

Shah, J.C., Chen, J.R., Chow, D., 1995. Preformulation study of etoposide. 2. Increased solubility and dissolution rate by solid-solid dispersions. Int. J. Pharm. 113, 103-111.

Shah, V.P., Tsong, Y., Sathe, P., Liu, J.P., 1998. In vitro dissolution profile comparison statistics and analysis of the similarity factor, f_2. Pharm. Res. 15, 889–896.

Shalon, D., Smith, S.J., Brown, P.O., 1996. A DNA microarray system for analyzing complex DNA samples using two color fluorescent probe hybridization. Genome. Res. 6, 639–45.

Shen, Q., Lin, Y., Handa, T., Doi, M., Sugie, M., Wakayama, K., Okada, N., Fujita, T., Yamamoto, A., 2006. Modulation of intestinal P-glycoprotein function by polyethylene glycols and their derivatives by in vitro transport and in situ absorption studies. Int. J. Pharm. 313(1-2), 49-56.

Sheu, M.T., Yeh, C.M., Sokoloski, T.D., 1994. Characterisation and dissolution of feno®brate solid dispersion systems. Int. J. Pharm. 103, 137-146.

Shimizu, H., Taniguchi, K., Hippo, Y., Hayashizaki, Y., Aburatani, H., Ishikawa, T., 2003. Characterisation of the mouse Abcc12 gene and its transcript encoding an`ATP-binding transporter, an orthologue of human ABCC12. Gene. 310, 17–28.

Shirihai, O. S., Gregory, T., Yu, C., Orkin, S. H., Weiss, M. J., 2000. ABC-me: a novel mitochondrial transporter induced by GATA-1 during erythroid differentiation. EMBO. J. 19, 2492–2502.

Shore, P.A., Brodie, B.B., Hogben, C.A.M., 1957. The gastric secretion of drugs: a pH partition hypothesis. J.Pharmacol. Exp. Ther. 119, 361–369.

Silverstein, R.M., Bassler, G.C., Morrill, T.C., 1991. Spectrometric Identification of Organic Compounds. John Wiley. New York. 109-130.

Simon-Assmann, P., Duclos, B., Orian-Rousseau, V., Arnold, C., Mathelin, C., Engvall, E., Kédinger, M., 1994. Differential expression of laminin isoforms and α6-β4 integrin subunits in the developing human and mouse intestina. Dev. Dyn. 201, 71-87.

Simoneli, A. P., Mehtha, S. C., Higuchi, W. I., 1976. Dissolution rates of high energy sulphathiazole-povidone coprecipitates II. Characterization of the form of drug controlling its dissolution rate via solubility studies. J. Pharm. Sci. 65, 355-361.

Simonelli, A.P. et al., 1969. Dissolution rates of high energy polyvinylpyrrolidone (PVP)-sulfathiazole coprecipitates. J. Pharm. Sci. 58, 538–549.

Sjokvist, E., Craig, D.Q.M, 1992. An investigation into the mechanism of dissolution of alkyl para-aminobenzoates from polyethylene glycol solid dispersions. Int. J. Pharm. 83, 211-219.

Sjokvist-Sears, E., Nystrom, C., 1988. Physicochemical aspects of drug release. VI. Drug dissolution rate from solid particulate dispersions and the importance of carrier and drug particle properties. Int. J. Pharm. 47, 51-66.

Sriamornsak, P., Thirawong, N., Nunthanid, Y.J., Sungthongjeen, S., 2007. Swelling and erosion of pectin matrix tablets and their impact on drug release behavior. Eur. J. Pharm. Biopharm. 67, 211–219.

Stein, W.D., 1997. Kinetics of the multidrug transporter (P-glycoprotein) and its reversal. Physiol Rev. 77*,* 545–590.

Stella, V., 1975. Prodrugs: An overview and definition. In: Pro-Drugs as Novel Drug Delivery System, American Chemical Society, Washington, Higuchi, T., Stclla, V. Eds. 1-115.

Stewart, B., Chan, O.H., Lu, R.H., Reyner, E.L., Schmid, H.L., Hamilton, H.W., Steinbaugh, B.A., Taylor, M.D., 1995. Comparison of intestinal permeabilities determined in multiple in vitro and in situ models: Relations to absorption in humans. Pharm. Res. 12, 693–699.

Straughn, A. B., Meyer, M. C., Raghow, G., Rotenberg, K., 1980. Bioavailability of microsize and ultramicrosize griseofulvin products in man. J. Pharmacokinet. Biopharm. 8, 347-362.

Suzuki, H., Sunada, H., 1997. Comparison of nicotinamide, ethylurea and polyethylene glycol as carriers for nifedipine solid dispersion systems. Chem. Pharm. Bull. 45, 1688-1693.

Sweetman, S.C., 2002. Martindale. The Complete Drug Reference. 33. ed. London: Pharm. Press.

Sweetman, S.C., 2004. Martindale: The complete drug reference. Electronic version. London UK: Pharmaceutical Press; Greenwood Village, Colorado: Thomson MICROMEDEX.

Sweetman, S.C., 2005. Martindale: The Complete Drug Reference. Pharm. Press. p. 47.

Takeuchi, M., Ueno, S., Yano, J., Floter, E., & Sato, K., (2000). Polymorphic transformation of 1, 3-distearoyl-sn-linoleoyl-glycerol. J. Amer. Oil. Chem. Soc. 77, 1243–1249.

Tammela, P., Laitinen, L., Galkin, A., Wennberg, T., Heczko, R., Vuorela, H., Slotte, J.P., Vuorela, P., 2004. Permeability characteristics and membrane affinity of flavonoids and alkyl gallates in Caco-2 cells and in phospholipid vesicles. Arch. Biochem. Biophys. 425, 193–199.

Tanaka, Y., Taki, Y., Sakane, T., Nadai, T., Sezaki, H., Yamashita, S., 1995. Characterization of drug transport through tight-junctional pathway in Caco-2 monolayer: Comparison with isolated rat jejunum and colon. Pharm. Res. 12, 523–528.

Tantishaiyakul, V., Kaewnopparat, N., Ingkatawornwong, S., 1999. Properties of solid dispersions of piroxicam in polyvinylpyrrolidone. Int. J. Pharm. 181, 143–151.

Taylor, L.S., Zografi, G., 1997. Spectroscopic characterization of interactions between PVP and indomethacin in amorphous molecular dispersions. Pharm. Res. 14, 1691-1698.

Taylor, M. D., 1996. Improved passive oral drug delivery via prodrugs. Adv. Drug Dev. Rev. 19, 131-148.

Terao, T., Hisanaga, E., Sai, Y., Tamai, I., Tsuji, A., 1996. Active secretion of drugs from the small intestinal epithelium in rats by P-Glycoprotein functioning as an absorption barrier. J. Pharm. Pharmaco. 48, 1083–1089.

Teresa, L., 2006. Recent Applications of DNA Microarray Technology to Toxicology and Ecotoxicology. Environ. Health. Perspect. 114(1), 4–9.

Teresa, M.M., Victoria, M.M., Gloria, E., Salcedo., 2002. Characterization and solubility study of solid dispersions of flunarizine and polyvinylpyrrolidone. Il Farmaco. 57(9), 723-727.

Thiebaut, F., Tsuruo, T., Hamada, H., Gottesman, M.M., Pastan, I., Willingham, M.C., 1987. Cellular localization of the multidrug-resistance gene product P-glycoprotein in normal human tissues. Proc. Natl. Acad. Sci. USA. 84, 7735–7738.

Thwaites, D.T., Armstrong, G., Hirst, B.H., Simmons, N.L., 1995a. D-cycloserine transport in human intestinal epithelial (Caco-2) cells mediated by a H+ -coupled amino acid transporter. Brit. J. Pharmaco. 115, 761-766.

Thwaites, D.T., Brown, C.D.A., Hirst, B.H., Simmons, N.L., 1993. Transepithelial glycylsarcosine transport in intestinal Caco-2 cells mediated by expression of H+ coupled carriers at both apical and basal membranes. J. Bio. Chem. 268, 7640-7642.

Thwaites, D.T., McEwan, G.T.A., Hirst, B.H., Simmons, N.L., 1995b. H^+-coupled α methylaminoisobutyric acid transport in human intestinal Caco-2 cells. Biochem. Biophys. Acta. 1234, 111-118.

Tibshirani, R., Hastie, T., Eisen, M., Ross, D., Botstein, D., Brown, P., 1999. Clustering methods for the analysis of DNA microarray data. Technical report. Stanford: Department of Statistics, Stanford University.

Tomi, M., Mori, M., Tachikawa, M., Katayama, K., Terasaki, T., Hosoya, K., 2005. l-type amino acid transporter 1-mediated l-leucine transport at the inner blood–retinal barrier. Invest. Ophthalmol. Vis. Sci. 46**,** 2522–2530.

Tozer, T.N., 1995. Clinical pharmacokinetics. Concepts and applications. 3rd ed. Williams and Wilkins. Media. PA.

Trapani, G., Franco, M., Latrofa, A., Pantaleo, M.R., Provenzano, M.R., Sanna, E., Maciocco, E., Liso, G., 1999. Physicochemical characterization and in vivo properties of Zolpidem in solid dispersions with polyethylene glycol 4000 and 6000. Int. J. Pharm. 184, 121-130.

Urbanetz, N.A., 2006. Stabilization of solid dispersions of nimodipine and polyethylene glycol 2000. Eur. J. Pharm. Sci. 28, 67–76.

Usui, F., Maeda. K., Kusai, A., Ikeda, M., Nishimura, K., Yamamoto, K., 1997. Inhibitory effects of water soluble polymers on precipitation of RS-8359. Int. J. Pharm.154, 59-66.

Van Aubel, R. A. M. H., Smeets, P.H.E., Peters, J.G.P., Bindels, R.J. M., Russel, F.G.M., 2002. The MRP4/ABCC4 Gene Encodes a Novel Apical Organic Anion Transporter in Human Kidney Proximal Tubules: Putative Efflux Pump for Urinary cAMP and cGMP. J. Am. Soc. Nephrol. 13, 595–603.

Van Drooge, D.J. et al., 2006. Characterization of the molecular distribution of drugs in glassy solid dispersions at the nano-meter scale, using differential scanning calorimetry and gravimetric water vapour sorption techniques. Int. J. Pharm. 310, 220–229.

Vilhelmsen, T. et al., 2005. Effect of a melt agglomeration process on agglomerates containing solid dispersions. Int. J. Pharm. 303, 132–142.

Vippagunta, S.R. et al., 2006. Factors affecting the formation of eutectic solid dispersions and their dissolution behavior. J. Pharm. Sci. 96, 294–304.

Von Mering, J., 1893. Beitrage zur Kenntniss der Antipyretica. Ther. Monatsch. 7, 577–587.

Vulevic, B., Chen, Z., Boyd, J. T., Davis, W., Jr., Walsh, E. S., Belinsky, M. G., Tew, K. D., 2001. Cloning and characterization of human adenosine 5′-triphosphate-binding cassette, sub-family A, transporter 2 (ABCA2). Cancer. Res. *61*, *3339* –3347.

Walter, E., Kissel, T., Reers, M., Dicneite, G., Hofmann, D, Stuber, W., 1995. Transepithelial properties of peptidomimetic thrombin inhibitors in monolayers of human intestinal cell line (Caco-2) and their correlation to *in vivo* data. Pharm. Res. 12, 360-365.

Wei, H., Dalton, C., Di Maso, M., Kanfer, I., Löbenberg, R., 2008. Physicochemical characterization of five glyburide powders: a BCS based approach to predict oral absorption. Eur. J. Pharm. Biopharm. 69, 1046–1056.

Wenzel, J, J., Kaminski, W, E., Piehler, A., Heimerl, S., Langmann, T., Schmitz, G., 2003. ABCA10, a novel cholesterol-regulated ABCA6-like ABC transporter. Biochem. Biophys. Res. Commun**.** 306**,**1089–1098.

Weuts, I., Kempen, D., Verreck, G., Decorte, A., Heymans, K., Peeters, J., Brewster, M., Van den, G.M., 2005. Study of physicochemical properties and stability of solid dispersions of loperamide and PEG 6000 prepared by spray drying. Eur. J. Pharm. Biopharm. 59, 119–126.

Wiseman, T., Williston, S., Brandts, J.F., Lin, L.N., 1989. Rapid measurement of binding constants and heats of binding using a new titration calorimeter. Anal. Biochem. 179, 131–137.

Wolters, J.C., Abele, R., Tampé, R., 2005. Selective and ATP-dependent translocation of peptides by the homodimeric ATP binding cassette transporter TAP-like (ABCB9). J. Biol. Chem. 280, 23631–23636.

Wong, T. W., Chan, L. W., Kho, S. B., Heng, P. W. S., 2002. Design of controlled-release solid dosage forms of alginate and chitosan using microwave. J. Contl. Rel. 84(3), 99–114.

http://www.drugbank.ca/

Yabuuchi, H., Shimizu, H., Takayanagi, S., Ishikawa, T., 2001. Multiple splicing variants of two new human ATP-binding cassette transporters, ABCC11 and ABCC12. Biochem. Biophys. Res. Commun. 288, 933–939.

Yabuuchi,H., Takayanagi, S., Yoshinaga, K., Taniguchi, N., Aburatani, H., Ishikawa, T., 2002. ABCC13, an unusual truncated ABC transporter, is highly expressed in fetal human liver. Biochem. Biophys. Res. Commun. 299, 410–417.

Yamashita, S., Furubayashi, T., Kataoka, M., Sakane, T., Sezaki, H., Tokuda, H., 2000. Optimized conditions for prediction of intestinal drug permeability using Caco-2 cells. Eur. J. Pharm. Sci.10, 195–204.

Yamashita, S., Tanaka, T., Endoh, Y., Taki, Y., Sakane, T., Nadai, T., Sezaki, H., 1997. Analysis of drug permeation across Caco-2 monolayer: Implication for predicting in vivo drug absorption. Pharm. Res. 14, 486–491.

Yee, S., 1997. In vitro permeability across caco-2 cells (colonic) can predict in vivo (small intestinal) absorption in man—fact or myth. Pharm. Res. 14, 763–766.

Yoshioka, M., Hancock, B.C., Zografi, G., 1995. Inhibition of indomethacin crystallization in poly(vinylpyrrolidone) coprecipitates. J. Pharm. Sci. 84, 983–986

Yoshioka, S., Aso, Y., 2007. Correlations between molecular mobility and chemical stability during storage of amorphous pharmaceuticals. J. Pharm. Sci. 96, 960–981.
Yu, L., 2001. Amorphous pharmaceutical solids: preparation, characterization and stabilization. Adv. Drug Deliv. Rev. 48, 27–42.

Zaplisky, S., Harris, J.M., 1997. Introduction to chemistry and biological applications of poly(ethylene glycol), poly(ethylene glycol) chemistry and biological applications, American Chemical Society, San Francisco, CA. 1–11.

Zelcer, N., Saeki, T., Reid, G., Beijnen J.H., Borst. P., 2001. Characterization of drug transport by the human multidrug resistance protein 3 (ABCC3), J. Biol. Chem. 276**(**49), 46400–46407.